1-31-2013

Communication-aware motion planning in mobile networks

Alireza Ghaffarkhah

Alireza Ghaffarkhah

Candidate

Electrical and Computer Engineering

Department

This dissertation is approved, and it is acceptable in quality and form for publication:

Approved by the Dissertation Committee:

Yasamin Mostofi , Chairperson

Chaouki Abdallah

Rafael Fierro

Lydia Tapia

Communication-Aware Motion Planning in Mobile Networks

by

Alireza Ghaffarkhah

B.S., Sharif University of Technology, 2005
M.S., Sharif University of Technology, 2007

DISSERTATION

Submitted in Partial Fulfillment of the
Requirements for the Degree of

Doctor of Philosophy
Engineering

The University of New Mexico

Albuquerque, New Mexico

December 2012

Dedication

To my mother and father

Acknowledgments

First and foremost, I would like to thank my advisor Prof. Yasamin Mostofi. She is a great teacher, an excellent mentor, an intelligent researcher and most importantly a trustworthy friend. I learnt a great deal from our numerous technical discussions. She is indeed the most hardworking person I have ever known and I will always admire her professionalism, enthusiasm for new ideas and dedication to research.

I would like to thank Prof. Chaouki Abdallah, Prof. Rafael Fierro and Prof. Lydia Tapia for serving on my dissertation committee. They are among the most knowledgeable people I have had the pleasure to meet at UNM. Prof. Abdallah has always been so supportive of me and I need to thank him for agreeing to be on my dissertation committee despite his extremely busy schedule as the Interim Provost at UNM. My special thanks also go to Prof. Fierro for always being so nice and helpful and for letting us use his lab during our experiments. Without his help doing experiments could be very painful. And I need to thank Prof. Tapia who agreed to be on my committee on short notice.

I would like to thank all the members of our research group at the Cooperative Network Lab at UNM, specially Mehrzad Malmirchegini, Alejandro Gonzalez-Ruiz and Yuan Yan, for being such great friends.

Finally, I want to thank my family, specially my mother Mahnaz and father Mehrdad, for their infinite love and support. To them, I owe everything.

Communication-Aware Motion Planning in Mobile Networks

by

Alireza Ghaffarkhah

B.S., Sharif University of Technology, 2005
M.S., Sharif University of Technology, 2007

Ph.D., University of New Mexico, 2012

Abstract

Over the past few years, considerable progress has been made in the area of networked robotic systems and mobile sensor networks. The vision of a mobile sensor network cooperatively learning and adapting in harsh unknown environments to achieve a common goal is closer than ever. In addition to sensing, communication plays a key role in the overall performance of a mobile network, as nodes need to cooperate to achieve their tasks and thus have to communicate vital information in environments that are typically challenging for communication. Therefore, in order to realize the full potentials of such networks, *an integrative approach to sensing (information gathering), communication (information exchange), and motion planning* is needed, such that each mobile sensor considers the impact of its motion decisions on both sensing and communication, and optimizes its trajectory accordingly. This is the main motivation for this dissertation.

This dissertation focuses on communication-aware motion planning of mobile networks in the presence of realistic communication channels that experience path loss,

shadowing and multipath fading. This is a challenging multi-disciplinary task. It requires an assessment of wireless link qualities at places that are not yet visited by the mobile sensors as well as a proper co-optimization of sensing, communication and navigation objectives, such that each mobile sensor chooses a trajectory that provides the best balance between its sensing and communication, while satisfying the constraints on its connectivity, motion and energy consumption. While some trajectories allow the mobile sensors to sense efficiently, they may not result in a good communication. On the other hand, trajectories that optimize communication may result in poor sensing. The main contribution of this dissertation is then to address these challenges by proposing a new paradigm for communication-aware motion planning in mobile networks. We consider three examples from networked robotics and mobile sensor network literature: *target tracking*, *surveillance* and *dynamic coverage*. For these examples, we show how probabilistic assessment of the channel can be used to integrate sensing, communication and navigation objectives when planning the motion in order to guarantee satisfactory performance of the network in realistic communication settings. Specifically, we characterize the performance of the proposed framework mathematically and unveil new and considerably more efficient system behaviors. Finally, since multipath fading cannot be assessed, proper strategies are needed to increase the robustness of the network to multipath fading and other modeling/channel assessment errors. We further devise such robustness strategies in the context of our communication-aware surveillance scenario. Overall, our results show the superior performance of the proposed motion planning approaches in realistic fading environments and provide an in-depth understanding of the underlying design trade-off space.

Contents

List of Figures

List of Tables

Chapter 1

Introduction

Over the past few years, considerable progress has been made in the area of robotic and mobile networks [1–3]. The vision of a mobile network cooperatively learning and adapting in harsh unknown environments to achieve a common goal is closer than ever. Such mobile networks consist of a group of unmanned sensors/agents/robots, equipped with sensing, processing and communication capabilities, that cooperate to perform a task jointly. Mobile networks can have a tremendous impact in many different areas, such as search and rescue [4,5], target tracking [6–12], surveillance [13–15], exploration and field estimation [16–20], environmental monitoring [21, 22] and military reconnaissance [23, 24]. Since each mobile sensor has a limited sensing and communication capability, the group relies on a networked operation to accomplish its task. Limited sensing and communication capabilities, distributed decision making and other constraints, thus, make designing robust and efficient mobile networks challenging.

Several different problems in designing mobile networks have been studied by different communities in recent years. In robotics and control community, problems such as motion planning and group coordination [25–33], cooperative task accom-

plishment [6–21] and control over networks [34–42] have been extensively studied. In the communication community, on the other hand, a rather different class of problems such as cross-layer design [43, 44], power management [45, 46], cooperative routing [47–49], diversity schemes [50, 51] and capacity [52, 53] have been considered. In this dissertation, we are interested in *communication-aware motion planning*, a problem that requires concepts from both communities. By communication-aware motion planning, we refer to the co-optimization of sensing (information gathering) and communication (information exchange) through proper trajectory design. This is a very challenging task and requires 1) an assessment of wireless link qualities at places that are not yet visited by the mobile sensors, and 2) a proper integration of sensing, communication and navigation objectives such that each mobile sensor chooses a trajectory that provides the best balance between its sensing and communication. While some trajectories allow the mobile sensors to sense the environment and gather information extensively, they may not result in a good communication performance. On the other hand, trajectories that optimize communication may result in poor sensing. Proper motion optimization, thus, requires understanding the underlying trade-offs and integrating sensing, communication and navigation objectives when planning the motion. Presenting such an *integrative strategy to communication, sensing and motion planning* in mobile networks is the key novelty of this dissertation. The proposed communication-aware motion planning approaches of this dissertation plan the motion of the mobile sensors by designing proper integrated objective functions, and using a probabilistic assessment of realistic fading channels to evaluate these objective functions at unvisited locations. The proposed approaches can be used to optimize the trajectories of the mobile sensors (and possibly their transmission powers and rates along their trajectories) to accomplish the sensing task of the network, while satisfying the constraints on the connectivity of the mobile sensors (as well as their motion and energy constraints).

Specifically, we design our communication-aware motion planning approaches for

a number of scenarios from robotic and mobile sensor network literature. The scenarios considered in this dissertation are as follows: *target tracking*, *surveillance* and *dynamic coverage*. Communication plays a key role in the overall performance of the network in all these cases, as mobile sensors need to communicate vital information in environments that are typically challenging for communication. Each scenario is studied in detail in a separate chapter, where we show the effects of realistic fading communication channels on the overall network performance and propose our communication-aware motion planning strategies. To the best of our knowledge, this is the first time that communication-aware motion planning strategies that consider realistic fading communication channels are designed for these scenarios, as we explain more throughout the dissertation.

1.1 Contributions of the Dissertation

In this section, we explain the organization of the dissertation and summarize its contributions. Each chapter of this dissertation deals with a specific problem. Thus, we explain the contributions of each chapter separately. Note that a more detailed discussion on the contributions of each chapter is provided at the beginning of the chapter.

Chapter 2: Probabilistic Assessment of Wireless Channels and Motion Planning for Improving Channel Prediction Quality

In this chapter, we first review the probabilistic modeling of wireless channels and propose a probabilistic channel assessment framework to predict the channel variations at unvisited locations, based on a small number of channel measurements. We then show how to plan motion of a mobile sensor to collect channel measurements

that improve its channel assessment performance. The probabilistic channel model introduced in this chapter is the well-established multi-scale random field model from the wireless communication literature. This model gives the distribution of the path loss, shadowing and multipath fading components of the channel as well as their spatial correlations. Our proposed probabilistic channel assessment framework is built on this model and enables a mobile sensor to efficiently predict the channel along its trajectory. In order to use the mobility of the mobile sensor to improve its channel assessment performance, we then propose two motion planning approaches. In the first approach, the trajectory of the mobile sensor is optimized to collect channel measurements that improve its estimate of the underlying channel parameters (specially the path loss parameters). In the second approach, the trajectory is optimized to collect measurements that directly minimize the channel assessment error variance at the mobile sensor.

We use this channel assessment framework extensively throughout the rest of the dissertation, when proposing our communication-aware motion planning approaches.

The results of this chapter are based on our journal papers [6, 54] and the conference papers [7, 55, 56].

Chapter 3: Communication-Aware Target Tracking Using Mobile Networks

In Chapter 3 of this dissertation, we study the problem of remotely tracking a moving target in realistic communication environments. We consider the scenario where a fixed remote station utilizes a number of mobile sensors for keeping track of the position of a moving target. The communication links between the mobile sensors and the remote station are realistic wireless links that experience path loss, shadowing and multipath fading. We first characterize the effects of realistic fading channels and a packet-dropping receiver on Kalman filtering for estimating the target position

at the remote station. By using an information-theoretic measure of uncertainty at the remote station, we then propose local communication-aware motion planning approaches to minimize the estimation error covariance (maximize the received Fisher information) of the target position at the remote station. Our novel motion planning approaches of this chapter properly integrate the sensing and communication objectives to accomplish the sensing task of the mobile sensors, while maintaining proper connectivity to the remote station. To the best of our knowledge, this is the first time that such communication-aware motion planning approaches are proposed for networked target tracking in realistic fading communication environments. This is the key contribution of this chapter.

The results of this chapter are based on our journal paper [6] and the conference paper [7].

Chapter 4: Communication-Aware Surveillance Using Mobile Networks

In Chapter 4 of this dissertation, we build on Chapter 3 to consider the case where the information is generated in a more complex manner in the environment. More specifically, we consider a networked surveillance operation where a number of mobile sensors are deployed to survey an environment, detect an unknown number of static targets, and inform a remote station of their findings. The mobile sensors detect the targets along their trajectories, using their collected sensory data. To inform the remote station, they send fixed-size binary vectors, referred to as *target maps*, to the remote station. In a target map, a one (zero), at any element, indicates that the mobile sensor has detected a target (or not) in the corresponding cell of the discretized version of the environment. The remote station then fuses the target maps received from the mobile sensors and builds a more reliable map of targets over the entire environment.

In this chapter, we start with analyzing the impact of the trajectories of the mobile sensors and the resulting sensing and communication qualities on the probability of target detection error at the remote station. We then propose a communication-aware motion planning framework that can guarantee, under certain assumptions, that each sensor explores the environment and gathers as much information as possible regarding target locations, while maintaining the required connectivity to the remote station. The proposed framework consists of two decentralized switching approaches to satisfy the requirements on the connectivity of the mobile sensors to the remote station: *communication-constrained* and *hybrid*. Our communication-constrained approach plans the motion of each mobile sensor such that it explores the workspace while maximizing its probability of connectivity to the remote station during the entire operation. This approach is appropriate for the case where the remote station needs to be constantly informed of the most updated map of the targets, which puts a constraint on the motion of the mobile sensors to constantly maintain their connectivity. Constant connectivity, however, is not required if the mission is such that the remote station only needs to be informed of the map of the targets at the end of a given operation time. In this case, the mobile sensors can explore the environment with less connectivity constraints, provided that they get connected to and inform the remote station at the end of the given operation time. Our hybrid motion planning approach is then appropriate for this case. This approach builds on our communication-constrained one and allows the mobile sensors to explore the area more extensively than the communication-constrained approach, while maximizing their probability of connectivity at the end of the operation. Both approaches make use of the probabilistic channel assessment framework of Chapter 2 to predict the path loss and shadowing components of the channel at unvisited locations, based on a small number of channel samples that are collected online or *a priori*. Proposing these two approaches is the main key contribution of this chapter. Another important contribution of this chapter is proposing strategies to increase the robustness of

our communication-constrained and hybrid approaches to multipath fading. Such strategies are specially desired since multipath fading cannot be predicted efficiently based on the sparse sampling of the channel and, therefore, is a source of uncertainty.

The results of this chapter are based on our journal paper [13] and the conference papers [14, 16].

Chapter 5: Communication-Aware Dynamic Coverage of Time-Varying Environments Using Mobile Networks

Chapter 5 of this dissertation is dedicated to the problem of communication-aware dynamic coverage of time-varying environments. We consider the problem where a number of mobile agents,[1] with limited energy budgets and sensing/actuation capabilities, are deployed to cover a set of point of interests (POIs) in a time-varying environment. By a time-varying environment, we refer to an environment where a quantity of interest that needs to be controlled at the POIs is time-varying and increasing in time at every POI that is not in the effective range of any mobile agent. Several real-world applications can be modeled as a dynamic coverage problem. Examples include surveillance of a time-varying environment, information collection from a set of data logging devices distributed over a spatially large environment, collecting hazardous materials from a set of POIs, distributed task accomplishment, and mobility-on-demand systems. In this chapter, we also consider a communication-oriented scenario where the mobile agents are required to communicate to a fixed remote station in order to complete their coverage task. The goal is then to plan the motion and communication policies of the mobile agents in order to guarantee the boundedness of the quantity of interest at all the POIs, while meeting the constraints on the connectivity of mobile agents to the remote station, the frequency of covering the POIs, and the total energy budget of the mobile agents. Note that since the

[1] In this chapter, we intentionally use the term "mobile agents" as opposed to "mobile sensors" to emphasize that the nodes may be active nodes that are able to actuate or change the environment.

quantity of interest is continuously increasing at the POIs, *periodic* trajectories need to be devised for the mobile agents in order to repeatedly cover the POIs. Next, we explain our communication-aware approach for dynamic coverage of time-varying environments in more detail.

We consider a linear dynamics for the time-variation of the quantity of interest at the POIs.[2] We then propose motion and communication policies for the mobile agents to minimize the total energy consumption of the mobile agents in each period, while guaranteeing that the quantity of interest at the POIs remains bounded, and the constraints on the connectivity of the mobile agents, the frequency of covering the POIs, and the total energy budget of the mobile agents are satisfied. We start with the case where the sensing/actuation range of the mobile agents is small such that each agent is required to move to the position of each POI and stop there for some time to sense/service it (this assumption is then relaxed at the end of the chapter). We also assume a limited total energy budget for the mobile agents. To keep our framework general, we consider two variants of the problem: *communication-intensive* and *communication-efficient*. Communication-intensive case refers to the case where the mobile agents are required to be connected at all the POIs they visit, in order to send their collected information to the remote station in real-time. Communication-efficient case, on the other hand, refers to the case where the mobile agents are only required to connect to the remote station once along their trajectories, decreasing the communication burden considerably. In both communication-intensive and communication-efficient cases, we show how to optimally find the trajectories of the mobile agents, as well as their stop times and transmission powers at the POIs, using mixed-integer linear programs (MILPs). The properties of the optimal solutions of the MILPs, as well as their asymptotic properties, are also characterized

[2]While the dynamics of the quantity of interest in the aforementioned problems could be nonlinear, a linear approximation may be a close enough approximation depending on the system parameters.

mathematically.

We next continue with extending our framework by considering a non-zero range for the sensing/actuation device of the mobile agents and adapting their velocities and transmission rates (in addition to their transmission powers) along their trajectories. Unlike the previous case, here we take into account the amount of information (the number of information bits) that is transmitted to and correctly received by the remote station along the trajectories of the mobile agents. For the sake of simplicity, however, we consider only one mobile agent. We then show how the trajectory of the mobile agent, as well as its transmission power, transmission rate and velocity, can be optimally found using an MILP. Finally, the solution of the proposed MILP in this case is characterized mathematically.

To the best of our knowledge, this is the first time that dynamic coverage is solved optimally, in the presence of realistic communication channels, and under several constraints on the connectivity and total energy consumption of the mobile agents. Also, there is no existing work that mathematically analyzes the dynamic coverage problem, as we do so in this chapter. We should emphasize that the proposed dynamic coverage framework of this chapter is quite general. Several communication-oriented dynamic coverage scenarios can be solved using the dynamic coverage strategies proposed in this chapter. A more detailed discussion can be found at the beginning of the chapter.

The results presented in this chapter are based on our recently submitted journal paper [57] and the conference paper [58].

1.2 Related Work

In this section, we review the current literature as related to different parts of this dissertation. This further highlights the contributions of the dissertation explained

in the previous section.

1.2.1 Probabilistic Assessment of Wireless Channels and Motion Planning for Improving Channel Prediction Quality

The probabilistic channel model utilized in Chapter 2 is the well-established multi-scale random field model proposed in the wireless communication literature [54, 59, 60]. This model gives the distribution of the path loss, shadowing and multipath fading components of the channels and their spatial correlations. We then use this model to propose our channel assessment framework in Chapter 2, based on concepts from Gaussian random fields. Our channel assessment framework can also be thought of in the context of krigging and active sensing of a general 2D field [19–21, 61–64]. For the implication of this framework for other applications not considered in this thesis, such as robotic routers, readers are referred to [65]. For more on transmitter position localization based on a probabilistic modeling of the channel, the readers are referred to [64, 66].

In Chapter 2, we also propose a motion planning framework for improving channel predictability in robotic/sensor networks.

1.2.2 Target Tracking Using Mobile Networks

Target tracking have been explored extensively in the robotics, control and mobile sensor network community [8–12,67]. The techniques that are based on optimizing an information-theoretic objective function are the most related to the target tracking approach of Chapter 3. Such techniques are often referred to as active sensing in the literature. In active sensing, the idea is to use a distributed sensor fusion technique, based on a Kalman filter, and then find the trajectories of the mobile sensors to

optimize an information-theoretic objective function that is designed to improve the overall sensor fusion performance. For instance, the authors in [9–11] propose analyzing the effects of possible motions or configurations of mobile sensors on the performance of Kalman filtering. To improve the performance, they then consider choosing the best local motion at each step [10,11] or navigating the mobile sensors to the optimal configuration asymptotically [9]. In these works, the resulting objective functions are nonlinear functions of the positions of the mobile agents at each step and are optimized using gradient-based, greedy or receding horizon techniques when planning the motion. Motion planning approaches based on vector fields have also been proposed [12]. Note that the communication links between the mobile sensors and the fusion center are assumed ideal in the aforementioned works. Recently a number of papers started to consider the effect of realistic communication links on the performance of Kalman filtering over wireless links. In [68,69], the authors study the problem of Kalman filtering over packet-dropping links. Kalman filtering in the presence of fading channels is also studied in [41], where the authors analyze the effect of SNR-dependant packet drops and communication noise on the filtering performance.[3]

The first attempts to consider realistic communication channels when tracking a moving target appeared in [70–72]. The proposed method in [70] considers a distance-dependant probability of drop for the mobile sensors and uses that to formulate the average Fisher information at the remote station. Also, in [71, 72] path loss models are used to find the overall observation error covariance (the summation of sensing and communication noise covariances) at the remote station. Greedy motion planning approaches are then used to minimize the total estimation error covariance of a best linear unbiased estimator (BLUE) of the remote station to estimate the target

[3]Note that Kalman filtering over packet-dropping links falls in the category of the *networked control systems* [34–39,69]. In the networked control systems, the goal is to consider the effect of communication links on the performance and stability of the estimation/conrol of a dynamical system over wireless links.

position. The communication-aware motion planning approaches of Chapter 3 can be considered as extensions of the motion planning approaches of [70–72] to the case that 1) the communication links are realisitic channels that experience path loss, shadowing and multipath fading, 2) the mobile sensors utilize a probabilistic assessment of wireless channels using the channel measurements they gather along their trajectories, and 3) sensing and communication goals are integrated in the design of the motion planner. By designing novel integrated sensing and communication objectives and using the channel assessment framework of Chapter 2, we can guarantee a large improvement in the target estimation performance in the presence of realistic fading channels, as we show in Chapter 3.

1.2.3 Surveillance, Exploration and Field Estimation Using Mobile Networks

The results of Chapter 4 are related to the current results on robotic surveillance, exploration, coverage, field estimation and environmental monitoring. For instance, in [15], the authors consider a surveillance scenario, using a team of unmanned aerial vehicles (UAVs) and unmanned ground vehicles (UGVs), for detecting and localizing an unknown number of features within a given search area. They then design an information-theoretic framework for coordination of the UAVs and UGVs, which maximizes the mutual information gain for target localization. However, only sensing objectives are considered for coordination. In the robotic exploration/coverage context, related works are [17, 18, 73, 74], where the authors propose gradient-based controllers to navigate the robots along trajectories that provide the best sensing coverage performance [73, 74] or guarantee exploration of the entire environment asymptotically [17, 18]. Motion planning for field estimation has also been studied by several works such as [19, 20]. In [19], a distributed kriged Kalman filter is used to estimate the spatio-temporal variations of a field. The author then pro-

poses a gradient-based motion controller to find the maxima of the field. A similar field estimation approach, based on kriging, is also considered in [20]. The authors, however, consider solving a dynamic program to find the optimal trajectories. In the environmental monitoring context, the authors in [21] address the problem of adaptive exploration for an autonomous ocean monitoring system. Feedback control laws are then derived to coordinate the robots along the trajectories that optimize a predefined exploration performance metric.

The aforementioned works, however, are not concerned with communication issues. In other words, the authors effectively consider the sensing objectives, i.e., goals that are aimed at maximizing the exploration and coverage performance of the robots when planning the motion. Although, proper communication objectives, i.e., goals that are aimed at maximizing the probability of connectivity to the remote station, are not taken into account [15, 17–21, 73–75]. Considering both objectives requires a new design paradigm as new challenges arise. Our proposed communication-aware framework addresses these challenges by properly co-optimizing sensing, communication and navigation objectives. This is not possible using the existing approaches in the literature.

1.2.4 Dynamic Coverage of Time-Varying Environments Using Mobile Networks

The existing literature related to the dynamic coverage problem of Chapter 5 is categorized based on the type of the environment (time-invariant or time-varying) and motion planning approach (analytical or algorithmic). For instance, the exploration strategies of [17, 18] can be considered dynamic coverage strategies used to cover a time-invariant environment based on analytical motion planning approaches (gradient-based approaches). The algorithmic motion planning approaches of [76–78]

can also be used for dynamic coverage of a time-invariant environment. In these works, the authors determine the paths that pass through a set of points or cells in a known [76] or unknown [77] environment. Their proposed approaches involve cellular decomposition for known environments and Morse decomposition for unknown ones, as well as devising heuristic and exact algorithms to achieve coverage. In their more recent work in [78], the authors also extend their algorithmic approach to the case of sensing ranges that go beyond the size of the robot. These works, however, do not consider planning periodic trajectories for dynamic coverage of time-varying environments. Furthermore, none of these works consider realistic communication and energy constraints when planning the motion of the mobile agents.

In terms of the class of the trajectories considered, the proposed approaches of Chapter 5 are related to current literature on sweep coverage and patrolling [79–83] and persistent monitoring [84, 85], where periodic trajectories for the mobile agents are planned to repeatedly cover a set of POIs in the environment. The approaches of [79–84] are based on designing heuristic near-optimal algorithms for covering the POIs (under a constraint on the frequency of visiting the points or by maximizing the frequency of the visits). The authors, however, do not consider a time-varying environment and realistic communication and energy constraints. The authors in [85] propose a trajectory planning algorithm, based on a constrained version of the Bellman-Ford algorithm, to persistently visit a set of cells in a discretized version of the environment. Their goal is to maximize a reward function and meet the constraint on the maximum allowable time for an agent to complete a cycle, without considering the communication and energy issues. Realistic communication links are considered in [86], where the authors propose on-line adaptation of the velocity of a single mobile agent to the channel quality (along a fixed trajectory). However, they do not consider path planning, sensing objectives, link prediction, or energy issues. The formal definition of a time-varying environment that we utilize in this chapter is first presented in [75], where the authors introduce the dynamics

of the quantity of interest at the POIs. In order to stabilize the dynamic coverage task, they then propose strategies to adapt the velocities of the mobile agents along predefined periodic trajectories. Similarly, no communication or energy constraint is considered in [75]. In Chapter 5, we extend the previous work on multi-agent coverage to a time-varying environment and in the presence of communication, time and energy constraints. More specifically, we consider a generalized version of the linear dynamical model of [75] to capture the time variations of the quantity of interest in the presence of realistic fading channels. We then propose optimal motion, transmission power and transmission rate policies for the mobile agents to stabilize the dynamic coverage task, while meeting the constraints on the connectivity of the mobile agents along their trajectories, the frequency of covering the POIs, and the total energy consumption of the mobile agents. Our proposed approach enables networked multi-agent dynamic coverage in realistic communication settings and in the presence of energy constraints, which is not possible using the current methods.

1.3 Notations

Throughout this dissertation, the following common notations are used:

- The dependency of a quantity f to any quantity x is shown by $f(x)$ when the x is continuous and by f_x when x is discrete. For instance, if a quantity f at mobile sensor k is a continuous function of time t and position q, we show this dependency by $f_k(q,t)$.

- We use calligraphic letters ($\mathcal{X}$, $\mathcal{Y}$, $\cdots$) to show finite or infinite sets. Then, the notation $|\mathcal{X}|$ denotes the number of elements (cardinality) of $\mathcal{X}$ if $\mathcal{X}$ is finite, while it shows the volume of $\mathcal{X}$ if $\mathcal{X}$ is a subset of $\mathbb{R}^N$.

- We traditionally assume that if $\mathcal{I} = \emptyset$, then 1) $\prod_{i\in\mathcal{I}} x_i = 1$, 2) $\sum_{i\in\mathcal{I}} x_i = 0$ and 3) $\bigcup_{i\in\mathcal{I}} \mathcal{X}_i = \emptyset$, where x_i and $\mathcal{X}_i$ denote arbitrary numbers and sets, respectively.

Chapter 2

Probabilistic Assessment of Wireless Channels and Motion Planning for Improving Channel Prediction Quality

Consider a spatially-distributed sensing operation, in a workspace $\mathcal{W} \subset \mathbb{R}^2$, where a a number of mobile sensors[1] need to maintain their connectivity to a fixed remote station while accomplishing their sensing task. A fundamental parameter that characterizes the performance of the communication channel from a mobile sensor to the remote station is the instantaneous channel power or equivalently the received signal power or the received signal-to-noise ratio (SNR).

In the wireless communication literature [59, 60], it is well established that the channel power (or the received signal power or the received SNR), can be modeled

[1]In this dissertation, we use terms "mobile sensor", "mobile agent" and "robot" interchangeably.

as a multi-scale non-stationary random field with three major dynamics: *path loss*, *shadowing (or shadow fading)* and *multipath fading*. Fig. 2.1 shows the received signal power across a route in the basement of the Electrical and Computer Engineering (ECE) building at the University of New Mexico (UNM). The three main dynamics of the received signal power are marked on the figure. Path loss is the slowest dynamic which is associated with the signal attenuation due to the distance-dependent power fall-off. Depending on the environment, blocking objects may result in a faster variation of the channel power referred to as shadowing. Finally, multiple replicas of the transmitted signal can arrive at the receiver due to the reflection from the surrounding objects, resulting in even a faster variation in the channel power called multipath fading.

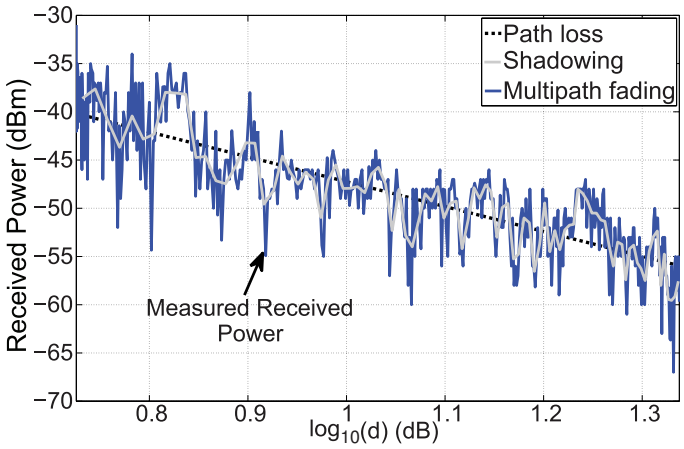

Figure 2.1: Underlying dynamics of the received signal power across a route in the basement of the ECE building at UNM. d is the distance to the transmitter.

In this chapter, we first summarize the well-established multi-scale probabilistic modeling of wireless channels and develop a channel prediction/assessment framework based on that. We then show how to plan the motion of a mobile sensor to improve its channel assessment performance. Using our probabilistic channel assessment framework a mobile sensor can assess the channel along its trajectory well, given only a small number of *a priori* channel measurements. In the following chap-

ters, the proposed channel assessment framework of this chapter is integrated with motion planning in order to maintain the connectivity of the mobile sensors while accomplishing their sensing task.

The rest of this chapter is organized as follows. In Section 2.1, we summarize the multi-scale probabilistic modeling of wireless channels, as discussed in the wireless communication literature. We introduce our probabilistic channel assessment framework in Section 2.2, where we explain how to estimate the channel parameters and predict the spatial variations of the channel power at unvisited locations. In Section 2.3, we analyze the sensitivity of our channel assessment approach to errors in the estimation of channel parameters and show that it is more sensitive to the estimation errors of the path loss parameters. In Section 2.4, we propose a framework for planning the motion of a mobile sensor to improve its channel assessment. A summary of the results of the chapter is provided in Section 2.5.

2.1 Probabilistic Modeling of Wireless Channels

The probabilistic modeling of wireless channels characterizes the distribution of a sample of the channel as well as its spatial correlation. In this section, we briefly explain a probabilistic model of wireless channels as discussed in the the wireless communication literature [54, 56, 59, 60]. Let $G(q)$ denote the channel power in the transmission from a mobile sensor at position $q \in \mathcal{W}$ to a remote station at position $q_b \in \mathbb{R}^2$. By using the multi-scale non-stationary random field model of wireless channels [59, 60], we have the following characterization for $G(q)$:

$$G(q) = G_{\mathrm{PL}}(q) G_{\mathrm{SH}}(q) G_{\mathrm{MP}}(q), \tag{2.1}$$

where $G_{\mathrm{SH}}(q)$ and $G_{\mathrm{MP}}(q)$ are random variables representing the impact of shadowing and multipath fading components respectively, and $G_{\mathrm{PL}}(q) = \frac{K_{\mathrm{PL}}}{\|q-q_b\|^{n_{\mathrm{PL}}}}$ is the

distance-dependent path loss. In this model, the multipath fading term, $G_{\rm MP}(q)$, has a unit average. Let $G_{\rm dB}(q) \triangleq 10\log_{10}\big(G(q)\big)$ represent the channel power in dB. We have

$$G_{\rm dB}(q) = K_{\rm dB} - 10\,n_{\rm PL}\log_{10}\big(\|q-q_b\|\big) + G_{\rm SH,dB}(q) + G_{\rm MP,dB}(q), \qquad (2.2)$$

where $K_{\rm dB} \triangleq 10\log_{10}(K_{\rm PL}) + \overline{G}_{\rm MP,dB}$, $\overline{G}_{\rm MP,dB} \triangleq 10\mathbb{E}\big\{\log_{10}\big(G_{\rm MP}(q)\big)\big\}$ is the average of the multipath fading term in dB, $G_{\rm SH,dB}(q) = 10\log_{10}\big(G_{\rm SH}(q)\big)$ is a zero-mean random variable representing the shadowing effect in dB, and $G_{\rm MP,dB}(q) = 10\log_{10}\big(G_{\rm MP}(q)\big) - \overline{G}_{\rm MP,dB}$ is a zero-mean random variable, independent of $G_{\rm SH,dB}(q)$, which denotes the impact of multipath fading in dB. Note that the average of the multipath fading term in the dB domain has been moved to $K_{\rm dB}$ in order to make the mean of $G_{\rm MP,dB}(q)$ zero.

In the communication literature, the distributions of $G_{\rm SH}(q)$ and $G_{\rm MP}(q)$, or equivalently $G_{\rm SH,dB}(q)$ and $G_{\rm MP,dB}(q)$, are established based on empirical data [59,60]. As for the shadowing component, log-normal is shown to be a good match for the distribution of $G_{\rm SH}(q)$, resulting in the following probability density function (pdf) for $G_{\rm SH,dB}(q)$: $f_{G_{\rm SH,dB},\rm norm}(x) = \frac{1}{\sqrt{2\pi}\vartheta}e^{\frac{-x^2}{2\vartheta^2}}$, where $\vartheta^2 = \mathbb{E}\big\{G^2_{\rm SH,dB}(q)\big\}$ is the variance of the shadow fading variations of the channel power around the path loss component in the dB domain. Distributions such as Rayleigh, Rician, Nakagami and log-normal are also shown to match the pdf of $G_{\rm MP}(q)$.[2] Rayleigh distribution is a good match when the channel has no line-of-sight (LOS) component. In this case, the pdf of $G_{\rm MP}(q)$ is given by $f_{G_{\rm MP},\rm Ray}(x) = e^{-x}$. If the channel has a LOS component, Rician distribution is shown to be a better match than Rayleigh. The pdf of $G_{\rm MP}(q)$ in this case is given by $f_{G_{\rm MP},\rm Ric}(x) = (K_r+1)e^{-K_r-(K_r+1)x}I_0\big(2\sqrt{xK_r(K_r+1)}\,\big)$, where $I_0(.)$ is the zeroth-order modified Bessel function and K_r is the Rician K-parameter, that determines the ratio of the power of the LOS component to the power of the non-LOS component of the channel. Note that Rayleigh fading is a special case

[2]We assume narrowband fading channels [59, 60] throughout this dissertation.

of the Rician fading for $K_r = 0$. Nakagami is the most general distribution for multipath fading, which is shown to be a good match in several environments [59]. The pdf of $G_{\text{MP}}(q)$ in case of a unit-average Nakagami multipath fading is given by $f_{G_{\text{MP}},\text{Nak}}(x) = \frac{m^m}{\Gamma(m)} x^{m-1} e^{-mx}$, where $\Gamma(.)$ represents the Gamma function and parameter m is referred to as the fading figure. For $m = 1$, Nakagami distribution reduces to Rayleigh, and for $m = \frac{(K_r+1)^2}{2K_r+1}$ it approximately reduces to Rician. Note that for Rayleigh, Rician and Nakagami multipath fading, the pdf of $G_{\text{MP,dB}}(q)$ can be calculated by a simple change of variable, using the pdf of $G_{\text{MP}}(q)$. Finally, some experimental measurements have shown log-normal to be a good enough yet simple fit for the distribution of $G_{\text{MP}}(q)$, in which case the pdf of $G_{\text{MP,dB}}(q)$ is given as follows: $f_{G_{\text{MP,dB}},\text{norm}}(x) = \frac{1}{\sqrt{2\pi}\omega} e^{\frac{-x^2}{2\omega^2}}$, with $\omega^2 = \mathbb{E}\{G^2_{\text{MP,dB}}(q)\}$ denoting the power of the multipath component in the dB domain.

Characterizing the spatial correlations of $G_{\text{SH,dB}}(q)$ and $G_{\text{MP,dB}}(q)$ is also important, specially for channel prediction purposes. As for the spatial correlation of multipath fading, there is no single model that can be a good match for different environments.[3] Due to the lack of a general model, in this paper we assume independent multipath fading components, i.e., for any two $q_1, q_2 \in \mathcal{W}$, if $q_1 \neq q_2$ then $G_{\text{MP,dB}}(q_1)$ and $G_{\text{MP,dB}}(q_2)$ are taken independent (and therefore uncorrelated). The spatial correlation of shadowing is more important as it stays correlated over larger distances. In the communication literature, this correlation is typically modeled with an exponential function [59]: $\mathbb{E}\{G_{\text{SH,dB}}(q_1)G_{\text{SH,dB}}(q_2)\} = \vartheta^2 e^{-\frac{\|q_1-q_2\|}{\beta}}$, for all $q_1, q_2 \in \mathcal{W}$. Here, the *decorrelation distance*, β, controls how correlated the channel is spatially. In the wireless communication literature, the value of β is reported between 10 m and 50 m for outdoor environments [59]. A typical range for ϑ, on the other hand, is between 4 dB and 13 dB [59].

[3] If the environment is rich in scatterers and the antenna has an isotropic angle of arrival, for instance, the Fourier transform of the auto-correlation function of multipath fading, $G_{\text{MP}}(q)$, will have a form that is referred to as Jakes' spectrum [59].

It is important to note that the probabilistic models introduced for channel power is readily applicable to received SNR too. This is due to the fact that the instantaneous received SNR in transmission from a mobile sensor at position $q \in \mathcal{W}$ to the remote station is given by $\mathrm{SNR}(q) = \frac{P_{\mathrm{TX}}(q)G(q)}{BN_0}$, where $P_{\mathrm{TX}}(q)$ is the transmission (TX) power of the mobile sensor at position $q \in \mathcal{W}$, B is the transmission bandwidth and $\frac{N_0}{2}$ is the power spectral density (PSD) of the thermal noise at the receiver of the remote station. Since BN_0 is fixed, for a given transmission power the probabilistic models of $\mathrm{SNR}(q)$ and $G(q)$ are the same.

Next, we show how each mobile sensor can probabilistically assess/predict the spatial variations of the channel power at unvisited locations, using a small number of channel power measurements.[4] Note that since the channel to the remote station is time-invariant, the delay in the communication among the mobile sensors, in the case of cooperative channel assessment, does not make the communicated information obsolete. Also, we emphasize that we are not suggesting that a wireless channel is fully predictable, as it is not. That is why instead of trying to capture and learn all the underlying dynamics of the channel, our proposed framework is aimed at probabilistically assessing the channel. As a result, our assessment of channel spatial variations is not going to be perfect, unless several measurements are gathered, but will be informative for the communication-aware motion planning, as we will see in next chapters.

[4]In this dissertation, we assume symmetric uplink and downlink channels, i.e., the channel from a mobile sensor to the remote station is taken identical to the one from the remote station to the mobile sensor. This is the case, for instance, if both transmissions occur in the same frequency band and are separated using Time Division Duplexing (TDD). If uplink and downlink use different frequency bands, then we assume that a few uplink channel measurements are sent back to the mobile sensor, using a feedback channel, as is common in the communication literature [59]. These uplink measurements then form the basis of uplink channel assessment.

2.2 Probabilistic Channel Assessment Based on a Small Number of Channel Measurements

In this section, we show how each mobile sensor can predict the spatial variations of the channel at unvisited locations based a small number of channel measurements. Let $\mathcal{M}_{k,t} = \{q_{k,t,\ell}\}_{\ell=1}^{m_{k,t}}$, for $m_{k,t} = |\mathcal{M}_{k,t}|$, denote the (possibly time-varying) set of the positions corresponding to the small number of channel power measurements available to the k^{th} mobile sensor at time instant t. These measurements can be gathered by the mobile sensor along its trajectory during the operation, gathered and communicated to it by other sensors (with similar receivers) operating in the same environment, or collected *a priori*. Consider negligible receiver thermal noise power, as compared to the received signal power, such that a mobile sensor can measure the received channel power with good accuracy. The stacked vector of the received channel power measurements (in dB), available to the k^{th} mobile sensor at time instant t, can then be expressed by

$$Y_{k,t} = \underbrace{\begin{bmatrix} 1 & -10\log_{10}\left(\|q_{k,t,1} - q_b\|\right) \\ \vdots & \vdots \\ 1 & -10\log_{10}\left(\|q_{k,t,m_{k,t}} - q_b\|\right) \end{bmatrix}}_{H_{k,t}} \theta + \underbrace{\begin{bmatrix} G_{\text{SH,dB}}(q_{k,t,1}) \\ \vdots \\ G_{\text{SH,dB}}(q_{k,t,m_{k,t}}) \end{bmatrix}}_{\Xi_{k,t}} + \underbrace{\begin{bmatrix} G_{\text{MP,dB}}(q_{k,t,1}) \\ \vdots \\ G_{\text{MP,dB}}(q_{k,t,m_{k,t}}) \end{bmatrix}}_{\Omega_{k,t}}, \tag{2.3}$$

where $\theta = [K_{\text{dB}} \quad n_{\text{PL}}]^{\text{T}}$ denote the vector of path loss parameters. Based on the introduced log-normal distribution for shadow fading and its exponential spatial correlation, $\Xi_{k,t}$ is a zero-mean Gaussian random vector with the covariance matrix $R_{k,t} \in \mathbb{R}^{m_{k,t} \times m_{k,t}}$, where $\left[R_{k,t}\right]_{\ell_1,\ell_2} = \vartheta^2 \exp\left(-\frac{\|q_{k,t,\ell_1} - q_{k,t,\ell_2}\|}{\beta}\right)$, for $1 \leq \ell_1, \ell_2 \leq m_{k,t}$. We also assume log-normal multipath fading and a resulting Gaussian distribution for $\Omega_{k,t}$. Note that Rayleigh, Rician and Nakagami provide a better fit than log-normal in general. However, mathematical derivations of online channel assessment are easier

with a log-normal distribution. This over-simplification, however, is only for our modeling and assessment purposes. When we present our results in the subsequent section, multipath component of the considered channels has a Rician (or Nakagami) distribution. We also take the elements of $\Omega_{k,t}$ to be uncorrelated due to the following reasons. First, there is no one good model that characterizes the correlation of multipath fading in all the environments since its correlation depends on the angle of arrival as well as receiver antenna pattern. Second, multipath component typically decorrelates very fast, making adaptation to its changes infeasible. As a result, we take $\Omega_{k,t}$ to be a zero-mean Gaussian random vector with the covariance $\omega^2 I_{m_{k,t}}$, where ω^2 is the power of multipath fading component (in dB) and $I_{m_{k,t}}$ is the $m_{k,t}$-dimensional identity matrix.

The first step in our probabilistic channel assessment is to estimate the parameters of the underlying model (θ, ϑ, β and ω), based on the available measurements. We have the following theorem [6]:

Theorem 2.2.1. *Define $\alpha \triangleq \vartheta^2 + \omega^2$. Then, the least-square (LS) estimation of the channel parameters, at the k^{th} mobile sensor and at time t, are given as follows:*

$$\begin{aligned}
\hat{\theta}_{k,t} &= \left(H_{k,t}^{\mathrm{T}} H_{k,t}\right)^{-1} H_{k,t}^{\mathrm{T}} Y_{k,t}, \\
\hat{\alpha}_{k,t} &= \frac{1}{m_{k,t}} Y_{k,t,c}^{\mathrm{T}} Y_{k,t,c}, \\
\begin{bmatrix} \log(\hat{\vartheta}_{k,t}^2) \\ \hat{\beta}_{k,t}^{-1} \end{bmatrix} &= \left(X_{k,t}^{\mathrm{T}} W_{k,t} X_{k,t}\right)^{-1} X_{k,t}^{\mathrm{T}} W_{k,t} \hat{x}_{k,t}, \\
\hat{\omega}_{k,t}^2 &= \hat{\alpha}_{k,t} - \hat{\vartheta}_{k,t}^2,
\end{aligned} \tag{2.4}$$

where $Y_{k,t,c} = \left(I_{m_{k,t}} - H_{k,t}(H_{k,t}^{\mathrm{T}} H_{k,t})^{-1} H_{k,t}^{\mathrm{T}}\right) Y_{k,t}$ represents the centered version of the measurement vector, $\hat{r}_{k,t}(d) = \log\left(\frac{1}{|\mathcal{A}_{k,t}(d)|} \sum_{(\ell_1,\ell_2)\in\mathcal{A}_{k,t}(d)} \left[Y_{k,t,c}\right]_{\ell_1} \left[Y_{k,t,c}\right]_{\ell_2}\right)$, for non-empty $\mathcal{A}_{k,t}(d) = \left\{(\ell_1,\ell_2) \;\middle|\; q_{k,t,\ell_1}, q_{k,t,\ell_2} \in \mathcal{M}_{k,t}, \|q_{k,t,\ell_1} - q_{k,t,\ell_2}\| = d\right\}$, denotes the log of the numerical estimate of the spatial correlation at distance d, $\mathcal{B}_{k,t} =$

$\{d_1, \cdots, d_{|\mathcal{B}_{k,t}|}\} = \{d | 0 < e^{\hat{r}_{k,t}(d)} < \hat{\alpha}_{k,t}\}$, $X_{k,t} = \begin{bmatrix} 1 & -d_1 \\ \vdots & \vdots \\ 1 & -d_{|\mathcal{B}_{k,t}|} \end{bmatrix}$, $\hat{x}_{k,t} = \begin{bmatrix} \hat{r}_{k,t}(d_1) \\ \vdots \\ \hat{r}_{k,t}(d_{|\mathcal{B}_{k,t}|}) \end{bmatrix}$, $W_{k,t} = \text{diag}\{w(d_1), \cdots, w(d_{|\mathcal{B}_{k,t}|})\}$, *and* $w(d)$ *is an associated weight that can be chosen based on the assessment of the accuracy of the estimation of* $\hat{r}_{k,t}(d)$.

Proof. It is straightforward to confirm that $\hat{\theta}_{k,t}$ minimizes $\|Y_{k,t} - H_{k,t}\theta\|^2$. The LS estimate of α is then given by $\frac{1}{m_{k,t}}\big(Y_{k,t} - H_{k,t}\hat{\theta}_{k,t}\big)^{\mathrm{T}}\big(Y_{k,t} - H_{k,t}\hat{\theta}_{k,t}\big)$, which can be easily confirmed to be $\hat{\alpha}_{k,t} = \frac{1}{m_{k,t}} Y_{k,t,c}^{\mathrm{T}} Y_{k,t,c}$. Then, ϑ and β can be estimated by minimizing the square error between the log of the estimated spatial correlation ($\hat{r}_{k,t}(d)$) and the modeled spatial correlation ($\vartheta^2 e^{-d/\beta}$):

$$[\hat{\vartheta}^2_{k,t}, \hat{\beta}_{k,t}] = \underset{\vartheta^2, \beta > 0}{\text{argmin}} \sum_{d \in \mathcal{B}_{k,t}} w(d) \Big(\log\big(\vartheta^2 e^{-d/\beta}\big) - \hat{r}_{k,t}(d) \Big)^2. \tag{2.5}$$

Using the definition of $X_{k,t}$, $\hat{x}_{k,t}$ and $W_{k,t}$, we can write this optimization problem as follows:

$$[\hat{\vartheta}^2_{k,t}, \hat{\beta}_{k,t}] = \underset{\vartheta^2, \beta > 0}{\text{argmin}} \left(X_{k,t} \begin{bmatrix} \log(\vartheta^2) \\ \beta^{-1} \end{bmatrix} - \hat{x}_{k,t} \right)^{\mathrm{T}} W_{k,t} \left(X_{k,t} \begin{bmatrix} \log(\vartheta^2) \\ \beta^{-1} \end{bmatrix} - \hat{x}_{k,t} \right). \tag{2.6}$$

It can then be easily confirmed that $\begin{bmatrix} \log(\hat{\vartheta}^2_{k,t}) \\ \hat{\beta}^{-1}_{k,t} \end{bmatrix} = \big(X_{k,t}^{\mathrm{T}} W_{k,t} X_{k,t}\big)^{-1} X_{k,t}^{\mathrm{T}} W_{k,t} \hat{x}_{k,t}$ minimizes the objective function of (2.6). Finally, given $\hat{\alpha}_{k,t}$ and $\hat{\vartheta}^2_{k,t}$, we have $\hat{\omega}^2_{k,t} = \hat{\alpha}_{k,t} - \hat{\vartheta}^2_{k,t}$. □

It should be noted that if the location of the fixed remote station is not known, path loss parameters can be estimated by finding the best line fit to the log of the received measurements. Then, α can be estimated by calculating the deviation from the estimated path loss curve, followed by estimating ϑ, β and ω as described in Theorem 2.2.1. Alternatively, the location of the remote station can also be added to the set of unknown parameters and jointly estimated.

Once the underlying channel parameters are estimated, the k^{th} mobile sensor can probabilistically assess the channel power, at an unvisited location, as given by the following theorem [6]:

Theorem 2.2.2. *Conditioned on the channel parameters (θ, β, ϑ and ω), a Gaussian distribution with mean $\hat{G}_{\text{dB},k,t}(q) = \mathbb{E}\big\{G_{\text{dB}}(q) \,\big|\, Y_{k,t}, \theta, \beta, \vartheta, \omega\big\}$ and variance $\sigma^2_{k,t}(q) = \mathbb{E}\Big\{\big(G_{\text{dB}}(q) - \hat{G}_{\text{dB},k,t}(q)\big)^2 \,\Big|\, Y_{k,t}, \theta, \beta, \vartheta, \omega\Big\}$ can best characterize the channel power at an unvisited position $q \in \mathcal{W} \setminus \mathcal{M}_{k,t}$, based on the measurements available to the k^{th} mobile sensor at time t. We then have*

$$\begin{aligned} \hat{G}_{\text{dB},k,t}(q) &= h^{\text{T}}(q)\,\theta + \phi^{\text{T}}_{k,t}(q) U^{-1}_{k,t}\big(Y_{k,t} - H_{k,t}\theta\big), \\ \sigma^2_{k,t}(q) &= \vartheta^2 + \omega^2 - \phi^{\text{T}}_{k,t}(q) U^{-1}_{k,t}\phi_{k,t}(q), \end{aligned} \tag{2.7}$$

where $\phi_{k,t}(q) = \Big[\vartheta^2\, e^{-\|q - q_{k,t,1}\|/\beta} \;\ldots\; \vartheta^2\, e^{-\|q - q_{k,t,m_{k,t}}\|/\beta}\Big]^{\text{T}}$, $h(q) = \big[1 \;\; -10\log_{10}\big(\|q - q_b\|\big)\big]^{\text{T}}$ *and* $U_{k,t} = R_{k,t} + \omega^2\, I_{m_{k,t}}$.

Proof. Consider variables $z_1 \in \mathbb{R}^{d_1}$ and $z_2 \in \mathbb{R}^{d_2}$ that are jointly Gaussian, with mean vectors μ_{z_1} and μ_{z_2}, covariance matrices Σ_{z_1} and Σ_{z_2}, and cross covariance matrix Σ_{z_1,z_2}. Then the conditional distribution of z_1 given z_2 is also Gaussian with mean vector $\mu_{z_1} + \Sigma_{z_1,z_2}\Sigma^{-1}_{z_2}(z_2 - \mu_{z_2})$ and covariance matrix $\Sigma_{z_1} - \Sigma_{z_1,z_2}\Sigma^{-1}_{z_2}\Sigma^{\text{T}}_{z_1,z_2}$ [87]. Setting $z_1 = G_{\text{dB}}(q)$, for $q \in \mathcal{W} \setminus \mathcal{M}_{k,t}$, and $z_2 = Y_{k,t}$ completes the proof. Note that $\hat{G}_{\text{dB},k,t}(q)$ represents the minimum mean-square error (MMSE) estimate of $G_{\text{dB}}(q)$. □

Note that Theorem 2.2.2 assumes perfect parameter estimation. The k^{th} mobile sensor then substitutes its estimated channel parameters of Theorem 2.2.1 to calculate $\hat{G}_{\text{dB},k,t}(q)$ and $\sigma^2_{k,t}(q)$. Throughout this dissertation, $\phi_{k,t,\text{est}}(q)$, $U_{k,t,\text{est}}$, $\hat{G}_{\text{dB},k,t,\text{est}}(q)$ and $\sigma^2_{k,t,\text{est}}(q)$ indicate the k^{th} sensor's assessment of $\phi_{k,t}(q)$, $U_{k,t}$, $\hat{G}_{\text{dB},k,t}(q)$ and $\sigma^2_{k,t}(q)$ respectively, when the exact channel parameters are replaced by their

estimated values. We consider the impact of parameter estimation error on the performance of channel assessment in the next section.[5]

Fig. 2.2 shows the reconstruction of a channel using our proposed channel assessment framework and based on a small number of *a priori* gathered measurements. The original channel is simulated using our probabilistic channel simulator [54], with the following parameters: $\theta = [-10 \quad 2.0]^{\mathrm{T}}$, $\vartheta = 4.0$ dB, $\beta = 20$ m, $\omega = 1.13$ dB (corresponding to a Rician distribution with parameter $K_r = 30$), and with uncorrelated multipath fading. A detailed description of this channel simulator can be found in [54, 56]. The total number of *a priori* gathered channel samples is 515, which is 0.5% of the grid size (the grid is 320×320). These measurements are randomly distributed over the workspace. The channel is then predicted in the rest of the workspace based on these measurements. The predicted channel is the mean of its probability distribution ($\hat{G}_{\mathrm{dB},k,t}(q)$ in Theorem 2.2.2), which is the MMSE estimate of the channel at an unvisited location. The average normalized mean-square error (ANMSE) of channel reconstruction is -29.55 dB in this example, which is calculated using the following formula at the k^{th} mobile sensor and at time t:

$$\mathrm{ANMSE}_{k,t} = \frac{1}{|\mathcal{W}|} \int_{\mathcal{W} \setminus \mathcal{M}_{k,t}} \frac{\left(\hat{G}_{\mathrm{dB},k,t,\mathrm{est}}(q) - G_{\mathrm{dB}}(q)\right)^2}{G^2_{\mathrm{dB}}(q)} \mathrm{d}q, \tag{2.8}$$

for $|\mathcal{W}|$ denoting the area of the workspace. While the number of channel measurements is considerably small, it can be seen that the trends of shadow fading and path loss are correctly assessed. However, since we considered uncorrelated multipath fading, rapid variations of the channel due to multipath could not be assessed.

In order to show the performance of the proposed channel assessment framework

[5] As we pointed out in Chapter 1, our channel assessment approach in Theorem 2.2.2 is conceptually similar to field estimation approaches based on kriging [19, 21, 61]. Kriging is a popular method for predicting the spatio-temporal variations of Gaussian random fields [19, 21, 61]. Our channel assessment approach can be considered an application of kriging for prediction of wireless channels.

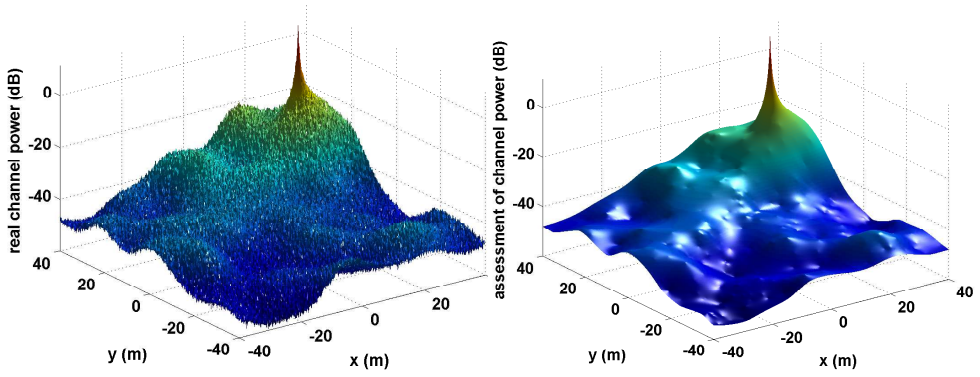

Figure 2.2: A simulated channel (left) and the mean of its probability distribution ($\hat{G}_{\mathrm{dB},k,t}(q)$ in Theorem 2.2.2) (right). The channel is simulated using our probabilistic channel simulator, with the following parameters: $\theta = [-10 \;\; 2.0]^{\mathrm{T}}$, $\vartheta = 4.0$ dB, $\beta = 20$ m and $\omega = 1.13$ dB (corresponding to a Rician distribution with parameter $K_r = 30$). The total number of *a priori* gathered channel samples is 515, which is 0.5% of the grid size (the grid is 320×320).

with real channels, Fig. 2.3 shows the reconstruction of two real channels using our channel assessment framework. The left figure shows an outdoor channel measurement across a street in downtown San Francisco (data is courtesy of Mark Smith [88]) with its reconstruction. The right figure, on the other hand, shows the reconstruction of an indoor channel measurement along a route in our basement. For both cases, the path loss parameters are estimated by finding the best line fit to the log of the received measurements. After subtracting the path loss term, the channel parameters are estimated using an approach similar to (2.4). The number of *a priori* channel measurements used for parameter estimation and reconstruction is 5% of the total samples for both channels. The channel observations are randomly distributed over the workspace. It can be seen that the outdoor channel can be reconstructed with a considerably better quality. This is expected as the indoor channel suffers from a more severe multipath fading, as can be seen. Fig. 2.4 shows the reconstruction performance as a function of the percentage of the measurements taken for the channels of Fig. 2.3. It can be seen that channel estimation performance improves as more measurements are collected.

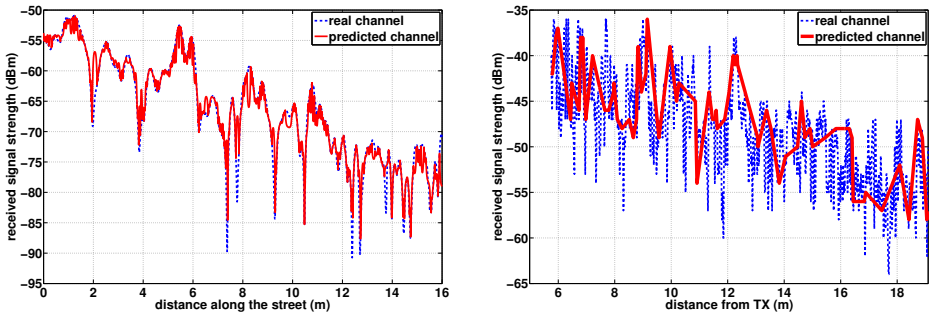

Figure 2.3: The received signal strength across a street in downtown San Francisco along with its reconstructed version (left) and an indoor received signal strength along a route in the basement of the ECE building at UNM and its reconstruction (right). The outdoor data is courtesy of Mark Smith. In both cases, the reconstruction is based on only 5% *a priori* channel measurements.

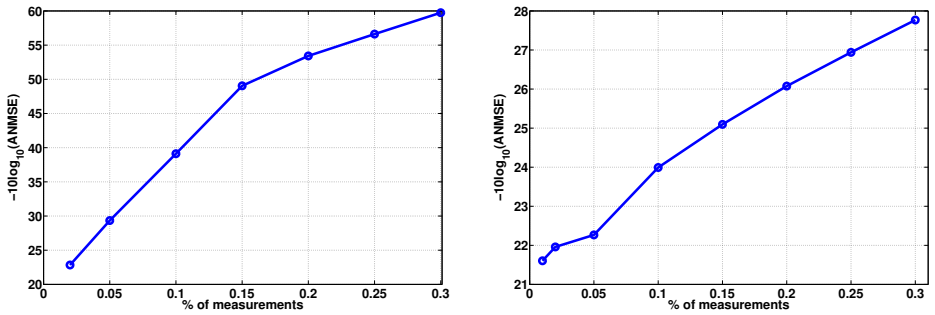

Figure 2.4: Channel prediction quality for the outdoor (left) and indoor (right) channels of Fig. 2.3, as a function of the percentage of the measurements gathered.

In the previous examples, we considered cases where the samples were randomly distributed over the workspace. Next, we consider a more realistic case where each mobile sensor measures the channel along its trajectory. Assume a scenario where a number of mobile sensors are tasked with cooperatively building a map of the spatial variations of a channel to a fixed remote station, as shown in Fig. 2.5. Each mobile sensor measures the channel along its trajectory and shares its observations with others for cooperative channel assessment (we assume each mobile sensor can communicate its measurements with all the other sensors during the operation). Fig. 2.5 (left) shows the trajectories of the mobile sensors superimposed on a 2D map of the channel power. The middle and right figures then show a snapshot of the true

channel power map and its estimate respectively, for the case where the total number of gathered samples is 350, which is 0.34% of the grid size (the grid is 320×320). The original channel is taken to be the same as in Fig. 2.2. In this case, the ANMSE of channel reconstruction is -25.3 dB, for all the mobile sensors.

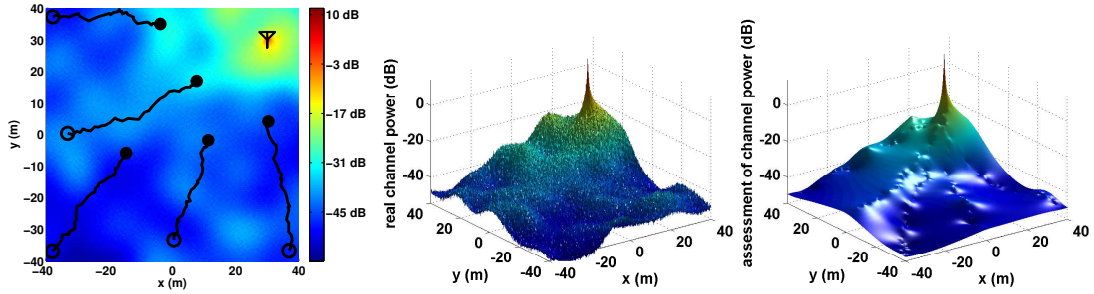

Figure 2.5: Performance of the channel assessment framework in a cooperative channel assessment scenario – trajectories of the mobile sensors (left), a snapshot of the true channel power map (middle) and the average of its probabilistic reconstruction using our framework ($\hat{G}_{\mathrm{dB},k,t}(q)$ in Theorem 2.2.2) (right). The empty circles and the filled ones in the left figure show the initial and final positions of the mobile sensors respectively. The original channel is the same as in Fig. 2.2. The total number of gathered samples is 350, which is 0.34% of the grid size.

Having an assessment of the spatial variations of the channel can be considerably valuable in maintaining the connectivity of the mobile sensors in a cooperative operation. In the following chapters, we show how each mobile sensor can use our proposed channel assessment framework in order to optimize its trajectory for communication-aware task accomplishment. More detailed discussion on our proposed channel assessment framework can be found in our recent paper [89].

2.3 Sensitivity of Channel Assessment to the Estimation Error of the Channel Parameters

In this section, we explore the impact of error in channel parameters on the overall channel assessment performance. Assume that estimated parameters are used for

the MMSE estimation of the channel in Theorem 2.2.2. For any $q \in \mathcal{W} \setminus \mathcal{M}_{k,t}$, we have

$$G_{\mathrm{dB}}(q) - \hat{G}_{\mathrm{dB},k,t,\mathrm{est}}(q) = h^{\mathrm{T}}(q)\tilde{\theta}_{k,t} + G_{\mathrm{SH,dB}}(q) + G_{\mathrm{MP,dB}}(q) \\ - \phi^{\mathrm{T}}_{k,t,\mathrm{est}}(q)U^{-1}_{k,t,\mathrm{est}}H_{k,t}\tilde{\theta}_{k,t} - \phi^{\mathrm{T}}_{k,t,\mathrm{est}}(q)U^{-1}_{k,t,\mathrm{est}}\big(\Xi_{k,t} + \Omega_{k,t}\big), \tag{2.9}$$

where $\tilde{\theta}_{k,t} = \theta - \hat{\theta}_{k,t}$. Let us define the following:

$$\Delta^2_{k,t}(q) \triangleq \mathbb{E}\Big\{ \big(G_{\mathrm{dB}}(q) - \hat{G}_{\mathrm{dB},k,t,\mathrm{est}}(q)\big)^2 \;\Big|\; \theta, \vartheta, \beta, \omega, \hat{\theta}_{k,t}, \hat{\vartheta}_{k,t}, \hat{\beta}_{k,t}, \hat{\omega}_{k,t} \Big\}. \tag{2.10}$$

By conditioning on both the estimated and real parameters and using the fact that

$$\mathbb{E}\Big\{ \big(G_{\mathrm{SH,dB}}(q) + G_{\mathrm{MP,dB}}(q)\big)\big(\Xi_{k,t} + \Omega_{k,t}\big) \;\Big|\; \vartheta, \beta, \omega \Big\} = \phi_{k,t}(q), \\ \mathbb{E}\Big\{ \big(\Xi_{k,t} + \Omega_{k,t}\big)\big(\Xi_{k,t} + \Omega_{k,t}\big)^{\mathrm{T}} \;\Big|\; \vartheta, \beta, \omega \Big\} = U_{k,t}, \\ \mathbb{E}\Big\{ \big(G_{\mathrm{SH,dB}}(q) + G_{\mathrm{MP,dB}}(q)\big)^2 \;\Big|\; \vartheta, \beta, \omega \Big\} = \vartheta^2 + \omega^2, \tag{2.11}$$

we obtain:

$$\Delta^2_{k,t}(q) = \vartheta^2 + \omega^2 - \phi^{\mathrm{T}}_{k,t,\mathrm{est}}(q)U^{-1}_{k,t,\mathrm{est}}\Big[2\phi_{k,t}(q) - U_{k,t}U^{-1}_{k,t,\mathrm{est}}\phi_{k,t,\mathrm{est}}(q)\Big] \\ + \Big[h(q) - H^{\mathrm{T}}_{k,t}U^{-1}_{k,t,\mathrm{est}}\phi_{k,t,\mathrm{est}}(q)\Big]^{\mathrm{T}}\tilde{\theta}_{k,t}\,\tilde{\theta}^{\mathrm{T}}_{k,t}\Big[h(q) - H^{\mathrm{T}}_{k,t}U^{-1}_{k,t,\mathrm{est}}\phi_{k,t,\mathrm{est}}(q)\Big]. \tag{2.12}$$

Then, we have the following important question: *which parameters have the most impact on channel assessment?* While we leave the proof of this to our future work, we observed, from several channel assessments, that the channel assessment framework is most sensitive to the error in path loss estimation (mainly the slope error), which is also intuitive. Fig. 2.6 shows the impact of parameter estimation uncertainty on the overall channel assessment quality, where the spatial average of $\Delta^2_{k,t}(q)$, i.e., $\frac{\int_{\mathcal{W}} \Delta^2_{k,t}(q)\mathrm{d}q}{|\mathcal{W}|}$ is plotted at a sample mobile sensor and for an indoor channel with the following parameters: $\theta = [-10 \;\; 2.0]^{\mathrm{T}}$, $\vartheta = 2.0$ dB, $\beta = 1.0$ m and $\omega = 2.78$ dB (corresponding to a Rician distribution with parameter $K_r = 5$). The number of available channel measurements is 0.1% of the total samples (102 measurements for

a 320×320 grid), with the measurements randomly distributed over the workspace. For each curve, only one parameter is perturbed while the rest are assumed perfect. It can be seen that channel assessment is considerably more sensitive to path loss parameters (specially the path loss exponent n_{PL}). As such, it becomes important to estimate the path loss parameters as accurately as possible. In the next section, we show how to do so by designing a proper motion planning objective function that is aimed at improving the estimation of path loss parameters.

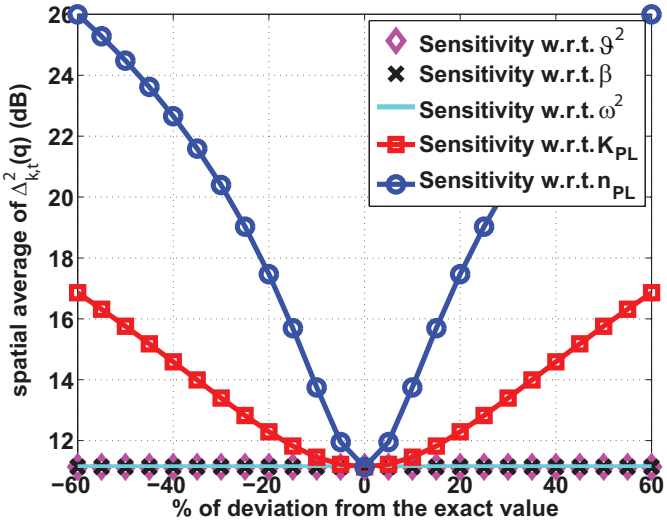

Figure 2.6: Spatial average of $\Delta^2_{k,t}(q)$, as a function of the % of estimation error in $\hat{\theta}_{k,t}$, $\hat{\vartheta}^2_{k,t}$, $\hat{\beta}_{k,t}$ and $\hat{\omega}_{k,t}$.

2.4 Motion Planning for Improving Wireless Channel Assessment in Mobile Networks

In this section, we show how each mobile sensor can use its mobility to improve its wireless channel assessment. Consider the case that a mobile sensor is assessing the spatial variations of its channel to a fixed remote station, using the channel measurements it collects along its trajectory, as discussed in the previous section.

Since the mobile sensor measures the channel along its trajectory, its motion directly impacts its channel assessment quality. In this section, we want to answer the following question: *How should a mobile sensor plan its trajectory in order to improve its channel assessment quality?* We first show how a mobile sensor can plan its trajectory in order to improve its estimate of the underlying channel parameters. This is then followed by planning the motion of a mobile sensor to decrease its channel assessment/prediction error variance.

Note that the motion planning approaches proposed in this section are greedy approaches, i.e., they choose the locally optimal choice at each step. Generally, a greedy approach does not guarantee finding the globally optimal solution which, in case of our motion planning approaches, is the solution of a highly-nonlinear optimal control problem. The reason we chose to use greedy approaches is twofold. First, solving an optimal control problem, with a highly-nonlinear objective and over a long time horizon, has a high computational complexity. Second, greedy approaches can easily support adaptation. In other words, the objective function can be modified at each step based on the newly gathered information. As shown in this section, such adaptation is in particular useful for our motion planning approaches as the proposed motion planning objective functions change based on the new channel measurements that the mobile sensors gather along their trajectories (and possibly share among each other).

2.4.1 Motion Planning for Improving the Estimation of the Underlying Channel Parameters

Our model for the spatial variations of the channel depends on the parameters θ, ϑ, β and ω, as discussed previously in this chapter. While the trajectory of a mobile sensor can be optimized to improve the estimation quality of all these parameters,

we saw in Section 2.3 that channel estimation is considerably more sensitive to the accuracy of the estimation of θ than the rest of the parameters. Therefore, in this part we devise a motion planning strategy that aims at improving the quality of the estimation of θ, assuming that the estimation error of the rest of the parameters is negligible. Consider the k^{th} mobile sensor in a multi-sensor scenario. Assume $m_{k,t} > 0$ channel measurements are available to the k^{th} mobile sensor at time instant t, as discussed previously in this chapter. Then, the mobile sensor needs to plan its trajectory such that the next channel measurement it gathers optimally improves its estimation of θ, as characterized by the next theorem. In this theorem, we consider the more challenging case of maximum likelihood (ML) estimation of the path loss parameters. The result can be easily modified for the simpler case of LS estimation.

Theorem 2.4.1. *Assume negligible error in the estimation of ϑ, β and ω. Let $C_{\text{ML},k,t}$ denote the error covariance of the ML estimation of the path loss parameters at the k^{th} mobile sensor and at time t, conditioned on shadowing and multipath parameters. Assume that the k^{th} mobile sensor gathers one more channel power measurement along its trajectory at time $t+1$. Then we have the following recursion for $C_{\text{ML},k,t}$:*

$$C^{-1}_{\text{ML},k,t+1} = C^{-1}_{\text{ML},k,t} + \frac{\left[h^{\text{T}}(\xi_{k,t+1}) - \phi^{\text{T}}_{k,t}(\xi_{k,t+1})U^{-1}_{k,t}H_{k,t}\right]^{\text{T}}\left[h^{\text{T}}(\xi_{k,t+1}) - \phi^{\text{T}}_{k,t}(\xi_{k,t+1})U^{-1}_{k,t}H_{k,t}\right]}{\sigma^2_{k,t}(\xi_{k,t+1})}, \tag{2.13}$$

where $\xi_{k,t+1}$ is the position of the j^{th} mobile sensor at time $k+1$.

Proof. Based on the probabilistic modeling of the previous section, the ML estimation of θ and its corresponding estimation error covariance, using the channel power measurements up to time $t+1$ and conditioned on ϑ, β and ω, are given as follows:

$$\begin{aligned}\hat{\theta}_{\text{ML},k,t+1} &= \left(H^{\text{T}}_{k,t+1}U^{-1}_{k,t+1}H_{k,t+1}\right)^{-1}H^{\text{T}}_{k,t+1}U^{-1}_{k,t+1}Y_{k,t+1},\\ C_{\text{ML},k,t+1} &= \left(H^{\text{T}}_{k,t+1}U^{-1}_{k,t+1}H_{k,t+1}\right)^{-1},\end{aligned} \tag{2.14}$$

where $U_{k,t+1} = \begin{bmatrix} \vartheta^2 + \omega^2 & \phi_{k,t}^{\mathrm{T}}\big(\xi_{k,t+1}\big) \\ \phi_{k,t}\big(\xi_{k,t+1}\big) & U_{k,t} \end{bmatrix}$ and $H_{k,t+1} = \big[h(\xi_{k,t+1}) \;\; H_{k,t}^{\mathrm{T}}\big]^{\mathrm{T}}$. Note that we take $\xi_{k,t+1} \notin \mathcal{M}_{k,t}$. By using matrix inversion lemma [90] for $U_{k,t+1}^{-1}$ we have:

$$U_{k,t+1}^{-1} = \begin{bmatrix} \frac{1}{\sigma_{k,t}^2(\xi_{k,t+1})} & \frac{\phi_{k,t}^{\mathrm{T}}(\xi_{k,t+1})U_{k,t}^{-1}}{\sigma_{k,t}^2(\xi_{k,t+1})} \\ \frac{U_{k,t}^{-1}\phi_{k,t}(\xi_{k,t+1})}{\sigma_{k,t}^2(\xi_{k,t+1})} & U_{k,t}^{-1} + \frac{U_{k,t}^{-1}\phi_{k,t}(\xi_{k,t+1})\phi_{k,t}^{\mathrm{T}}(\xi_{k,t+1})U_{k,t}^{-1}}{\sigma_{k,t}^2(\xi_{k,t+1})} \end{bmatrix} \tag{2.15}$$

where $\sigma_{k,t}^2\big(\xi_{k,t+1}\big) = \vartheta^2 + \omega^2 - \phi_{k,t}^{\mathrm{T}}\big(\xi_{k,t+1}\big)U_{k,t}^{-1}\phi_{k,t}\big(\xi_{k,t+1}\big)$. By multiplying $U_{k,t+1}^{-1}$ from left by $H_{k,t+1}^{\mathrm{T}}$ and from right by $H_{k,t+1}$, and by using the fact that $C_{\mathrm{ML},k,t}^{-1} = H_{k,t}^{\mathrm{T}}U_{k,t}^{-1}H_{k,t}$, (2.13) is obtained. □

Our proposed approach to minimize the estimation error covariance of θ in the next step is to have the k^{th} mobile sensor maximize the second term on the right hand side of (2.13) at any time t. Consider the following discrete dynamical model for the k^{th} mobile sensor: $\xi_{k,t+1} = \Upsilon_k(\xi_{k,t}, u_{k,t})$, where $u_{k,t} \in \mathcal{U}_k$ is the control input at time t, $\mathcal{U}_k$ is the set of admissible control inputs and $\Upsilon_k(.,.)$ is a known function. We then have the following next-step motion optimization problem, considering the trace of the right hand side of (2.13):

$$\begin{aligned} u_{k,t}^* &= \underset{u_{k,t}}{\operatorname{argmax}}\; J_{\mathrm{PL},k,t}(\xi_{k,t+1}) \triangleq \frac{\big\|h^{\mathrm{T}}(\xi_{k,t+1}) - \phi_{k,t,\mathrm{est}}^{\mathrm{T}}(\xi_{k,t+1})U_{k,t,\mathrm{est}}^{-1}H_{k,t}\big\|^2}{\sigma_{k,t,\mathrm{est}}^2(\xi_{k,t+1})} \\ &\text{s.t. 1) } \xi_{k,t+1} = \Upsilon_k\big(\xi_{k,t}, u_{k,t}\big),\ 2)\ u_{k,t} \in \mathcal{U}_k,\ 3)\ \xi_{k,t+1} \in \mathcal{W} \setminus \mathcal{O}_{k,t}, \end{aligned} \tag{2.16}$$

where $\phi_{k,t,\mathrm{est}}(q)$, $U_{k,t,\mathrm{est}}$ and $\sigma_{k,t,\mathrm{est}}^2(q)$ are the estimates of $\phi_{k,t}(q)$, $U_{k,t}$ and $\sigma_{k,t}^2(q)$, with the shadowing and multipath parameters replaced by their estimated values. Also, $\mathcal{O}_{k,t}$ denotes the set of forbidden areas for obstacle/collision avoidance, estimated by the k^{th} mobile sensor at time t.

Note that we do not consider coordination among the mobile sensors when planning their motion in (2.16). However, the sensors can share their gathered channel measurements and their positions as they move. The shared information can be used

by each mobile sensor in two ways. First, it can can combine these measurements with its own measurements to estimate the channel parameters and plan its motion more efficiently. In this case, the set $\mathcal{M}_{k,t}$ includes the positions of the channel measurements of the k^{th} mobile sensor as well as the positions of the channel measurements it has received from the other sensors up to time t. Second, the current positions of the other sensors at time t (included in $\mathcal{M}_{k,t}$) can be used to avoid collisions with other sensors more efficiently by estimating more precise $\mathcal{O}_{k,t}$. The resulting motion planner, however, does not change its form when the channel measurements are shared among the mobile sensors. More specifically, only the sets $\mathcal{M}_{k,t}$ and $\mathcal{O}_{k,t}$ change.

Fig. 2.7 shows the performance of the motion planner of (2.16) in an indoor environment that has obstacles (denoted by gray areas). A mobile sensor starts with no *a priori* channel measurement in this environment. It then solves for its next position by locally optimizing (2.16) in a small area around its current position. In this example, the dynamical model of the mobile sensor is given by the first-order system $\xi_{t+1} = \xi_t + u_t$, where $\|u_t\| \leq 1.75$ (1.75 is the radius of the local search area which is the maximum velocity times the sampling time interval of the discretized system). Here, we dropped index k since there is only one sensor. The left and right figures show the trajectory of the mobile sensor and its normalized path loss estimation error variance respectively. The indoor channel is simulated with the same parameters of Fig. 2.6. Note that the ratio of the power of the uncorrelated part of the channel (ω^2) to the correlated part (ϑ^2) is relatively high in this example, in order to simulate a typical indoor environment that is rich in multipath. The right figure also compares the performance with the case where the mobile sensor has a random trajectory (the random case is averaged over 50 runs). It can be seen that we gain considerably (around 10dB) by using the motion optimization framework of (2.16). Next, we continue with proposing a motion planning approach for directly improving the channel prediction error variance.

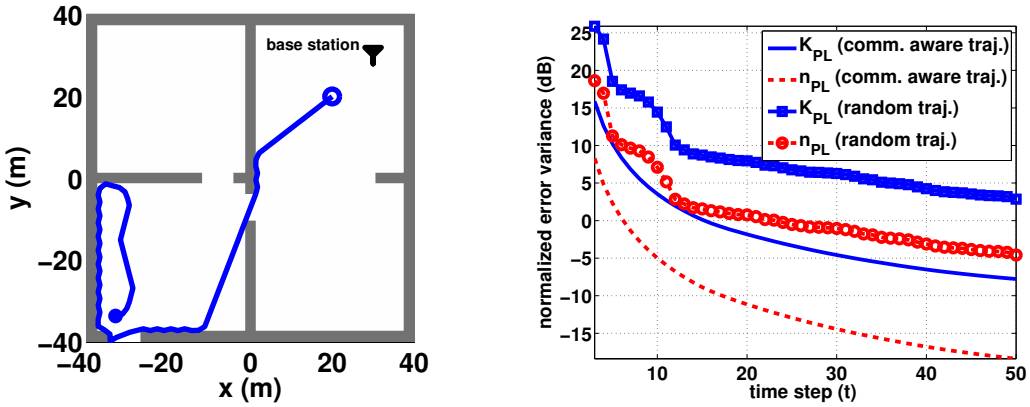

Figure 2.7: Trajectory of a mobile mobile sensor in communication-aware motion planning for improving path loss parameter estimation in an indoor environment (left) and the corresponding normalized estimation error variance (right). The empty circle and the filled one in the left figure denote the initial and final positions of the mobile sensor.

2.4.2 Motion Planning for Reducing the Channel Assessment Uncertainty

Once the parameters of the underlying model are estimated, the mobile sensor can plan its trajectory in order to reduce its channel assessment/prediction uncertainty. As characterized in Theorem 2.2.2, the error variance of the channel assessment at the k^{th} mobile sensor at time t is as follows: $\sigma^2_{k,t}(q) = \vartheta^2 + \omega^2 - \phi^{\text{T}}_{k,t}(q) U^{-1}_{k,t} \phi_{k,t}(q)$, for any $q \in \mathcal{W} \setminus \mathcal{M}_{k,t}$ and assuming negligible error in the underlying parameters. Consider the case where a number of channel measurements are available to the k^{th} mobile sensor at time t. Then, the mobile sensor can plan its motion to go towards the location with the highest channel assessment uncertainty, i.e., the largest $\sigma^2_{k,t}(q)$, based on the available measurements.[6] Define the following objective function:

$$J_{\text{CH},k,t}(q) \triangleq \max\left\{0, \sigma^2_{k,t,\text{est}}(q) - \sigma^2_{\text{TH}}\right\} \psi\big(\|q - \xi_{k,t}\|\big), \tag{2.17}$$

where $\sigma^2_{k,t,\text{est}}(q)$ is the estimate of $\sigma^2_{k,t}(q)$, with the exact parameters replaced by the estimated ones, σ^2_{TH} is a fixed threshold and $\psi(.)$ is a non-increasing function

[6] Alternatively, the mobile sensor can plan its motion in order to minimize the spatial average of the channel assessment uncertainty over the entire workspace of interest [7].

of its argument. By thresholding $\sigma^2_{k,t,\mathrm{est}}(q)$, we remove the positions with negligible channel assessment uncertainty. Then, $\psi\big(\|q-\xi_{k,t}\|\big)$ weighs the remaining space based on closeness to the current position, favoring less movement. Let $q^*_{k,t}$ denote the maximizing argument of the $J_{\mathrm{CH},k,t}(q)$ over the workspace:

$$q^*_{k,t} \triangleq \underset{q\in\mathcal{W}\setminus\mathcal{M}_{k,t}\cup\mathcal{O}_{k,t}}{\operatorname{argmax}} J_{\mathrm{CH},k,t}(q) \tag{2.18}$$

Here, $q^*_{k,t}$ is an obstacle/collision free position with high channel assessment uncertainty, that is also close to the current position of the mobile sensor. If motion cost is not an issue, ψ can be chosen one. In our results, we take $\psi(d)=e^{-\zeta d}$, for $\zeta\geq 0$. The motion of the k^{th} mobile sensor at time t (the corresponding control input) is then the solution of the following optimization problem:

$$\begin{aligned} &u^*_{k,t} = \underset{u_{k,t}}{\operatorname{argmin}} \left\|\xi_{k,t+1}-q^*_{k,t}\right\| \text{ for } q^*_{k,t} = \underset{q\in\mathcal{W}\setminus\mathcal{M}_{k,t}\cup\mathcal{O}_{k,t}}{\operatorname{argmax}} J_{\mathrm{CH},k,t}(q) \\ &\text{s.t. 1) } \xi_{k,t+1}=\Upsilon_k\big(\xi_{k,t},u_{k,t}\big),\ 2)\ u_{k,t}\in\mathcal{U}_k,\ 3)\ \xi_{k,t+1}\in\mathcal{W}\setminus\mathcal{O}_{k,t}. \end{aligned} \tag{2.19}$$

As can be seen from (2.19), the motion of the k^{th} mobile sensor is planned based on its current estimate of the channel assessment error variance. Similar to motion planning for improving the estimation of the channel parameters, sharing the channel measurements and the positions of the mobile sensors can be useful in two ways. First, each mobile can combine these measurements with its own ones to assess the channel and plan its motion more efficiently. The extra channel measurements prevent the mobile sensor from visiting previously-explored areas by other sensors, which results in a much faster reduction in the overall channel assessment error variance. Second, the current positions of the other sensors at time t can be used to avoid collisions with other sensors by estimating a more precise $\mathcal{O}_{k,t}$. However, the form of the motion planner does not change by sharing the channel measurements and positions among the mobile sensors.

Fig. 2.8 shows the performance of this motion planning approach for a single mobile sensor in an outdoor environment with obstacles (denoted by gray areas),

where we assumed negligible error in the estimation of the modeling parameters. The dynamical model of the mobile sensor is given by $\xi_{t+1} = \xi_t + u_t$, where $\|u_t\| \leq 5.5$. The outdoor channel is simulated with the following parameters: $\theta = [-10 \quad 2]$, $\vartheta = 4$ dB, $\beta = 10.0$ m and $\omega = 2$ dB (for a Rician distribution with $K_r = 10$). Furthermore, $\sigma^2_{\text{TH}} = 4$ and $\zeta = 0.02$. The mobile sensor starts with 0.016% *a priori* channel measurements, randomly chosen in the space (0.016% of the total number of workspace samples, i.e., 16 measurements for a 320×320 grid). Fig. 2.8 (left) and (right) show the trajectory of the mobile sensor and the time evolution of ANMSE of the channel assessment respectively. For the sake of comparison, the right figure also compares the performance with the case where the mobile sensor has a random trajectory (the random case is averaged over 50 runs). It can be seen that channel assessment uncertainty reduces considerably as the mobile sensor intelligently plans its motion. In terms of computational complexity, solving the optimization problem of (2.19) at each step, for a 320×320 grid, took 2.4 seconds (on average) on a desktop with the Intel Core 2 vPro processor and 2 GB of RAM.

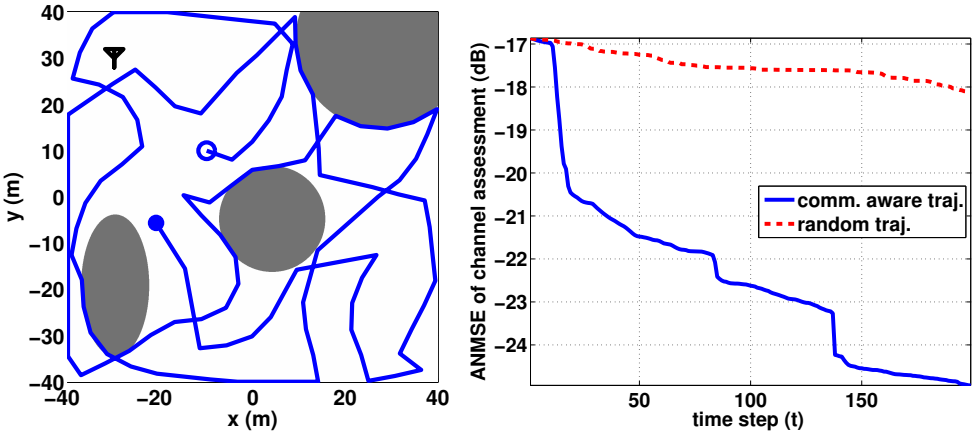

Figure 2.8: Trajectory of a mobile mobile sensor in communication-aware motion planning for reducing channel assessment uncertainty in an outdoor environment (left) and the corresponding ANMSE (right). The empty circle and the filled one in the left figure denote the initial and final positions of the mobile sensor.

Finally, Fig. 2.9 shows the snapshots of the spatial variations of the channel assessment error variance over the workspace and for four different time instants. It can be seen that channel prediction improves considerably with time, as the mobile sensor intelligently optimizes its motion accordingly.

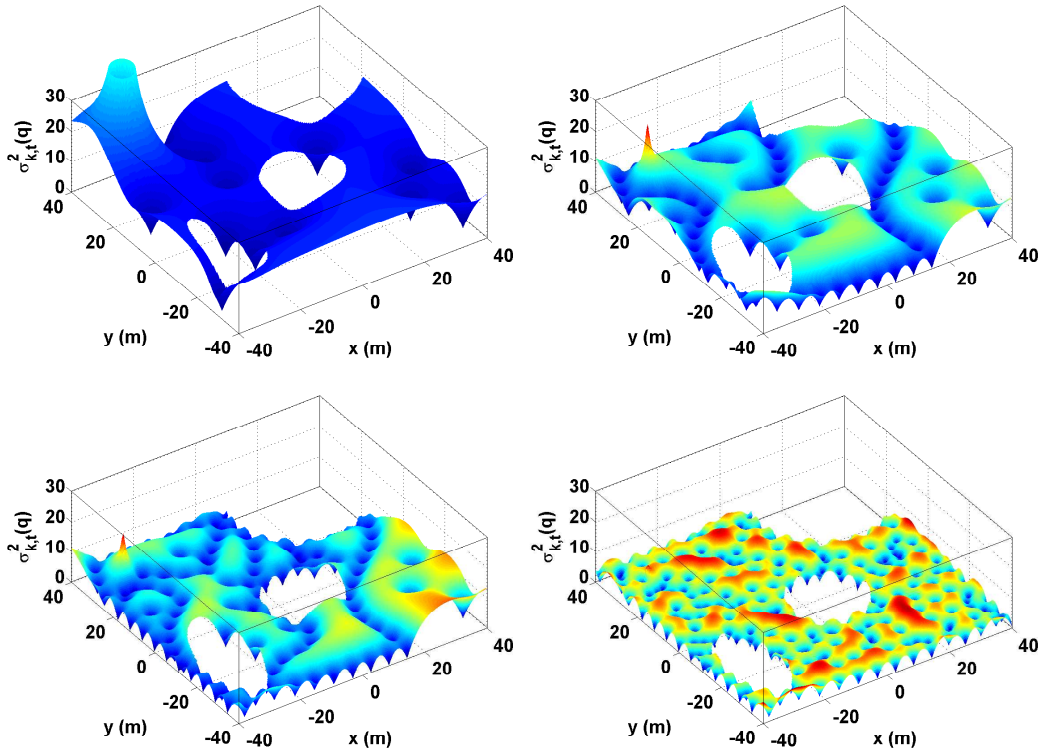

Figure 2.9: Snapshots of the channel assessment error variance over the workspace (top left for $t = 0$, top right for $t = 50$, bottom left for $t = 100$ and bottom right for $t = 200$)

2.5 Summary

In this chapter, we first showed how a mobile sensor can assess (predict) the spatial variations of a wireless channel based on a small number of channel measurements. We then showed how to plan motion of the mobile sensor to improve its channel assessment performance. Our proposed probabilistic channel assessment framework

is built on the well-established multi-scale model of wireless channels and enables a mobile sensor to efficiently predict the channel along its trajectory. To improve its channel assessment performance, the mobile sensor can then use one of the two proposed motion planning strategies of this chapter to either improve its estimate of the underlying model parameters or decrease the channel predication error variance.

In the following chapters, we show how the proposed channel assessment framework of this chapter can be integrated with motion planning in order to improve the connectivity of the mobile sensors while accomplishing their networked task.

Chapter 3

Communication-Aware Target Tracking Using Mobile Networks

In this chapter, we study the problem of networked target tracking in realistic communication environments. We consider the scenario where a fixed remote station utilizes a mobile sensor (or a number of them) for keeping track of the position of a moving target. The communication links between the mobile sensor and the remote station are realistic wireless link that experiences path loss, shadowing and multipath fading. We first characterize the estimation error covariance of target position at the remote station when 1) a realistic packet-dropping receiver is used at the remote station which drops the received packets based on the instantaneous received SNR and 2) a Kalman filter is used to fuse the received noisy sensory data at the remote station. This error covariance depends on both the sensing quality of the mobile sensors along their trajectories and the quality of their channels to the remote station. We then propose novel decentralized communication-aware motion planning approaches that integrate sensing and communication objectives to minimize the estimation error covariance of target position at the remote station. A schematic of the networked target tracking scenario considered in this chapter is shown in Fig.

3.1.

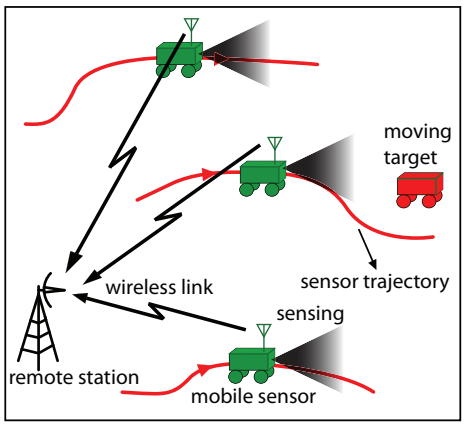

Figure 3.1: A schematic of the networked target tracking operation considered in this chapter.

Note that in order for the mobile sensors to assess the proposed objective functions (or constrains) at positions that have not yet been visited by any mobile sensor, the channel assessment framework of Chapter 2 is used. Also note that we do not consider any coordination among the nodes for the purpose of target tracking. In other words, each mobile sensor plans its motion individually. However, as explained in Section 2.4, the mobile sensors can still share their channel measurements and their positions in order to assess the channel and avoid collisions more efficiently. Finally, similar to the motion planning approaches of Section 2.4, the proposed motion planning approaches of this chapter are greedy to avoid high computational complexity and better facilitate adaptation.

The rest of the chapter is organized as follows. In Section 3.1, we describe our system model and present the Kalman filtering equations for target tracking over realistic communication links. In Section 3.2, we propose our communication-aware motion planning approaches and mathematically analyze their performance. We present our simulation and experimental results in Section 3.3, followed by a summary of the chapter in Section 3.4.

3.1 Problem Formulation

Consider the case where a fixed remote station utilizes n mobile sensors for keeping track of a position of a moving target in a workspace $\mathcal{W} \subset \mathbb{R}^2$, which is assumed to be closed and convex [91]. The overall goal is for the station to constantly have a good assessment of the target position. The communication links between the mobile sensors and the base station experience path loss, shadowing and multipath fading. We consider a realistic packet-dropping receiver [6, 92] at the remote station, i.e., the remote station drops all the packets with the received SNR (or equivalently the received channel power) below a predefined threshold. Note that in practice, the receiver drops the packets based on the quality of decoding. However, in [93], the authors show that this is equivalent to having a received SNR threshold. Let $\mathrm{SNR}_{\mathrm{TH}}$ denote this SNR threshold. Then, the received packet from the k^{th} mobile sensor is dropped at time t if $\mathrm{SNR}(\xi_{k,t}) < \mathrm{SNR}_{\mathrm{TH}}$, and is kept otherwise. Here, $\mathrm{SNR}(q)$ is the received SNR at the remote station when mobile sensor is at position $q \in \mathcal{W}$. Without loss of generality, assume that all the mobile sensors use a fixed transmit power P_{TX}. From Chapter 2, for any $q \in \mathcal{W}$ we have $\mathrm{SNR}(q) = \frac{P_{\mathrm{TX}} G(q)}{B N_0}$, where B is the transmission bandwidth and $\frac{N_0}{2}$ is the power spectral density (PSD) of the thermal noise at the receiver of the remote station. Then, $\mathrm{SNR}(\xi_{k,t}) < \mathrm{SNR}_{\mathrm{TH}}$ results in

$$G_{\mathrm{dB}}(\xi_{k,t}) < 10 \log_{10} \left(\frac{\mathrm{SNR}_{\mathrm{TH}} B N_0}{P_{\mathrm{TX}}} \right) \triangleq G_{\mathrm{dB,TH}}, \tag{3.1}$$

where $G_{\mathrm{dB,TH}}$ is the equivalent packet dropping threshold for channel power in dB (see Chapter 2 for more details).

Let us define $x_t \triangleq \left[p_t^{\mathrm{T}} \;\; \dot{p}_t^{\mathrm{T}} \right]^{\mathrm{T}}$, with $p_t \in \mathbb{R}^2$ and $\dot{p}_t \in \mathbb{R}^2$ denoting the position and velocity of the target respectively at time t. Also, let $y_{k,t} \in \mathbb{R}^2$ represent the measurement of the k^{th} mobile sensor of x_t at time t. We consider the following

dynamical and observation models [94]:

$$x_{t+1} = \underbrace{\begin{bmatrix} I_2 & t_s I_2 \\ 0 & I_2 \end{bmatrix}}_{A} x_t + \underbrace{\begin{bmatrix} \frac{1}{2} t_s^2 I_2 \\ t_s I_2 \end{bmatrix}}_{B} w_t, \quad y_{k,t} = \underbrace{\begin{bmatrix} I_2 & 0 \end{bmatrix}}_{C} x_t + v_{k,t}, \tag{3.2}$$

where t_s is the sampling period used to discretize the dynamics of the target, $w_t \in \mathbb{R}^2$ and $v_{k,t} \in \mathbb{R}^2$ are zero-mean Gaussian noises, with $W = \mathbb{E}\{w_k w_k^{\mathrm{T}}\}$ and $V_{k,t} = \mathbb{E}\{v_{k,t} v_{k,t}^{\mathrm{T}}\}$ representing their covariance matrices respectively, and I_2 is the 2×2 identity matrix. Note that $V_{k,t}$ depends on the position of the k^{th} mobile sensor as well as the position of the target [7, 94]: $V_{k,t} = \Phi(\xi_{k,t}, p_t)$, where $\Phi(.,.)$ is assumed known.

The remote station constantly estimates the position of the target, based on its received observations and by using a Kalman filter. We assume that when the received packet from a mobile sensor is kept at the remote station, it is error-free. This is the case when $\mathrm{SNR}_{\mathrm{TH}}$ is large enough. We therefore consider the following assumption throughout the rest of this chapter:

Assumption 3.1.1. *The packet-dropping threshold* $\mathrm{SNR}_{\mathrm{TH}}$ *is large enough, or equivalently the performance of the decoding algorithm at the remote station is good enough, such that the packets that are kept at the remote station can be considered error-free.*

Note that Assumption 3.1.1 is a valid for a large class of existing receivers used in robotics and sensor network applications. Now, let $\hat{x}_{t_1|t_2}$ represent the estimate of x_{t_1} at the remote station, using all the received observations up to and including time t_2. Also, let $\Pi_{t_1|t_2}$ denote the corresponding estimation error covariance at the remote station, given $G_{\mathrm{dB}}(\xi_{k,0}), \cdots, G_{\mathrm{dB}}(\xi_{k,t_2})$, for $t_2 \leq t_1$ and $k = 1, \cdots, n$. Assuming i.i.d. observations and based on Assumption 3.1.1, the Kalman filter equations for

estimating x_t is given as follows [95]:

$$\begin{aligned}
\hat{x}_{t+1|t} &= A\,\hat{x}_{t|t},\\
\Pi_{t+1|t} &= A\Pi_{t|t}A^{\mathrm{T}} + BWB^{\mathrm{T}},\\
\hat{x}_{t+1|t+1} &= \hat{x}_{t+1|t} + \Pi_{t+1|t}\overline{C}^{\mathrm{T}}\big(\overline{C}\Pi_{t+1|t}\overline{C}^{\mathrm{T}} + \overline{V}_{t+1}\big)^{-1}\big(\overline{y}_{t+1} - \overline{C}\hat{x}_{t+1|t}\big),\\
\Pi_{t+1|t+1} &= \Pi_{t+1|t} - \Pi_{t+1|t}\overline{C}^{\mathrm{T}}\big(\overline{C}\Pi_{t+1|t}\overline{C}^{\mathrm{T}} + \overline{V}_{t+1}\big)^{-1}\overline{C}\Pi_{t+1|t},
\end{aligned} \tag{3.3}$$

where $\overline{C} \triangleq \big[C^{\mathrm{T}} \cdots C^{\mathrm{T}}\big]^{\mathrm{T}}$ is the matrix of the stacked observation matrices of all the mobile sensors, $\overline{y}_{t+1} \triangleq \big[y_{1,t+1}^{\mathrm{T}} \cdots y_{n,t+1}^{\mathrm{T}}\big]^{\mathrm{T}}$ is the vector of stacked observations of the mobile sensors and $\overline{V}_{t+1} = \mathrm{diag}\left(\frac{V_{1,t+1}}{\lambda_{1,t+1}}, \cdots, \frac{V_{n,t+1}}{\lambda_{n,t+1}}\right)$. Here, the binary variable $\lambda_{k,t}$ captures the effect the packet-dropping receiver of the remote station and is defined as follows:

$$\lambda_{k,t} \triangleq \begin{cases} 1, & G_{\mathrm{dB}}(\xi_{k,t}) \geq G_{\mathrm{dB,TH}},\\ 0, & \text{else} \end{cases} \tag{3.4}$$

Using the definition of $\overline{V}_{t+1}$, one can see that whenever the received packet from the k^{th} mobile sensor is dropped at time $t+1$, its corresponding diagonal block in $\overline{V}_{t+1}$ becomes infinite, which implies that the observation of the k^{th} mobile sensor does not contribute to the estimation process at that time. This becomes more clear by using the information form of the Kalman filters [95]. Let us define the Fisher information matrix as $\Gamma_{t_1|t_2} \triangleq \Pi_{t_1|t_2}^{-1}$. Then, by using the information form of Kalman filter, which is a direct result of applying the matrix inversion lemma, a recursion for $\Gamma_{t|t}$ is given as follows:

$$\begin{aligned}
\Gamma_{t+1|t} &= \Big(A\Gamma_{t|t}^{-1}A^{\mathrm{T}} + BWB^{\mathrm{T}}\Big)^{-1},\\
\Gamma_{t+1|t+1} &= \Gamma_{t+1|t} + \sum_{k=1}^{n} \underbrace{\lambda_{k,t+1}C^{\mathrm{T}}V_{k,t+1}^{-1}C}_{\triangleq\Lambda_{k,t+1}},
\end{aligned} \tag{3.5}$$

where $\Lambda_{k,t+1}$ is the information contribution of the k^{th} mobile sensor at time $t+1$. As can be seen, the Fisher information at the remote station will be dictated by

the dynamics of the target as well as the summation of the information contribution terms, i.e., $\sum_{k=1}^{n} \Lambda_{k,t+1}$. Next we show how to plan the motion of the mobile sensors at each step to maximize the average Fisher information at the remote station.

3.2 Communication-Aware Target Tracking Using Probabilistic Assessment of Wireless Channels

The information innovation term $\Lambda_{k,t+1}$ in (3.5) depends on both the sensing quality of the k^{th} mobile sensor as well as its communication link quality to the remote station. Since our assessment of the link qualities is probabilistic, $\Lambda_{k,t+1}$ also becomes stochastic due to its dependency on the link qualities. By averaging over channel distributions, we have

$$\mathbb{E}\big\{\Gamma_{t+1|t+1}\big\} = \mathbb{E}\big\{\Gamma_{t+1|t}\big\} + \sum_{k=1}^{n} \mathbb{E}\big\{\Lambda_{k,t+1}\big\}, \tag{3.6}$$

where

$$\begin{aligned}\mathbb{E}\big\{\Lambda_{k,t+1}\big\} &= \mathbb{E}\big\{\lambda_{k,t+1}\big\} C^{\mathrm{T}} V_{k,t+1}^{-1} C \\ &= \mathbb{P}\Big\{G_{\mathrm{dB}}\big(\xi_{k,t+1}\big) \geq G_{\mathrm{dB,TH}}\Big\} C^{\mathrm{T}} V_{k,t+1}^{-1} C. \end{aligned} \tag{3.7}$$

In this equation, $\mathbb{P}\Big\{G_{\mathrm{dB}}\big(\xi_{k,t+1}\big) \geq G_{\mathrm{dB,TH}}\Big\}$ is the probability that the received packet from the k^{th} mobile sensor is kept at the remote station at time $t+1$. At any time t, the next step average Fisher information at the remote station is maximized if the k^{th} mobile sensor maximizes its assessment of $\mathbb{E}\big\{\Lambda_{k,t+1}\big\}$. The k^{th} mobile mobile sensor can assess $\mathbb{P}\Big\{G_{\mathrm{dB}}\big(\xi_{k,t+1}\big) \geq \Upsilon_{\mathrm{dB,TH}}\Big\}$ by using the channel assessment framework of Chapter 2 as follows:

$$\mathbb{P}\Big\{G_{\mathrm{dB}}\big(\xi_{k,t+1}\big) \geq G_{\mathrm{dB,TH}}\Big\} = Q\left(\frac{G_{\mathrm{dB,TH}} - \hat{G}_{\mathrm{dB},k,t,\mathrm{est}}(\xi_{k,t+1})}{\sigma_{k,t,\mathrm{est}}(\xi_{k,t+1})}\right), \tag{3.8}$$

where $Q(a) = \frac{1}{\sqrt{2\pi}} \int_a^\infty e^{-s^2/2} \mathrm{d}s$ is the Q-function (the tail probability of normal distribution). Also, $\hat{G}_{\mathrm{dB},k,t,\mathrm{est}}(q)$ and $\sigma_{k,t,\mathrm{est}}(q)$ are the estimates of $\hat{G}_{\mathrm{dB},k,t}(q)$ and $\sigma_{k,t}(q)$ respectively (see Theorem 2.2.2), with the exact parameters replaced by the estimated ones.

Our first proposed approach is to plan the motion of the mobile sensors at time t such that the trace of $\mathbb{E}\{\Gamma_{t+1|t+1}\}$ is maximized. This is equivalent to maximizing the trace of $\sum_{k=1}^{n} \mathbb{E}\{\Lambda_{k,t+1}\}$, which results in the following optimization problem for finding the control input of the k^{th} mobile sensor at time t:

$$u_{k,t}^* = \underset{u_{k,t}}{\operatorname{argmax}}\ J_{\mathrm{TRCK1},k,t}(\xi_{k,t+1}) \triangleq \underbrace{Q\left(\frac{G_{\mathrm{dB,TH}} - \hat{G}_{\mathrm{dB},k,t,\mathrm{est}}\big(\xi_{k,t+1}\big)}{\sigma_{k,t,\mathrm{est}}\big(\xi_{k,t+1}\big)}\right)}_{\text{Comm. obj.}} \times \underbrace{\mathrm{tr}\Big\{\Phi^{-1}\big(\xi_{k,t+1}, \hat{p}_{k,t+1|t}\big)\Big\}}_{\text{Sensing obj.}}$$

$$\text{s.t. 1) } \xi_{k,t+1} = \Upsilon_k\big(\xi_{k,t}, u_{k,t}\big),\ 2)\ u_{k,t} \in \mathcal{U}_k,\ 3)\ \xi_{k,t+1} \in \mathcal{W} \setminus \mathcal{O}_{k,t}. \tag{3.9}$$

Here, $\xi_{k,t+1} = \Upsilon_k(\xi_{k,t}, u_{k,t})$, for known $\Upsilon_k(.,.)$, denotes the dynamical model of the k^{th} mobile sensor, $u_{k,t} \in \mathcal{U}_k$ is the control input of the k^{th} mobile sensor at time t and $\mathcal{U}_k$ is the set of its admissible control inputs. Also, $\hat{p}_{k,t+1|t}$ is the prediction of the k^{th} mobile sensor of the target position at time $t+1$, which it can assess by using a local Kalman filter. The set $\mathcal{O}_{k,t}$ includes the forbidden positions that are excluded to avoid obstacles/collisions. The objective function of (3.9) shows how channel learning is integrated with sensing objectives in order to ensure communication-aware operation. A mobile sensor can start with *a priori* channel measurements in the environment for channel assessment. It then improves its channel assessment as it gathers more measurements along its trajectory, while simultaneously tracking the target using (3.9).

As can be seen, by using the trace of $\mathbb{E}\{\Gamma_{t+1|t+1}\}$, the overall objective of the next step information maximization at the remote station decouples into maximizing n

localized objective functions at the individual mobile sensors. In case other metrics are used (e.g. det(.) or $\|.\|$), the objective function may not be decentralizable, requiring coordination and sharing the position of the mobile sensors among them. Note that sharing the positions (and the channel measurements) is useful even when the decentralized motion planning approach of (3.9) is used. As explained in Section 2.4, each mobile sensor can use the channel measurements and the positions of the other sensors up to time t to better assess the channel. This makes the Q-function term in the objective function of (3.9) a more precise estimate of the probability of connectivity. Additionally, by using the current positions of other mobile sensors, the set $\mathcal{O}_{k,t}$ will be a more reliable set for collision avoidance.

Using the motion planning approach of (3.9), the mobile sensors improve their probability of connectivity while tracking the target. Next, we mathematically show that in case the channel is *assessed perfectly*, the motion planning approach of (3.9) maintain the connectivity of the mobile sensors. By perfect channel assessment we mean the following:

Definition 3.2.1. *Perfect channel assessment refers to the case where the channel is predicted perfectly. For instance, if the multipath fading power is negligible, the channel parameters are known perfectly and the number of channel measurements are large enough such that $\sigma_{k,t}(q) \to 0$, for all k, $q \in \mathcal{W}$ and $t \geq 0$, then the channel is predicted perfectly.*

We then have the following theorem in case of perfect channel assessment:

Theorem 3.2.1. *Assume that the channel is assessed perfectly. Define the time-invariant set $\mathcal{W}_c \triangleq \left\{q \in \mathcal{W} \middle| \hat{G}_{\mathrm{dB},k,t,\mathrm{est}}(q) \geq G_{\mathrm{dB,TH}}\right\}$ as the connected region, which is assumed to be closed. Then, if $\xi_{k,0} \in \mathcal{W}_c$ for all k, the motion planning approach of (3.9) maintain the connectivity of the mobile sensors, i.e., it ensures $\xi_{k,t} \in \mathcal{W}_c$ for all k and $t > 0$.*

Proof. In case the channel is assessed perfectly, the Q-function in (3.9) acts as a hard limiter and becomes one if $\xi_{k,t+1} \in \mathcal{W}_c$, and zero otherwise. Therefore, if $\xi_{k,t} \in \mathcal{W}_c$, the solution of (3.9) is a point $\xi_{k,t+1} \in \mathcal{W}_c$, which has this property that the k^{th} mobile sensor can be navigated to this point at time $t+1$, without any collision or violating the constraints imposed by its dynamics. This proves that if $\xi_{k,0} \in \mathcal{W}_c$, then $\xi_{k,t} \in \mathcal{W}_c$ for all $t > 0$. Note that we assumed that 1) $\mathcal{U}_k \ni 0$ and 2) when $u_{k,t} = 0$ then $\Upsilon_k\big(\xi_{k,t}, u_{k,t}\big) = \xi_{k,t}$. □

From Theorem 3.2.1, one can observe that in case of perfect channel assessment, the optimization problem of (3.9) is equivalent to the following:

$$u^*_{k,t} = \underset{u_{k,t}}{\operatorname{argmax}}\ \operatorname{tr}\Big\{\Phi^{-1}\big(\xi_{k,t+1}, \hat{p}_{k,t+1|t}\big)\Big\} \tag{3.10}$$
$$\text{s.t. 1) } \xi_{k,t+1} = \Upsilon_k\big(\xi_{k,t}, u_{k,t}\big),\ 2)\ u_{k,t} \in \mathcal{U}_k,\ 3)\ \xi_{k,t+1} \in \mathcal{W}_c \setminus \mathcal{O}_{k,t}.$$

In other words, in order to ensure communication-awareness in this case, it is sufficient to limit the motion of the mobile sensors to the connected region $\mathcal{W}_c$ and only consider the sensing objective. This motivates our second motion planning approach for communication-aware target tracking. In this approach, we limit the motion of the mobile sensors to the areas with good probability of connectivity. More specifically, we plan the motion of the k^{th} mobile sensor to guarantee that, if the channel is not assessed perfectly, $\mathbb{P}\Big\{G_{\text{dB}}\big(\xi_{k,t+1}\big) \geq G_{\text{dB,TH}}\Big\} \geq 1-\varepsilon$, for all k and an arbitrary small $0 < \varepsilon < 1$, while maximizing the trace of $C^{\text{T}} V^{-1}_{k,t+1} C$. This results in the following motion optimization problem to find the control input of the k^{th} mobile sensor at time t:

$$u^*_{k,t} = \underset{u_{k,t}}{\operatorname{argmax}}\ J_{\text{TRCK2},k,t}(\xi_{k,t+1}) \triangleq \underbrace{\operatorname{tr}\Big\{\Phi^{-1}\big(\xi_{k,t+1}, \hat{p}_{k,t+1|t}\big)\Big\}}_{\text{Sensing obj.}}$$
$$\text{s.t. 1) } \underbrace{Q\left(\frac{G_{\text{dB,TH}} - \hat{G}_{\text{dB},k,t,\text{est}}\big(\xi_{k,t+1}\big)}{\sigma_{k,t,\text{est}}\big(\xi_{k,t+1}\big)}\right) \geq 1-\varepsilon,}_{\text{Comm. constraint}}$$
$$2)\ \xi_{k,t+1} = \Upsilon_k\big(\xi_{k,t}, u_{k,t}\big),\ 3)\ u_{k,t} \in \mathcal{U}_k,\ 4)\ \xi_{k,t+1} \in \mathcal{W} \setminus \mathcal{O}_{k,t}. \tag{3.11}$$

It can be seen that in case of perfect channel assessment, (3.9) and (3.11) are equivalent and are reduced to (3.10).

We next continue with analyzing the convergence properties of the proposed motion planning approaches. We have the following theorem:

Theorem 3.2.2. *Consider the case where the channel is assessed perfectly. Assume that the collision among the mobile sensors is negligible. Let $\mathcal{O} \subset \mathcal{W}$ denote the open set of obstacles and define $\mathcal{W}_{c,f} \triangleq \mathcal{W}_c \setminus \mathcal{O}$ to be the obstacle-free connected region (obstacle-free region with $\hat{G}_{\mathrm{dB},k,t,\mathrm{est}}(q) \geq G_{\mathrm{dB,TH}}$). Assume that $\mathcal{W}_{c,f}$ is a closed set and $\xi_{k,0} \in \mathcal{W}_{c,f}$ for all k. Also, assume that the target is static and located at $p_0 \in \mathcal{W}$. Define the function $\varphi : \mathcal{W}_{c,f} \to \mathbb{R}_+$ such that $\varphi(q) = \mathrm{tr}\big\{\Phi^{-1}(q, p_0)\big\}$. Also, for any $q \in \mathbb{R}^2$, define the reachable set of the k^{th} sensor as $\mathcal{R}_k(q) \triangleq \big\{q' \in \mathbb{R}^2 \big| q' = \Upsilon_k(q, u), u \in \mathcal{U}_k\big\}$, which is assumed to be a closed and connected set (not to be confused with the connected region $\mathcal{W}_c$). Assume there exists an $r > 0$ such that $\mathcal{R}_k(q) \supseteq \mathcal{B}(q, r)$, where $\mathcal{B}(q, r)$ is the disk with radius r centered at $q \in \mathcal{W}_{c,f}$. Then, each mobile sensor converges to a local maximum of φ over $\mathcal{W}_{c,f}$ (which could be on the boundary of $\mathcal{W}_{c,f}$) using (3.9) or (3.11).*

Proof. As proved by Theorem 3.2.1, in case the collision among the mobile sensors is negligible and they start in $\mathcal{W}_{c,f}$, they will remain in $\mathcal{W}_{c,f}$ using (3.9) or (3.11). At each time t, the next position of the k^{th} sensor is found as follows: $\xi_{k,t+1} = \mathrm{argmax}_{q \in \mathcal{R}_{k,f}(q)} \mathrm{tr}\Big\{\Phi^{-1}\big(q, \hat{p}_{k,t+1|t}\big)\Big\}$, where $\mathcal{R}_{k,f}(q) \triangleq \mathcal{R}_k(q) \cap \mathcal{W}_{c,f}$. Since the target is stationary, each mobile sensor can asymptotically estimate the position of the target using its local Kalman filter, i.e., $\hat{p}_{k,t+1|t} \to p_0$. Also, since both $\mathcal{W}_{c,f}$ and $\mathcal{R}_k(q)$ are closed and $\mathcal{R}_k(q) \supseteq \mathcal{B}(q, r)$ for some $r > 0$, then there always exists a $\rho(q) > 0$ such that $\mathcal{R}_{k,f}(q) \supseteq \mathcal{B}\big(q, \rho(q)\big)$ for each $q \in \mathcal{W}_{c,f} \setminus \partial\mathcal{W}_{c,f}$, where $\partial\mathcal{W}_{c,f}$ denotes the boundary of $\mathcal{W}_{c,f}$ (note that $\mathcal{W}_{c,f}$ is a closed set). This ensures that the dynamics of the mobile sensor is such that it can move in any direction unless it hits the boundary of $\mathcal{W}_{c,f}$. Thus, it will eventually converge to a local maximum of $\varphi(q)$

over $\mathcal{W}_{c,f}$, which could be in $\mathcal{W}_{c,f} \setminus \partial\mathcal{W}_{c,f}$ or on the boundary $\partial\mathcal{W}_{c,f}$. □

Using Theorem 3.2.2, one can immediately conclude that if the smooth $\varphi(q)$ has a unique maximum and attains its global maximum inside $\mathcal{W}_{c,f}$, then the mobile sensors will eventually converge to this global maximum of $\varphi(q)$, provided that the conditions of Theorem 3.2.2 hold. Note that the condition $\mathcal{R}_k(q) \supseteq \mathcal{B}(q, r)$ in Theorem 3.2.2 guarantees that the mobile sensor can move in every direction at any point along its trajectory unless it is on the boundary of the workspace. In case the dynamical model of the mobile sensor limits its direction of the movement, convergence may not happen.

3.2.1 Discussion on Local Extrema Avoidance

Local extrema avoidance is an important issue in motion planning [28, 29]. Researchers have proposed several methods to design motion planners that can avoid local extrema. The approaches based on the well-known Navigation Functions, for instance, are good examples [29, 96].

In our proposed motion planning framework of this chapter, we solve the resulting optimization problems through a local greedy search (dictated by constraints 1 and 2 of (3.9) or constraints 2 and 3 of (3.11)). Thus, our framework naturally suffers from local extrema. Although, we emphasize that by enlarging the search space (if permitted computationally) and/or separating the optimization of the best next step from path planning, local extrema could be avoided. For instance, by enlarging the reachable set $\mathcal{R}_k(q)$ (defined in Theorem 3.2.2), we can lower the chance of getting trapped in a local extremum. In the extreme case where the workspace is obstacle-free, $\mathcal{W} \subseteq \mathcal{R}_k(q)$, the channel is assessed perfectly as $t \to \infty$, and the target is stationary, asymptotically the mobile sensors converge to the global maxima of $\varphi(q)$. There is, however, a constraint on the size of the reachable set of the mobile sensors.

Generally, the size of $\mathcal{R}_k(q)$ is dictated by the sampling period t_s and the dynamics of the k^{th} sensor. For a very small t_s the size of $\mathcal{R}_k(q)$ is small unless the mobile sensors can move very fast. So, the reachable sets should be chosen as larger as possible within the constraints imposed by the dynamics of the mobile sensors.

Also, note that the time variation of the objective function/constraints, due to the movement of the target and/or the new channel measurements gathered along the trajectory, is also a mechanism that may prevent the mobile sensors from being trapped in local extrema. This mechanism is specially useful in practical applications where the channel assessment is not perfect.

3.3 Simulation and Experimental Results

In this section, we present the results of applying the proposed communication-aware framework to two examples with simulated and real channels. For the sake of brevity, we use the motion optimization approach of (3.9) in these example. Similar behaviors can be observed if (3.11) is instead used.

Fig. 3.2 shows a target tracking scenario in an outdoor environment that contains obstacles (gray areas), using three mobile sensors. We use mobile agents with the following dynamics: $\xi_{k,t+1} = \xi_{k,t} + u_{k,t}$, for $\|u_{k,t}\| \leq 2.0$. We furthermore assume the position-dependent model of [7] for the observation noise covariance: $\text{tr}\big\{\Phi^{-1}(\xi_{k,t}, p_t)\big\} = \frac{1}{g(\|\xi_{k,t}-p_t\|)}$, where $g(r) = \varpi(r - r_s)^2 + \nu$, $\varpi > 0$ and $\nu > 0$ are scaling constants, and r_s is the sweet spot radius at which the sensing quality is the best. For this example we use $\varpi = 0.008$, $\nu = 0.08$ and $r_s = 1.0$ m. The outdoor channel is simulated using the following parameters: $\theta = [-10 \;\; 2.0]^{\text{T}}$, $\vartheta = 4.0$ dB, $\beta = 20$ m and $\omega = 1.13$ dB (corresponding to a Rician distribution with $K_r = 30$). Furthermore, $t_s = 0.5$ s, $W = 0.001 I_2$ and $G_{\text{dB,TH}} = -40$ dB. In order to compare the performance of our communication-aware framework with more traditional

approaches, the figure shows four different cases: 1) *comm-aware*, 2) *comm-aware (PL-only)*, 3) *informed disk model* and 4) *comm-unaware*. Comm-aware case is the full communication-aware framework of (3.9). On the other hand, comm-aware (PL-only) is a simplified yet probabilistic version of our framework where the correlation of the shadowing part is not utilized. In this case, the average of the channel is estimated by considering only the path loss parameters in (3.9) ($\hat{G}_{\mathrm{dB},k,t,\mathrm{est}}(q) = h^{\mathrm{T}}(q)\hat{\theta}_{k,t}$ in Theorem 2.2.2) and the variance is calculated accordingly. As we shall see from our results, this approach is more suitable for the cases where the environment is multipath dominant (experiencing a small ratio of the correlated channel component to the uncorrelated part). Informed disk model is the case where each mobile sensor models the link with a disk model (which is common in the robotics literature). However, it is a more informed approach, in which our channel assessment framework is utilized to assess the path loss decay rate. Then a disk is specified based on $G_{\mathrm{dB,TH}}$. Finally, the comm-unaware case is the case where each mobile sensor only considers its sensing objectives. Fig. 3.2 (left) shows the trajectories of the mobile sensors for comm-aware (solid magenta lines) and comm-unaware (dashed red lines) cases, superimposed on the connectivity map of the received channel power to the remote station, with the white (black) regions denoting the connected (disconnected) areas. For better visualization, we did not include the trajectories of the other two cases. The performance of all the four cases is then compared in Fig. 3.2 (right), where the trace of the average normalized error covariance of target position estimation at the remote station (averaged over 30 runs) is plotted as a function of time. It can be seen that the communication-aware case performs considerably better than the other approaches as it maintains the connectivity of the mobile sensors to the remote station with high probability. This is then followed by the performance of the PL-only case, informed disk model and the unaware case, as expected. Note that in all the cases, each mobile sensor solves for its corresponding next-step motion optimization problem locally, in a small area around it. Furthermore, in all the cases, the mobile

sensors start with 0.1% randomly-positioned *a priori* channel measurements in the environment (102 measurements for a 320×320 grid).

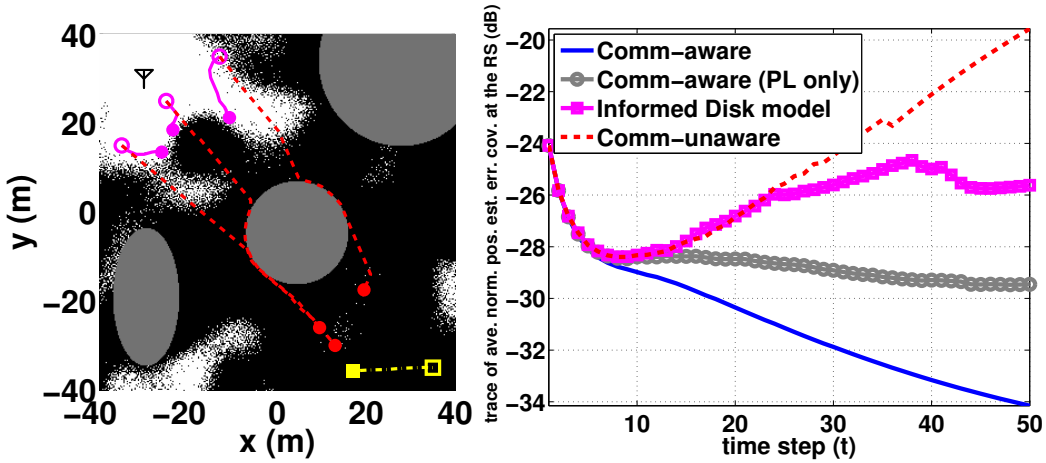

Figure 3.2: Performance of the proposed communication-aware target tracking framework in an outdoor environment – The left figure shows the trajectories of the mobile sensors and the target. The solid magenta and dashed red lines correspond to the trajectory of the mobile sensors in communication-aware and communication-unaware cases respectively, while the yellow dash-dot line represents the trajectory of the target. The empty circles/box and the filled ones show the initial and final positions of the mobile sensors/target respectively. The right figure compares the performance of four approaches, with different levels of communication-awareness, in terms estimation error covariance at the remote station (RS).

Fig. 3.3 compares the performance of the aforementioned four approaches in an indoor environment. In this case, the performance is simulated in a real environment in our building, in terms of channel measurements. The figure shows the blueprint of the basement of the Electrical and Computer Engineering building at the University of New Mexico, with the true connectivity map to the remote station superimposed on it. Aside from the underlying channel, all the other parameters are the same as for Fig. 3.2, except that we only have one mobile sensor with $\|u_{k,t}\| \leq 0.8$ and $G_{\text{dB,TH}} = -50$ dB. As can be seen, the aforementioned four approaches compare similar to Fig. 3.2. In this case, however, the performance of comm-aware (PL only) is very close to that of the comm-aware case since the ratio of the power of the correlated channel component to that of the uncorrelated part is lower ($\vartheta^2/\omega^2 = 1.13$

as compared to $\vartheta^2/\omega^2 = 13.22$ for Fig. 3.2) and the decorrelation distance is also smaller ($\beta = 0.32$ m as compared to $\beta = 20$ m for Fig. 3.2), as expected. Overall, the results indicate that networked robotic operations can benefit considerably from probabilistic channel assessment and the integration of communication and sensing objectives.

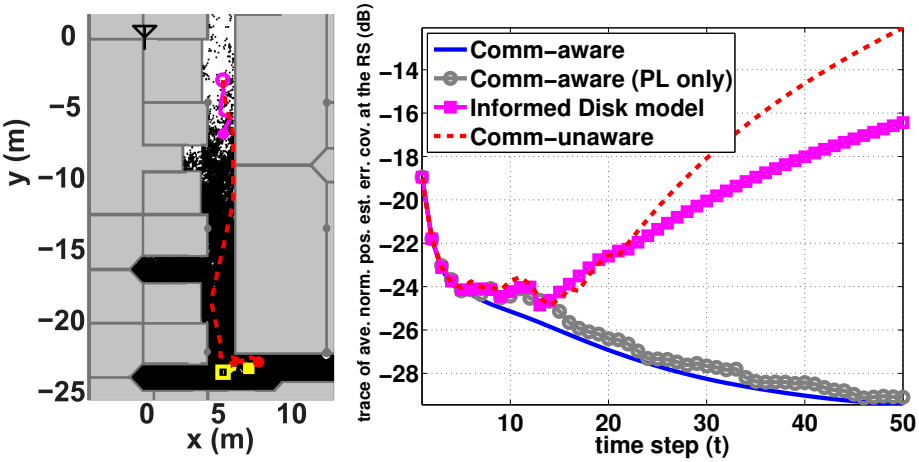

Figure 3.3: Performance of the proposed communication-aware target tracking framework in an indoor environment (basement of the Electrical and Computer Engineering building at the University of New Mexico) – The left figure shows the trajectories of the mobile sensor and the target (see the explanation of Fig. 3.2). The right figure compares the performance of four approaches, with different levels of communication-awareness, in terms estimation error covariance at the remote station (RS).

3.4 Summary

In this chapter, we proposed a communication-aware motion planning framework to remotely track a target in realistic communication environments, using a number of mobile sensors. We formulated the filtering equations in the presence of realistic communication links and a packet-dropping receiver at the remote station. By using the probabilistic channel assessment framework of Chapter 2, we then designed communication-aware motion planning approaches that properly combine sensing and communication objectives. Our proposed approaches plan the motion of mobile

sensors such that the increase in the Fisher information at the remote station is maximized. Finally, we showed the good performance of our framework, using both real and simulated channel measurements.

In the next chapter, we consider the problem of multi sensor surveillance using mobile sensor networks and develop a communication-aware data fusion and motion planning framework for surveillance in the presence of realistic fading channels.

Chapter 4

Communication-Aware Surveillance Using Mobile Networks

In this chapter, we build on the previous chapters to consider the case where the information is generated in a more complex manner in the environment. More specifically, we consider a networked surveillance operation where a number of mobile sensors/robots are deployed to survey an environment, for the possible presence of an unknown number of static (stationary) targets, and inform a remote station of their findings. We discretize the environment into several non-overlapping cells. The cells are assumed small enough, such that there exists at most one target in each cell. The mobile sensors detect the targets along their trajectories, using their collected sensory data. Each mobile sensor is equipped with an omni-directional sensor with a limited sensing range. The sensing quality within the sensing range also degrades as the distance to the sensor increases. To inform the remote station, the mobile sensors send fixed-size binary vectors, referred to as *target maps*, to the remote station. In a target map, a one (zero), at any element, indicates that the mobile sensor has

detected a target (or not) in the corresponding cell of the discretized version of the environment. Additionally, the communication links between the mobile sensors and the remote station are realistic narrowband communication channels that experience path loss, shadowing and multipath fading. The remote station then fuses the target maps received from the mobile sensors, by running its target detection algorithm, and builds a more reliable map of targets over the entire environment. Fig. 4.1 shows a schematic of the networked surveillance operation considered in this chapter.

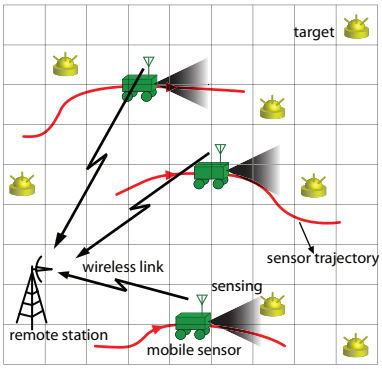

Figure 4.1: A schematic of the networked surveillance operation considered in this chapter.

In this chapter, we start with analyzing the impact of the trajectories of the mobile sensors and the resulting sensing and communication qualities on the probability of target detection error at the remote station. We then proceed with solving the main problem considered in this chapter, which is stated as follows: *How can each mobile sensor plan its trajectory such that it explores the environment and gathers as much information as possible regarding target locations, while maintaining the required connectivity to the remote station?*

Following the terminology of Chapter 3, we refer to such a motion design as communication-aware motion planning in this chapter. This is a challenging task that requires 1) evaluating the probability of connectivity to the remote station at unvisited locations and 2) co-optimization of sensing (information gathering) and communication (information exchange) through proper trajectory design.

In this chapter, we develop the mathematical framework of communication-aware motion planning for networked surveillance. As explained in Chapter 1, in the current literature on surveillance and exploration using robots/mobile sensors, the authors effectively consider the sensing objectives, i.e., goals that are aimed at maximizing the exploration and sensing performance of the mobile sensors when planning the motion. However, proper communication objectives, i.e., goals that are aimed at maximizing the probability of connectivity to the remote station, are not taken into account [15, 17, 19–21, 73, 75]. Most of the current works on the motion planning of mobile networks typically assume non-realistic communication links. For instance, it is common to assume either perfect links [15] or links that are perfect within a certain radius of a mobile sensor [97, 98], a significant over-simplification of communication channels. In this chapter, we extend our results on communication-aware motion planning for target tracking, presented in Chapter 3, to a surveillance scenario using mobile sensors. Our framework enables robust networked surveillance operation in realistic communication settings which is not possible using traditional communication-unaware approaches. The main contributions of this chapter are summarized as follows:

- The first key contribution of this chapter is introducing a communication-aware motion planning framework for networked surveillance. The proposed framework consists of two decentralized switching approaches to satisfy the requirements on the connectivity of the mobile sensors to the remote station. Our *communication-constrained* approach plans the motion of each mobile sensor such that it explores the workspace while maximizing its probability of connectivity to the remote station during the entire operation. This approach is appropriate for the case where the remote station needs to be constantly informed of the most updated map of the targets, which puts a constraint on the motion of the mobile sensors to constantly maintain their connectivity.

Constant connectivity, however, is not required if the mission is such that the remote station only needs to be informed of the map of the targets at the end of a given operation time. In this case, the mobile sensors can explore the environment with less connectivity constraints, provided that they get connected to and inform the remote station at the end of the given operation time. Our *hybrid* motion planning approach is then appropriate for this case. This approach builds on our communication-constrained one and allows the mobile sensors to explore the area more extensively than the communication-constrained approach, while maximizing their probability of connectivity at the end of the operation. Both approaches make use of the probabilistic channel assessment framework of Chapter 2 to predict the path loss and shadowing components of the channel at unvisited locations, based on a small number of channel samples that are collected online or *a priori*. A considerable part of this chapter is then dedicated to designing these two switching approaches, mathematically characterizing their asymptotic behaviors, and discussing their underlying trade-offs.

- Another important contribution of this chapter is proposing strategies to increase the robustness of the proposed communication-constrained and hybrid approaches to multipath fading. Such strategies are specially desired since multipath fading cannot be predicted efficiently using our channel assessment framework and, therefore, is a source of uncertainty.[1]

Similar to the previous chapter, we are not concerned with the interference among the mobile sensors. We assume that the number of mobile sensors is small enough, with respect to the available resources, such that each mobile sensor can have a pre-assigned slot for communication to the remote station. Similarly, we do not

[1]Multipath fading typically gets uncorrelated over small distances [59]. Thus, it cannot be predicted at unvisited locations based on a few spatial samples of the channel, as discussed in Chapter 2.

consider coordination among the mobile sensors when motion planning. Instead, each mobile sensor optimizes its motion locally, to maintain proper connectivity to the remote station, while exploring the area efficiently. We are also not concerned with obstacle/collision avoidance in this chapter. However, our framework can be extended to include obstacle avoidance, as we have considered such cases in Chapter 2 and 3. Also, similar to those chapters, the motion planning approaches proposed in this chapter are greedy with time-varying objective functions/constraints.

The rest of the chapter is organized as follows. In Section 4.1, we describe our sensing and communication models . In Section 4.2, we mathematically characterize the target detection quality of the mobile sensors and the remote station. This forms the base of our analysis for Section 4.3, where we introduce our communication-constrained and hybrid motion planning approaches. In Section 4.4, we propose strategies to increase the robustness of our motion planning approaches to multipath fading and other channel assessment errors. The performance of our approaches is analyzed mathematically in Section 4.5. We present our simulation and experimental results in Section 4.6, followed by a summary of the chapter in Section 4.7.

4.1 Problem Formulation

Consider a convex and closed [91] workspace $\mathcal{W} \subset \mathbb{R}^2$, which contains an unknown number of fixed targets that need to be detected. Let $\{\mathcal{W}_i\}_{i=1}^m$ denote a partition (or tessellation) of $\mathcal{W}$ into m non-overlapping subsets, such that $\bigcup_{i=1}^m \mathcal{W}_i = \mathcal{W}$ and $\mathcal{W}_i \cap \mathcal{W}_j = \emptyset$ for $i \neq j$. We refer to each $\mathcal{W}_i$ as a *cell* in this chapter. We assume small enough cells such that there exists at most one target in each cell. Furthermore, we assume that the events, corresponding to the presence of a target in different cells, are independent.

The remote station deploys n mobile sensors to detect the targets in $\mathcal{W}$. Each

mobile sensor k, for $k = 1, \cdots, n$, uses a local detection algorithm to fuse its gathered sensory data at any time t and update its binary target map. The target map of the k^{th} mobile sensor at time t refers to a binary vector $x_{k,t} = [x_{1,k,t} \cdots x_{m,k,t}]^{\text{T}}$, in which $x_{i,k,t} = 1$ (or $x_{i,k,t} = 0$) indicates that the mobile sensor has detected a target (or not) in the i^{th} cell, based on its observations up to time t. The mobile sensors then send their most updated maps to the remote station, over realistic wireless communication links that experience path loss, shadowing and multipath fading. The remote station fuses the most updated target maps received from the mobile sensors and builds its more reliable target map $x_{b,k} = [x_{1,b,k} \cdots x_{m,b,k}]^{\text{T}}$. The goal is for the remote station to obtain an accurate assessment of all the cells that contain the targets, using the information received from the mobile sensors as they move along their trajectories.

The trajectories of the mobile sensors affect both their sensing/exploration and communication link qualities, impacting the overall performance at the remote station. While some motion trajectories could result in the best sensing quality, they may not satisfy the constraints on connectivity of the mobile sensors to the remote station. Similarly, the trajectories that solely optimize connectivity may result in poor sensing/exploration quality and a resulting high probability of target detection error. Thus, the desired trajectories are the ones that combine sensing and communication objectives to satisfy the constraints on connectivity of the mobile sensors to the remote station, while improving the sensing quality of the mobile sensors, as we mathematically characterize in this chapter. Based on the requirement on the connectivity of the mobile sensors to the remote station, we propose two switching motion planning approaches, called communication-constrained and hybrid, to improve the performance of the remote station, in the presence of realistic fading channels. These two approaches are explained in details in Section 4.3.

Note that in case the distribution of the targets is known to be very sparse, instead of sending its whole target map, each mobile sensor can only send the difference

between its current map and the one that was last received by the remote station. This strategy saves power as the number of bits that need to be sent is smaller, compared to the case that the whole target map is sent. Proper compression techniques [99] can also be used to decrease the number of bits sent to the remote station. In either case, the proposed framework of this chapter is still valid and can be used with minor modifications. For the sake of simplicity, however, we assume that the mobile sensors send their whole binary maps without any compression.

4.1.1 Sensing and Dynamical Models of the Mobile Sensors

Assuming small enough cells, each cell i can be effectively represented by a single position $q_i \in \mathcal{W}_i$. We assume omni-directional onboard sensors such that a target in the i^{th} cell can be sensed by the k^{th} mobile sensor if $\|\xi_{k,t} - q_i\| < d_{\text{sen},k}$, where $\xi_{k,t}$ denotes the position of the k^{th} mobile sensor at time t and $d_{\text{sen},k}$ is its sensing radius. The time-varying set $\mathcal{S}_{k,t} = \big\{1 \leq i \leq m \;\big|\; \|\xi_{k,t} - q_i\| < d_{\text{sen},k}\big\}$, referred to as the sensing region or the footprint of the k^{th} mobile sensor, then contains the indices of all the cells that are in the sensing range of the k^{th} mobile sensor at time t.

Let hypothesis H_1 (H_0) refer to the case that there exists a target (there is no target) in a cell. Also, let $y_{i,k,t}$ represent the observation of the k^{th} mobile sensor of the i^{th} cell at time t, when $i \in \mathcal{S}_{k,t}$. Under hypotheses H_1 and H_0, the distribution of $y_{i,k,t}$ is given by two probability density functions $p(y_{i,k,t}|H_1)$ and $p(y_{i,k,t}|H_0)$, respectively. Note that $p(y_{i,k,t}|H_1)$ and $p(y_{i,k,t}|H_0)$ are time-varying functions that depend on the positions of the k^{th} mobile sensor and the i^{th} cell. A well-known example is the Gaussian observation model: $y_{i,k,t} = v_{i,k,t}$ under H_0, and $y_{i,k,t} = 1 + v_{i,k,t}$ under H_1, where $v_{i,k,t} \in \mathbb{R}$ is a zero-mean white Gaussian noise representing the effect of sensing error. The variance of $v_{i,k,t}$ is then given by $V_{i,k,t} = \Phi_k\big(\|\xi_{k,t} - q_i\|\big)$, where $\Phi_k(.)$ is a non-decreasing function of its argument [17, 73].[2]

[2]Our proposed framework is general in terms of the sensing model and does not pre-

As for the dynamics of the mobile sensors, we consider holonomic mobile sensors [100] with the following first order dynamics:[3] $\xi_{k,t+1} = \xi_{k,t} + u_{k,t}$, where $u_{k,t}$ is the motion control input of the k^{th} mobile sensor at time t. We assume $\|u_{k,t}\| \leq u_{\max,k}$, where $u_{\max,k}$ denotes the maximum step size of the k^{th} mobile sensor. We furthermore assume that the mobile sensors are small enough, compared to the dimension of the workspace, such that each mobile sensor can be considered a point in $\mathcal{W}$.

Note that it is straightforward to extend the result of this chapter to consider directional sensors. Similarly, more complicated non-holonomic and/or nonlinear dynamics can be used for the mobile sensors. We, however, consider the simpler case of omni-directional sensing models and holonomic dynamics to focus on the main purpose of this chapter which is communication-aware motion planning for networked surveillance.

4.1.2 The Communication Model and Probabilistic Characterization of Wireless Links

Each mobile sensor k updates the remote station on its current target map, at a number of points along its trajectory. In case of realistic communication settings, the remote station receives a corrupted version of the transmitted target map. Let $\text{SNR}_{k,t}$ denote the instantaneous received signal-to-noise ratio (SNR) in the transmission from the k^{th} mobile sensor to the remote station at time t. As explained in Chapter 2, we have $\text{SNR}_{k,t} = \frac{P_{\text{TX},k,t} G_{k,t}}{B N_0}$, where $P_{\text{TX},k,t}$ represents the transmission (TX) power of the k^{th} mobile sensor at time t, $G_{k,t} > 0$ is the channel power in the transmission from the k^{th} mobile sensor to the remote station at time t, B is the channel bandwidth

sume the validity of the Gaussian model. This model is, however, used extensively in our simulation results.

[3] By a holonomic mobile sensor, we refer to a mobile sensor whose degrees of freedom are all controllable, i.e., it can be controlled to move in any direction by changing its control input [100].

and $\frac{N_0}{2}$ is the power spectral density (PSD) of the receiver thermal noise [59]. Similar to Chapter 3, in this chapter we consider a packet-dropping receiver at the remote station, where a received packet from the k^{th} mobile sensor is kept if $\text{SNR}_{k,t} \geq \text{SNR}_{\text{TH}}$, for a fixed threshold SNR_{TH}, and is dropped otherwise. Then, at any time t, we refer to the k^{th} mobile sensor as connected (disconnected) if $\text{SNR}_{k,t} \geq \text{SNR}_{\text{TH}}$ ($\text{SNR}_{k,t} < \text{SNR}_{\text{TH}}$). To facilitate the mathematical derivations, we also assume that SNR_{TH} is large-enough such that the packets that are kept at the remote station can be assumed to be error-free.

As explained in Chapter 2, the channel power $G_{k,t}$ is a function of the position of the k^{th} mobile sensor at time t, i.e., $G_{k,t} = G(\xi_{k,t})$, where $G(q)$ denotes the channel power at position $q \in \mathcal{W}$. We consider realistic communication channels between the mobile sensors and the remote station, where $G(q)$ experiences path loss, shadowing and multipath fading. We model $G(q)$ probabilistically using the multi-scale non-stationary random process model introduced in Chapter 2. Each mobile sensor then uses its *a priori* collected channel samples to predict the channel at unvisited places, as discussed in Section 2.2. Refer to Chapter 2 for more details on probabilistic modeling of wireless channel. A plot of a real channel, measured along a route in the basement of the ECE building at UNM, is also shown in Fig. 2.1 of Chapter 2.

4.2 Multi-Sensor Surveillance in the Presence of Fading Channels

In order to find the optimum communication-aware motion decisions and characterize the underlying sensing and communication trade-offs, we need to first derive expressions for the detection performance of a mobile sensor and the remote station, at any time instant, as a function of channel and sensing qualities. In this section, we design

target detection algorithms, for both the mobile sensors and the remote station, and analyze their performance. In Section 4.2.1, a sequential detection algorithm is proposed for the mobile sensors. A target detection algorithm for the remote station is then introduced in Section 4.2.2, where the exact probability of error at the remote station, as well as its Chernoff bound, are characterized. Our derived expressions are then used in Section 4.3, when devising a framework for communication-aware surveillance.

4.2.1 Optimal Sequential Detection at Mobile Sensors

Let $0 \leq \pi_{i,0} \leq 1$ denote the prior probability that a target exists in the i^{th} cell, in the absence of any observation. Also, let $\mathcal{I}_{i,k,t} \triangleq \left\{1 \leq \ell \leq t \,\middle|\, i \in \mathcal{S}_{k,\ell}\right\}$ be the set of all the time instants, up to and including time t, when the i^{th} cell has been observed by the k^{th} mobile sensor. The k^{th} mobile sensor uses a maximum *a posteriori* (MAP) test to decide whether there exist a target in the i^{th} cell, based on its set of observations $\mathcal{Y}_{i,k,t} \triangleq \left\{y_{i,k,\ell} \,|\, \ell \in \mathcal{I}_{i,k,t}\right\}$. We have $x_{i,k,t} = 1$ if $p(H_1|\mathcal{Y}_{i,k,t}) > p(H_0|\mathcal{Y}_{i,k,t})$, and $x_{i,k,t} = 0$ otherwise, where $p(H_1|\mathcal{Y}_{i,k,t})$ and $p(H_0|\mathcal{Y}_{i,k,t})$ are the *a posteriori* probabilities of having a target or not in the i^{th} cell [87]. In the Bayesian paradigm, $p(H_1|\mathcal{Y}_{i,k,t}) = \frac{p(\mathcal{Y}_{i,k,t}|H_1)p(H_1)}{p(\mathcal{Y}_{i,k,t})}$ and $p(H_0|\mathcal{Y}_{i,k,t}) = \frac{p(\mathcal{Y}_{i,k,t}|H_0)p(H_0)}{p(\mathcal{Y}_{i,k,t})}$, where $p(H_1) = \pi_{i,0}$ and $p(H_0) = 1 - \pi_{i,0}$. Assuming i.i.d. observations, we can see that the MAP test is equivalent to the following likelihood ratio test (LRT) [87]:

$$\prod_{\ell \in \mathcal{I}_{i,k,t}} L_{i,k,\ell} \underset{x_{i,k,t}=0}{\overset{x_{i,k,t}=1}{\gtrless}} \frac{1 - \pi_{i,0}}{\pi_{i,0}}, \tag{4.1}$$

where $L_{i,k,\ell} = \frac{p(y_{i,k,\ell} \,|\, H_1)}{p(y_{i,k,\ell} \,|\, H_0)}$ is the likelihood ratio using observation $y_{i,k,\ell}$. This LRT can be also implemented in a sequential fashion as follows:

$$\begin{aligned} L_{i,k,t} &\underset{x_{i,k,t}=0}{\overset{x_{i,k,t}=1}{\gtrless}} \frac{1 - \pi_{i,k,t-1}}{\pi_{i,k,t-1}}, \\ \pi_{i,k,t} &= \frac{\pi_{i,k,t-1}\, L_{i,k,t}}{\pi_{i,k,t-1}\, L_{i,k,t} + 1 - \pi_{i,k,t-1}}, \end{aligned} \tag{4.2}$$

where $\pi_{i,k,t}$ denotes the updated posterior of the k^{th} mobile sensor, regarding the presence of a target in the i^{th} cell, using its observations up to time instant $t \geq 1$. Note that we set $\pi_{i,k,0} = \pi_{i,0}$ for $1 \leq k \leq n$. Also, in case $i \notin \mathcal{S}_{k,t}$, we set $L_{i,k,t} = 1$, which results in $\pi_{i,k,t} = \pi_{i,k,t-1}$. Finally, if the i^{th} cell has not been observed by the k^{th} mobile sensor for all the time instants $\ell \leq t$, i.e., $\mathcal{I}_{i,k,t} = \emptyset$, the decision regarding the presence of a target is made solely based on the value of the initial prior, i.e., $x_{i,k,t} = 1$ if $\pi_{i,0} > 0.5$, and $x_{i,k,t} = 0$ otherwise. More details on sequential likelihood ratio testing can be found in [87].

The performance of the local detectors of the mobile sensors is characterized by their detection, false-alarm and the corresponding error probabilities at each time instant. Let $\eta_{i,k,t}$, $\mu_{i,k,t}$ and $\gamma_{i,k,t}$ denote the detection, false-alarm and error probabilities of the k^{th} mobile sensor, for detection of a target in the i^{th} cell at time t. We have

$$\begin{aligned}
\eta_{i,k,t} &= \mathbb{P}\Big\{ \prod_{\ell \in \mathcal{I}_{i,k,t}} L_{i,k,\ell} > \frac{1-\pi_{i,0}}{\pi_{i,0}} \;\Big|\; H_1 \Big\}, \\
\mu_{i,k,t} &= \mathbb{P}\Big\{ \prod_{\ell \in \mathcal{I}_{i,k,t}} L_{i,k,\ell} > \frac{1-\pi_{i,0}}{\pi_{i,0}} \;\Big|\; H_0 \Big\}, \\
\gamma_{i,k,t} &= \pi_{i,0}(1-\eta_{i,k,t}) + (1-\pi_{i,0})\mu_{i,k,t}.
\end{aligned} \tag{4.3}$$

These probabilities can be characterized using the sensing model of the mobile sensor. Note that since $p(y_{i,k,t} \,|\, H_1)$ and $p(y_{i,k,t} \,|\, H_0)$ depend on the position of the k^{th} mobile sensor at time t, the probabilities $\eta_{i,k,t}$, $\mu_{i,k,t}$, and as a direct result $\gamma_{i,k,t}$, will be functions of the whole trajectory of the k^{th} mobile sensor from the beginning up to time t. To show this, consider the Gaussian observation model of Section 4.1.1. It is easy to confirm that in this case

$$\prod_{\ell \in \mathcal{I}_{i,k,t}} L_{i,k,\ell} = \prod_{\ell \in \mathcal{I}_{i,k,t}} \frac{\exp\left(-\frac{(y_{i,k,\ell}-1)^2}{2V_{i,k,\ell}}\right)}{\exp\left(-\frac{y_{i,k,\ell}^2}{2V_{i,k,\ell}}\right)} = \exp\left(\sum_{\ell \in \mathcal{I}_{i,k,t}} \frac{2y_{i,k,\ell}-1}{2V_{i,k,\ell}}\right). \tag{4.4}$$

Therefore, the detection probability in this case is given by

$$\eta_{i,k,t} = \mathbb{P}\left\{ \sum_{\ell \in \mathcal{I}_{i,k,t}} \frac{y_{i,k,\ell}}{V_{i,k,\ell}} > \log\left(\frac{1-\pi_{i,0}}{\pi_{i,0}}\right) + \sum_{\ell \in \mathcal{I}_{i,k,t}} \frac{1}{2V_{i,k,\ell}} \,\middle|\, H_1 \right\}. \tag{4.5}$$

Under hypothesis H_1, the distribution of $\sum_{\ell \in \mathcal{I}_{i,k,t}} \frac{y_{i,k,\ell}}{V_{i,k,\ell}}$ is given by a Gaussian distribution with mean $\sum_{\ell \in \mathcal{I}_{i,k,t}} \frac{1}{V_{i,k,\ell}}$ and variance $\sum_{\ell \in \mathcal{I}_{i,k,t}} \frac{1}{V_{i,k,\ell}}$. We therefore have

$$\begin{aligned} \eta_{i,k,t} &= Q\left(\frac{\log\left(\frac{1-\pi_{i,0}}{\pi_{i,0}}\right) - \frac{1}{2}\sum_{\ell \in \mathcal{I}_{i,k,t}} V_{i,k,\ell}^{-1}}{\sqrt{\sum_{\ell \in \mathcal{I}_{i,k,t}} V_{i,k,\ell}^{-1}}} \right) \\ &= Q\left(\frac{\log\left(\frac{1-\pi_{i,0}}{\pi_{i,0}}\right) - \frac{1}{2}\sum_{\ell \in \mathcal{I}_{i,k,t}} \Phi_k^{-1}\big(\|\xi_{k,\ell} - q_i\|\big)}{\sqrt{\sum_{\ell \in \mathcal{I}_{i,k,t}} \Phi_k^{-1}\big(\|\xi_{k,\ell} - q_i\|\big)}} \right) \end{aligned} \tag{4.6}$$

where $Q(.)$ is the Q-function (the tail probability of the Gaussian distribution). Similarly,

$$\mu_{i,k,t} = Q\left(\frac{\log\left(\frac{1-\pi_{i,0}}{\pi_{i,0}}\right) + \frac{1}{2}\sum_{\ell \in \mathcal{I}_{i,k,t}} \Phi_k^{-1}\big(\|\xi_{k,\ell} - q_i\|\big)}{\sqrt{\sum_{\ell \in \mathcal{I}_{i,k,t}} \Phi_k^{-1}\big(\|\xi_{k,\ell} - q_i\|\big)}} \right) \tag{4.7}$$

In the simpler case of $\pi_{i,0} = 0.5$ (no initial prior on the positions of the targets), this results in

$$\gamma_{i,k,t} = \mu_{i,k,t} = 1 - \eta_{i,k,t} = Q\left(\frac{1}{2}\sqrt{\sum_{\ell \in \mathcal{I}_{i,k,t}} \Phi_k^{-1}\big(\|\xi_{k,\ell} - q_i\|\big)} \right). \tag{4.8}$$

As can be seen, the target detection performance of each mobile sensor is a function of its entire trajectory. Finally, for the special case of $\mathcal{I}_{i,k,t} = \emptyset$, we have $\gamma_{i,k,t} = \min\big\{\pi_{i,0},\, 1-\pi_{i,0}\big\}$, as expected.

4.2.2 Optimal Detection at the Remote Station

Similar to Chapter 3, let us define the binary variable $\lambda_{k,t}$ as follows:

$$\lambda_{k,t} \triangleq \begin{cases} 1, & \mathrm{SNR}_{k,t} > \mathrm{SNR}_{\mathrm{TH}} \\ 0, & \text{otherwise} \end{cases} \tag{4.9}$$

Also, let $\tau_{k,t}$ denote the last time instant that the k^{th} mobile sensor was connected to the remote station, up to time $t \geq 1$:

$$\tau_{k,t} \triangleq \max \big\{ \{0\} \cup \{1 \leq \ell \leq t \mid \lambda_{k,\ell} = 1\} \big\}. \tag{4.10}$$

Note that since $t \geq 1$, we define $\tau_{k,t} = 0$ to indicate the case that the k^{th} mobile sensor has not been yet connected to the remote station up to time $t \geq 1$, i.e., $\lambda_{k,\ell} = 0$ for $\ell = 1, \cdots, t$. At any time instant, the remote station fuses the last received decisions of all the mobile sensors (if available), regarding the presence of a target in a cell. Let us define $\mathcal{K}_{i,t}$ as the set of the mobile sensors that have been connected to the remote station at least once up to time $t \geq 1$ and visited the i^{th} cell at least once before their last connection to the remote station.

$$\mathcal{K}_{i,t} \triangleq \left\{ 1 \leq k \leq n \;\middle|\; q_i \in \bigcup_{\ell=1}^{\tau_{k,t}} \mathcal{S}_{k,\ell},\ \tau_{k,t} \geq 1 \right\}. \tag{4.11}$$

Assuming independent received observations from the mobile sensors, we then have the following LRT at the remote station:[4]

$$\prod_{k \in \mathcal{K}_{i,t}} \widetilde{L}_{i,k,\tau_{k,t}} \underset{x_{i,b,t}=0}{\overset{x_{i,b,t}=1}{\gtrless}} \frac{1-\pi_{i,0}}{\pi_{i,0}}, \tag{4.12}$$

where $\widetilde{L}_{i,k,\tau_{k,t}}$ denotes the LR corresponding to the last received observation from the k^{th} mobile sensor and is given by the following at any time $1 \leq \ell \leq t$:

$$\widetilde{L}_{i,k,\ell} = \frac{p(\hat{x}_{i,k,\ell}|H_1)}{p(\hat{x}_{i,k,\ell}|H_0)} = \begin{cases} \frac{p(\hat{x}_{i,k,\ell}=1|H_1)}{p(\hat{x}_{i,k,\ell}=1|H_0)}, & \hat{x}_{i,k,\ell} = 1 \\ \frac{p(\hat{x}_{i,k,\ell}=0|H_1)}{p(\hat{x}_{i,k,\ell}=0|H_0)}, & \hat{x}_{i,k,\ell} = 0 \end{cases}, \tag{4.13}$$

where $\hat{x}_{i,k,\ell}$ denotes the decoded version of $x_{i,k,\ell}$ at the remote station. We have

$$\begin{aligned} &\frac{p(\hat{x}_{i,k,\ell}=1|H_1)}{p(\hat{x}_{i,k,\ell}=1|H_0)} \\ &\quad = \frac{p(\hat{x}_{i,k,\ell}=1|x_{i,k,\ell}=1)p(x_{i,k,\ell}=1|H_1) + p(\hat{x}_{i,k,\ell}=1|x_{i,k,\ell}=0)p(x_{i,k,\ell}=0|H_1)}{p(\hat{x}_{i,k,\ell}=1|x_{i,k,\ell}=1)p(x_{i,k,\ell}=1|H_0) + p(\hat{x}_{i,k,\ell}=1|x_{i,k,\ell}=0)p(x_{i,k,\ell}=0|H_0)} \\ &\quad = \frac{p(\hat{x}_{i,k,\ell}=1|x_{i,k,\ell}=1)\eta_{i,k,\ell} + p(\hat{x}_{i,k,\ell}=1|x_{i,k,\ell}=0)(1-\eta_{i,k,\ell})}{p(\hat{x}_{i,k,\ell}=1|x_{i,k,\ell}=1)\mu_{i,k,\ell} + p(\hat{x}_{i,k,\ell}=1|x_{i,k,\ell}=0)(1-\mu_{i,k,\ell})}. \end{aligned} \tag{4.14}$$

[4]We implicitly assume that the remote station is aware of the sensing model of the mobile sensors and can calculate their corresponding detection and false-alarm probabilities, using their instantaneous positions.

Using the assumption of large $\mathrm{SNR}_{\mathrm{TH}}$, the packets that are kept at the remote station are error-free. Therefore, $p(\hat{x}_{i,k,\ell}=1|x_{i,k,\ell}=1)=1$ and $p(\hat{x}_{i,k,\ell}=1|x_{i,k,\ell}=0)=0$. Then, $\frac{p(\hat{x}_{i,k,\ell}=1|H_1)}{p(\hat{x}_{i,k,\ell}=1|H_0)}=\frac{\eta_{i,k,\ell}}{\mu_{i,k,\ell}}$. Similarly, $\frac{p(\hat{x}_{i,k,\ell}=0|H_1)}{p(\hat{x}_{i,k,\ell}=0|H_0)}=\frac{1-\eta_{i,k,\ell}}{1-\mu_{i,k,\ell}}$, which results in

$$\widetilde{L}_{i,k,\ell}=\begin{cases}\frac{\eta_{i,k,\ell}}{\mu_{i,k,\ell}}, & \hat{x}_{i,k,\ell}=1\\ \frac{1-\eta_{i,k,\ell}}{1-\mu_{i,k,\ell}}, & \hat{x}_{i,k,\ell}=0\end{cases}, \tag{4.15}$$

Note that in case $\mathcal{K}_{i,t}=\emptyset$, we have $\prod_{k\in\mathcal{K}_{i,t}}\widetilde{L}_{i,k,\tau_{k,t}}=1$. Then $x_{i,b,t}=1$ if $\pi_{i,0}>0.5$, and $x_{i,b,t}=0$ otherwise.

Detection, false-alarm and error probabilities at the remote station, as functions of target detection performance of the mobile sensors and their channel to the remote station, are also very important to characterize. Let $\eta_{i,b,t}$, $\mu_{i,b,t}$ and $\gamma_{i,b,t}$ denote the detection, false-alarm and error probabilities at the remote station, for detection of a target in the i^{th} cell at time t. We have

$$\begin{aligned}\eta_{i,b,t}&=\mathbb{P}\left\{\prod_{k\in\mathcal{K}_{i,t}}\widetilde{L}_{i,k,\tau_{k,t}}>\frac{1-\pi_{i,0}}{\pi_{i,0}}\;\middle|\;H_1\right\},\\ \mu_{i,b,t}&=\mathbb{P}\left\{\prod_{k\in\mathcal{K}_{i,t}}\widetilde{L}_{i,k,\tau_{k,t}}>\frac{1-\pi_{i,0}}{\pi_{i,0}}\;\middle|\;H_0\right\},\\ \gamma_{i,b,t}&=\pi_{i,0}(1-\eta_{i,b,t})+(1-\pi_{i,0})\mu_{i,b,t}.\end{aligned} \tag{4.16}$$

Next, we show how to characterize these quantities.

4.2.3 Mathematical Characterization of the Performance at the Remote Station

The trajectories of the mobile sensors affect both their sensing (target detection) and communication qualities. In order to optimize the motion planning accordingly, we need to mathematically characterize the impact of both on the probability of error at the remote station. Let us define $\mathcal{B}_{i,t}\triangleq\left\{b=[b_1\;\cdots\;b_n]^{\mathrm{T}}\middle|\;b_k\in\{0,1\},\;b_k=\right.$

$0\ \forall k \notin \mathcal{K}_{i,t}\big\}$, with the size of $|\mathcal{B}_{i,t}| = 2^{|\mathcal{K}_{i,t}|}$. This set contains all the possible binary decisions of the mobile sensors of the i^{th} cell, up to the last time they were connected to the remote station (if $k \notin \mathcal{K}_{i,t}$, then the k^{th} mobile sensor will not cooperate in the decision making process at the remote station). By calculating the probability of occurrence of each member of $\mathcal{B}_{i,t}$, under the both hypotheses H_0 and H_1, and considering the cases where $\prod_{k\in\mathcal{K}_{i,t}} \widetilde{L}_{i,k,\tau_{k,t}} > \frac{1-\pi_{i,0}}{\pi_{i,0}}$, we get

$$\begin{aligned}
\eta_{i,b,t} = &\sum_{b\in\mathcal{B}_{i,t}} \left[\prod_{k\in\mathcal{K}_{i,t}} \eta_{i,k,\tau_{k,t}}^{b_k} \big(1-\eta_{i,k,\tau_{k,t}}\big)^{1-b_k} \right] \\
&\times \text{Heav}\left(\prod_{k\in\mathcal{K}_{i,t}} \left(\frac{\eta_{i,k,\tau_{k,t}}}{\mu_{i,k,\tau_{k,t}}}\right)^{b_k} \left(\frac{1-\eta_{i,k,\tau_{k,t}}}{1-\mu_{i,k,\tau_{k,t}}}\right)^{1-b_k} - \frac{1-\pi_{i,0}}{\pi_{i,0}} \right), \\
\mu_{i,b,t} = &\sum_{b\in\mathcal{B}_{i,t}} \left[\prod_{k\in\mathcal{K}_{i,t}} \mu_{i,k,\tau_{k,t}}^{b_k} \big(1-\mu_{i,k,\tau_{k,t}}\big)^{1-b_k} \right] \\
&\times \text{Heav}\left(\prod_{k\in\mathcal{K}_{i,t}} \left(\frac{\eta_{i,k,\tau_{k,t}}}{\mu_{i,k,\tau_{k,t}}}\right)^{b_k} \left(\frac{1-\eta_{i,k,\tau_{k,t}}}{1-\mu_{i,k,\tau_{k,t}}}\right)^{1-b_k} - \frac{1-\pi_{i,0}}{\pi_{i,0}} \right),
\end{aligned} \tag{4.17}$$

where Heav(.) denotes the Heaviside step function:

$$\text{Heav}(x) = \begin{cases} 1, & x > 0 \\ 0.5, & x = 0 \\ 0, & x < 0 \end{cases} \tag{4.18}$$

Also, as explained previously, the detection error probability $\gamma_{i,b,t}$ is calculated as follows:

$$\gamma_{i,b,t} = \pi_{i,0}(1-\eta_{i,b,t}) + (1-\pi_{i,0})\mu_{i,b,t}. \tag{4.19}$$

Similar to optimal detection at the mobile sensors, if $\mathcal{K}_{i,t} = \emptyset$, we have $\gamma_{i,b,t} = \min\big\{\pi_{i,0},\ 1-\pi_{i,0}\big\}$, as confirmed next. Using (4.17), we have $\eta_{i,b,t} = \mu_{i,b,t} = \text{Heav}\left(1 - \frac{1-\pi_{i,0}}{\pi_{i,0}}\right) = \text{Heav}\left(\pi_{i,0} - 0.5\right)$, for $\mathcal{K}_{i,t} = \emptyset$. Therefore,

$$\gamma_{i,b,t} = \pi_{i,0}\,\text{Heav}\left(-\pi_{i,0}+0.5\right) + (1-\pi_{i,0})\,\text{Heav}\left(\pi_{i,0}-0.5\right) = \min\big\{\pi_{i,0},\ 1-\pi_{i,0}\big\}. \tag{4.20}$$

Furthermore, for the special case where $\pi_{i,0} = 0.5$ (no initial prior) and $\mu_{i,k,\tau_{k,t}} = 1 - \eta_{i,k,\tau_{k,t}}$,[5] the detection error probability takes a more simplified form. First, consider the following lemma:

Lemma 4.2.1. *Let $\mathcal{B}$ denote the set of all the binary permutations of an n-dimensional binary vector b. Assume η_k, for $k = 1, \cdots, n$, denotes the probability that $b_k = 1$. Define*

$$\eta_b = \sum_{b\in\mathcal{B}} \left[\prod_{k=1}^{n} \eta_k^{b_k}(1-\eta_k)^{1-b_k}\right] \text{Heav}\left(\prod_{k=1}^{n}\left(\frac{\eta_k}{1-\eta_k}\right)^{2b_k-1} - 1\right).$$
$$\mu_b = \sum_{b\in\mathcal{B}} \left[\prod_{k=1}^{n} (1-\eta_k)^{b_k}\eta_k^{1-b_k}\right] \text{Heav}\left(\prod_{k=1}^{n}\left(\frac{\eta_k}{1-\eta_k}\right)^{2b_k-1} - 1\right). \tag{4.21}$$

Then, $\eta_b + \mu_b = 1$.

Proof. We have

$$\begin{aligned}\eta_b + \mu_b &= \sum_{b\in\mathcal{B}} \left[\prod_{k=1}^{n} \eta_k^{b_k}(1-\eta_k)^{1-b_k}\right] \\ &\quad \times \left[\text{Heav}\left(\prod_{k=1}^{n}\left(\frac{\eta_k}{1-\eta_k}\right)^{2b_k-1} - 1\right) + \text{Heav}\left(\prod_{k=1}^{n}\left(\frac{1-\eta_k}{\eta_k}\right)^{2b_k-1} - 1\right)\right] \\ &= \sum_{b\in\mathcal{B}} \left[\prod_{k=1}^{n} \eta_k^{b_k}(1-\eta_k)^{1-b_k}\right] = 1, \end{aligned} \tag{4.22}$$

where we used the fact that $\text{Heav}(x-1) + \text{Heav}(\frac{1}{x} - 1) = 1$. □

Using Lemma 4.2.1, we can immediately conclude that by setting $1 - \eta_{i,k,\tau_{k,t}} = \mu_{i,k,\tau_{k,t}}$ (for each mobile sensor) and $\frac{1-\pi_{i,0}}{\pi_{i,0}} = 1$ in (4.17), we have $\eta_{i,b,t} = 1 - \mu_{i,b,t}$ (the same relationship between the detection and false-alarm probabilities hold at the remote station). Therefore,

$$\gamma_{i,b,t} = \sum_{b\in\mathcal{B}_{i,t}} \left[\prod_{k\in\mathcal{K}_{i,t}} \eta_{i,k,\tau_{k,t}}^{1-b_k}\, \mu_{i,k,\tau_{k,t}}^{b_k}\right] \text{Heav}\left(\prod_{k\in\mathcal{K}_{i,t}}\left(\frac{\eta_{i,k,\tau_{k,t}}}{\mu_{i,k,\tau_{k,t}}}\right)^{2b_k-1} - 1\right). \tag{4.23}$$

[5]This is the case for several realistic sensing models, such as the Gaussian observation model introduced in Section 4.1.1.

Similarly, for the case that $\mathcal{K}_{i,t} = \emptyset$, (4.23) results in $\gamma_{i,b,t} = 0.5$.

The derived expressions for the performance at the remote station are useful for the analysis purposes. However, their computational complexity makes them improper choices for real-time motion planning applications. Next, we characterize the Chernoff bound [87] on the probability of error at the remote station, which can be calculated more efficiently and is a better choice for motion planning approaches of Section 4.3.

4.2.4 Chernoff Bound On the Probability of Error at the Remote Station

With the assumption of independent received observations from the mobile sensors, the probability of detection error at the remote station is upper bounded by its Chernoff bound as follows [87]: $\gamma_{i,b,t} \leq \bar{\gamma}_{i,b,t}$, where

$$\begin{aligned}
\bar{\gamma}_{i,b,t} &= \inf_{0<s<1} \pi_{i,0}^{s}\big(1-\pi_{i,0}\big)^{1-s} \prod_{k\in\mathcal{K}_{i,t}} \mathbb{E}\Big\{ \exp\Big(s \log\big(\widetilde{L}_{i,k,\tau_{k,t}}\big)\Big) \;\Big|\; H_0 \Big\} \qquad (4.24)\\
&= \inf_{0<s<1} \pi_{i,0}^{s}\big(1-\pi_{i,0}\big)^{1-s} \prod_{k\in\mathcal{K}_{i,t}} \Bigg[\left(\frac{\eta_{i,k,\tau_{k,t}}}{\mu_{i,k,\tau_{k,t}}}\right)^{s} p(\hat{x}_{i,k,\tau_{k,t}} = 1|H_0) \\
&\qquad\qquad + \left(\frac{1-\eta_{i,k,\tau_{k,t}}}{1-\mu_{i,k,\tau_{k,t}}}\right)^{s} p(\hat{x}_{i,k,\tau_{k,t}} = 0|H_0) \Bigg] \\
&= \inf_{0<s<1} \pi_{i,0}^{s}\big(1-\pi_{i,0}\big)^{1-s} \prod_{k\in\mathcal{K}_{i,t}} \Big[\eta_{i,k,\tau_{k,t}}^{s}\, \mu_{i,k,\tau_{k,t}}^{1-s} + \big(1-\eta_{i,k,\tau_{k,t}}\big)^{s}\big(1-\mu_{i,k,\tau_{k,t}}\big)^{1-s} \Big].
\end{aligned}$$

Finding the optimum s in (4.24) is not easy in general. However, for the special case of $\pi_{i,0} = 0.5$ and $\mu_{i,k,\tau_{k,t}} = 1 - \eta_{i,k,\tau_{k,t}}$, the optimum exponent is $s = 0.5$, as proved by the following lemma:[6]

[6]In case $s = 0.5$ is used, the Chernoff bound is called the Bhattacharyya bound [87].

Lemma 4.2.2. *Assume $\eta_k > 0.5$ for $k \in \mathcal{K}$, where $\mathcal{K} \subseteq \{1, \cdots, n\}$. Then,*

$$\text{argmin}_{0<s<1} \prod_{k\in\mathcal{K}} \left[\eta_k^s \left(1-\eta_k\right)^{1-s} + \eta_k^{1-s}(1-\eta_k)^s\right] = 0.5. \tag{4.25}$$

Proof. Define $f(s) \triangleq \sum_{k\in\mathcal{K}} \log\left[\eta_k^s \left(1-\eta_k\right)^{1-s} + \eta_k^{1-s}(1-\eta_k)^s\right]$. Then, the optimum s is the one that minimizes $f(s)$ for $s \in (0,1)$. We have

$$\begin{aligned}\frac{\mathrm{d}}{\mathrm{d}s}f(s) &= \sum_{k\in\mathcal{K}} \frac{\eta_k^s \left(1-\eta_k\right)^{1-s} \log\left(\frac{\eta_k}{1-\eta_k}\right) - \eta_k^{1-s}(1-\eta_k)^s \log\left(\frac{\eta_k}{1-\eta_k}\right)}{\eta_k^s \left(1-\eta_k\right)^{1-s} + \eta_k^{1-s}(1-\eta_k)^s} \\ &= \sum_{k\in\mathcal{K}} \log(\alpha_k)\left(\frac{\alpha_k^{2s-1}-1}{\alpha_k^{2s-1}+1}\right),\end{aligned} \tag{4.26}$$

where $\alpha_k \triangleq \frac{\eta_k}{1-\eta_k}$. It can be seen that $\frac{\mathrm{d}}{\mathrm{d}s}f(s) = 0$ for $s = 0.5$, $\frac{\mathrm{d}}{\mathrm{d}s}f(s) < 0$ for $0 < s < 0.5$ and $\frac{\mathrm{d}}{\mathrm{d}s}f(s) > 0$ for $0.5 < s < 1$, which completes the proof. □

Using Lemma 4.2.2, the Chernoff bound, for the case of $\pi_{i,0} = 0.5$ (no initial prior) and $\mu_{i,k,\tau_{k,t}} = 1 - \eta_{i,k,\tau_{k,t}}$, is given by $\bar{\gamma}_{i,b,t} = 0.5\prod_{k\in\mathcal{K}_{i,t}} \left[2\sqrt{\eta_{i,k,\tau_{k,t}}\left(1-\eta_{i,k,\tau_{k,t}}\right)}\ \right]$. Finally, in case $\mathcal{K}_{i,t} = \emptyset$, the Chernoff bound on the probability of error will be $\bar{\gamma}_{i,b,t} = \inf\limits_{0<s<1} \pi_{i,0}^s \big(1-\pi_{i,0}\big)^{1-s} = \min\big\{\pi_{i,0},\ 1-\pi_{i,0}\big\}$, which is the same as what we found previously for the probability of error in this case.

4.3 Motion Planning and Power Management Strategies for Minimizing the Detection Error Probability at the Remote Station

Based on the explanations of the previous section, a communication-aware surveillance problem in a mobile sensor network can be stated as follows: Given a limited operation time, T, limited average transmission powers for the mobile sensors, $P_{\text{TX,AV},k}$, for $k = 1, \cdots, n$, and their dynamical models, find the positions of the

mobile sensors, $\xi_{k,t}$, as well as the instantaneous TX powers, $P_{\mathrm{TX},k,t}$, for $k = 1, \cdots, n$ and over the entire time interval $t = 1, \cdots, T$, such that one of the followings holds:

(i) $\sum_{t=1}^{T} \sum_{i=1}^{m} \mathbb{E}\{\gamma_{i,b,t}\}$ is minimized, while maximizing the probability of connectivity of all the mobile sensors during the entire operation, i.e., $\mathbb{E}\{\lambda_{k,t}\}$, for $k = 1, \cdots, n$ and over the entire time interval $t = 1, \cdots, T$.

(ii) $\sum_{i=1}^{m} \mathbb{E}\{\gamma_{i,b,T}\}$ is minimized, while maximizing the probability of connectivity of the mobile sensors at the end of the operation, i.e., $\mathbb{E}\{\lambda_{k,T}\}$, for $k = 1, \cdots, n$.

As explained before, problem (i) is applicable to the case where the remote station requires a constant update on the target positions. Then, the mobile sensors are required to maximize their probability of connectivity to the remote station during the entire operation and improve their exploration performance within connectivity constraints. In problem (ii), on the other hand, maximizing the probability of connectivity during the entire operation is not a goal and the probability of error at the end of the operation is the only performance measure. In this case, the mobile sensors can freely explore the environment, provided that their probability of connectivity, at the end of the operation, is maximized.

Solving problems (i) and (ii) is considerably challenging, without any approximation. Furthermore, the distribution of the channel at unvisited locations, which is used to calculate $\mathbb{E}\{\gamma_{i,b,t}\}$, is time-varying. This makes solving the problem even more challenging. Therefore, more efficient but approximate approaches are desired.

In this section, we propose a communication-aware motion planning framework for suboptimally solving problems (i) and (ii). This is the main contribution of this chapter. The proposed framework consists of two switching greedy approaches: communication-constrained approach for problem (i) and hybrid approach for problem (ii). This framework can account for the time-varying distribution of channel

variations, using a probabilistic assessment of wireless channels. We also introduce robustness strategies, such as TX power adaptation, motion jittering and robustness margins, to increase the robustness of the proposed framework to multipath fading and channel assessment errors.[7]

Similar to Chapter 3, we use the channel assessment framework of Chapter 2 to evaluate our proposed objective functions at unvisited locations. This is discussed in more details when explaining the proposed motion planning approaches in the next two sections.

4.3.1 Communication-Constrained Motion Planning

Consider planning the motion of the mobile sensors in order to constantly update the remote station on the positions of the targets, while improving the exploration performance of each individual mobile sensor. Assume $\pi_{i,0} = 0.5$ for $1 \leq i \leq m$ and $\eta_{i,k,t} = 1 - \mu_{i,k,t}$ for $1 \leq i \leq m$ and $1 \leq k \leq n$. By using the optimal $s = 0.5$, we get

$$\log\big(\bar{\gamma}_{i,b,t+1}\big) = \log(0.5) + \sum_{k \in \mathcal{K}_{i,t+1}} \log\Big(2\sqrt{\eta_{i,k,\tau_{k,t+1}}\big(1 - \eta_{i,k,\tau_{k,t+1}}\big)}\,\Big). \tag{4.27}$$

Let $\mathrm{KL}(\eta)$ denote the Kullback-Leibler (KL) distance between two discrete distributions Bern(0.5) and Bern(η), where Bern(η) represents the Bernoulli distribution with the success probability of η. We have $\mathrm{KL}(\eta) = -\log\big(2\sqrt{\eta(1-\eta)}\,\big)$. Using the definition of $\mathrm{KL}(\eta)$ and $\lambda_{k,t}$, we have

$$\log\big(\bar{\gamma}_{i,b,t+1}\big) = \log(0.5) - \sum_{k=1}^{n} \Big[\lambda_{k,t+1}\mathrm{KL}\big(\eta_{i,k,t+1}\big) + \big(1 - \lambda_{k,t+1}\big)\mathrm{KL}\big(\eta_{i,k,\tau_{k,t}}\big)\Big], \tag{4.28}$$

where we set $\eta_{i,k,\tau_{k,t}} = 0.5$ for $\tau_{k,t} = 0$ (the case where the k^{th} mobile sensor has not yet been connected to the remote station up to time $t \geq 1$). The average of

[7]Note that in this chapter, we are not concerned with energy conservation. Instead, our goal is to schedule a limited average TX power for communication. In case energy conservation is a goal, the current framework can be extended to consider communication and motion powers and optimize the trajectories to minimize the total energy consumption.

$\log\big(\bar{\gamma}_{i,b,t+1}\big)$, conditioned on the channel values up to time t, is then given by the following:

$$\mathbb{E}\Big\{\log\big(\bar{\gamma}_{i,b,t+1}\big)\Big|\lambda_t\Big\} = \log(0.5) - \sum_{k=1}^{n}\Big[\mathbb{E}\{\lambda_{k,t+1}\}\Big(\mathrm{KL}\big(\eta_{i,k,t+1}\big) - \mathrm{KL}\big(\eta_{i,k,\tau_{k,t}}\big)\Big) + \mathrm{KL}\big(\eta_{i,k,\tau_{k,t}}\big)\Big], \tag{4.29}$$

where $\lambda_t = [\lambda_{1,1} \cdots \lambda_{n,t}]^{\mathrm{T}}$. Using the probabilistic channel assessment framework of Chapter 2, the k^{th} mobile sensor can assess the probability of being connected to the remote station at time $t+1$ as follows:

$$\mathbb{E}\big\{\lambda_{k,t+1}\big\} = \mathbb{P}\big\{G_{\mathrm{dB}}(\xi_{k,t+1}) > G_{\mathrm{dB,TH},k,t+1}\big\} = Q\left(\frac{G_{\mathrm{dB,TH},k,t+1} - \hat{G}_{\mathrm{dB},k,t,\mathrm{est}}(\xi_{k,t+1})}{\sigma_{k,t,\mathrm{est}}(\xi_{k,t+1})}\right), \tag{4.30}$$

where $Q(.)$ is the Q-function, $\hat{G}_{\mathrm{dB},k,t,\mathrm{est}}(q)$ and $\sigma^2_{k,t,\mathrm{est}}(q)$ are the estimates of $G_{\mathrm{dB},k,t}(q)$ and $\sigma^2_{k,t}(q)$ respectively (see Theorem 2.2.2), with the exact channel parameters replaced by the estimated ones (similar to Chapter 3). Furthermore, $G_{\mathrm{dB,TH},k,t+1}$ denotes the (possibly time-varying) channel power threshold of the k^{th} mobile sensor at time $t+1$ (in dB), which depends on the power management strategy that we introduce in Section 4.4.1. We then propose the following decentralized greedy motion optimization framework for the k^{th} mobile sensor at time t, based on minimizing its contribution to the average detection error probability of the next time step at the remote station:

$$u^*_{k,t} = \underset{u_{k,t}}{\operatorname{argmax}}\ J_{\mathrm{cc},k,t}\big(\xi_{k,t+1}\big) \triangleq \underbrace{\mathbb{E}\big\{\lambda_{k,t+1}\big\}}_{\text{Comm. obj.}} \underbrace{\Big[\sum_{i=1}^{m}\mathrm{KL}(\eta_{i,k,t+1}) - C_{k,t}\Big]}_{\text{Sensing obj.}}$$

$$\text{s.t. 1) } \xi_{k,t+1} = \xi_{k,t} + u_{k,t},\ \text{2) } \xi_{k,t+1} \in \mathcal{V}_{k,t}, \tag{4.31}$$

where $C_{k,t} \triangleq \sum_{i=1}^{m}\mathrm{KL}\big(\eta_{i,k,\tau_{k,t}}\big)$ is a constant (is not a function of $\xi_{k,t+1}$) and

$$\mathcal{V}_{k,t} \triangleq \Big\{q \in \mathcal{W}\ \Big|\ \|q - \xi_{k,t}\| \le u_{\max,k}, \mathbb{P}\big\{G_{\mathrm{dB}}(q) > G_{\mathrm{dB,TH},k,t+1}\big\} \ge \Delta_{\mathrm{conn}}\Big\}, \tag{4.32}$$

for a positive threshold Δ_{conn}. Note that larger Δ_{conn} will result in a more conservative (in terms of connectivity maintenance) but less sensing-effective strategy. This threshold is chosen based on how much we need the communication-constrained approach to be robust to multipath fading (and other channel assessment errors). Also, the sensing part of (4.31) is always non-negative as $\text{KL}\big(\eta_{i,k,t+1}\big) \geq \text{KL}\big(\eta_{i,k,\tau_{k,t}}\big)$ for every $1 \leq i \leq m$.

Equation (4.31) is a key equation that shows 1) the separation of communication and sensing objectives for the purpose of navigation, 2) that solely from a sensing perspective, each mobile sensor should minimize its surveillance uncertainty at the next step by maximizing its KL distance to Bern(0.5), 3) that solely from a communication perspective, each mobile sensor should maximize the probability of being connected to the remote station at the next step and 4) that the optimal trajectory is the one that provides the right balance between these objectives. In other words, *the optimal communication-constrained navigation strategy is the one that minimizes the sensing uncertainty while maximizing the probability of being connected to the remote station at the next step, based on what the mobile sensor can assess about the connected regions.*

One drawback of the localized motion planning strategy of (4.31) is its feasibility. Based on the available knowledge on channel link qualities, there may be situations where $\mathcal{V}_{k,t} = \emptyset$ (for example the case where the mobile sensor starts in a disconnected area far from the remote station). In such cases, the k^{th} mobile sensor can get stuck in a region with a poor link quality. Furthermore, even if the problem does not become infeasible, if $\text{Area}\big(\mathcal{V}_{k,t}\big)$ is too small, the proposed approach will be less robust to channel assessment errors. In order to avoid such undesired conditions, next we propose a switching strategy to navigate each mobile sensor to unvisited locations with good link qualities, in case the link quality is poor in the local region around the current position of the mobile sensor.

A Switching Strategy for Avoiding Undesired Local Extrema

Let $\mathrm{idx}(q)$, for $q \in \mathcal{W}$, denote the index of the cell that contains q, i.e., the unique i such that $q \in \mathcal{W}_i$. Also, let us define the following sets:

$$\mathcal{E}_{k,t} \triangleq \Big\{ q \in \mathcal{W} \;\Big|\; \mathbb{P}\big\{ G_{\mathrm{dB}}(q) > G_{\mathrm{dB,TH},k,t+1} \big\} \geq \Delta_{\mathrm{conn}} \Big\},$$
$$\mathcal{F}_{k,t} \triangleq \Big\{ q \in \mathcal{W} \;\Big|\; \eta_{\mathrm{idx}(q),k,t} < \Delta_{\mathrm{sens}} \Big\}, \tag{4.33}$$

where Δ_{conn} is as defined before and Δ_{sens} is another positive threshold. The idea behind the switching approach is to add another mode of operation, referred to as the *sensing-aware communication seeking mode*, to navigate the k^{th} mobile sensor to the closest point in $\mathcal{E}_{k,t} \cap \mathcal{F}_{k,t}$ whenever $\big|\mathcal{V}_{k,t}\big| < \varepsilon_{\mathrm{conn}}$, for a small positive $\varepsilon_{\mathrm{conn}}$. Here, $\big|\mathcal{V}_{k,t}\big|$ represents the area of $\mathcal{V}_{k,t}$. In other words, this mode navigates the k^{th} mobile sensor towards the closest unexplored (or poorly explored) region where the probability of connection (using the current assessment of the channel at the mobile sensor) is good enough. Then, as soon as we have $\big|\mathcal{V}_{k,t}\big| \geq \varepsilon_{\mathrm{conn}}$, we switch back to the motion planning strategy of (4.31), which we refer to as *communication-aware exploration mode*. The control input of the k^{th} mobile sensor in the sensing-aware communication seeking mode can then be found as follows:

$$u^*_{k,t} = \underset{u_{k,t}}{\mathrm{argmin}} \; \|\xi_{k,t+1} - q^*_{\mathrm{comm},k,t}\| \tag{4.34}$$
$$\text{s.t. 1) } q^*_{\mathrm{comm},k,t} = \underset{q \in \mathcal{E}_{k,t} \cap \mathcal{F}_{k,t}}{\mathrm{argmin}} \; \|q - \xi_{k,t}\|,\ 2)\ \xi_{k,t+1} = \xi_{k,t} + u_{k,t},\ 3)\ \|u_{k,t}\| \leq u_{k,\max}.$$

Using the control strategy of (4.34), whenever $\big|\mathcal{V}_{k,t}\big| < \varepsilon_{\mathrm{conn}}$, the k^{th} mobile sensor is navigated directly towards $q^*_{\mathrm{comm},k,t}$, which is the closest point of $\mathcal{E}_{k,t} \cap \mathcal{F}_{k,t}$ to the current position of the mobile sensor. Fig. 4.2 summarizes the proposed switching strategy, which prevents the mobile sensor from getting stuck in undesired local extrema. Furthermore, it increases the robustness to channel assessment errors (mainly caused by multipath), by introducing extra design parameters such as Δ_{conn}. In Sec-

tion 4.4, we discuss more strategies for improving the performance and increasing the robustness of the switching approach.

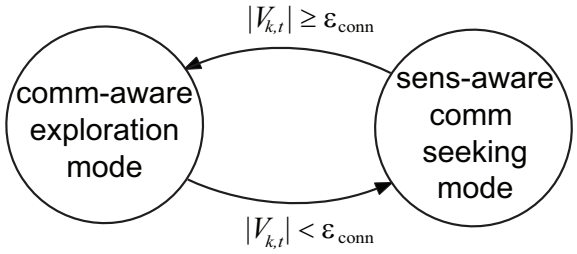

Figure 4.2: Illustration of the proposed communication-constrained motion planning approach.

4.3.2 Hybrid Motion Planning

Consider the communication-constrained motion planning approach of (4.31). The communication part of the objective function in (4.31), i.e., the Q-function in the definition of $J_{\text{cc},k,t}\big(\xi_{k,t+1}\big)$, enforces the k^{th} mobile sensor to move to the positions with a higher chance of experiencing a better channel quality. As the quality of channel learning gets better, $\sigma_{k,t,\text{est}}(\xi_{k,t+1})$ becomes smaller. In the limit of perfect channel learning, the Q-function acts as a hard limiter, enforcing the mobile sensor to only explore the connected regions. This property of the communication-constrained approach can be considerably useful for the applications that require constant communication of the most updated binary maps to the remote station, which requires constant improvement of the probability of connection of individual mobile sensors. However, for a limited operation time T and a time-invariant field, the mobile sensors may only be concerned with the probability of detection error of the remote station at the end of operation, i.e., $\sum_{i=1}^{m} \mathbb{E}\{\gamma_{i,b,T}\}$ as explained before. Minimizing this will result in a different motion planning approach, with a different balance between exploration and communication, which we refer to as *hybrid* motion planning. The idea

behind the hybrid motion planning approach is to have each mobile sensor explore the environment extensively and communicate its binary target map at the end of the mission (note that the remote station only uses the last communication of each mobile sensor). This proposed approach has four modes of operation:

- Mode 1 (*sensing-aware exploration mode*): In this mode, each mobile sensor optimizes its motion only based on its sensing and exploration objectives, without taking communication constraints into account. The purpose of this mode is to explore the environment as much as possible, in the given operation time. Each mobile sensor k, therefore, chooses its next motion decision such that its local detection probability, $\eta_{i,k,t+1}$, is maximized. The controller input of the k^{th} mobile sensor is then calculated using the following optimization problem:

$$u^*_{k,t} = \underset{u_{k,t}}{\operatorname{argmax}}\ J_{\text{sens},k,t}\big(\xi_{k,t+1}\big) \triangleq \sum_{i=1}^{m} \eta_{i,k,t+1} \tag{4.35}$$
$$\text{s.t. 1) } \xi_{k,t+1} = \xi_{k,t} + u_{k,t},\ \text{2) } \|u_{k,t}\| \leq u_{\max,k},\ \text{3) } \xi_{k,t+1} \in \mathcal{W},$$

  where the k^{th} mobile sensor assesses its detection probability based on its sensing model. In this mode, communication objectives are not considered in local motion planning. However, it is possible that the mobile sensor transmits its current decision vector if it randomly moves to a connected spot. This can increase the robustness, in case the operation was terminated abruptly and earlier than planned. However, from power consumption perspective, it may be better if the mobile sensor does not communicate in this stage and leaves all its power for optimizing the connectivity at the end of operation.

- Mode 2 (*local extrema avoidance mode*): Using the localized exploration strategy of (4.35), each mobile sensor tries to explore the environment as much as possible. However, there can be undesirable situations where it gets stuck in a given area, while there are still unvisited areas that can be explored in the

given operation time. Similar to the communication-constrained case, in order to avoid such undesirable situations, we add a mode to navigate a mobile sensor to poorly explored locations, whenever the estimated improvement of its sensing quality is small. Using the definition of $\mathcal{F}_{k,t}$ in Section 4.3.1, the mobile sensor switches to the local extrema avoidance mode, to move towards the closest point in $\mathcal{F}_{k,t}$, whenever

$$\psi_{k,t} \triangleq \frac{\max_{\xi_{k,t+1}\in\mathcal{R}_{k,t}} \sum_{i=1}^{m} |\eta_{i,k,t+1} - \eta_{i,k,t}|}{\sum_{i=1}^{m} \eta_{i,k,t}} < \varepsilon_{\text{sens}}, \tag{4.36}$$

for a small positive $\varepsilon_{\text{sens}}$ and $\mathcal{R}_{k,t} \triangleq \big\{q \in \mathcal{W} \;\big|\; \|q - \xi_{k,t}\| \leq u_{\max,k}\big\}$. In other words, we navigate the mobile sensor towards the closest poorly explored point in the workspace in order to improve its sensing performance. We then switch back to the sensing-aware exploration mode as soon as we have $\psi_{k,t} \geq \varepsilon_{\text{sens}}$. The control input of the k^{th} mobile sensor, in this mode, is also found by following the same approach of the sensing-aware communication seeking mode of the previous case:

$$u^*_{k,t} = \underset{u_{k,t}}{\operatorname{argmin}} \; \|\xi_{k,t+1} - q^*_{\text{sens},k,t}\| \tag{4.37}$$

$$\text{s.t. 1) } q^*_{\text{sens},k,t} = \underset{q\in\mathcal{F}_{k,t}}{\operatorname{argmin}} \; \|q - \xi_{k,t}\|,\ 2)\ \xi_{k,t+1} = \xi_{k,t} + u_{k,t},\ 3)\ \|u_{k,t}\| \leq u_{k,\max}.$$

- Mode 3 (*connection-seeking mode*): Once the environment is explored extensively and the limited operation time is approaching, each mobile sensor needs to move to positions with high chance of connectivity, where it can send its most updated binary decision vector to the remote station. Based on its most recent predicted channel, each mobile sensor has an estimate of how many steps it takes for it to move to a connected position. Based on this knowledge and by considering the remaining number of operation steps, each mobile sensor can decide when to switch from the sensing-aware exploration mode or the local extrema avoidance mode to the connection-seeking mode. Consider the

set $\mathcal{E}_{k,t}$, defined in Section 4.3.1. The closest point in $\mathcal{E}_{k,t}$ is then found as follows: $q^*_{\text{seek},k,t} = \underset{q\in\mathcal{E}_{k,t}}{\text{argmin}}\|q-\xi_{k,t}\|$. Using the fist-order dynamics of the mobile sensors, the minimum number of steps required to get to $q^*_{\text{seek},k,t}$, at time t, is $\zeta_{k,t} = \left\lfloor \frac{\|\xi_{k,t}-q^*_{\text{seek},k,t}\|}{u_{\max,k}} \right\rfloor + 1$. The k^{th} mobile sensor switches to the connection-seeking mode at time t if 1) it is not connected to the remote station at time t and 2) $\zeta_{k,t} \geq T - t - M$, where M is a positive and small offset, which can add a robustness margin to the operation. Once a decision to switch to the connection-seeking mode is made, the control input of each mobile sensor is found as follows:

$$u^*_{k,t} = \underset{u_{k,t}}{\text{argmin}}\ \|\xi_{k,t+1} - q^*_{\text{seek},k,t}\| \tag{4.38}$$

$$\text{s.t. 1) } q^*_{\text{seek},k,t} = \underset{q\in\mathcal{E}_{k,t}}{\text{argmin}}\ \|q-\xi_{k,t}\|,\ 2)\ \xi_{k,t+1} = \xi_{k,t} + u_{k,t},\ 3)\ \|u_{k,t}\| \leq u_{k,\max}.$$

Similar to the communication-constrained approach, as we increase Δ_{conn} in $\mathcal{E}_{k,t}$, the motion planner becomes more robust to the variations of multipath fading and other assessment uncertainties, by acting more conservatively.

- Mode 4 (*communication-aware exploration mode*): Once a mobile sensor moves to a region where $\left|\mathcal{V}_{k,t}\right| \geq \varepsilon_{\text{conn}}$, it utilizes the proposed communication-aware exploration mode of Section 4.3.1, in order to maintain its connectivity to the remote station till the end of operation. In this mode, the mobile sensor still senses the connected area, as described in the previous section. However, its main goal is connectivity maintenance. Note that in case the k^{th} mobile sensor is still disconnected after switching to this mode (possibly due to its poor assessment of the channel in the presence of large multipath fading), it can take advantage of a jittery movement around its current location, in order to increase its chance of connectivity. In the next section, we explain such strategies to further increase the robustness of both communication-constrained and hybrid approaches.

Fig. 4.3 demonstrates an overview of the hybrid approach where transition between the modes is illustrated.

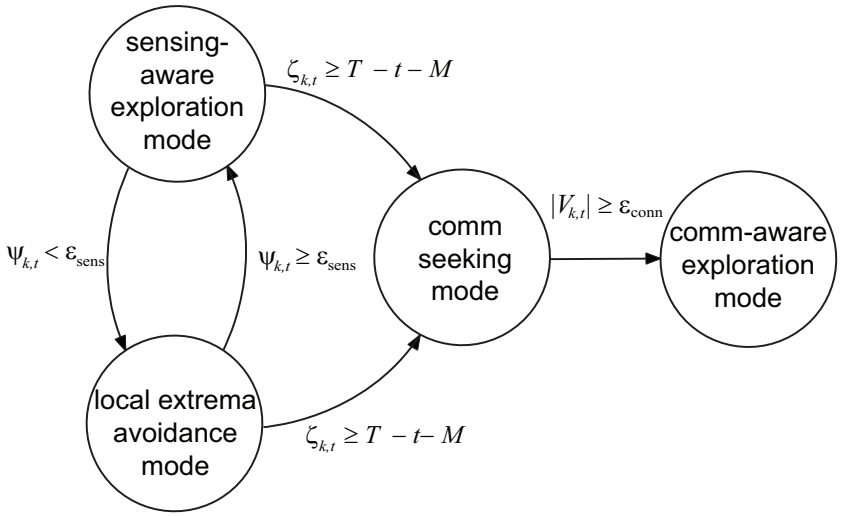

Figure 4.3: Illustration of the proposed hybrid motion planning approach.

4.4 Further Robustness to Multipath Fading and other Channel Assessment/Modeling Errors

In Chapter 2, we explained how our probabilistic channel assessment framework can be used by each mobile sensor to learn the shadowing and path loss components and characterize the channel learning uncertainty, in the presence of multipath fading and other channel assessment errors. This enabled our probabilistic motion control approaches in Section 4.3.1 and 4.3.2. We also showed how to increase the robustness, by introducing a number of design parameters (such as Δ_{conn}). In this section, we discuss more strategies to increase the robustness to multipath fading and other channel assessment/modeling errors. These strategies can be combined with our communication-constrained or hybrid motion planners to further improve the performance. Fig. 4.4 summarizes how our proposed framework handles different

elements of wireless channels using 1) probabilistic assessment of the shadowing and path loss components and 2) strategies to increase robustness to multipath fading and other modeling errors. We will discuss the robustness strategies in the subsequent sections.

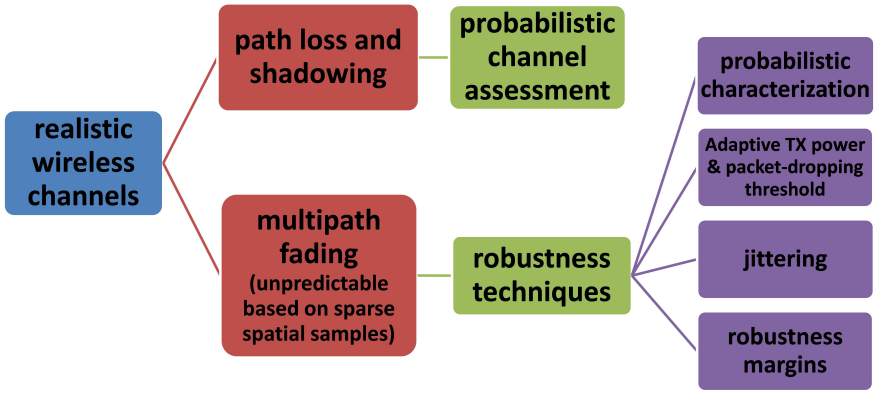

Figure 4.4: Illustration of the proposed probabilistic channel assessment framework and robustness techniques.

4.4.1 Adaptive Transmit Power and Packet Dropping Threshold for Increasing the Robustness to Multipath Fading

The threshold $G_{\mathrm{dB,TH},k,t+1}$ in the formulation of $\mathbb{E}\{\lambda_{k,t+1}\}$ in (4.30), as well as in the definitions of $\mathcal{V}_{k,t}$ and $\mathcal{E}_{k,t}$, depends on the TX power adaptation strategy of the k^{th} mobile sensor. Consider the case where the k^{th} mobile sensor is given the total average TX power of $P_{\mathrm{TX,AV},k}$. It can use the fixed TX power of $P_{\mathrm{TX},k,t} = P_{\mathrm{TX,AV},k}$ during its operation, independent of the channel quality. In this case, we have $G_{\mathrm{dB,TH},k,t+1} = 10\log_{10}\left(\frac{\mathrm{SNR_{TH}}BN_0}{P_{\mathrm{TX,AV},k}}\right) + \Delta G_{\mathrm{dB,TH}}$, where $\Delta G_{\mathrm{dB,TH}} \geq 0$ is added to increase the robustness to multipath fading. The idea is that by increasing the packet-dropping threshold, the mobile sensor is then forced to operate in regions with higher channel power, resulting in more robustness to multipath fading.

Alternatively, each mobile sensor can adapt its TX power to channel quality. Power adaptation strategies have been heavily explored in the communication literature [45, 46, 101]. In this chapter, the goal of TX power adaptation is to increase the robustness of the proposed motion planning algorithm by saving power at positions with high channel qualities, with the goal of satisfying the connectivity requirements at positions with low channel qualities. Similar to [101], we consider the following simple TX power adaptation strategy for each mobile sensor:

$$P_{\mathrm{TX},k,t} = \begin{cases} 0, & \min\left(P_{\mathrm{TX,AV},k,t}, P_{\mathrm{TX,max},k}\right) < \frac{\mathrm{SNR_{TH}}BN_0}{G(\xi_{k,t})} \\ \frac{\mathrm{SNR_{TH}}BN_0}{G(\xi_{k,t})}, & \text{otherwise} \end{cases}, \tag{4.39}$$

where $P_{\mathrm{TX,max},k}$ is the maximum TX power of the k^{th} mobile sensor and $P_{\mathrm{TX,AV},k,t}$ is the average of the remaining power budget of the k^{th} mobile sensor at time instant t:

$$P_{\mathrm{TX,AV},k,t} = \frac{1}{T-t+1}\left(TP_{\mathrm{TX,AV},k} - \sum_{\ell=1}^{t-1} P_{\mathrm{TX},k,\ell}\right). \tag{4.40}$$

Based on (4.39), the k^{th} mobile sensor sends its binary decision vector to the remote station at time t when the minimum required TX power to make the mobile sensor connected is no larger than $\min\left(P_{\mathrm{TX,AV},k,t}, P_{\mathrm{TX,max},k}\right)$. The channel power threshold is then selected to be:

$$G_{\mathrm{dB,TH},k,t+1} = 10\log_{10}\left(\frac{\mathrm{SNR_{TH}}BN_0}{\min(P_{\mathrm{TX,AV},k,t}, P_{\mathrm{TX,max},k})}\right) + \Delta G_{\mathrm{dB,TH}}. \tag{4.41}$$

Note that in this chapter, we are not concerned with minimizing the total energy consumption. In other words, our goal is to schedule a limited average TX power for communication. However, the current framework can be extended to consider both communication and motion powers and optimize the trajectories of the mobile sensors such that the total energy consumption is minimized, while the main networked task is accomplished. It is also worth mentioning that, in the hybrid approach, the mobile

sensors may decide not to send anything, while operating in modes 1 and 2, to save power for the end of the operation when they need to be connected. This strategy is particularly useful for long operations with limited power budgets. However, if power is not a constraint, the mobile sensors can always send their most updated target maps to the remote station if they move to a connected spot by chance. This can further increase the robustness, in case the operation terminates abruptly and earlier than planned.

4.4.2 Jittery Movements for Increasing the Probability of Connectivity in the Presence of Large Multipath Fading

Consider the communication-constrained approach. This strategy guides each mobile sensor to an area that has a high probability of connectivity. However, a specific position may or may not have the connectivity requirement, as our channel learning framework cannot predict the fine variations of multipath fading and is also prone to errors. Since the mobile sensor is guided to an area that has a high probability of connectivity (high average channel power), then small jittering can help the mobile sensor find a better location in terms of connectivity. In case a jittery movement is added, after the proposed communication-constrained or hybrid motion planner is executed at each step, the mobile sensor picks N_{jitt} random points in a small circular region around its current location. It then moves to each point one by one, measures the channel there, and then simply chooses the point with the best channel quality for sending. The radius of the circular region for jittering is chosen such that the path loss and shadowing parts of channel remain stationary in the region, based on the assessment of the channel available to each mobile sensor. Note that in case the adaptive TX power strategy of (4.39) is used, if none of the N_{jitt} points satisfy the

the connectivity requirement at some steps, nothing will be sent.

4.5 Performance Analysis of the Proposed Motion Planning Strategies

With some assumptions, it is possible to analyze the final performance of the proposed communication-constrained and hybrid approaches. The following theorems summarize our key results:

Theorem 4.5.1. *Assume that 1) the mobile sensors use the fixed TX power strategy of $P_{\mathrm{TX},k,t} = P_{\mathrm{TX,AV},k}$, for $k = 1, \cdots, n$, 2) based on the assessment of the channel at all the mobile sensors, $\mathcal{W} \setminus \cup_{t=1}^{\infty} \cup_{k=1}^{n} \mathcal{E}_{k,t} \neq \emptyset$ (refer to Section 4.3.1 for the definition of $\mathcal{E}_{k,t}$), and 3) the sensing radius of each mobile sensor and the size of each cell are small, compared to the size of the workspace, such that some of the cells in $\mathcal{W} \setminus \cup_{t=1}^{\infty} \cup_{k=1}^{n} \mathcal{E}_{k,t}$ cannot be sensed by any mobile sensor k, while it moves inside $\cup_{t=1}^{\infty} \mathcal{E}_{k,t}$. Then, the average of the probability of error at the remote station in the communication-constrained approach (averaged over the space and the conditional distribution[8] of the channel) is lower bounded by a positive value at any time, i.e., there exists $\underline{\gamma} > 0$ such that $\frac{1}{m} \sum_{i=1}^{m} \mathbb{E}\{\gamma_{i,b,t}\} \geq \underline{\gamma}$, for all $k \geq 1$.*

Proof. For every $t \geq 1$, we have

$$\frac{1}{m} \sum_{i=1}^{m} \mathbb{E}\{\gamma_{i,b,t}\} \geq \frac{1}{m} \sum_{i=1}^{m} \mathbb{E}\{\gamma_{i,b,T}\} \geq \lim_{T \to \infty} \frac{1}{m} \sum_{i=1}^{m} \mathbb{E}\{\gamma_{i,b,T}\}, \tag{4.42}$$

where the expected values are calculated over the conditional distribution of the channel. Assuming $\pi_{i,0} = 0.5$, for $1 \leq i \leq m$, and $\eta_{i,k,t} = 1 - \mu_{i,k,t}$, for $1 \leq i \leq m$

[8]The distribution of the channel conditioned on the finite set of channel measurements.

and $1 \leq k \leq n$, we obtain

$$\lim_{T\to\infty} \gamma_{i,b,T} = \sum_{b\in\mathcal{B}} \left[\prod_{k=1}^{n} (1-\mu_{i,k,\infty})^{1-b_k}\, \mu_{i,k,\infty}^{b_k}\right] \text{Heav}\left(\prod_{k=1}^{n}\left(\frac{1-\mu_{i,k,\infty}}{\mu_{i,k,\infty}}\right)^{2b_k-1} - 1\right), \tag{4.43}$$

where $\mu_{i,k,\infty} \triangleq \lim_{T\to\infty} \mu_{i,k,\tau_{k,T}}$ and $\mathcal{B}$ is the set of all the binary vectors of size n. Note that $\mu_{i,k,\infty} = 0.5$ in case $\lim_{T\to\infty} \tau_{k,T} = 0$. Consider the communication-constrained approach, where $P_{\text{TX},k,t} = P_{\text{TX,AV},k}$ and $\mathcal{W} \setminus \cup_{t=1}^{\infty} \cup_{k=1}^{n} \mathcal{E}_{k,t} \neq \emptyset$. If the sensing radius of each mobile sensor and the size of each cell are small, we can find some cell i inside $\mathcal{W} \setminus \cup_{t=1}^{\infty} \cup_{k=1}^{n} \mathcal{E}_{k,t} \neq \emptyset$ and some $\underline{\mu}_i > 0$, such that $\mu_{i,k,\infty} \geq \underline{\mu}_i$, $\forall k$. This cell i can be any cell inside $\mathcal{W} \setminus \cup_{t=1}^{\infty} \cup_{k=1}^{n} \mathcal{E}_{k,t}$, which is not visited by any mobile sensor during the entire operation or is sensed for a finite number of steps before each mobile sensor reaches $\mathcal{E}_{k,t}$, for $k = 1, \cdots, n$. This implies that there exists a positive lower bound on $\lim_{T\to\infty} \frac{1}{m} \sum_{i=1}^{m} \gamma_{i,b,T}$ and, by averaging over the conditional channel distribution, on $\lim_{T\to\infty} \frac{1}{m} \sum_{i=1}^{m} \mathbb{E}\{\gamma_{i,b,T}\}$. In other words, there exists $\underline{\gamma} > 0$ such that $\lim_{T\to\infty} \frac{1}{m} \sum_{i=1}^{m} \mathbb{E}\{\gamma_{i,b,T}\} \geq \underline{\gamma}$. The same result can be obtained for the more general case where $\pi_{i,0} \neq 0.5$, for some $1 \leq i \leq m$, or $\eta_{i,k,t} \neq 1 - \mu_{i,k,t}$, for some $1 \leq i \leq m$ and $1 \leq k \leq n$, using (4.17). This completes the proof. □

Theorem 4.5.2. *Assume that 1) the channel is assessed perfectly,*[9] *2) the mobile sensors are connected to the remote station at the beginning of the operation, 3) the sensing radius of each mobile sensor and the size of each cell are small, compared to the size of the workspace, such that the maximum area covered by a mobile sensor k, while moving in $\mathcal{E}_{k,t}$, is approximately equal to the area of $\mathcal{E}_{k,t}$ (refer to Section 4.3.1 for the definition of $\mathcal{E}_{k,t}$), for $k = 1, \cdots, n$, 4) the mobile sensors use the same fixed TX power strategy of $P_{\text{TX},k,t} = P_{\text{TX,AV}}$, for $k = 1, \cdots, n$, 5) $\pi_{i,0} =$*

[9]By this assumption we automatically assume that the multipath fading power is zero, the channel parameters are estimated perfectly and the number of channel measurements in the environment are large such that $\sigma_{k,t}(q) \to 0$ for all k, $q \in \mathcal{W}$ and $t \geq 1$. See Definition 3.2.1 in Chapter 3 for more details.

0.5, for $i = 1, \cdots, m$, and 6) the workspace is a circular region with the remote station located at the center of the circle. Then, in the communication-constrained approach, a lower bound for $\lim_{T\to\infty} \frac{1}{m}\sum_{i=1}^{m} \mathbb{E}\{\gamma_{i,b,T}\}$ (averaged over every possible channel) is approximately given by $0.5\Big[Q(a) - \exp\Big(\frac{2+2a\rho}{\rho^2}\Big)Q\Big(\frac{2+a\rho}{\rho}\Big)\Big]$, where $a = \frac{K_{\mathrm{dB}} - 10n_{\mathrm{PL}}\log_{10}(R_{\mathcal{W}}) - G_{\mathrm{dB,TH}}}{\vartheta}$, $\rho = \frac{10n_{\mathrm{PL}}}{\vartheta\log(10)}$, $G_{\mathrm{dB,TH}} = 10\log_{10}\big(\frac{BN_0\mathrm{SNR_{TH}}}{P_{\mathrm{TX,AV}}}\big)$ and $R_{\mathcal{W}}$ is the radius of the workspace.

Proof. In case the mobile sensors start connected and the channel is assessed perfectly, each mobile sensor k only explores $\mathcal{E}_{k,t}$ in the communication-constrained approach. Then, if there exists only one connected region around the remote station and the size of the cells and the sensing radii of the mobile sensors are small, we approximately have

$$\lim_{T\to\infty} \frac{1}{m}\sum_{i=1}^{m} \gamma_{i,b,T} \geq \frac{\big|\mathcal{W} \setminus \cup_{t=1}^{\infty}\cup_{k=1}^{n}\mathcal{E}_{k,t}\big|}{2\big|\mathcal{W}\big|}. \tag{4.44}$$

In case of perfect channel assessment, the area of $\mathcal{W}\setminus\cup_{t=1}^{\infty}\cup_{k=1}^{n}\mathcal{E}_{k,t}$ is equal to the area of the disconnected region. Therefore, by averaging over the channel distribution, we get

$$\begin{aligned}
\lim_{T\to\infty} \frac{1}{m}\sum_{i=1}^{m} \mathbb{E}\{\gamma_{i,b,T}\} &\geq \frac{0.5}{\pi R_{\mathcal{W}}^2}\int_{\mathcal{W}} \mathbb{P}\{G_{\mathrm{dB}}(q) < G_{\mathrm{dB,TH}}\}\mathrm{d}q \\
&= \frac{1}{R_{\mathcal{W}}^2}\int_0^{R_{\mathcal{W}}} rQ\bigg(\frac{K_{\mathrm{dB}} - 10n_{\mathrm{PL}}\log_{10}(r) - G_{\mathrm{dB,TH}}}{\vartheta}\bigg)\mathrm{d}r \\
&= 0.5\bigg[Q(a) - \exp\Big(\frac{2+2a\rho}{\rho^2}\Big)Q\Big(\frac{2+a\rho}{\rho}\Big)\bigg],
\end{aligned} \tag{4.45}$$

for $\rho = \frac{10n_{\mathrm{PL}}}{\vartheta\log(10)}$, $a = \frac{K_{\mathrm{dB}} - 10n_{\mathrm{PL}}\log_{10}(R_{\mathcal{W}}) - G_{\mathrm{dB,TH}}}{\vartheta}$ and $G_{\mathrm{dB,TH}} = 10\log_{10}\big(\frac{BN_0\mathrm{SNR_{TH}}}{P_{\mathrm{TX,AV}}}\big)$, where we used the method of Chapter 2 of [59] to calculate the integral. □

Theorem 4.5.3. *Assume that the channel is assessed perfectly, $\pi_{i,0} = 0.5$, for $1 \leq i \leq m$, and $\eta_{i,k,t} = 1 - \mu_{i,k,t}$, for $1 \leq i \leq m$ and $1 \leq k \leq n$. In the hybrid approach, if we select $\Delta_{\mathrm{sens}} = 1 - \delta_{\mathrm{sens}}$ (see Section 4.3.1 for the definition of the Δ_{sens}), for an*

arbitrary small positive δ_{sens}, then we have the following for the asymptotic average probability of detection error at the remote station: $\lim_{T\to\infty} \frac{1}{m} \sum_{i=1}^{m} \mathbb{E}\{\gamma_{i,b,T}\} \leq \delta_{\text{sens}}$*, where averaging is done over every possible channel.*

Proof. Assume that the mobile sensors start with the sensing-aware exploration mode in the hybrid approach. Consider the k^{th} mobile sensor, for $1 \leq k \leq n$. For this mobile sensor, the exploration continues (the spatial average of its detection error probability decreases) until $\psi_{k,t} < \varepsilon_{\text{sens}}$ (see Section 4.3.2 for the definition of the variables). In this case, we have either $\mathcal{F}_{k,t} = \emptyset$, which means that $\mu_{i,k,t} \leq \delta_{\text{sens}}$, for $1 \leq i \leq m$, or $\mathcal{F}_{k,t} \neq \emptyset$. For the latter, the proposed local extrema avoidance mode of the hybrid approach navigates the mobile sensor to a point in $\mathcal{F}_{k,t}$. Then, two different cases may happen. If a situation where $\psi_{k,t} \geq \varepsilon_{\text{sens}}$ does not happen, while in the local extrema avoidance mode, the mobile sensor will remain in this mode and visit every point in $\mathcal{F}_{k,t}$ until $\mathcal{F}_{k,t} = \emptyset$. On the other hand, if the mobile sensor switches back to the sensing-aware exploration mode at some point, the exploration continues similar to the previous case, which also proves that $\mathcal{F}_{k,t} = \emptyset$ after some steps. Therefore, we have $\mu_{i,k,t} \leq \delta_{\text{sens}}$, for $1 \leq i \leq m$ and t greater than a positive constant. Then, assuming that the channel is assessed almost perfectly, we have $\mu_{i,k,\infty} \leq \delta_{\text{sens}}$ (see the proof of Lemma 4.5.1 for the definition of $\mu_{i,k,\infty}$), for $1 \leq i \leq m$ and $1 \leq k \leq n$. This implies that $\lim_{T\to\infty} \gamma_{i,b,T} \leq \delta_{\text{sens}}$, for $1 \leq i \leq m$. By averaging over the channel distribution, we have $\lim_{T\to\infty} \mathbb{E}\{\gamma_{i,b,T}\} \leq \delta_{\text{sens}}$, for $1 \leq i \leq m$, which completes the proof. □

As indicated by Theorem 4.5.3, the hybrid approach almost always outperforms the communication-constrained one, in terms of the final probability of error at the remote station, for large enough T. We compare the performance of the two approaches in the next section, using both simulated and experimental data.

4.6 Simulation and Experimental Results

In this section, we evaluate the performance of the proposed communication-aware surveillance framework using both simulated and real channel measurements. Our results highlight the underlying trade-offs in the design space as summarized later in this section. For instance, they show that while the hybrid approach outperforms the communication-constrained one in terms of the final probability of networked detection error, the latter has a higher probability of constant connectivity and is therefore more robust to the abrupt termination of the operation. Also, we further compare these two approaches with communication-unaware strategies (strategies that consider only sensing objectives for planning the motion of the mobile sensors) and show the effectiveness of the proposed framework in realistic fading environments.

Consider a surveillance scenario where three mobile sensors are tasked to explore a given environment for the possible presence of targets. We use the Gaussian observation model of Section 4.1.1, where the following form is chosen for the observation error variance [17, 73]:

$$\Phi_k(d) = \begin{cases} \varrho\, d^2 + \nu, & d < d_{\text{sen}} \\ \infty, & \text{otherwise} \end{cases} \tag{4.46}$$

for positive constants $\varrho > 0$ and $\nu > 0$ and a limited sensing radius d_{sen} for each mobile sensor. The communication channel between the mobile sensors and the remote station is simulated using our probabilistic channel simulator, which can simulate path loss, shadow fading and multipath fading, with realistic spatial correlations. A detailed description of this channel simulator can be found in [54, 56].

First we compare the trajectories of communication-constrained and hybrid planning approaches, for a fixed TX power case, where the following parameters are used: $u_{\max,k} = 3.0$ m for $k = 1, 2, 3$, $\varrho = 0.02$, $\nu = 0.04$, $d_{\text{sen}} = 3.0$ m, $K_{\text{dB}} = -10$ dB, $n_{\text{PL}} = 2.5$, $\vartheta = 2$ dB, $\beta = 4$ m, $\omega = 2$ dB, $BN_0 = -85$ dB, $P_{\text{TX,AV},k} = -20$ dB, for

$k = 1, 2, 3$, $P_{\mathrm{TX,max},k} = -10$ dB, for $k = 1, 2, 3$, and $\mathrm{SNR}_{\mathrm{TH}} = 23$ dB, with a Rician multipath fading. Note that Rician multipath fading was simulated to make the simulated more realistic. Furthermore, we use the following design parameters when implementing our communication-aware and hybrid motion planners: $\Delta_{\mathrm{conn}} = 0.8$, $\Delta_{\mathrm{sens}} = 0.65$, $\varepsilon_{\mathrm{conn}} = 0.25$, $\varepsilon_{\mathrm{sens}} = 0.002$, $\Delta G_{\mathrm{dB,TH}} = 0$ and $M = 5$ (see Section 4.3.1 and 4.3.2 for the definition of these parameters). For the purpose of channel learning, the mobile sensors use 0.01% of the total channel samples (64 samples in a 800×800 grid), which are assumed to be randomly collected during an initial learning phase. Then, they collect more samples as they move along their trajectories. The collected samples are used to estimate the underlying channel parameters and assess the spatial variations of the channel at unvisited areas. Fig. 4.5 shows the trajectories of the mobile sensors for one simulated channel in both cases. The black regions in Fig. 4.5 represent the areas where the mobile sensors are not connected to the remote station (received SNR is below the acceptable threshold), given $P_{\mathrm{TX},k,t} = P_{\mathrm{TX,AV},k}$. It can be seen that by using the communication-constrained approach, the mobile sensors converge to the regions where they are connected to the remote station (if they are not connected at the beginning) and stay connected afterwards. In other words, this approach forces the mobile sensors to mostly explore the regions with better link qualities, so that they can constantly update the remote station and minimize its detection error probability, as we explained in Section 4.3.1. The hybrid navigation strategy, on the other hand, allows the mobile sensors to explore the environment more freely. It, however, enables the mobile sensors to be connected to the remote station at the end of operation. Also, as can be seen from the figure, some regions may be revisited by the mobile sensors several times along their trajectories. Note that in both cases, the mobile sensors take advantage of a jittery movement, in areas of radius 0.3 m around their current locations and by testing $N_{\mathrm{jitt}} = 45$ points at each step. In this specific example, jittery movement in the communication-constrained case results in 10%, 15% and 17% increase in the percentage of time that Mobile

Sensor #1, Mobile Sensor #2 and Mobile Sensor #3 are connected along their trajectories, respectively. Similarly, in the hybrid approach, by using the jittery movement we have 24%, 20% and 41% increase in the percentage of time that Mobile Sensor #1, Mobile Sensor #2 and Mobile Sensor #3 are connected along their trajectories, respectively.

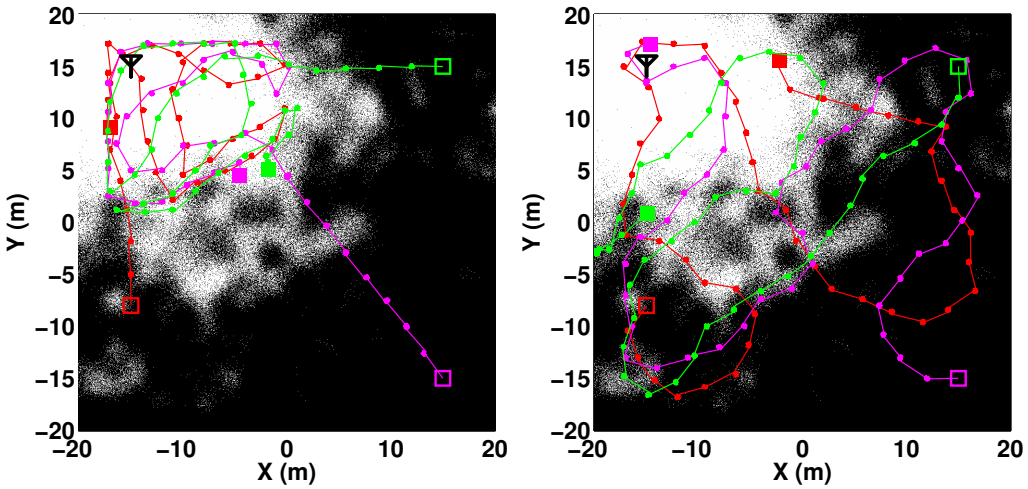

Figure 4.5: Trajectories of three mobile sensors for communication-constrained (left) and hybrid (right) cases, with fixed TX powers. The red, magenta and green lines correspond to the trajectories of the Mobile Sensor #1, Mobile Sensor #2 and Mobile Sensor #3, respectively. The empty boxes and the filled ones denote the initial and final positions respectively. The location of the remote station is denoted on the top left corner of the figures. See the pdf file for more visual clarity.

Next, consider the case where the adaptive TX power strategy of (4.39) is used for both communication-constrained and hybrid approaches.[10] Then, the connectivity regions will become time-varying and different for different mobile sensors (since their TX powers are different). One would expect that the white regions (connectivity regions), corresponding to the k^{th} mobile sensor, expand as its instantaneous average

[10]As explained before, in case energy conservation is not an issue, a mobile sensor can transmit any time it is connected by luck in the hybrid approach too and hence apply the adaptive TX power strategy of (4.39). Multiple transmissions (as opposed to transmission only at the end of the operation) in the hybrid case will increase the robustness, although it is not required.

TX power, $P_{\mathrm{TX,AV},k,t}$, increases. Fig. 4.6 shows the evolution of the connectivity regions for both strategies, for one of the mobile sensors of Fig. 4.5, when the TX power adaptation technique of (4.39) is used. The communication channel is taken to be the same as the one used in Fig. 4.5. In such an adaptive strategy, the connectivity region of the mobile sensor expands with time with high probability, as can be seen from the figure, for two reasons. First, in case of poor channel quality at time t, the mobile sensor does not send anything, which results in an increase in $P_{\mathrm{TX,AV},k,t+1}$ and an expansion in its next step connectivity region. Second, in case the mobile sensor decides to send its updated target map to the remote station using (4.39), it uses the minimum required power for connectivity, given by $\frac{\mathrm{SNR_{TH}}BN_0}{G(\xi_{k,t})}$, using its measured channel power at time t. Note that we did not simulate any jittery movement in this case.

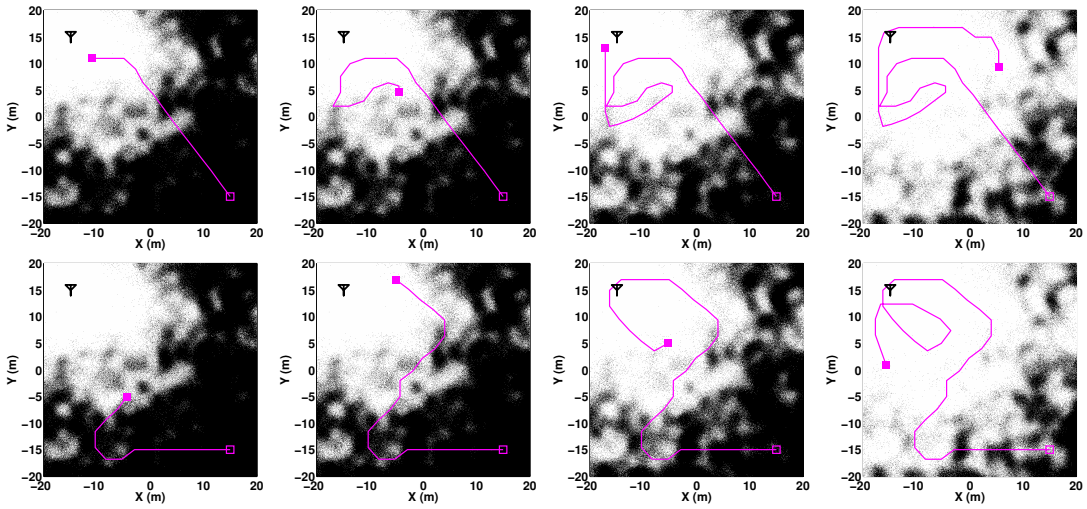

Figure 4.6: Impact of the adaptive TX power on connectivity regions. Time-varying connectivity regions (white areas) in communication-constrained (top row) and hybrid (bottom row) cases are shown for one of the mobile sensors of Fig. 4.5, at time steps $t = 15$, $t = 25$, $t = 35$ and $t = 45$ (from left to right). The communication channel is taken to be the same as the one used in Fig. 4.5. Empty boxes and filled ones denote the initial and final positions respectively. See the pdf file for more visual clarity.

In order to further compare the communication-constrained and hybrid approaches, Fig. 4.7 (left) shows the average of the final detection error probability at the remote

station, i.e., $\frac{1}{m}\sum_{i=1}^{m}\mathbb{E}\{\gamma_{i,b,T}\}$, as a function of the given operation time T, for the three mobile sensors and the same system parameters of Fig. 4.5.[11] The averaging is done over the space and 20 different channels. In Fig. 4.7 (left), for every T, the whole trajectory of the mobile sensor is generated for 20 different channels and the average results at the end of the operation are then plotted. In order to simplify the scenario, TX power is not adaptive in this case and the mobile sensors, in both communication-constrained and hybrid approaches, use the constant TX power of $P_{\text{TX,AV},k} = -20$ dB at each step. They, however, make use of a jittery movement, at the end of each step, to increase their chance of connectivity to the remote station. It can be seen that the hybrid approach outperforms the communication-constrained one, in terms of the average of the final detection error probability at the remote station, as expected. The figure also shows that as $T \to \infty$, the average probability of error goes to zero in the hybrid case, while it reaches an error floor in the communication-constrained case. However, the communication-constrained approach provides smaller average detection error probability at the remote station, in case the operation terminates earlier than the planned time T. To see this, Fig. 4.7 (right) shows the average of the detection error probability at the remote station, i.e., $\frac{1}{m}\sum_{i=1}^{m}\mathbb{E}\{\gamma_{i,b,t}\}$, as a function of time step t, averaged over space and 20 different channels. We used $T = 50$ as the operation time in this case. As can be seen, if the operation ends while the hybrid approach is still in the exploration mode, it results in a worse performance, as it is designed to optimize the operation given a certain time.

Fig. 4.8 compares the performance of three approaches, with different levels of awareness, in terms of communication and sensing, for the same system parameters of Fig. 4.5. The results are averaged over 20 different channels. Similar to Fig. 4.7, TX power is not adaptive. Also, no jittery movement is simulated in this case, to show

[11]The spatial average or spatial integration of the quantity under control, is a popular choice for the performance measure in surveillance and exploration literature [17].

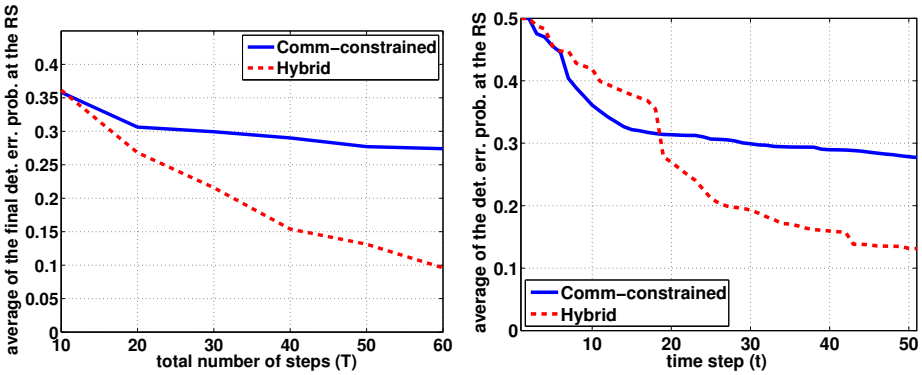

Figure 4.7: Average of the detection error probability at the remote station (RS) as a function of (left) the given operation time (T) and (right) time step (t) for communication-constrained and hybrid approaches. TX power is not adaptive in this case.

the underlying trade-off more clearly. For the sake of comparison, the results for a sensing-constrained case are also shown. A sensing-constrained case only optimizes the exploration objective and communicates with the remote station anytime its trajectory takes it to the connected regions, as was described in modes 1 and 2 of the hybrid case. Thus, it is unaware of communication objectives. The figure shows the average of the final detection error probability at the remote station, as a function of $\mathrm{SNR}_{\mathrm{TH}}$, for two cases of $T = 10$ (left) and $T = 50$ (right). Interesting trade-offs can be observed. Consider the left figure, where T is small. In this case, as $\mathrm{SNR}_{\mathrm{TH}}$ increases, the chance of connectivity becomes small over the whole space. As such, the performance of the sensing-constrained approach degrades considerably, for large $\mathrm{SNR}_{\mathrm{TH}}$, since it does not include communication objectives in its motion optimization. It can be see that the communication-constrained and hybrid cases perform almost the same and better than the sensing constrained approaches. Also, in this case, the average of the detection error probability in the communication-constrained and hybrid approaches are large (compared to detection error probability of hybrid approach in the right figure). This is because the operation time is limited and the requirement on link qualities is high. The right figure, on the other hand, shows the performance for the case of $T = 50$. In this case, since the given operation

time is longer than the left figure, the trajectory of the sensing-constrained approach crosses through more connected regions by luck, which improves its performance. For the communication-constrained case, the performance degrades as $\mathrm{SNR}_{\mathrm{TH}}$ increases since its exploration is limited to connected regions, which are shrinking as $\mathrm{SNR}_{\mathrm{TH}}$ increases. The hybrid approach, however, results in the best performance in both cases, providing the best trade-off between sensing and communication, as expected.

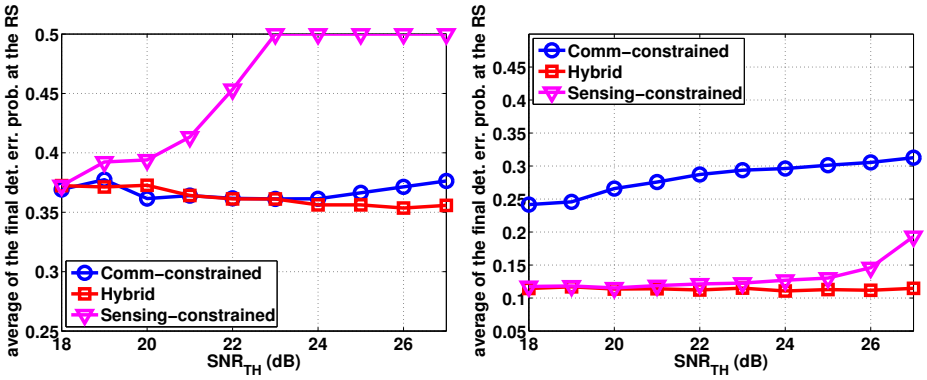

Figure 4.8: Communication and sensing trade-offs in a networked surveillance scenario. The figure shows average of the final detection error probability at the remote station (RS), averaged over the space and channel distribution, as a function of $\mathrm{SNR}_{\mathrm{TH}}$, for two cases of $T = 10$ (left) and $T = 50$ (right).

In order to show the performance of our framework with real channel measurements, Fig. 4.9 shows a surveillance scenario, using one mobile sensor and by considering the real channel measurements gathered in the basement of our building. The channel measurements are collected through a survey of the channel, using the onboard IEEE 802.11g WLAN card of a Pioneer 3-AT robot (shown in Fig. 4.11) and for a remote station (an IEEE 802.11g wireless router) located in one of the rooms in the basement. This channel samples are then used to simulate the surveillance scenario. During the surveillance operation, the channel is assessed based on 0.1% *a priori* channel samples (47 samples), as well as the samples the mobile sensor collects along its trajectory. The TX power is kept fixed and a received SNR threshold of 35 dB is chosen for packet dropping. The mobile sensor also takes advantage of a jittery movement, in areas of radius 0.15 m around its current locations and by

testing $N_{\text{jitt}} = 20$ points at each step. The sensing model is the same as the one used for the previous simulations, except that we use $d_{\text{sen}} = 1.0$ m in this case. The Pioneer robot is modeled by the holonomic dynamical model of this chapter, with $u_{\max,k} = 1.5$. A simple obstacle avoidance strategy, similar to the one proposed in [6], is also used. The left and right figures in Fig. 4.9 show the trajectory of the mobile sensor in the communication-constrained and hybrid approaches respectively, where the true connectivity map to the remote station is superimposed on the blueprint of the basement. Fig. 4.10 then compares the resulting average of the detection error probability at the remote station, as a function of time step t.

It can be seen that, although multipath fading power is large, the mobile sensor maintains its connectivity along its entire trajectory in the communication-constrained approach, as expected. More precisely, in this example it maintains its connectivity at 97.3% of the entire operation time. The hybrid approach, however, achieves a smaller average probability of detection error at the end of operation, compared to the communication-constrained approach. It also ensures that the mobile sensor is connected by the end of the operation.

Finally, Fig. 4.12 summarizes the results and observations of this chapter, in terms of the level of communication and sensing awareness of a motion planning strategy and its impact on the overall performance.

4.7 Summary

In this chapter, we considered the scenario where a team of mobile sensors are deployed by a remote station to explore a given environment, detect an unknown number of static targets and inform the remote station of their findings. We studied the problem of designing the trajectories of the mobile sensors to minimize the probability of target detection error at the remote station, while satisfying the requirements

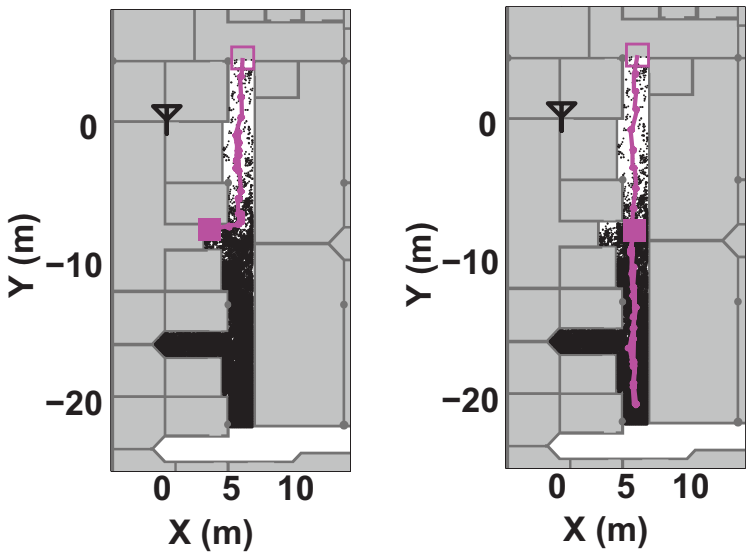

Figure 4.9: Performance of the proposed communication-aware surveillance framework using real channel measurements in an indoor environment (basement of the Electrical and Computer Engineering building at UNM). The left and right figures show the trajectory of the mobile sensor in the communication-constrained and hybrid approaches respectively, where the true connectivity map to the remote station is superimposed on the blueprint of the basement.

on the connectivity of the mobile sensors to the remote station. We showed how to design such trajectories by co-optimization of sensing (information gathering) and communication (information exchange). Based on the requirement on the connectivity of the mobile sensors to the remote station, we considered two cases. First, we considered the case where the mobile sensors need to constantly update the remote station on the locations of the targets. For this case, we proposed our *communication-constrained* motion planning approach which enables the mobile sensors to explore the workspace while maximizing their probability of connectivity to the remote station during the entire operation. We proved that the overall motion optimization objective function, in this case, is a multiplication of a sensing function that maximizes the Kullback-Leibler (KL) divergence between the maximum uncertainty state and the current one, with a communication function, that maximizes the probability

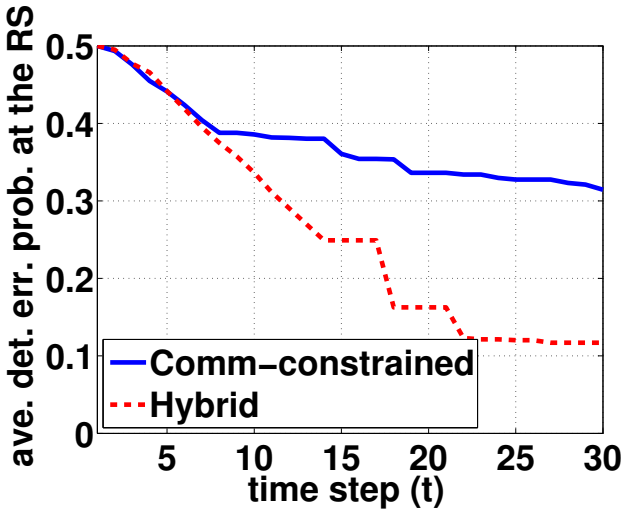

Figure 4.10: The resulting average of the detection error probability at the remote station (RS), as a function of time step t, for the indoor environment of Fig. 4.9.

of connectivity to the remote station.

Second, we considered the case where the remote station only needs to be informed of the locations of the targets at the end of a given operation time. By building on our communication-constrained results, we proposed our *hybrid* motion planning approach for this case. This approach plans the motion of the mobile sensors such that they explore the workspace with less connectivity constraint on their motion, as compared to the communication-constrained approach, while maximizing their probability of connectivity at the end of the operation. We mathematically characterized the asymptotic behavior of our proposed approaches under certain conditions. We showed that, in terms of the final detection error probability at the remote station, the hybrid approach outperforms the communication-constrained one, while the latter provides better constant connectivity and, therefore, is more robust to abrupt termination of the operation. We finally proposed strategies to further increase the robustness of both approaches to multipath fading.

Figure 4.11: The picture of the Pioneer 3-AT robot, equipped with directional and omni-directional antennas, used for channel measurements in the indoor surveillance scenario of Fig. 4.9. Only omni-directional channel measurement were used in this example.

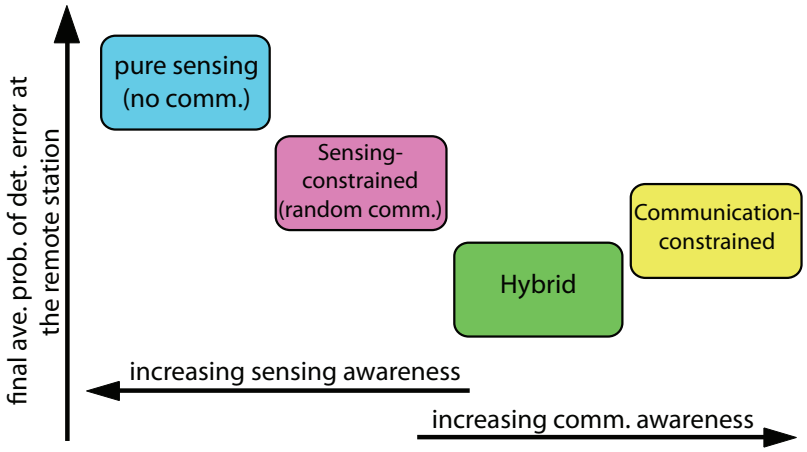

Figure 4.12: Comparison of different motion planning approaches, based on the level of communication and sensing awareness and its impact on the overall performance.

Chapter 5

Communication-Aware Dynamic Coverage of Time-Varying Environments Using Mobile Networks

Deployment of a group of mobile sensors/robots/agents[1] to dynamically cover a number of points of interest (POIs) in a spatially-large environment has a broad range of applications in robotics and mobile sensor networks [15,17,75,85]. Covering the POIs may refer to sensing the POIs using the onboard sensors of the mobile agents. It may also refer to servicing or performing a task at the POIs. By a spatially-large environment, we mean an environment in which the POIs cannot be fully covered by any static configuration of the mobile agents, possibly due to the small effective ranges of their onboard sensors/actuators, as compared to the size

[1]In this chapter, we intentionally use "mobile agents" as opposed to "mobile sensors" to emphasize that the nodes can also be active nodes that are able to actuate or change the environment.

of the environment. In the dynamic coverage problem, we are then interested in planning the motion of the mobile agents such that they can cover all the POIs in a spatially-large environment. This translates to planning the motion of the mobile agents to minimize/maximize a quantity of interest at the POIs [17, 75]. Such quantity is specifically defined for the given dynamic coverage problem (we explain this later in this section through some examples).

In this chapter, we consider an extended version of the dynamic coverage problem where a number of mobile agents, with limited energy budgets and sensing/actuation capabilities, are deployed to cover a set of POIs in a *time-varying* environment. By a time-varying environment, we refer to an environment where the quantity of interest is time-varying and increasing in time at every POI that is not in the effective range of any mobile agent. We also consider a communication-constrained scenario, where the mobile agents are required to communicate to a fixed remote station in order to complete their coverage task. Our goal in this chapter is then to plan the motion and communication policies of the mobile agents to minimize the total energy (the summation of the motion and communication energy) consumption of the mobile agents, while 1) guaranteeing the boundedness of the quantity of interest at all the POIs, and 2) meeting the constraints on the connectivity of the mobile agents to the remote station, the frequency of covering the POIs, and the total energy budget of the mobile agents. Note that since the quantity of interest is continuously increasing at the POIs, *periodic* trajectories need to be devised for the mobile agents in order to repeatedly cover the POIs. A schematic of the dynamic coverage problem considered in this chapter is shown in Fig. 5.1.

Several real-world applications can be modeled by a dynamic coverage problem. Next, we provide four examples from mobile sensor networks and robotics literature:

1. The first example is surveillance and monitoring of a time-varying environment using a team of mobile agents. Here, the remote station is a monitoring station

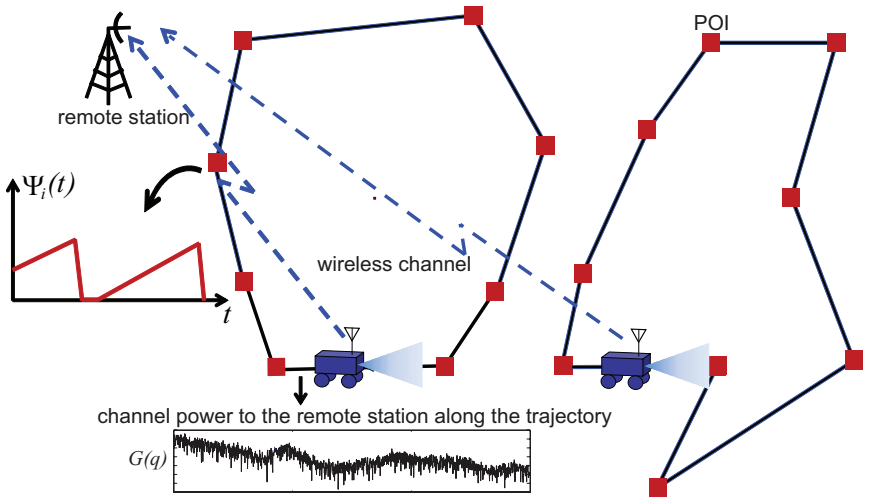

Figure 5.1: Dynamic coverage of a time-varying environment using a team of mobile agents. $\Psi_i(t)$ is the quantity of interest at the i^{th} POI that needs to be kept bounded by periodically visiting the POI.

and the quantity of interest that needs to be kept bounded is the uncertainty on the time-varying states of the POIs at the remote station. In this example, a POI is covered if it can be sensed by the onboard sensor of a mobile agent (e.g., a digital camera). This example can be considered as the extension of the surveillance problem of Chapter 4 to a time-varying environment.[2]

2. The second example is estimation over wireless communication links. The POIs in this example represent a number of dynamical systems, spatially distributed over the workspace, whose states need to be estimated at a remote station. A number of mobile agents then observe the dynamical systems along periodic trajectories and send their observations to the remote station over wireless

[2]To see this more clearly, consider the target detection problem of Chapter 4, where additionally the presence or absence of a target at a POI is modeled by a Markov process. The state of each POI is a binary value which is one if there is a target at the POI, and is zero otherwise. The problem of estimating the state of the POIs, using the observations collected by the sensing devices of the mobile agents, can be formulated by a hidden Markov model (HMM), which is an extension of the detection framework of Chapter 4. The quantity of interest to keep bounded is the uncertainty of the state estimation, i.e., the probability of detection error at the remote station.

communication links. A POI is covered in this examples if its state can be observed by a mobile agent and communicated to the remote station. The quantity of interest to keep bounded for each POI is then the uncertainty of its state estimation (e.g., the estimation error variance) at the remote station. This uncertainty is increasing in time when the POI is not covered by any agent.

3. The third example is information collection in a time-varying environment, where the POIs represent a number of stationary data loggers that are distributed over a spatially-large environment to log time-variations of an environmental feature (e.g. temperature, humidity, radioactive contamination). The information bits (which are increasing in time at each data logger) need to be collected and transmitted to a remote station. A number of mobile agents are then tasked to move along periodic trajectories, collect the information bits from the data loggers, and transmit them to the remote station at positions where they get connected along their trajectories. The quantity of interest to keep bounded in this example is the size of the queue of the POIs through proper information collection and communication.

4. The fourth example is a remotely controlled robotic operation for collecting hazardous materials that are continuously produced at some POIs in the environment. In this example, the remote station is in charge of remotely controlling the mobile agents. The quantity of interest to be kept bounded is also the volume of the hazardous materials at all the POIs. The coverage in this case means collecting the hazardous materials from the POIs, using the onboard actuators of the mobile agents.

In all these examples, the communication to a remote station is crucial. Therefore, considering the effect of realistic fading communication channels between the mobile agents and the remote station is considerably important. The dynamics of

the quantity of interest depends on both local coverage (sensing/servicing) performance and communication link qualities between the mobile agents and the remote station. Similar to the previous chapters, a communication-aware strategy is then required to co-optimize the information-gathering (local coverage) and information-exchange (communication) performance of the mobile agents. Next, we explain our communication-aware approach for dynamic coverage of time-varying environments in more detail.

We consider a linear dynamics for the time-variation of the quantity of interest at the POIs.[3] We then propose motion and communication policies for the mobile agents to minimize the total energy consumption of the mobile agents in each period, while guaranteeing that the quantity of interest at the POIs remains bounded, and the constraints on the connectivity of the mobile agents, the frequency of covering the POIs, and the total energy budget of the mobile agents are satisfied. We start with the case where the sensing/actuation range of the mobile agents is small such that each agent is required to move to the position of each POI and stop there for some time to sense/service it (this assumption is then relaxed at the end of the chapter). We also assume a limited total energy budget for the mobile agents. To keep our framework general, we consider two variants of the problem: *communication-intensive* and *communication-efficient*. Communication-intensive case refers to the case where the mobile agents are required to be connected at all the POIs they visit, in order to send their collected information to the remote station in real-time. Communication-efficient case, on the other hand, refers to the case where the mobile agents are only required to connect to the remote station once along their trajectories, decreasing the communication burden considerably. In both communication-intensive and communication-efficient cases, we show how to optimally find the trajectories of the

[3]While the dynamics of the quantity of interest in the aforementioned problems could be nonlinear, a linear approximation may be a close enough approximation depending on the system parameters.

mobile agents, as well as their stop times and transmission powers at the POIs, using mixed-integer linear programs (MILPs). The properties of the optimal solutions of the MILPs, as well as their asymptotic properties, are also characterized mathematically.

We next continue with extending our framework by considering a non-zero range for the sensing/actuation device of the mobile agents and adapting their velocities and transmission rates (in addition to their transmission powers) along their trajectories. Unlike the previous case, here we take into account the amount of information (the number of information bits) that is transmitted to and correctly received by the remote station along the trajectories of the mobile agents. For the sake of simplicity, however, we consider only one mobile agent. We then show how to plan the trajectory of the mobile agent, as well as its transmission power, transmission rate and velocity, can be optimally found using an MILP. Finally, the solution of the proposed MILP is also characterized mathematically in this case.

The rest of this chapter is organized as follows. In Section 5.1, we present our system model for dynamic coverage of a time-varying environment. In this section, we present a linear dynamics for the time-variations of the quantity of interest at the remote station, which depends on both the local sensing qualities of the mobile agents as well as their communication link qualities to the remote station. In Section 5.2, we then propose a novel MILP program to find the optimal trajectories of the mobile agents, as well as their optimal stop times and transmission powers at the POIs, in the communication-intensive case. In Section 5.3, we extend all the results of Section 5.2 to the communication-efficient case. In both Section 5.2 and Section 5.3, we also provide a probabilistic analysis of the solutions of the proposed MILPs. We present our extensive simulation results in Section 5.4. In Section 5.5, we then extend our framework to the case where the range of the sensing/actuation devices of the mobile agents is not zero, and the velocities, transmission powers and transmission

rates along the trajectories of the mobile agents are adaptive. The dynamic coverage problem in this case is solved optimally in Section 5.6 using a novel MILP program. A mathematical analysis of the solution of the MILP and its special cases (e.g. when sensing/actuation range goes to zero) is also provided in this section. We present our simulation results for this extended case in Section 5.7, followed by a summary of the results of the chapter in Section 5.8.

5.1 System Modeling

Consider an obstacle-free workspace $\mathcal{W} \subset \mathbb{R}^2$, which contains a set of m POIs $\mathcal{Q} = \{q_1, \cdots, q_m\}$. Let $\Psi_i(t)$, for $i = 1, \cdots, m$, represent the quantity of interest that needs to be controlled at the i^{th} POI. We assume a time-varying workspace, where $\Psi_i(t)$ increases with a certain rate as long as the i^{th} POI is not being covered (sensed/serviced) by any mobile agent. Then, as soon as the POI is covered by a connected mobile agent, $\Psi_i(t)$ decreases with a rate that depends on the onboard sensing capabilities of the mobile agent. In order to keep $\Psi_i(t)$ bounded at all the POIs, we therefore use a team of n mobile agents to repeatedly cover the POIs in the workspace. Each mobile agent is assigned to a nonempty subset of the POIs. A closed periodic trajectory is then planned for each agent to cover every point in this subset.

Let $\mathcal{V} = \{1, \cdots, m\}$ denote the set of the indices of the POIs. Also, let $\mathcal{V}_k$, for $k = 1, \cdots, n$, represent the nonempty subset of $\mathcal{V}$ assigned to the k^{th} agent. In this section, we consider the following assumptions:

Assumption 5.1.1. *The sets $\{\mathcal{V}_k\}_{k=1}^n$ define a partition of $\mathcal{V}$, i.e., $\bigcup_{k=1}^n \mathcal{V}_k = \mathcal{V}$ and $\mathcal{V}_{k_1} \cap \mathcal{V}_{k_2} = \emptyset$, for $k_1 \neq k_2$. Therefore, each POI is assigned to one agent only.*

Assumption 5.1.2. *The trajectory of each mobile agent k defines a Hamiltonian cycle, shown by $\mathcal{C}_k$, on $\mathcal{V}_k$. In other words, for each mobile agent k, we assume a*

piecewise-linear trajectory that passes through all the POIs in $\mathcal{V}_k$ and visits each POI exactly once in each period.

Assumption 5.1.3. *The effective ranges of the onboard sensors of the mobile agents are negligible, compared to the size of the workspace. Therefore, in order to cover each POI, each agent is required to physically move to the position of the POI.*

These assumptions imply that 1) the optimal trajectory for k^{th} agent, without loss of generality, can be selected from the set of the Hamiltonian cycles on the POIs in $\mathcal{V}_k$ and 2) due to negligible effective ranges, each agent is required to stop at each POI for a limited time to sense it. As explained previously, depending on the requirement on the connectivity of the mobile agents to the remote station, we consider two cases in this section: *communication-intensive* and *communication-efficient*. In the communication-intensive case, the mobile agent k is required to be connected to the remote station at all the POIs in $\mathcal{V}_k$. This case is suitable, for instance, for the scenario where communication is needed to permit local sensing/servicing. In the communication-efficient case, on the other hand, the connectivity at all the POIs is not a constraint. Each mobile agent k covers the POIs in $\mathcal{V}_k$ and completes its coverage task by communicating to the remote station at one pre-selected position along its trajectory, reducing the communication burden considerably. At this position, the mobile agent informs the remote station of the states of all the POIs it has covered in one period. In this chapter, we adopt two extended versions of the linear model proposed in [75], for the dynamics of $\Psi_i(t)$ in both communication-intensive and communication-efficient cases:

1. Communication-intensive case:

$$\dot{\Psi}_i(t) = \mathrm{I}\big(\Psi_i(t) \geq 0\big)\Big[\rho_i - \lambda_k(t)\mathrm{I}\big(\xi_k(t) = q_i\big)\alpha_{i,k}\Big], \;\; \forall i \in \mathcal{V}_k, \; k = 1, \cdots, n, \tag{5.1}$$

2. Communication-efficient case:

$$\Psi_i(t) = \Phi_i\big(\tau_k(t)\big) + \rho_i\big[t - \tau_k(t)\big],$$
$$\dot{\Phi}_i(t) = \mathrm{I}\big(\Phi_i(t) \geq 0\big)\Big[\rho_i - \mathrm{I}\big(\xi_k(t) = q_i\big)\alpha_{i,k}\Big], \quad \forall i \in \mathcal{V}_k,\ k = 1, \cdots, n, \qquad (5.2)$$

where I(.) denotes the indicator function, $\xi_k(t)$ is the position of the k^{th} mobile agent at time t, $\lambda_k(t)$ is a binary value which is one if the k^{th} agent is connected to the remote station at time t along its trajectory and zero otherwise and $\tau_k(t) \triangleq \max\big\{0 \leq \tau \leq t \big| \lambda_k(\tau) = 1\big\}$ specifies the last time the k^{th} agent has been connected to the remote station up to time t in the communication-efficient case. Furthermore, ρ_i determines the constant rate at which $\Psi_i(t)$ increases, while it is not being covered by any mobile agent, $\alpha_{i,k}$ represents the constant *service rate* of the k^{th} mobile agent at the i^{th} POI, and $\Phi_i(t)$ is an auxiliary function.[4] Characterization of the service rate depends on the sensing/servicing performance of each individual agent.

The dynamical model of (5.1) implies that $\Psi_i(t)$ increases with rate ρ_i, whenever the k^{th} mobile agent is not connected to the remote station or the POI is not covered by the mobile agent. This implies that the mobile agents need to maintain their connectivity, while covering the POIs, in order to bound $\Psi_i(t)$, for all $i \in \mathcal{V}$. On the other hand, in the dynamical model of (5.2), the mobile agents are not required to maintain their connectivity at the POIs, provided that they get connected to the remote station at least once along their trajectory.

5.1.1 Communication Model of the Mobile Agents

The binary value $\lambda_k(t)$ of (5.1) and (5.2), is a function of the signal-to-noise ratio (SNR) of the uplink channels from the k^{th} agent to the remote station at time

[4] In the communication-efficient case, $\Phi_i(t)$ can be treated as the local version of $\Psi_i(t)$ at the k^{th} agent, while $\Psi_i(t)$ is defined for the remote station.

t [59]. Similar to the previous chapters, in a realistic communication setting and in the presence of a packet-dropping receiver at the remote station, $\lambda_k(t)$ is given as follows:

$$\lambda_k(t) = \begin{cases} 1, & \frac{P_{\mathrm{TX},k}(t)G_k(t)}{N_0 B} \geq \mathrm{SNR}_{\mathrm{TH}}, \\ 0, & \text{otherwise}, \end{cases} \qquad k = 1, \cdots, n, \tag{5.3}$$

where $P_{\mathrm{TX},k}(t)$ is the transmission power of the k^{th} agent at time t along its trajectory, $G_k(t)$ represents the instantaneous channel power in transmission from the k^{th} agent to the remote station at time t along its trajectory, $\frac{N_0}{2}$ is the power spectral density (PSD) of the receiver noise, B is the channel bandwidth and $\mathrm{SNR}_{\mathrm{TH}}$ is the packet-dropping threshold of the receiver of the remote station, which depends on the quality of decoding at the remote station [59, 93]. The instantaneous channel power $G_k(t)$ is a function of the position of the k^{th} agent at time t: $G_k(t) = G\big(\xi_k(t)\big)$, where $G(q)$, for $q \in \mathcal{W}$, denotes the 2D map of channel power in the workspace. When designing our optimal coverage policies in Sections 5.2.2 and 5.3.2, we start by assuming that $G(q)$ is known for every $q \in \mathcal{W}$. This assumption, however, may not be feasible in practical applications, where the channel is only known at a small number of positions in the workspace. In such cases, similar to the previous chapters, we use the probabilistic channel assessment framework of Chapter 2 to assess the distribution of the channel power at unvisited locations. Considering such stochastic channel models, when designing the optimal dynamic coverage policies, is typically challenging. Our proposed approach is based on stochastic programming and is discussed in Sections 5.2.3 and 5.3.3.

Note that each mobile agent needs to be connected in order to communicate to the remote station at the positions of the POIs (in the communication-intensive case) or at one predefined point along its trajectory (in the communication-efficient case). Let $P_{\mathrm{TX},i,k}$, for $i \in \mathcal{V}_k$, denote the transmission power of the k^{th} mobile agent at the i^{th} POI in the communication-intensive case. Also, let t_c denote a fixed communication time assigned for communication to the remote station. We

assume that t_c is small enough such that sending/receiving the packets at each POI can be finished while the mobile agent is stopped at the POI (or is still very close to it). Then, in the communication-intensive case we have $P_{\text{TX},k}(t) = P_{\text{TX},i,k}$ for a total time period of length t_c at the i^{th} POI, and $P_{\text{TX},k}(t) = 0$ otherwise. Similarly, in the communication-efficient case, the mobile agent communicates to the remote station at one selected point along their trajectory. Let $\xi_{\text{TX},k}$ and $P_{\text{TX},k}$ denote the communication point and the fixed transmission power of the k^{th} mobile agent in the communication efficient case, respectively. Similar to the communication-intensive case, we then have $P_{\text{TX},k}(t) = P_{\text{TX},k}$ for a total time period of length t_c at position $\xi_{\text{TX},k}$, and $P_{\text{TX},k}(t) = 0$ otherwise. We find the optimal values of $P_{\text{TX},i,k}$, for $i \in \mathcal{V}_k$, in Section 5.2 and the optimal values of $\xi_{\text{TX},k}$ and $P_{\text{TX},k}$ in Section 5.3.

5.1.2 Energy Consumption Model of the Mobile Agents

The total energy consumed by a mobile agent in one period is the summation of its motion energy and its communication energy. The motion energy is the time integral of the motion power, which itself is a function of the velocity and power loss of the mobile agent. We adopt the following model for the motion power of the k^{th} agent [102, 103]:

$$P_{m,k}(t) = \begin{cases} P_{\text{loss},s,k}, & \xi_k(t) = q_i, \text{ for some } i \in \mathcal{V}_k, \\ P_{\text{loss},m,k} + w_k v_k, & \text{otherwise}, \end{cases} \tag{5.4}$$

where $P_{\text{loss},m,k}$ and v_k are the velocity and the power loss of the k^{th} agent while moving from one POI to another, $P_{\text{loss},s,k}$ denotes its power loss while stopping at one of the POIs, and w_k is a constant that depends on the dynamics of the k^{th} agent. Note that we include all the constant power losses (i.e., motion, computation and actuation losses) in $P_{\text{loss},m,k}$ and $P_{\text{loss},m,s}$ terms. Therefore, generally $P_{\text{loss},m,k}$ is different from (typically smaller than) $P_{\text{loss},s,k}$. Another note is that, without loss of generality, the velocity of the each mobile agent is assumed constant. The reason

is that both sensing/actuation and communication happen either at the positions of the POIs or at one point along the trajectory of the agent. Therefore, adaptation of speed is not required. In fact the optimal velocity for each mobile agent is the maximum possible velocity, as shown in the next section.

As explained previously, the periodic trajectory of each mobile agent defines a Hamiltonian cycle on the set of POIs assigned to it. Let $\mathcal{C}_k$ denote the Hamiltonian cycle defined on the set of POIs in $\mathcal{V}_k$, with $\mathrm{d}(\mathcal{C}_k)$ denoting its total Euclidean length. Also, let $t_{i,k}$, for $i \in \mathcal{V}_k$, denote the stop time of the k^{th} mobile agent at the i^{th} POI. The motion energy consumed in one period by the k^{th} agent, in both communication-intensive and communication-efficient cases, is then calculated as follows:

$$E_{m,k} = \int_{T_k} P_{m,k}(t)dt = P_{\text{loss},s,k} \sum_{i \in \mathcal{V}_k} t_{i,k} + \left(\frac{P_{\text{loss},m,k}}{v_k} + w_k \right) \mathrm{d}(\mathcal{C}_k), \tag{5.5}$$

where $T_k = \sum_{i \in \mathcal{V}_k} t_{i,k} + \frac{\mathrm{d}(\mathcal{C}_k)}{v_k}$ denotes the period of the movement of the k^{th} mobile agent along its trajectory (including the summation of the stop times at the POIs).

The communication energy, on the other hand, is consumed when a mobile agent transmits data to the remote station. Based on the connectivity model of the mobile agents discussed in the previous section, the communication energy consumed in one period by the k^{th} agent in the communication-intensive case becomes

$$E_{c,k} = \int_{T_k} P_{\text{TX},k}(t)dt = t_c \sum_{i \in \mathcal{V}_k} P_{\text{TX},i,k}. \tag{5.6}$$

In the communication-efficient case, on the other hand, we have the following for communication energy consumed in one period the k^{th} agent

$$E_{c,k} = \int_{T_k} P_{\text{TX},k}(t)dt = t_c P_{\text{TX},k}. \tag{5.7}$$

Finally, the total energy consumed by the k^{th} agent in one period is given as $E_k = E_{m,k} + E_{c,k}$.

5.2 Dynamic Coverage of Time-Varying Environments in the Communication-Intensive Case

In this section, we study the problem of dynamic coverage of time-varying environments in the communication-intensive case. More specifically, we provide a formal definition of feasible stabilizing dynamic coverage policies and formulate the dynamic coverage problem. We then show how to design optimal feasible stabilizing dynamic coverage policies for a given team of mobile agents using a mixed-integer linear program (MILP). Furthermore, we show how to modify the MILP, using methods from stochastic programming, to consider stochastic communication channels. We conclude this section by a probabilistic analysis of the dynamic coverage task, when both the channel and the positions of the POIs are stochastic and the number of POIs is large.

5.2.1 Problem Formulation

Consider the dynamical system of (5.1). In the communication-intensive case, we are interested in finding dynamic coverage policies that make this dynamical system stable, while meeting the constraints on 1) the connectivity of the mobile agents, 2) the minimum frequency (maximum period) of covering the POIs, and 3) the total energy consumption in one period. A dynamic coverage policy in the communication-intensive case is a tuple of all the design variables and is defined as follows:

Definition 5.2.1. *In the communication-intensive case, a dynamic coverage policy for the k^{th} mobile agent is a tuple $\mathcal{P}_k = \big(\mathcal{V}_k, \mathcal{C}_k, v_k, \{P_{\mathrm{TX},i,k}\}_{i\in\mathcal{V}_k}, \{t_{i,k}\}_{i\in\mathcal{V}_k}\big)$, where $\mathcal{V}_k$ is the non-empty set of POIs assigned to the k^{th} agent, $\mathcal{C}_k$ denotes the Hamiltonian cycle defined on $\mathcal{V}_k$, and v_k is the constant velocity of the k^{th} agent. Also, $P_{\mathrm{TX},i,k}$ and $t_{i,k}$, for $i \in \mathcal{V}_k$, are the transmission power and the stop time of the k^{th} agent at the i^{th}*

POI. The overall dynamic coverage policy to find is then the tuple $\mathcal{P} = (\mathcal{P}_1, \cdots, \mathcal{P}_n)$.

Given the channel powers at all the POIs, the available energy budget of each mobile agent, the constraint on the frequency of covering each POI, and the maximum transmission power of each agent, only a finite set of dynamic coverage policies is acceptable. This motivates the definition of *feasible dynamic coverage policies* in the communication-intensive case:

Definition 5.2.2. *A dynamic coverage policy* $\mathcal{P}$ *is feasible in the communication intensive case if the following are true:*

$$1)\ \sum_{i\in\mathcal{V}_k} t_{i,k} + \frac{\mathrm{d}(\mathcal{C}_k)}{v_k} \le T_{\max}, \qquad k = 1, \cdots, n, \tag{5.8}$$

$$2)\ P_{\mathrm{loss},s,k} \sum_{i\in\mathcal{V}_k} t_{i,k} + \left(\frac{P_{\mathrm{loss},m,k}}{v_k} + w_k\right) \mathrm{d}(\mathcal{C}_k) + t_c \sum_{i\in\mathcal{V}_k} P_{\mathrm{TX},i,k} \le E_{\max,k}, \quad k = 1, \cdots, n,$$

$$3)\ P_{\mathrm{TX},\max,k} \ge P_{\mathrm{TX},i,k} \ge \frac{P_{\mathrm{TH}}}{G(q_i)}, \qquad \forall i \in \mathcal{V}_k,\ k = 1, \cdots, n,$$

$$4)\ 0 \le v_k \le v_{\max,k}, \qquad k = 1, \cdots, n.$$

Here, $P_{\mathrm{TH}} \triangleq \mathrm{SNR}_{\mathrm{TH}} N_0 B$, $T_{\max}$ *is the given maximum acceptable period for covering all the POIs,* $E_{\max,k}$, $P_{\mathrm{TX},\max,k}$ *and* $v_{\max,k}$ *are the given maximum total energy, maximum transmission power and maximum velocity of the* k^{th} *agent, and* $\mathrm{SNR}_{\mathrm{TH}}$ *is the packet-dropping threshold of the receiver of the remote station, as defined in (5.3).*

Note that the lower-bound $\frac{P_{\mathrm{TH}}}{G(q_i)}$, on the feasible transmission power at the i^{th} POI, is the minimum transmission power required for being connected based on (5.3). Also note that, depending on the channel powers at the POIs and the thresholds $T_{\max}$, $P_{\mathrm{TX},\max,k}$ and $E_{\max,k}$, a feasible dynamic coverage policy may not exist. However, if such feasible policies exist, we are interested in finding those feasible policies that make the dynamic coverage task stable, while minimizing the total energy consumption. The formal definition of a stable coverage task is given as follows:

Definition 5.2.3. *A dynamic coverage task is called stable if there exists a finite* $\overline{\Psi}$*, independent of the initial conditions, such that* $\max_{1\leq i\leq m}\sup_{t\geq 0}\Psi_i(t)\leq\overline{\Psi}$.

The following lemma gives a necessary and sufficient condition for a feasible policy $\mathcal{P}$ to stabilize the dynamic coverage task:

Lemma 5.2.1. *A feasible dynamic coverage policy* $\mathcal{P}$ *is stabilizing, i.e., it stabilizes the dynamic coverage task, if and only if there exist non-negative stability margins* $\Delta_1,\cdots,\Delta_n$ *such that*

$$\alpha_{i,k}t_{i,k}-\rho_i\left(\sum_{j\in\mathcal{V}_k}t_{j,k}+\frac{\mathrm{d}(\mathcal{C}_k)}{v_k}\right)\geq\Delta_k,\qquad\forall i\in\mathcal{V}_k,\ k=1,\cdots,n. \tag{5.9}$$

Proof. Consider POI $i\in\mathcal{V}_k$ and dynamical system (5.1) and (5.2). When the dynamic coverage policy is feasible, the k^{th} mobile agent is connected to the remote station at all the POIs in the communication-intensive case, i.e., $\lambda_k(t)=1$ whenever $\mathrm{I}\big(\xi_k(t)=q_i\big)=1$, for $i\in\mathcal{V}_k$. Then, the dynamic coverage task is stable, based on Definition 5.2.3, if and only if $\Psi_i(t+T_k)\leq\Psi_i(t)$, for $i\in\mathcal{V}_k$, $k=1,\cdots,n$ and any t. Here, T_k is the period of movement of the k^{th} mobile agent. From (5.1), $\Psi_i(t+T_k)-\Psi_i(t)=\rho_iT_k-\alpha_{i,k}t_{i,k}$. Furthermore, we have $T_k=\sum_{i\in\mathcal{V}_k}t_{i,k}+\frac{\mathrm{d}(\mathcal{C}_k)}{v_k}$. Therefore, the necessary and sufficient condition for stability to satisfy $\Psi_i(t+T_k)\leq\Psi_i(t)$ is given by (5.9). Similar results also hold for a feasible coverage policy in the communication-efficient case. □

By an optimal feasible stabilizing policy, we then refer to a feasible stabilizing policy $\mathcal{P}$, based on conditions (5.8) and (5.9), that optimizes a performance measure defined for the dynamic coverage task. In this section, we focus on maximizing the *lifetime* of the mobile agents. We define the lifetime of each mobile agent as the number of times it covers its assigned POIs. Assuming a fixed total energy for each mobile agent for the entire operation, maximizing the lifetime is equivalent to

minimizing the total energy consumption of the mobile agent during one period. Therefore, we have the following optimization problem to find the optimal feasible stabilizing policies in the communication-intensive case:

Problem 5.2.1. *The maximum-lifetime feasible stabilizing dynamic coverage policy for coverage of a time-varying environment in the communication-intensive case is given as follows:*

$$\min_{\mathcal{P},E_1,\cdots,E_n} \sum_{k=1}^{n} \varpi_k E_k,$$

s.t.

$$1)\ \alpha_{i,k}t_{i,k} - \rho_i\left(\sum_{j\in\mathcal{V}_k} t_{j,k} + \frac{\mathrm{d}(\mathcal{C}_k)}{v_k}\right) \geq \Delta_k, \qquad \forall i \in \mathcal{V}_k,\ k = 1,\cdots,n,$$

$$2)\ \sum_{i\in\mathcal{V}_k} t_{i,k} + \frac{\mathrm{d}(\mathcal{C}_k)}{v_k} \leq T_{\max}, \qquad k = 1,\cdots,n,$$

$$3)\ P_{\mathrm{loss},s,k}\sum_{i\in\mathcal{V}_k} t_{i,k} + \left(\frac{P_{\mathrm{loss},m,k}}{v_k} + w_k\right)\mathrm{d}(\mathcal{C}_k) + t_c\sum_{i\in\mathcal{V}_k} P_{\mathrm{TX},i,k} \leq E_k,\ \ k = 1,\cdots,n,$$

$$4)\ P_{\mathrm{TX},\max,k} \geq P_{\mathrm{TX},i,k} \geq \frac{P_{\mathrm{TH}}}{G(q_i)}, \qquad \forall i \in \mathcal{V}_k,\ k = 1,\cdots,n,$$

$$5)\ 0 \leq v_k \leq v_{\max,k}, \qquad k = 1,\cdots,n,$$

$$6)\ E_k \leq E_{\max,k}, \qquad k = 1,\cdots,n, \tag{5.10}$$

where we set $\Delta_k \geq 0$ *and* $\varpi_k > 0$.

Note that $\Delta_k > 0$ is a given system design parameter that increases the robustness of the optimal policy to modeling errors and disturbances. Robustness, however, comes at the cost of consuming more energy, as expected. The next section is dedicated to solving this problem using an MILP.

5.2.2 Optimal Solution of the Dynamic Coverage Problem in the Communication-Intensive Case – Case of Known Channel Powers at the POIs

In the main theorem of this section (Theorem 5.2.1), we provide a closed form expression for the optimal policy of each agent, given a partition $\{\mathcal{V}_k\}_{k=1}^n$. We furthermore confirm that the optimal Hamiltonian cycle is the minimum-length Hamiltonian cycle and the optimal speed is $v_{\max}$.

Theorem 5.2.1. *Consider a partition $\{\mathcal{V}_k\}_{k=1}^n$ of $\mathcal{V}$. Then, assuming that $G(q_i)$, for $i \in \mathcal{V}$, are known, the following are true for the solution of Problem 5.2.1 in the communication-intensive case:*

1. *For a given set of non-negative stability margins Δ_k, $k = 1, \cdots, n$, Problem 5.2.1 is feasible if and only if the following are true, for $k = 1, \cdots, n$:*

   $$1)\ \frac{P_{\text{TH}}}{G(q_i)} \leq P_{\text{TX,max},k}, \qquad \forall i \in \mathcal{V}_k, \tag{5.11}$$

   $$2)\ \sum_{i \in \mathcal{V}_k} \frac{\rho_i}{\alpha_{i,k}} < 1,$$

   $$3)\ \frac{\mathrm{d}(\mathcal{H}_k)}{v_{\max,k}} \leq \min\left\{ T_{\max}\phi_k - \Delta_k \eta_k, \frac{\big(\overline{E}_{\max,k} - w_k \mathrm{d}(\mathcal{H}_k)\big)\phi_k - \Delta_k \eta_k P_{\text{loss},s,k}}{(1-\phi_k)P_{\text{loss},s,k} + \phi_k P_{\text{loss},m,k}} \right\},$$

   where $\mathcal{H}_k$ denotes the minimum-length Hamiltonian cycle on $\mathcal{V}_k$, $\overline{E}_{\max,k} \triangleq E_{\max,k} - t_c \sum_{i \in \mathcal{V}_k} \frac{P_{\text{TH}}}{G(q_i)}$, $\phi_k \triangleq 1 - \sum_{i \in \mathcal{V}_k} \frac{\rho_i}{\alpha_{i,k}}$ and $\eta_k \triangleq \sum_{i \in \mathcal{V}_k} \frac{1}{\alpha_{i,k}}$.

2. *The maximum stability margin that can be selected for each agent k, for $k = 1, \cdots, n$, is given as follows when $\sum_{i \in \mathcal{V}_k} \frac{\rho_i}{\alpha_{i,k}} < 1$:*

   $$\Delta_{\max,k} = \min\left\{ \frac{\overline{E}_{\max,k} - w_k \mathrm{d}(\mathcal{H}_k) + \big(P_{\text{loss},s,k} - P_{\text{loss},m,k}\big)\frac{\mathrm{d}(\mathcal{H}_k)}{v_{\max,k}}}{P_{\text{loss},s,k}}, T_{\max} \right\} \frac{\phi_k}{\eta_k} - \frac{1}{\eta_k}\frac{\mathrm{d}(\mathcal{H}_k)}{v_{\max,k}}. \tag{5.12}$$

3. *There exists a feasible stabilizing policy, i.e., Problem 5.2.1 is feasible for at least one set of non-negative Δ_k, if and only if the following are true, for $k = 1, \cdots, n$:*

$$1)\ \frac{P_{\mathrm{TH}}}{G(q_i)} \leq P_{\mathrm{TX,max},k}, \qquad \forall i \in \mathcal{V}_k, \tag{5.13}$$

$$2)\ \sum_{i \in \mathcal{V}_k} \frac{\rho_i}{\alpha_{i,k}} < 1,$$

$$3)\ \frac{\mathrm{d}(\mathcal{H}_k)}{v_{\max,k}} \leq \min\left\{T_{\max}, \frac{\overline{E}_{\max,k} - w_k \mathrm{d}(\mathcal{H}_k)}{(1-\phi_k)P_{\mathrm{loss},s,k} + \phi_k P_{\mathrm{loss},m,k}}\right\}\phi_k.$$

4. *If Problem 5.2.1 is feasible, the optimal Hamiltonian cycle, velocity and transmission power of the k^{th} agent, for $k = 1, \cdots, n$, are given as follows: $\mathcal{C}_k^* = \mathcal{H}_k$, $v_k^* = v_{\max,k}$ and $P_{\mathrm{TX},i,k}^* = \frac{P_{\mathrm{TH}}}{G(q_i)}$, for all $i \in \mathcal{V}_k$. We also have the following for the optimal stop times and total energy of the mobile agents:*

$$1)\ t_{i,k}^* = \Delta_k\left(\frac{1}{\alpha_{i,k}} + \frac{\rho_i \eta_k}{\alpha_{i,k}\phi_k}\right) + \frac{\rho_i}{\alpha_{i,k}\phi_k}\frac{\mathrm{d}(\mathcal{H}_k)}{v_{\max,k}}, \qquad \forall i \in \mathcal{V}_k, \tag{5.14}$$

$$2)\ E_k^* = P_{\mathrm{loss},s,k}\left(\frac{\Delta_k \eta_k}{\phi_k} + \frac{1-\phi_k}{\phi_k}\frac{\mathrm{d}(\mathcal{H}_k)}{v_{\max,k}}\right) + \left(\frac{P_{\mathrm{loss},m,k}}{v_{\max,k}} + w_k\right)\mathrm{d}(\mathcal{H}_k) + t_c \sum_{i \in \mathcal{V}_k} \frac{P_{\mathrm{TH}}}{G(q_i)}.$$

Proof. Consider (5.60) where a partition $\{\mathcal{V}_k\}_{k=1}^n$ is given. In this case, the problem becomes decoupled and can be solved individually for each mobile agent. It can be immediately seen that the optimal TX power for each mobile agent k is the minimum possible transmission power required to make the POIs in $\mathcal{V}_k$ connected, i.e., $P_{\mathrm{TX},i,k}^* = \frac{P_{\mathrm{TH}}}{G(q_i)}$, for $i \in \mathcal{V}_k$. Thus, the first set of conditions for feasibility of the problem are $\frac{P_{\mathrm{TH}}}{G(q_i)} \leq P_{\mathrm{TX,max},k}$, for $i \in \mathcal{V}_k$ and $k = 1, \cdots, n$. Moreover, for any set of stop times $t_{i,k}$, for $i \in \mathcal{V}_k$, the total energy and the period are increasing functions of $\mathrm{d}(\mathcal{C}_k)$ and decreasing functions of v_k. Thus, to obtain the minimum total energy, the optimal cycle is the one with the minimum total length, i.e., the minimum-length Hamiltonian cycle $\mathcal{H}_k$, and the optimal velocity is the maximum possible velocity, i.e., $v_{\max,k}$.

Let us replace $\mathrm{d}(\mathcal{C}_k)$ with $\mathrm{d}(\mathcal{H}_k)$ and v_k with $v_{\max,k}$ in (5.60). Also, let us define $\overline{E}_{\max,k} \triangleq E_{\max,k} - t_c \sum_{i\in\mathcal{V}_k} \frac{P_{\mathrm{TH}}}{G(q_i)}$. Then, the optimal stop times for each mobile agent k are given by the solution of the following optimization problem, provided that the optimal stop times are all positive:

$$\begin{aligned}
&\min \textstyle\sum_{i\in\mathcal{V}_k} t_{i,k},\\
&\text{s.t.}\\
&1)\ \alpha_{i,k}t_{i,k} - \rho_i\left(\textstyle\sum_{j\in\mathcal{V}_k} t_{j,k} + \frac{\mathrm{d}(\mathcal{H}_k)}{v_{\max,k}}\right) \geq \Delta_k, \qquad \forall i \in \mathcal{V}_k,\\
&2)\ \textstyle\sum_{i\in\mathcal{V}_k} t_{i,k} + \frac{\mathrm{d}(\mathcal{H}_k)}{v_{\max,k}} \leq T_{\max},\\
&3)\ P_{\mathrm{loss},s,k}\textstyle\sum_{i\in\mathcal{V}_k} t_{i,k} + \left(\frac{P_{\mathrm{loss},m,k}}{v_{\max,k}} + w_k\right)\mathrm{d}(\mathcal{H}_k) \leq \overline{E}_{\max,k}.
\end{aligned} \tag{5.15}$$

This optimal solution of this linear program satisfies the Karush-Kuhn-Tucker (KKT) conditions. The Lagrangian of the problem is given by

$$\begin{aligned}
L_k = &\sum_{i\in\mathcal{V}_k} t_{i,k} - \sum_{i\in\mathcal{V}_k} \mu_{i,k}\left(\alpha_{i,k}t_{i,k} - \rho_i\sum_{j\in\mathcal{V}_k} t_{j,k} - \rho_i\frac{\mathrm{d}(\mathcal{H}_k)}{v_{\max,k}} - \Delta_k\right) + \\
&\gamma_k\left(\sum_{i\in\mathcal{V}_k} t_{i,k} + \frac{\mathrm{d}(\mathcal{H}_k)}{v_{\max,k}} - T_{\max}\right) + \nu_k\left(P_{\mathrm{loss},s,k}\sum_{i\in\mathcal{V}_k} t_{i,k} + \frac{P_{\mathrm{loss},m,k}\mathrm{d}(\mathcal{H}_k)}{v_{\max,k}} + w_k\mathrm{d}(\mathcal{H}_k) - \overline{E}_{\max,k}\right),
\end{aligned} \tag{5.16}$$

where $\mu_{i,k}$, γ_k and ν_k are the Lagrange multipliers. The KKT conditions are then as follows:

$$\begin{aligned}
&1)\ \tfrac{\partial L_k}{\partial t_{i,k}} = 1 - \alpha_{i,k}\mu_{i,k} + \textstyle\sum_{j\in\mathcal{V}_k}\mu_{j,k}\rho_j + \gamma_k + \nu_k P_{\mathrm{loss},s,k} = 0, \qquad \forall i \in \mathcal{V}_k,\\
&2)\ \mu_{i,k}\left(\alpha_{i,k}t_{i,k} - \rho_i\textstyle\sum_{j\in\mathcal{V}_k} t_{j,k} - \rho_i\frac{\mathrm{d}(\mathcal{H}_k)}{v_{\max,k}} - \Delta_k\right) = 0, \qquad \forall i \in \mathcal{V}_k,\\
&3)\ \gamma_k\left(\textstyle\sum_{i\in\mathcal{V}_k} t_{i,k} + \frac{\mathrm{d}(\mathcal{H}_k)}{v_{\max,k}} - T_{\max}\right) = 0,\\
&4)\ \nu_k\left(P_{\mathrm{loss},s,k}\textstyle\sum_{i\in\mathcal{V}_k} t_{i,k} + \frac{P_{\mathrm{loss},m,k}\mathrm{d}(\mathcal{H}_k)}{v_{\max,k}} + w_k\mathrm{d}(\mathcal{H}_k) - \overline{E}_{\max,k}\right) = 0,\\
&5)\ \alpha_{i,k}t_{i,k} - \rho_i\textstyle\sum_{j\in\mathcal{V}_k} t_{j,k} - \rho_i\frac{\mathrm{d}(\mathcal{H}_k)}{v_{\max,k}} - \Delta_k \geq 0,\\
&6)\ \textstyle\sum_{i\in\mathcal{V}_k} t_{i,k} + \frac{\mathrm{d}(\mathcal{H}_k)}{v_{\max,k}} - T_{\max} \leq 0,\\
&7)\ P_{\mathrm{loss},s,k}\textstyle\sum_{i\in\mathcal{V}_k} t_{i,k} + \frac{P_{\mathrm{loss},m,k}\mathrm{d}(\mathcal{H}_k)}{v_{\max,k}} + w_k\mathrm{d}(\mathcal{H}_k) - \overline{E}_{\max,k} \leq 0,\\
&8)\ \mu_{i,k} \geq 0,\ \forall i \in \mathcal{V}_k,\ \gamma_k \geq 0,\ \nu_k \geq 0.
\end{aligned} \tag{5.17}$$

From the first set of conditions in (5.17), we conclude that $\mu_{i,k} > 0$, for $i \in \mathcal{V}_k$, which results in the following optimality conditions: $\alpha_{i,k}t_{i,k} - \rho_i\sum_{j\in\mathcal{V}_k} t_{j,k} - \rho_i\frac{\mathrm{d}(\mathcal{H}_k)}{v_{\max,k}} = \Delta_k$,

for $i \in \mathcal{V}_k$. By solving this set of equations, we get the following for the optimal stop times:

$$t^*_{i,k} = \Delta_k \left(\frac{1}{\alpha_{i,k}} + \frac{\rho_i \eta_k}{\alpha_{i,k}\phi_k} \right) + \frac{\rho_i}{\alpha_{i,k}\phi_k} \frac{\mathrm{d}(\mathcal{H}_k)}{v_{\max,k}}, \qquad \forall i \in \mathcal{V}_k, \tag{5.18}$$
$$\sum_{i \in \mathcal{V}_k} t^*_{i,k} = \Delta_k \frac{\eta_k}{\phi_k} + \frac{\mathrm{d}(\mathcal{H}_k)}{v_{\max,k}} \frac{1-\phi_k}{\phi_k},$$

where $\phi_k \triangleq 1 - \sum_{i \in \mathcal{V}_k} \frac{\rho_i}{\alpha_{i,k}}$ and $\eta_k \triangleq \sum_{i \in \mathcal{V}_k} \frac{1}{\alpha_{i,k}}$. It can be seen that the optimal stop times are all positive when $\sum_{i \in \mathcal{V}_k} \frac{\rho_i}{\alpha_{i,k}} < 1$, for $k = 1, \cdots, n$, which form the second set of conditions for the feasibility of the optimization problem. The third set of such conditions are also given as follows:

$$P_{\mathrm{loss},s,k} \left(\Delta_k \frac{\eta_k}{\phi_k} + \frac{\mathrm{d}(\mathcal{H}_k)}{v_{\max,k}} \frac{1-\phi_k}{\phi_k} \right) + \left(\frac{P_{\mathrm{loss},m,k}}{v_{\max,k}} + w_k \right) \mathrm{d}(\mathcal{H}_k) \leq \overline{E}_{\max,k},$$
$$\Delta_k \frac{\eta_k}{\phi_k} + \frac{\mathrm{d}(\mathcal{H}_k)}{v_{\max,k}} \frac{1}{\phi_k} \leq T_{\max,k}. \tag{5.19}$$

After combining these two constraints, we then obtain the third set of feasibility conditions in part 1 of Theorem 5.2.1. The maximum stability margin is also the maximum Δ_k that satisfies (5.19), which can be shown to be the same as $\Delta_{\max,k}$ in part 2 of Theorem 5.2.1. Finally, by setting $\Delta_k = 0$ in (5.19), we get the conditions of (5.13) in part 3 of Theorem 5.2.1. □

Theorem 5.2.1 can be used to determine whether there exists a feasible stabilizing policy for a given partition $\{\mathcal{V}_k\}_{k=1}^n$. Then, we can find the optimal solution to Problem 5.2.1 by searching through all the partitions $\{\mathcal{V}_k\}_{k=1}^n$ of $\mathcal{V}$ that satisfy (5.11), and finding the one with minimum $\sum_{k=1}^n \varpi_k E^*_k$. A more efficient alternative for solving Problem 5.2.1 is to use a mixed-integer program (MIP) to find the optimal partitions and optimal stopping times for the mobile agents, when the maximum allowed velocities and minimum possible transmission powers are used. Generally, there is more than one way to formulate the MIP. Since there are multiple mobile agents, some MIP formulations can be nonlinear, in which case the optimal solution

is very challenging to find. Next, we show how to formulate a mixed-integer linear program (MILP), by transforming the nonlinear mixed-integer constraints to linear ones. This makes finding the optimal dynamic coverage policies tractable even for large number of POIs. Note that MILPs can be solved much more efficiently than their nonlinear alternatives. There exists several solvers, such as IBM ILOG CPLEX [104] and SAS/OR [105], that can solve large-scale MILP considerably fast.

Let us consider auxiliary binary variables $x_{i,k}$ and $z_{i,j,k}$, for $i, j \in \mathcal{V}$ and $k = 1, \cdots, n$. We have $x_{i,k} = 1$ whenever the i^{th} POI is assigned to the k^{th} mobile agent, and $x_{i,k} = 0$ otherwise. Also, $z_{i,j,k} = 1$ if there exists an edge between the i^{th} and j^{th} POIs in the Hamiltonian cycle assigned to the k^{th} mobile agent, and $z_{i,j,k} = 0$ otherwise. To guarantee that every POI that is on the Hamiltonian cycle $\mathcal{V}_k$ have one degree in and one degree out, we can add the following set of constraints: $\sum_{j=1,j\neq i}^{m} z_{i,j,k} = x_{i,k}$, $\sum_{j=1,j\neq i}^{m} z_{j,i,k} = x_{i,k}$, for all $i \in \mathcal{V}$. Then, by defining $d_{i,j} \triangleq \|q_i - q_j\|$, we have the following constraints for the period and total energy per period of the k^{th} agent:

$$\sum_{i=1}^{m} x_{i,k} t_{i,k} + \frac{1}{v_{\max,k}} \sum_{i=1}^{m} \sum_{j=1,j\neq i}^{m} z_{i,j,k} d_{i,j} \leq T_{\max}, \tag{5.20}$$

$$P_{\text{loss},s,k} \sum_{i=1}^{m} x_{i,k} t_{i,k} + \left(\frac{P_{\text{loss},m,k}}{v_{\max,k}} + w_k \right) \sum_{i=1}^{m} \sum_{j=1,j\neq i}^{m} z_{i,j,k} d_{i,j} + t_c \sum_{i=1}^{m} \frac{x_{i,k} P_{\text{TH}}}{G(q_i)} \leq E_{\max,k},$$

with $t_{i,k} \geq 0$ for all i, k. As can be seen, the left-hand side of both constraints are nonlinear functions of $t_{i,k}$ and $x_{i,k}$. In order to make the constraints linear, we consider a large constant $\Omega > 0$. We then add the linear constraints $t_{i,k} \leq x_{i,k}\Omega$, for all i, k, to guarantee that $t_{i,k} = 0$ whenever $x_{i,k} = 0$ ($i \notin \mathcal{V}_k$), while there is no constraint on $t_{i,k}$ whenever $x_{i,k} = 1$ ($i \in \mathcal{V}_k$). This way we can replace the nonlinear term $x_{i,k} t_{i,k}$ with $t_{i,k}$ in (5.20), without changing the optimal solution. Furthermore, since the k^{th} mobile agent does not need to stabilize any POI out of $\mathcal{V}_k$, we should modify the stability constraints of the k^{th} mobile agent such that they automatically become true for all $i \notin \mathcal{V}_k$. This is done by considering the following stability

constraints:

$$\alpha_{i,k}t_{i,k} - \rho_i \left(\sum_{i=1}^{m} t_{i,k} + \frac{1}{v_{\max,k}} \sum_{i=1}^{m} \sum_{j=1, j\neq i}^{m} z_{i,j,k} d_{i,j} \right) + (1 - x_{i,k})\Omega \geq \Delta_k, \quad \forall i, k. \quad (5.21)$$

We can see that when $x_{i,k} = 0$, constraint (5.21) becomes true if $\Omega > 0$ is large enough. It is easy to confirm that any $\Omega \geq \max\left\{T_{\max}, \left(\max_i \rho_i\right) T_{\max} + \max_k \Delta_k\right\}$ can be considered large enough for this set of constraints. Such an Ω also guarantees that whenever $x_{i,k} = 1$, the constraint $t_{i,k} \leq x_{i,k}\Omega$ is always true. Based on this discussion, the MILP formulation for solving Problem 5.2.1 is given by Program 1.

Program 1 MILP for solving Problem 5.2.1 in the communication-intensive case

$\min \sum_{k=1}^{n} \varpi_k E_k,$

s.t.

1) $\alpha_{i,k}t_{i,k} - \rho_i \left(\sum_{i=1}^{m} t_{i,k} + \frac{1}{v_{\max,k}} \sum_{i=1}^{m} \sum_{j=1, j\neq i}^{m} z_{i,j,k} d_{i,j} \right) + (1 - x_{i,k})\Omega \geq \Delta_k, \ \forall i, k,$

2) $\sum_{i=1}^{m} t_{i,k} + \frac{1}{v_{\max,k}} \sum_{i=1}^{m} \sum_{j=1, j\neq i}^{m} z_{i,j,k} d_{i,j} \leq T_{\max}, \qquad \forall k,$

3) $P_{\text{loss},s,k} \sum_{i=1}^{m} t_{i,k} + \left(\frac{P_{\text{loss},m,k}}{v_{\max,k}} + w_k \right) \sum_{i=1}^{m} \sum_{j=1, j\neq i}^{m} z_{i,j,k} d_{i,j} + t_c \sum_{i=1}^{m} \frac{x_{i,k} P_{\text{TH}}}{G(q_i)} \leq E_k, \forall k,$

4) $\sum_{j=1, j\neq i}^{m} z_{i,j,k} = x_{i,k}, \ \sum_{j=1, j\neq i}^{m} z_{j,i,k} = x_{i,k}, \qquad \forall i, k,$

5) $\sum_{k=1}^{n} x_{i,k} = 1, \qquad \forall i,$

6) $\sum_{i=1}^{m} h_i = n,$

7) $u_i - u_j - m(h_i + h_j) + (m-1) \sum_{k=1}^{n} z_{i,j,k} \leq m - 2, \qquad \forall i, j \neq i,$

8) $2 - h_i \leq u_i \leq m, \qquad \forall i,$

9) $t_{i,k} \leq x_{i,k}\Omega, \qquad \forall i, k,$

10) $x_{i,k} \frac{P_{\text{TH}}}{G(q_i)} \leq P_{\text{TX},\max,k}, \qquad \forall i, k,$

11) $E_k \leq E_{\max,k}, \qquad \forall k,$

12) $z_{i,j,k} \in \{0, 1\}, \ x_{i,k} \in \{0, 1\}, \ h_i \in \{0, 1\}, \ u_i \in \mathbb{N}, \ 0 \leq t_{i,k} \leq \Omega, \qquad \forall i, j, k,$

Constraints 1, 2 and 3 in Program 1 are the stability, time and energy constraints, as introduced before. Constraint 4 forces each POI $i \in \mathcal{V}$ to have exactly one degree in

and one degree out. Constraint 5 guarantees that each POI is assigned to one mobile agent.[5] Constraints 6, 7 and 8 are the sub-tour elimination constraints (SECs), which are added to prevent any invalid sub-tour on the set of POIs assigned to each agent [106]. To prevent sub-tours, we have introduced $2m$ auxiliary variables h_i and u_i, for $i \in \mathcal{V}$, and used a modified version of the well-known Miller-Tucker-Zemlin (MTZ) constraints [106, 107]. Constraint 9 forces $t_{i,k} = 0$ whenever $x_{i,k} = 0$. Constraint 10 is the transmission power constraint, which implies that if a POI is assigned to a mobile agent, that mobile agent should be able to be connected at the position of the POI. Finally, constraint 11 is the constraint on the maximum total energy consumption in each period.

It is worth mentioning that MTZ formulations for sub-tour elimination, as used in vehicle routing problem (VRP) or multiple traveling salesman problem (mTSP), typically assume a fixed POI, called *depot*, through which all the mobile agents must pass [108]. The MTZ formulation used in Program 1 is different from those formulations, as it assumes no depot [107]. The idea here is to introduce floating depot variables h_i, for $i \in \mathcal{V}$, which guarantee that whenever $h_i = 1$ (the i^{th} POI is selected as a depot), constraint 7 in Program 1 is always true. Also note that, in general, the MTZ formulation has a polynomial size (i.e., the number of SECs is of polynomial order), compared to the exponential size of several alternative formulations in the literature [108].

For n mobile agents and m POIs, the MILP of Program 1 has $nm(m+1)+2m+n$ variables ($nm^2 + m$ binaries, $nm + n$ reals and n integers), $3nm + m(m + 1) + 2n$ inequality constraints and $2nm+m+1$ equality constraints. This MILP can be solved using several efficient solvers, such as IBM ILOG CPLEX [104] and SAS/OR [105].

[5]Note that if $x_{i,k} = 1$, the k^{th} mobile agent needs to visit at least one more POI (other than POI i) to satisfy constrain 4 in Program 1. Therefore, the case of one single POI assigned to one agent is automatically prevented, i.e., $|\mathcal{V}_k| > 1$ for all k.

Fig. 5.2 shows a sample plot of $\Psi_i(t)$ for one of the POIs after optimizing the dynamic coverage operation using the proposed MILP. Fig. 5.2 (left) corresponds to the case where $\Delta_k > 0$ (robust dynamic coverage with positive stability margin) and Fig. 5.2 (right) corresponds to the case where $\Delta_k = 0$ (zero stability margin). It can be seen that a positive stability margin results in a longer stop time and, as a direct result, more energy consumption at the point of interest, as proved by Theorem 5.2.1.

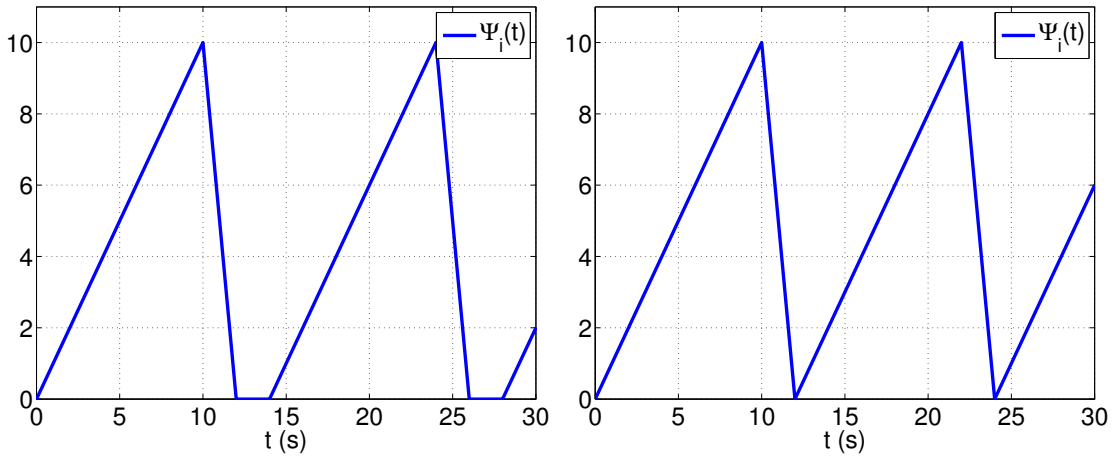

Figure 5.2: A sample plot of $\Psi_i(t)$ at the remote station in the communication-intensive case, for one of the POIs, after optimizing the dynamic coverage operation using the MILP of Program 1. The left figure corresponds to the case where $\Delta_k > 0$ (robust dynamic coverage with positive stability margin) and the right one corresponds to the case where $\Delta_k = 0$ (zero stability margin).

5.2.3 Optimal Solution of the Dynamic Coverage Problem in the Communication-Intensive Case – Case of Unknown Stochastic Channel Powers at the POIs

So far, we have assumed that the channel powers $G(q_i)$, for $i \in \mathcal{V}$, are known beforehand when solving Problem 5.2.1. This, however, may not be the case in practical applications, where the channel power may only be known at a small number of

positions in the workspace that are different from the positions of the POIs. For such cases, we can use the probabilistic channel prediction framework of Chapter 2 to assess the channel powers at the positions of the POIs. Stochastic channel powers, however, result in stochastic constraints in Problem 5.2.1. It is then desired to find alternative deterministic conditions that guarantee that the feasibility conditions hold with a probability larger than a given threshold. This is, however, very challenging in general, due to the fact that the conditions are complex functions of the stochastic channel powers. To simplify the problem in the case of stochastic channel powers, we propose using concepts from stochastic programming [109]. Stochastic programming provides a systematic *sub-optimal* approach to transform the stochastic constraints of an optimization problem to deterministic ones.

Several methods have been proposed in the stochastic programming literature for this purpose, such as the expectation constraint method, worse-case constraint method and chance constraint method [109]. In this section, we use the chance constraint method, as it provides more robustness to stochasticity of the channel and is yet easy to apply to our dynamic coverage problem. The idea behind the chance constraint method is to replace any constraint that is directly a function of the main random variables ($G(q_i)$ in our case) with its chance constrain. A chance constraint is simply a constraint that guarantees that the probability of meeting the stochastic constraint is larger than a given χ, for $0.5 < \chi < 1$, while assuming that all the other optimization variables are deterministic [109]. Next, we show how to solve the chance-constrained version of Problem 5.2.1, i.e., Problem 5.2.1, with its stochastic constraints replaced with the corresponding chance constraints. In this chapter, a feasible solution to this problem is called a *χ-probable feasible stabilizing dynamic coverage policy* and is defined as follows:

Definition 5.2.4. *The dynamic coverage policy $\mathcal{P}$ is called a χ-probable feasible stabilizing dynamic coverage policy in the communication-intensive case if for this*

policy the probability of meeting any stochastic constraint in Problem 5.2.1 is larger than χ, for $0.5 < \chi < 1$.

Let us start by calculating the probability of meeting the stochastic constraint in the chance-constrained version of Problem 5.2.1. Instead of deterministic $G(q_i)$, for $i \in \mathcal{V}$, we have the corresponding predicted channel $\hat{G}_{\text{dB}}(q_i)$ in dB (see Chapter 2). Then, the minimum transmission power constraint (constraint 4 of Problem 5.2.1) will have the following chance-constrained form:

$$\mathbb{P}\left\{P_{\text{TX},i,k} \geq \frac{P_{\text{TH}}}{G(q_i)}\right\} \geq \chi, \qquad i \in \mathcal{V}_k,\ k = 1, \cdots, n. \tag{5.22}$$

Similar to the previous chapters, in order to calculate $\mathbb{P}\left\{P_{\text{TX},i,k} \geq \frac{P_{\text{TH}}}{G(q_i)}\right\}$, we use the probabilistic channel assessment framework of Chapter 2. We then have

$$\mathbb{P}\left\{P_{\text{TX},i,k} \geq \frac{P_{\text{TH}}}{G(q_i)}\right\} = Q\left(\frac{10\log_{10}\left(\frac{P_{\text{TH}}}{P_{\text{TX},i,k}}\right) - \hat{G}_{\text{dB}}(q_i)}{\sigma(q_i)}\right), \tag{5.23}$$

where $Q(x) = \frac{1}{\sqrt{2\pi}}\int_x^\infty e^{-x^2/2}dx$ is the tail probability of a Gaussian distribution. Note that we have dropped the dependency of channel assessment on k and t in this case, as the channel is assessed beforehand, using a number of *a priori* channel measurements, and used for finding the optimal dynamic coverage policy for all the mobile agents. After some straightforward calculations, we can find the necessary and sufficient condition for (5.22) as follows:

$$P_{\text{TX},i,k} \geq 10^{-\left(\sigma(q_i)Q^{-1}(\chi)+\hat{G}_{\text{dB}}(q_i)\right)/10}\, P_{\text{TH}} \triangleq \Gamma(q_i,\chi), \qquad i \in \mathcal{V}_k,\ k = 1, \cdots, n, \tag{5.24}$$

with $Q^{-1}(x)$ denoting the inverse of $Q(x)$ (not to be confused with exponentiation). This shows that in order to account for stochastic channels when designing optimal dynamic coverage policies, it is sufficient to replace $\frac{P_{\text{TH}}}{G(q_i)}$ with $\Gamma(q_i,\chi)$ in Problem 5.2.1. After this modification, the MILP of Program 1 is readily applicable to this case as well. Similarly, the results of Theorem 5.2.1 also hold. For instance, we can

show that, given the partition $\{\mathcal{V}_k\}_{k=1}^n$, there exists a χ-probable feasible stabilizing policy for the k^{th} agent, for $k = 1, \cdots, n$, if and only if

$$\begin{aligned}
&1)\ \Gamma(q_i, \chi) \leq P_{\text{TX,max},k}, \qquad \forall i \in \mathcal{V}_k, \\
&2)\ \sum_{i \in \mathcal{V}_k} \frac{\rho_i}{\alpha_{i,k}} < 1, \\
&3)\ \frac{\mathrm{d}(\mathcal{H}_k)}{v_{\max,k}} \leq \min\left\{T_{\max}, \frac{E_{\max,k} - t_c \sum_{i \in \mathcal{V}_i} \Gamma(q_i, \chi) - w_k \mathrm{d}(\mathcal{H}_k)}{(1-\phi_k)P_{\text{loss},s,k} + \phi_k P_{\text{loss},m,k}}\right\} \phi_k.
\end{aligned} \tag{5.25}$$

It is worth mentioning that, from (5.24), the average minimum transmit power required, to meet the constraint on the transmission power with a probability larger than χ, for $0.5 < \chi < 1$, increases as the uncertainty in channel assessment ($\sigma(q_i)$) gets larger. Finally, in a realistic communication scenario, results of both cases of known and unknown channel powers can be useful. Since the dynamic coverage task is periodic, the results for the unknown probabilistic case can first be used for planning. Then, once the agents measure the channel at their corresponding POIs, they can share their channel measurements and solve the optimization problem for the case of known channels.

5.2.4 Probabilistic Analysis of the Dynamic Coverage Problem in the Communication-Intensive Case

By probabilistic analysis of the dynamic coverage problem, we mean deriving conditions for a policy $\mathcal{P}$ to be a χ-probable feasible stabilizing dynamic coverage policy in case both the channel and the positions of the POIs are stochastic. Such analysis provides *a priori* knowledge about the coverage task before the deployment of the mobile agents, which is extremely useful for high-level planning purposes. It characterizes the probability of having a feasible stabilizing dynamic coverage policy, when the channel power and the positions of the POIs are drawn from a certain distribution. Without loss of generality, we consider the following extra assumptions in this

section for the ease of mathematical derivations:[6]

Assumption 5.2.1. *The rate of increasing $\Psi_i(t)$ and the service rate of each agent k are identical at all the POIs, i.e., $\rho_i = \rho$ and $\alpha_{i,k} = \alpha_k$, for $i \in \mathcal{V}$ and $k = 1, \cdots, n$.*

Assumption 5.2.2. *The motion power loss, while a mobile agent is moving, is equal to its motion power loss when it stops at a POI, i.e., $P_{\text{loss},s,k} = P_{\text{loss},m,k} = P_{\text{loss},k}$, for $k = 1, \cdots, n$.*

Assumption 5.2.3. *The POIs assigned to the k^{th} mobile agent, for $k = 1, \cdots, n$, are independently and identically distributed (i.i.d.) according to an absolutely continuous pdf $\psi(q)$ which is defined over the workspace $\mathcal{W}$. Furthermore, the number of these POIs is large.*[7]

In order to better follow the discussion, it would be easier to assume the case of known channels, i.e., for any realization of the channel, the agents plan based on the full knowledge of the channel.

As explained in Section 5.2.3, in case of stochastic constraints in Problem 5.2.1, the optimal strategy is to directly calculate the probability of having a feasible stabilizing dynamic coverage policy and derive conditions that guarantee this probability is larger than a threshold. If both the channel powers at the POIs and their positions are stochastic, however, deriving such conditions is extremely challenging. Therefore, similar to Section 5.2.3, we use a sub-optimal approach based on stochastic programming, i.e., we treat the rest of the variables, aside from channel power and the positions of the POIs, deterministically.

[6]Note that these assumptions are made to simplify the theoretical analysis of this section. Similar results can be found for the case that either one of these assumptions does not hold. For instance, the results of this section can be easily extended to the case that ρ_i, for $i = 1, \cdots, n$, are i.i.d. random variables, independent of the channel and the positions of the POIs, or to the case where $P_{\text{loss},s,k} \neq P_{\text{loss},m,k}$.

[7]The meaning of a large number of POIs will be explained later in this section.

Let $m_k = |\mathcal{V}_k|$ represent the number of POIs assigned to the k^{th} mobile agent. We calculate the probabilities of meeting the stochastic constraints by first conditioning on the positions of the POIs and then averaging over their probability distributions. Using the results of the previous section, we conclude that in the case of randomly positioned POIs, we have

$$\mathbb{P}\left\{P_{\text{TX},i,k} \geq \frac{P_{\text{TH}}}{G(q_i)}\right\} = \int_{\mathcal{W}} Q\left(\frac{10\log_{10}\left(\frac{P_{\text{TH}}}{P_{\text{TX},i,k}}\right) - \widetilde{G}_{\text{dB}}(q)}{\widetilde{\sigma}(q)}\right)\psi(q)dq \geq \chi, \quad (5.26)$$

where $\widetilde{G}_{\text{dB}}(q)$ and $\widetilde{\sigma}^2(q)$ are the mean and variance of a Gaussian distribution that characterizes the channel power (in the dB domain) at a position $q \in \mathcal{W}$. Since the left-hand side of (5.26) is an increasing function of $P_{\text{TX},i,k}$, we have the following for all the POIs assigned to the k^{th} agent:

$$P_{\text{TX},i,k} \geq 10^{-\breve{G}_{\text{dB}}(\chi)/10}\, P_{\text{TH}} \triangleq \Gamma(\chi), \qquad i \in \mathcal{V}_k,\ k = 1, \cdots, n, \quad (5.27)$$

where $\breve{G}_{\text{dB}}(\chi)$ is the unique solution to the following equation as a function of G:

$$\int_{\mathcal{W}} Q\left(\frac{G - \widetilde{G}_{\text{dB}}(q)}{\widetilde{\sigma}(q)}\right)\psi(q)dq = \chi. \quad (5.28)$$

Next, consider all the constraints of Problem 5.2.1 that are functions of the $\mathrm{d}(\mathcal{C}_k)$. Based on the previous results, the optimum Hamiltonian cycles are the minimum-length Hamiltonian cycles. Therefore, we can find the probability of meeting the constraints as a function of $\mathrm{d}(\mathcal{H}_k)$ instead, where $\mathcal{H}_k$ is the minimum-length Hamiltonian cycle on $\mathcal{V}_k$. Since the constraints of Problem 5.2.1 are linear with respect to $\mathrm{d}(\mathcal{H}_k)$, we are then required to find the probabilities of the form $\mathbb{P}\{\mathrm{d}(\mathcal{H}_k) \leq c\}$, for a constant c. Such probabilities can be found using the following result from the probabilistic traveling salesman problem (TSP) literature [106]:

Lemma 5.2.2. *Assume that the spatial distribution of POIs is i.i.d., according to an absolutely continuous pdf $\psi(q)$ defined over the compact set $\mathcal{W}$. Then, there exists a*

constant $\theta_{\rm TSP}$ *such that*

$$\begin{aligned} &1)\ \ \mathbb{P}\left\{\lim_{m_k\to\infty}\frac{\mathrm{d}(\mathcal{H}_k)}{\sqrt{m_k}}=\theta_{\rm TSP}\int_{\mathcal{W}}\sqrt{\psi(q)}dq\right\}=1,\\ &2)\ \lim_{m_k\to\infty}\frac{\mathbb{E}\big\{\mathrm{d}(\mathcal{H}_k)\big\}}{\sqrt{m_k}}=\theta_{\rm TSP}\int_{\mathcal{W}}\sqrt{\psi(q)}dq, \end{aligned} \tag{5.29}$$

where $m_k=|\mathcal{V}_k|$ *is the number of POIs assigned to the* $k^{\rm th}$ *mobile agent.*

Proof. See [106]. □

The constant $\theta_{\rm TSP}$ is estimated to be around 0.765 [110]. Let us define $\zeta \triangleq \theta_{\rm TSP}\int_{\mathcal{W}}\sqrt{\psi(q)}dq$. By using Lemma 5.2.2 and by considering the constraint (5.27) on the transmission power of each mobile agent, we conclude that, for large m_k, the results of Theorem 5.2.1 hold in this case too, provided that $\mathrm{d}(\mathcal{H}_k)$ is replaced by $\zeta\sqrt{m_k}$, $\frac{P_{\rm TH}}{G(q_i)}$ is replaced by $\Gamma(\chi)$, and m_k remains large.[8] Therefore, given a partition $\{\mathcal{V}_k\}_{k=1}^n$, there exists a χ-probable feasible stabilizing dynamic coverage policy, i.e., the chance-constrained version of Problem 5.2.1 is feasible, if and only if the following are true, for $k=1,\cdots,n$:

$$\begin{aligned} &1)\ \Gamma(\chi)\le P_{\rm TX,max,k},\\ &2)\ m_k<\frac{\alpha_k}{\rho},\\ &3)\ \min\left\{\frac{E_{{\rm max},k}-t_c m_k\Gamma(\chi)-w_k\zeta\sqrt{m_k}}{P_{{\rm loss},k}},T_{\rm max}\right\}\left(1-m_k\frac{\rho}{\alpha_k}\right)\ge\frac{\zeta\sqrt{m_k}}{v_{{\rm max},k}}. \end{aligned} \tag{5.30}$$

Note that for (5.30) to be a precise condition, m_k is required to be large. That is why the second part of Assumption 5.2.3 is necessary for the analysis of this section. For convex environments, $m_k\ge 15$ can be assumed sufficiently large. In other words, for $m_k\ge 15$, $\zeta\sqrt{m_k}$ is a tight approximation for the length of the minimum-length Hamiltonian cycle on the set of POIs assigned to the $k^{\rm th}$ agent [110]. On the other hand, the set of constraints in (5.30) may not be feasible for very large m_k. In

[8] Note that no MILP needs to the be solved in this case.

fact, there is an upper-bound on the maximum number of access points that can be assigned to each agent, as we characterize next.

An Upper Bound on the Maximum Number of POIs Covered by a Mobile Agent in the Communication-Intensive Case

Consider the following theorem:

Theorem 5.2.2. *Assume that for the k^{th} agent and for the given χ, we have $\Gamma(\chi) \leq P_{\text{TX,max},k}$, where $\Gamma(\chi)$ is given by (5.27). Then, under Assumptions 5.2.1, 5.2.2 and 5.2.3, an upper-bound on the maximum number of POIs that can be assigned to the k^{th} agent, to guarantee a χ-probable feasible stabilizing dynamic coverage policy in the communication-intensive case, is given as follows:*

$$\overline{m}_k = \begin{cases} \min\left\{s_{k,1}^2, s_{k,2}^2\right\}, & \mathcal{A}_k \cap \mathcal{B}_k = \emptyset,\ E_{\max,k} > P_{\text{loss},k} T_{\max} \\ \max\left\{s^2 \middle| s \in \mathcal{A}_k \cap \mathcal{B}_k\right\}, & \mathcal{A}_k \cap \mathcal{B}_k \neq \emptyset,\ E_{\max,k} > P_{\text{loss},k} T_{\max} \\ \max\left\{s^2 \middle| s \in \mathcal{A}'_k \cap \mathcal{B}_k\right\}, & \mathcal{A}'_k \cap \mathcal{B}_k \neq \emptyset,\ E_{\max,k} \leq P_{\text{loss},k} T_{\max} \end{cases}, \tag{5.31}$$

provided that such $\overline{m}_k$ exists (chance-constrained version of Problem 5.2.1 is feasible) and it is sufficiently large. Here,

$$s_{k,1} = \frac{-\zeta/v_{\max,k} + \sqrt{\zeta^2/v_{\max,k}^2 + 4T_{\max}^2 \rho/\alpha_k}}{2T_{\max}\rho/\alpha_k}, \tag{5.32}$$

$$s_{k,2} = \frac{-\zeta w_k + \sqrt{\zeta^2 w_k^2 + 4t_c\Gamma(\chi)\left(E_{\max,k} - P_{\text{loss},k}T_{\max}\right)}}{2t_c\Gamma(\chi)},$$

$$s_{k,3} = \min\left\{\sqrt{\frac{\alpha_k}{\rho}}, \frac{-\zeta w_k + \sqrt{\zeta^2 w_k^2 + 4t_c\Gamma(\chi)E_{\max,k}}}{2t_c\Gamma(\chi)}\right\},$$

$$\mathcal{A}_k = \left\{s \middle| s_{k,2} \leq s \leq s_{k,3}\right\},\ \mathcal{A}'_k = \left\{s \middle| 0 \leq s \leq s_{k,3}\right\},$$

$$\mathcal{B}_k = \left\{s \middle| \left(\frac{\zeta P_{\text{loss},k}}{v_{\max,k}} + \zeta w_k\right)s + \left(t_c\Gamma(\chi) + \frac{E_{\max,k}\rho}{\alpha_k}\right)s^2 - \frac{\zeta w_k \rho}{\alpha_k}s^3 - \frac{t_c\Gamma(\chi)\rho}{\alpha_k}s^4 \leq E_{\max,k}\right\}.$$

Proof. Consider the constraints in (5.30) and assume that m_k is large enough. By defining the variable $s \triangleq \sqrt{m_k}$ and after some straightforward derivations, we can

conclude that any feasible $s \geq 0$ satisfies one of the following sets of constraints: 1) $\frac{T_{\max}\rho}{\alpha_k}s^2 + \frac{\zeta}{v_{\max,k}}s \leq T_{\max}, t_c\Gamma(\chi)s^2 + w_k\zeta s \leq E_{\max,k} - P_{\text{loss},k}T_{\max}$, or 2) $E_{\max,k} \geq t_c\Gamma(\chi)s^2 + w_k\zeta s \geq E_{\max,k} - P_{\text{loss},k}T_{\max}, \left(\frac{\zeta P_{\text{loss},k}}{v_{\max,k}} + \zeta w_k\right)s + \left(t_c\Gamma(\chi) + \frac{E_{\max,k}\rho}{\alpha_k}\right)s^2 - \frac{\zeta w_k\rho}{\alpha_k}s^3 - \frac{t_c\Gamma(\chi)\rho}{\alpha_k}s^4 \leq E_{\max,k}, s^2 \leq \frac{\alpha_k}{\rho}$. First assume that $E_{\max,k} > P_{\text{loss},k}T_{\max}$. Then, the maximum $s \geq 0$ that satisfies the first set of constraints is simply the minimum of the positive roots of $\frac{T_{\max}\rho}{\alpha_k}s^2 + \frac{\zeta}{v_{\max,k}}s = T_{\max}$ and $t_c\Gamma(\chi)s^2 + w_k\zeta s = E_{\max,k} - P_{\text{loss},k}T_{\max}$, which are $s_{k,1}$ and $s_{k,2}$ in (5.32), respectively. Similarly, any $s \geq 0$ that satisfies the second set of constraints 1) must be greater than or equal to $s_{k,2}$ and less than or equal to the minimum of $\sqrt{\frac{\alpha_k}{\rho}}$ and the positive root of $t_c\Gamma(\chi)s^2 + w_k\zeta s = E_{\max,k}$, which is $s_{k,3}$ in (5.32), and 2) must satisfy the fourth-order polynomial inequality in the second set of constraints. Therefore, the maximum s that satisfies the second set of constraints is simply the maximum s in $\mathcal{A}_k \cap \mathcal{B}_k$, for $\mathcal{A}_k$ and $\mathcal{B}_k$ defined in (5.32). Note that all the elements of $\mathcal{A}_k \cap \mathcal{B}_k$ are necessarily greater than or equal to $\min\left\{s_{k,1}, s_{k,2}\right\}$. Therefore, if $\mathcal{A}_k \cap \mathcal{B}_k \neq \emptyset$, the upper bound on s is the maximum element of $\mathcal{A}_k \cap \mathcal{B}_k$. However, if $\mathcal{A}_k \cap \mathcal{B}_k = \emptyset$, the upper bound on s is given by $\min\left\{s_{k,1}, s_{k,2}\right\}$.

Next, assume that $E_{\max,k} \leq P_{\text{loss},k}T_{\max}$. In this case the first set of constraints does not hold for any $s \geq 0$ and only the second set of constraints needs to be considered. Following a similar procedure, we can conclude that the maximum possible s that satisfies the second set of constraints is the maximum s in $\mathcal{A}'_k \cap \mathcal{B}_k$. This completes the proof. □

Average Minimum Energy Per Period Consumed to Cover a Set of POIs by a Mobile Agent in the Communication-Intensive Case

Another interesting quantity to characterize probabilistically is the average of the minimum energy consumed in one period by the k^{th} mobile agent to feasibly stabilize its assigned POIs. This is given by the following theorem in case of large m_k:

Theorem 5.2.3. *Consider Assumptions 5.2.1, 5.2.2 and 5.2.3. Then, the average of the minimum energy consumed in one period by the k^{th} mobile agent to feasibly stabilize its assigned POIs is given as follows in the communication-intensive case:*

$$E_{\min,\text{ave},k} = \left[\frac{P_{\text{loss},k}}{\left(1 - m_k \frac{\rho}{\alpha_k}\right) v_{\max,k}} + w_k\right] \zeta\sqrt{m_k} + t_c m_k P_{\text{TH}} \int_{\mathcal{W}} \frac{\exp\left(\frac{1}{2}\bar{\sigma}^2(q)\right)}{10^{\frac{\widetilde{G}_{\text{dB}}(q)}{10}}} \psi(q) dq, \tag{5.33}$$

where $\widetilde{G}_{\text{dB}}(q)$ and $\widetilde{\sigma}^2(q)$ are the mean and variance of a Gaussian distribution that characterizes the channel power at a position $q \in \mathcal{W}$ in the dB domain, $\bar{\sigma}(q) \triangleq \frac{\log(10)}{10}\widetilde{\sigma}(q)$, $m_k < \frac{\alpha_k}{\rho}$, and m_k remains large enough.

Proof. The minimum energy occurs when the stability margin is zero. By setting $\Delta_k = 0$ in (5.14), and based on Assumptions 5.2.1, 5.2.2 and 5.2.3, we obtain

$$\begin{aligned} E_{\min,\text{ave},k} = \mathbb{E}\left\{E_k^*\right\} = &\left[\frac{P_{\text{loss},k}}{\left(1 - m_k \frac{\rho}{\alpha_k}\right) v_{\max,k}} + w_k\right] \mathbb{E}\big\{d(\mathcal{H}_k)\big\} \\ &+ t_c m_k P_{\text{TH}} \int_{\mathcal{W}} \mathbb{E}\left\{\frac{1}{G(q)}\middle| q\right\} \psi(q) dq, \end{aligned} \tag{5.34}$$

where averaging is done over every possible distribution of the channel. The channel power $G(q)$ is log-normally distributed in linear domain (Gaussian distributed, with mean $\widetilde{G}_{\text{dB}}(q)$ and variance $\widetilde{\sigma}^2(q)$, in the dB domain). We have

$$\begin{aligned} \mathbb{E}\left\{\frac{1}{G(q)}\middle| q\right\} &= \int_0^\infty \frac{10}{\log(10)\sqrt{2\pi}\widetilde{\sigma}(q) G^2} \exp\left(-\frac{\left(10\log_{10}(G) - \widetilde{G}_{\text{dB}}(q)\right)^2}{2\widetilde{\sigma}^2(q)}\right) dG \\ &= \frac{\exp\left(\frac{1}{2}\bar{\sigma}^2(q)\right)}{10^{\frac{\widetilde{G}_{\text{dB}}(q)}{10}}}. \end{aligned} \tag{5.35}$$

Also, using Lemma 5.2.2, $\mathbb{E}\big\{d(\mathcal{H}_k)\big\} = \zeta\sqrt{m_k}$ for large m_k. After substituting $\mathbb{E}\left\{\frac{1}{G(q)}\middle| q\right\}$ and $\mathbb{E}\big\{d(\mathcal{H}_k)\big\}$ into (5.34), (5.33) is obtained. □

Note that Theorem 5.2.3 characterizes the exact average minimum energy consumption, as it directly calculates the average of E_k^* in (5.14) over the distributions of the channel and POIs.

5.3 Dynamic Coverage of Time-Varying Environments in the Communication-Efficient Case

In this section, we study dynamic coverage of time-varying environments in the communication-efficient case. Unlike the communication-intensive case, the mobile agents are not required to be connected at the positions of all POIs in this case, as long as they are connected at least once along their trajectories. Next, we present the definition of the dynamic coverage policy in the communication-efficient case and formulate the problem. We then show how to design optimal feasible stabilizing policies for the mobile agents in this case.

5.3.1 Problem Formulation

Consider the dynamical system of (5.2). Similar to the communication-intensive case, a dynamic coverage policy in the communication-efficient case is defined as follows:

Definition 5.3.1. *In the communication-efficient case, a dynamic coverage policy for the k^{th} mobile agent is a tuple $\mathcal{P}_k = \big(\mathcal{V}_k, \mathcal{C}_k, v_k, \xi_{\mathrm{TX},k}, P_{\mathrm{TX},k}, \{t_{i,k}\}_{i\in\mathcal{V}_k}\big)$, where $\mathcal{V}_k$ is the non-empty set of POIs assigned to the k^{th} agent, $\mathcal{C}_k$ is the Hamiltonian cycle defined on $\mathcal{V}_k$, v_k is the constant velocity of the k^{th} agent, $\xi_{\mathrm{TX},k}$ is the only position along the Hamiltonian cycle $\mathcal{C}_k$ assigned for communication, $P_{\mathrm{TX},k}$ is the transmission power of the k^{th} agent at $\xi_{\mathrm{TX},k}$, and $t_{i,k}$, for $i \in \mathcal{V}_k$, is the stop time of the k^{th} mobile agent at the i^{th} POI. The overall dynamic coverage policy to find is then the tuple $\mathcal{P} = (\mathcal{P}_1, \cdots, \mathcal{P}_n)$.*

Note that we have assumed only one transmission in one period.[9] The definitions

[9]The results can be easily extended to the case of multiple transmissions in one period. Multiple transmission is, in particular, useful to increase the spatial diversity and therefore the robustness of the proposed scheme to multipath fading and other channel assessment errors.

of the feasible coverage policies, stable coverage tasks, and the conditions for a policy $\mathcal{P}$ to be a feasible stabilizing policy in the communication-efficient case are also similar to the communication-intensive case. The only differences are as follows: 1) the total communication energy $t_c \sum_{i\in\mathcal{V}_k} P_{\mathrm{TX},i,k}$ in the second condition of (5.8) is replaced by $t_c P_{\mathrm{TX},k}$, 2) $P_{\mathrm{TX},i,k}$ in the third condition of (5.8) is replaced by $P_{\mathrm{TX},k}$, for all $i \in \mathcal{V}_k$, and 3) the channel powers $G(q_i)$, in the third condition of (5.8), are replaced by $G(\xi_{\mathrm{TX},k})$. Here, the communication-time t_c is as defined in the communication-intensive case.

In order to maximize the lifetime of the mobile agents, we therefore have the following optimization problem to find the optimal feasible stabilizing policies in the communication-efficient case:

Problem 5.3.1. *The maximum-lifetime feasible stabilizing dynamic coverage policy for coverage of time-varying environments in the communication-efficient case is given as follows:*

$$\min_{\mathcal{P},E_1,\cdots,E_n} \sum_{k=1}^{n} \varpi_k E_k, \tag{5.36}$$

s.t.

$$\begin{aligned}
&1)\ \alpha_{i,k} t_{i,k} - \rho_i \left(\sum_{i\in\mathcal{V}_k} t_{i,k} + \frac{\mathrm{d}(\mathcal{C}_k)}{v_k} \right) \geq \Delta_k, \qquad \forall i \in \mathcal{V}_k,\ k = 1,\cdots,n,\\
&2)\ \sum_{i\in\mathcal{V}_k} t_{i,k} + \frac{\mathrm{d}(\mathcal{C}_k)}{v_k} \leq T_{\max}, \qquad k = 1,\cdots,n,\\
&3)\ P_{\mathrm{loss},s,k} \sum_{i\in\mathcal{V}_k} t_{i,k} + \left(\frac{P_{\mathrm{loss},m,k}}{v_k} + w_k \right) \mathrm{d}(\mathcal{C}_k) + t_c P_{\mathrm{TX},k} \leq E_k, \qquad k = 1,\cdots,n,\\
&4)\ P_{\mathrm{TX},\max,k} \geq P_{\mathrm{TX},k} \geq \frac{P_{\mathrm{TH}}}{G(\xi_{\mathrm{TX},k})}, \qquad k = 1,\cdots,n,\\
&5)\ 0 \leq v_k \leq v_{\max,k}, \qquad k = 1,\cdots,n,\\
&6)\ E_k \leq E_{\max,k}, \qquad k = 1,\cdots,n,
\end{aligned} \tag{5.37}$$

where we set $\Delta_k \geq 0$ *and* $\varpi_k > 0$.

Note that in the communication-efficient case, the communication points $\xi_{\mathrm{TX},k}$, for $k = 1, \cdots, n$, also need to be optimized. Also, here the mobile agents do not stop to communicate at the communication points, i.e., they transmit for a time interval with length t_c as they move.[10] Next we show how this dynamic coverage problem can be optimally solved using an MILP, similar to the communication-intensive case.

5.3.2 Optimal Solution of the Dynamic Coverage Problem in the Communication-Efficient Case – Case of Known Channel Powers at the POIs

Consider Problem 5.3.1. Based on the definition of the dynamic coverage policy in the communication-efficient case, $\xi_{\mathrm{TX},k}$ can be any point on the Hamiltonian cycle $\mathcal{C}_k$ of the k^{th} agent. Finding the optimal coverage policy in this case is very challenging. This is due to the fact that given the partition $\{\mathcal{V}_k\}_{k=1}^n$ and conditioned on the channel power over the workspace, the optimal Hamiltonian cycle for an agent k may be different from the minimum-length Hamiltonian cycle $\mathcal{H}_k$. In other words, since there is no requirement for transmission at the POIs, moving to a point out of the minimum-length Hamiltonian cycle can possibly minimize the communication energy and the resulting overall energy consumption. To simplify the problem, we consider the following assumption in this section:

Assumption 5.3.1. *The communication point $\xi_{\mathrm{TX},k}$ is selected from the set of POIs $\mathcal{V}_k$, i.e., $\xi_{\mathrm{TX},k} = q_i$, for some $i \in \mathcal{V}_k$.*

Based on this assumption and given a partition $\{\mathcal{V}_k\}_{k=1}^n$, the optimal policy in the communication-efficient case is then given by the following theorem:

[10] As compared to the communication-intensive case, t_c could be larger in the communication-efficient case, since more data is sent to the remote station in each transmission. Still, we assume that t_c is small enough such that the movement of the k^{th} mobile agent while communicating, i.e., $v_{\max,k} t_c$, is negligible for all k.

Theorem 5.3.1. *Consider a partition $\{\mathcal{V}_k\}_{k=1}^n$ of $\mathcal{V}$. Then, assuming that the channel powers $G(q_i)$, for $i \in \mathcal{V}$, are known, the following are true for the solution of Problem 5.3.1, in the communication-efficient case:*

1. *For a given set of non-negative stability margins Δ_k, $k = 1, \cdots, n$, Problem 5.3.1 is feasible if and only if the following are true, for $k = 1, \cdots, n$:*

$$1)\ \frac{P_{\mathrm{TH}}}{\max_{i\in\mathcal{V}_k}\{G(q_i)\}} \leq P_{\mathrm{TX,max},k}, \tag{5.38}$$
$$2)\ \sum_{i\in\mathcal{V}_k} \frac{\rho_i}{\alpha_{i,k}} < 1,$$
$$3)\ \frac{\mathrm{d}(\mathcal{H}_k)}{v_{\max,k}} \leq \min\left\{T_{\max}\phi_k - \Delta_k\eta_k, \frac{\big(\overline{E}_{\max,k} - w_k\mathrm{d}(\mathcal{H}_k)\big)\phi_k - \Delta_k\eta_k P_{\mathrm{loss},s,k}}{(1-\phi_k)P_{\mathrm{loss},s,k} + \phi_k P_{\mathrm{loss},m,k}}\right\},$$

where $\mathcal{H}_k$ denotes the minimum-length Hamiltonian cycle on $\mathcal{V}_k$, $\overline{E}_{\max,k} \triangleq E_{\max,k} - t_c\frac{P_{\mathrm{TH}}}{\max_{i\in\mathcal{V}_k}\{G(q_i)\}}$, $\phi_k \triangleq 1 - \sum_{i\in\mathcal{V}_k}\frac{\rho_i}{\alpha_{i,k}}$ and $\eta_k \triangleq \sum_{i\in\mathcal{V}_k}\frac{1}{\alpha_{i,k}}$.

2. *The maximum stability margin that can be selected for each agent k, for $k = 1, \cdots, n$, is given as follows when $\sum_{i\in\mathcal{V}_k}\frac{\rho_i}{\alpha_{i,k}} < 1$:*

$$\Delta_{\max,k} = \min\left\{\frac{\overline{E}_{\max,k} - w_k\mathrm{d}(\mathcal{H}_k) + \big(P_{\mathrm{loss},s,k} - P_{\mathrm{loss},m,k}\big)\frac{\mathrm{d}(\mathcal{H}_k)}{v_{\max,k}}}{P_{\mathrm{loss},s,k}}, T_{\max}\right\}\frac{\phi_k}{\eta_k} - \frac{1}{\eta_k}\frac{\mathrm{d}(\mathcal{H}_k)}{v_{\max,k}}. \tag{5.39}$$

3. *There exists a feasible stabilizing policy, i.e., Problem 5.2.1 is feasible for at least one set of non-negative Δ_k, if and only if the following are true, for $k = 1, \cdots, n$:*

$$1)\ \frac{P_{\mathrm{TH}}}{\max_{i\in\mathcal{V}_k}\{G(q_i)\}} \leq P_{\mathrm{TX,max},k}, \tag{5.40}$$
$$2)\ \sum_{i\in\mathcal{V}_k} \frac{\rho_i}{\alpha_{i,k}} < 1,$$
$$3)\ \frac{\mathrm{d}(\mathcal{H}_k)}{v_{\max,k}} \leq \min\left\{T_{\max}, \frac{\overline{E}_{\max,k} - w_k\mathrm{d}(\mathcal{H}_k)}{(1-\phi_k)P_{\mathrm{loss},s,k} + \phi_k P_{\mathrm{loss},m,k}}\right\}\phi_k.$$

4. If Problem 5.3.1 is feasible, the optimal Hamiltonian cycle, velocity, transmission power and transmission point of the k^{th} agent, for $k = 1, \cdots, n$, are given as follows: $\mathcal{C}_k^* = \mathcal{H}_k$, $v_k^* = v_{\max,k}$, $P_{\text{TX},k}^* = \frac{P_{\text{TH}}}{\max_{i\in\mathcal{V}_k}\{G(q_i)\}}$ and $\xi_{\text{TX},k}^* = q_{i_k^*}$, where $i_k^* = \text{argmax}_{i\in\mathcal{V}_k} G(q_i)$. We also have the following for the optimal stop times and total energy of the mobile agents:

$$1)\ t_{i,k}^* = \Delta_k \left(\frac{1}{\alpha_{i,k}} + \frac{\rho_i \eta_k}{\alpha_{i,k}\phi_k} \right) + \frac{\rho_i}{\alpha_{i,k}\phi_k} \frac{\mathrm{d}(\mathcal{H}_k)}{v_{\max,k}}, \qquad \forall i \in \mathcal{V}_k, \tag{5.41}$$

$$2)\ E_k^* = P_{\text{loss},s,k} \left(\frac{\Delta_k \eta_k}{\phi_k} + \frac{1-\phi_k}{\phi_k} \frac{\mathrm{d}(\mathcal{H}_k)}{v_{\max,k}} \right) + \left(\frac{P_{\text{loss},m,k}}{v_{\max,k}} + w_k \right) \mathrm{d}(\mathcal{H}_k) + t_c \frac{P_{\text{TH}}}{\max_{i\in\mathcal{V}_k}\{G(q_i)\}}.$$

Proof. The proof is similar to the proof of Theorem 5.2.1 and is omitted for brevity. □

Similar to the communication-intensive case, we next propose an MILP to solve Problem 5.3.1. This MILP can be used to find the optimal partitions, optimal Hamiltonian cycles, optimal communication points and optimal stopping times for the mobile agents when the maximum allowed velocities and minimum possible transmission powers are used. However, the MILP formulation is more complicated in this case, since the optimal transmission points and, therefore, the optimal transmission powers of the mobile agent are not known beforehand. The MILP formulation for solving Problem 5.3.1 is given in Program 2.

In Program 2, the constant Ω' is selected large enough, similar to Ω in Program 1. Furthermore, in addition to the variables used in Program 1, we have introduced mn auxiliary binary variables $y_{i,k}$, for $i \in \mathcal{V}$ and $k = 1, \cdots, n$. For each mobile agent k, $y_{i,k} = 1$ if the i^{th} POI is selected as the communication point, and $y_{i,k} = 0$ otherwise. Constraint 10 in Program 2 guarantees that only one POI in $\mathcal{V}_k$ is selected as the communication point. Constraint 11 also forces $y_{i,k} = 0$ whenever $x_{i,k} = 0$. Explanation of other constraints is similar to Program 1. Fig. 5.3 shows sample

Program 2: MILP for solving Problem 5.3.1 in the communication-efficient case

$\min \sum_{k=1}^{n} \varpi_k E_k,$

s.t.

1) $\alpha_{i,k} t_{i,k} - \rho_i \left(\sum_{i=1}^{m} t_{i,k} + \frac{1}{v_{\max,k}} \sum_{i=1}^{m} \sum_{j=1, j\neq i}^{m} z_{i,j,k} d_{i,j} \right) + (1 - x_{i,k}) \Omega' \geq \Delta_k, \ \forall i, k,$

2) $\sum_{i=1}^{m} t_{i,k} + \frac{1}{v_{\max,k}} \sum_{i=1}^{m} \sum_{j=1, j\neq i}^{m} z_{i,j,k} d_{i,j} \leq T_{\max}, \qquad \forall k,$

3) $P_{\text{loss},s,k} \sum_{i=1}^{m} t_{i,k} + \left(\frac{P_{\text{loss},m,k}}{v_{\max,k}} + w_k \right) \sum_{i=1}^{m} \sum_{j=1, j\neq i}^{m} z_{i,j,k} d_{i,j} + t_c \sum_{i=1}^{m} \frac{y_{i,k} P_{\text{TH}}}{G(q_i)} \leq E_k, \forall k,$

4) $\sum_{j=1, j\neq i}^{m} z_{i,j,k} = x_{i,k}, \ \sum_{j=1, j\neq i}^{m} z_{j,i,k} = x_{i,k}, \qquad \forall i, k,$

5) $\sum_{k=1}^{n} x_{i,k} = 1, \qquad \forall i,$

6) $\sum_{i=1}^{m} h_i = n,$

7) $u_i - u_j - m(h_i + h_j) + (m-1) \sum_{k=1}^{n} z_{i,j,k} \leq m - 2, \qquad \forall i, j \neq i,$

8) $2 - h_i \leq u_i \leq m, \qquad \forall i,$

9) $t_{i,k} \leq x_{i,k} \Omega', \qquad \forall i, k,$

10) $\sum_{i=1}^{m} y_{i,k} = 1, \qquad \forall k,$

11) $y_{i,k} \leq x_{i,k} \Omega', \qquad \forall i, k,$

12) $y_{i,k} \frac{P_{\text{TH}}}{G(q_i)} \leq P_{\text{TX},\max,k}, \qquad \forall i, k,$

13) $E_k \leq E_{\max,k}, \qquad \forall k,$

14) $z_{i,j,k} \in \{0,1\}, x_{i,k} \in \{0,1\}, y_{i,k} \in \{0,1\}, h_i \in \{0,1\}, u_i \in \mathbb{N}, 0 \leq t_{i,k} \leq \Omega', \forall i, j, k,$

plots of $\Psi_i(t)$ and $\Phi_i(t)$ for one of the POIs after optimizing the dynamic coverage operation using the MILP of Program 2. Fig. 5.3 (left) corresponds to the case where $\Delta_k > 0$ (robust dynamic coverage with positive stability margin) and Fig. 5.3 (right) corresponds to the case where $\Delta_k = 0$ (zero stability margin). It can be seen that, similar to the communication-intensive case, a positive stability margin results in longer stop time and more energy consumption at the point of interest, as proved in Theorem 5.3.1. It can also be seen how $\Psi_i(t)$ at the remote station becomes equal to $\Phi_i(t)$ any time the mobile agent communicates to the remote station (in this example

the communication point is located at another POI).

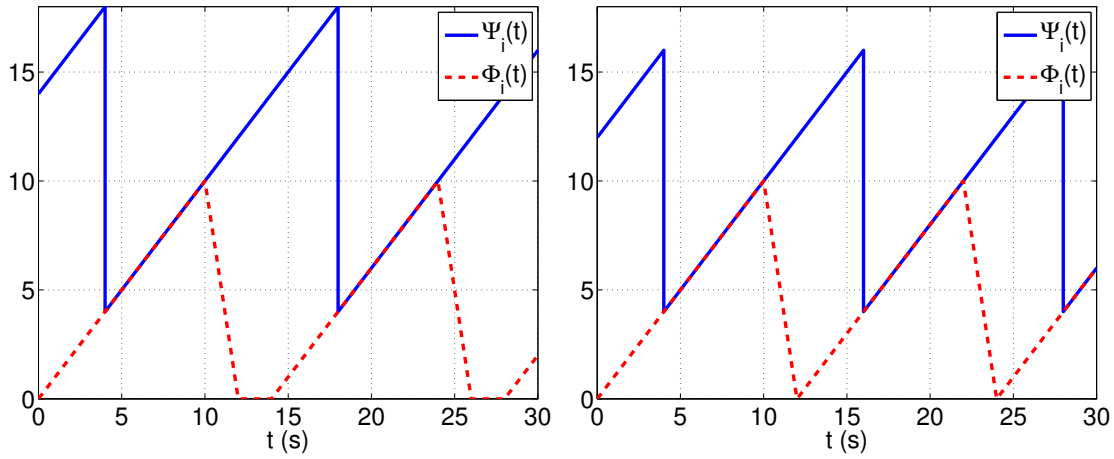

Figure 5.3: Sample plots of $\Psi_i(t)$ and $\Phi_i(t)$ in the communication-efficient case for one of the POIs after optimizing the dynamic coverage operation using the MILP of Program 2. The left figure corresponds to the case where $\Delta_k > 0$ (robust dynamic coverage with positive stability margin) and the right figure corresponds to the case where $\Delta_k = 0$ (zero stability margin).

Virtual POIs in the Communication-Efficient Case

The coverage task in the communication-efficient case can be feasibly stabilized if at least one POI is connected along the Hamiltonian cycle of each mobile agent (as opposed to all POIs in the communication-intensive case). In case there is no feasible stabilizing dynamic coverage policy in the communication-efficient case, due to a poor channel quality at the POIs, we may be able to feasibly stabilize the coverage task by adding a number of *virtual* POIs. These are points close enough to the actual POIs, which have a good channel quality. Adding virtual POIs does not guarantee the existence of a feasible stabilizing coverage policy. It, however, increases the chance of finding such a policy in case the channel quality is low at the positions of the actual POIs.

5.3.3 Optimal Solution of the Dynamic Coverage Problem in the Communication-Efficient Case – Case of Unknown Stochastic Channel Powers at the POIs

The definitions of the chance constraints and χ-probable feasible stabilizing dynamic coverage policies, presented in Section 5.2.3 for Problem 5.2.1, can also be applied to Problem 5.3.1 as well. Similarly, the minimum transmission power constraint (constraint 4 of Problem 5.3.1) will have the following chance-constrained form:

$$\mathbb{P}\left\{P_{\mathrm{TX},k} \geq \frac{P_{\mathrm{TH}}}{G(\xi_{\mathrm{TX},k})}\right\} \geq \chi, \qquad k = 1, \cdots, n. \tag{5.42}$$

Using the distribution of the channel power in the dB domain given by our channel assessment framework of Chapter 2, we can show that this condition is equivalent to

$$P_{\mathrm{TX},k} \geq 10^{-\left(\sigma(\xi_{\mathrm{TX},k})Q^{-1}(\chi)+\hat{G}_{\mathrm{dB}}(\xi_{\mathrm{TX},k})\right)/10} P_{\mathrm{TH}} \triangleq \Gamma(\xi_{\mathrm{TX},k}, \chi), \qquad k = 1, \cdots, n. \tag{5.43}$$

Similar to the communication-intensive case, this result shows that in order to account for stochastic channels, when designing optimal dynamic coverage policies in the communication-efficient case, it is sufficient to replace $\frac{P_{\mathrm{TH}}}{G(\xi_{\mathrm{TX},k})}$ with $\Gamma(\xi_{\mathrm{TX},k}, \chi)$ in Problem 5.3.1. Then, the results of Theorem 5.3.1 and the MILP of Program 2 can readily be used in this case as well. We can see that, given the partition $\{\mathcal{V}_k\}_{k=1}^n$, the optimum communication point $\xi^*_{\mathrm{TX},k}$ is given by $\xi^*_{\mathrm{TX},k} = q_{i^*_k}$, where $i^*_k = \mathrm{argmin}_{i\in\mathcal{V}_k}\Gamma(q_i, \chi)$. Also, there is a χ-probable feasible stabilizing policy for the k^{th} agent, for $k = 1, \cdots, n$, if and only if

$$\begin{aligned}
&1)\ \min_{i\in\mathcal{V}_k}\Gamma(q_i,\chi) \leq P_{\mathrm{TX,max},k}, \\
&2)\ \sum_{i\in\mathcal{V}_k}\frac{\rho_i}{\alpha_{i,k}} < 1, \\
&3)\ \min\left\{\frac{E_{\max,k} - t_c \min_{i\in\mathcal{V}_k}\Gamma(q_i,\chi) - w_k \mathrm{d}(\mathcal{H}_k)}{(1-\phi_k)P_{\mathrm{loss},s,k} + \phi_k P_{\mathrm{loss},m,k}}, T_{\max}\right\}\phi_k \geq \frac{\mathrm{d}(\mathcal{H}_k)}{v_{\max,k}}.
\end{aligned} \tag{5.44}$$

5.3.4 Probabilistic Analysis of the Dynamic Coverage Problem in the Communication-Efficient Case

The same approach we used in Section 5.2.4 can be followed to probabilistically analyze the dynamic coverage problem in the communication-efficient case. Assume that the POIs are independently and identically distributed (i.i.d.) according to an absolutely continuous pdf $\psi(q)$, defined over the workspace $\mathcal{W}$. Also, assume that, conditioned on every $q \in \mathcal{W}$, the channel power $G(q)$ is Gaussian-distributed in the dB domain, with $\widetilde{G}_{\mathrm{dB}}(q)$ and $\widetilde{\sigma}^2(q)$ representing its mean and variance respectively. By following the same (sub-optimal) chance constraint approach of Section 5.2.4 and by considering Assumptions 5.2.1, 5.2.2 and 5.2.3, we can show that, given a partition $\{\mathcal{V}_k\}_{k=1}^n$, there exists a χ-probable feasible stabilizing dynamic coverage policy for this case if the following are true, for all $k = 1, \cdots, n$:

$$\begin{aligned} &1)\ \Gamma(\chi) \leq P_{\mathrm{TX,max},k}, \\ &2)\ m_k < \frac{\alpha_k}{\rho}, \\ &3)\ \min\left\{\frac{E_{\max,k} - t_c\Gamma(\chi) - w_k\zeta\sqrt{m_k}}{P_{\mathrm{loss},k}}, T_{\max}\right\}\left(1 - m_k\frac{\rho}{\alpha_k}\right) \geq \frac{\zeta\sqrt{m_k}}{v_{\max,k}}, \end{aligned} \tag{5.45}$$

where m_k is the number of POIs assigned to the k^{th} agent, which is assumed large enough (refer to Section 5.2.4), and $\Gamma(\chi)$ is a function of $\widetilde{G}_{\mathrm{dB}}(q)$ and $\widetilde{\sigma}^2(q)$, as defined in (5.27). Next, similar to the communication-intensive case, we use (5.45) to find an upper bound on the maximum number of POIs that can be assigned to each agent.

An Upper Bound on the Maximum Number of POIs Covered by a Mobile Agent in the Communication-Efficient Case

Consider the following theorem:

Theorem 5.3.2. *Assume that for the k^{th} agent and for the given χ, we have $\Gamma(\chi) \leq P_{\mathrm{TX,max},k}$, where $\Gamma(\chi)$ is given by (5.27). Then, under Assumptions 5.2.1, 5.2.2 and*

5.2.3, an upper-bound on the maximum number of POIs that can be assigned to the k^{th} agent, to guarantee a χ-probable feasible stabilizing dynamic coverage policy in the communication-efficient case, is given by the following:

$$\overline{m}_k = \begin{cases} \min\left\{s_{k,1}^2, s_{k,2}^2\right\}, & \mathcal{A}_k \cap \mathcal{B}_k = \emptyset,\ E_{\max,k} - t_c\Gamma(\chi) > P_{\text{loss},k} T_{\max} \\ \max\left\{s^2 \middle| s \in \mathcal{A}_k \cap \mathcal{B}_k\right\}, & \mathcal{A}_k \cap \mathcal{B}_k \neq \emptyset,\ E_{\max,k} - t_c\Gamma(\chi) > P_{\text{loss},k} T_{\max} \\ \max\left\{s^2 \middle| s \in \mathcal{A}'_k \cap \mathcal{B}_k\right\}, & \mathcal{A}'_k \cap \mathcal{B}_k \neq \emptyset,\ E_{\max,k} - t_c\Gamma(\chi) \leq P_{\text{loss},k} T_{\max} \end{cases}, \tag{5.46}$$

provided that such $\overline{m}_k$ exists (chance-constrained version of Problem 5.3.1 is feasible) and it is sufficiently large. Here,

$$\begin{aligned} s_{k,1} &= \frac{-\zeta/v_{\max,k} + \sqrt{\zeta^2/v_{\max,k}^2 + 4T_{\max}^2\rho/\alpha_k}}{2T_{\max}\rho/\alpha_k}, \\ s_{k,2} &= \frac{E_{\max,k} - t_c\Gamma(\chi) - P_{\text{loss},k}T_{\max}}{\zeta w_k}, \\ s_{k,3} &= \min\left\{\sqrt{\frac{\alpha_k}{\rho}}, \frac{E_{\max,k} - t_c\Gamma(\chi)}{\zeta w_k}\right\}, \\ \mathcal{A}_k &= \left\{s \middle| s_{k,2} \leq s \leq s_{k,3}\right\},\ \mathcal{A}'_k = \left\{s \middle| 0 \leq s \leq s_{k,3}\right\}, \\ \mathcal{B}_k &= \left\{s \middle| \left(\frac{\zeta P_{\text{loss},k}}{v_{\max,k}} + \zeta w_k\right) s + \frac{\left(E_{\max,k} - t_c\Gamma(\chi)\right)\rho}{\alpha_k} s^2 - \frac{\zeta w_k \rho}{\alpha_k} s^3 \leq E_{\max,k}\right\}. \end{aligned} \tag{5.47}$$

Proof. Consider the constraints in (5.45) and assume that m_k is large enough. By defining the variable $s \triangleq \sqrt{m_k}$ and after some straightforward derivations, we can conclude that any feasible $s \geq 0$ satisfies the following sets of constraints: 1) $\frac{T_{\max}\rho}{\alpha_k}s^2 + \frac{\zeta}{v_{\max,k}}s \leq T_{\max},\ s \leq \frac{E_{\max,k} - t_c\Gamma(\chi) - P_{\text{loss},k}T_{\max}}{\zeta w_k}$ or 2) $\frac{E_{\max,k} - t_c\Gamma(\chi)}{\zeta w_k} \geq s \geq \frac{E_{\max,k} - t_c\Gamma(\chi) - P_{\text{loss},k}T_{\max}}{\zeta w_k},\ s^2 \leq \frac{\alpha_k}{\rho},\ \left(\frac{\zeta P_{\text{loss},k}}{v_{\max,k}} + \zeta w_k\right) s + \frac{\left(E_{\max,k} - t_c\Gamma(\chi)\right)\rho}{\alpha_k} s^2 - \frac{\zeta w_k \rho}{\alpha_k} s^3 \leq E_{\max,k}$. The maximum s that satisfies one of these constraints is then found using a procedure similar to that of Theorem 5.2.2 for two cases of $E_{\max,k} - t_c\Gamma(\chi) > P_{\text{loss},k}T_{\max}$ and $E_{\max,k} - t_c\Gamma(\chi) \leq P_{\text{loss},k}T_{\max}$. □

Average Minimum Energy Per Period Consumed to Cover a Set of POIs by a Mobile Agent in the Communication-Efficient Case

An approach similar to that of the communication-intensive case can be followed to calculate the average of the minimum energy consumed in one period by the k^{th} mobile agent to feasibly stabilize its assigned POIs in the communication-efficient case. Unlike communication-intensive case, however, the joint pdf of the channel powers at the POIs is required in this case. From Chapter 2, we know that, given a set of channel positions, the joint pdf of the channel powers is given by a multi-variate Gaussian distribution. Without loss of generality, assume that we order the POIs assigned to the k^{th} agent as follows: $\mathcal{V}_k = \{1, \cdots, m_k\}$. Let $\widetilde{G}_{\text{dB}}(Q_k)$ and $\widetilde{\Sigma}(Q_k)$, for $Q_k \triangleq \left[q_1^{\text{T}}, \cdots, q_{m_k}^{\text{T}}\right]^{\text{T}}$, denote the $m_k \times 1$ mean vector and $m_k \times m_k$ covariance matrix of the multi-variate Gaussian distribution that gives the joint pdf of the channel powers at these POIs. We then have the following theorem:

Theorem 5.3.3. *Consider Assumptions 5.2.1, 5.2.2 and 5.2.3. Then, the average of the minimum energy consumed in one period by the k^{th} mobile agent, to feasibly stabilize its assigned POIs, is given as follows in the communication-efficient case:*

$$E_{\text{min,ave},k} = \left[\frac{P_{\text{loss},k}}{\left(1 - m_k \frac{\rho}{\alpha_k}\right) v_{\max,k}} + w_k\right] \zeta \sqrt{m_k} + t_c P_{\text{TH}} \int_{\mathcal{W}} \cdots \int_{\mathcal{W}} \int_{-\infty}^{\infty} 10^{-x/10} \frac{\partial}{\partial x} \Upsilon(x, Q_k) \psi(q_1) \cdots \psi(q_{m_k}) dx dQ_k, \quad (5.48)$$

where $Q_k \triangleq \left[q_1^{\text{T}}, \cdots, q_{m_k}^{\text{T}}\right]^{\text{T}}$ is the stacked vector of the positions of the POIs in $\mathcal{V}_k$, $m_k < \frac{\alpha_k}{\rho}$,

$$\Upsilon(x, Q_k) \triangleq \int_{-\infty}^{x} \cdots \int_{-\infty}^{x} \frac{\exp\left(-\frac{1}{2}\left(G_{\text{dB}} - \widetilde{G}_{\text{dB}}(Q_k)\right)^{\text{T}} \widetilde{\Sigma}^{-1}(Q_k) \left(G_{\text{dB}} - \widetilde{G}_{\text{dB}}(Q_k)\right)\right)}{(2\pi)^{\frac{m_k}{2}} \left|\widetilde{\Sigma}(Q_k)\right|^{\frac{1}{2}}} dG_{\text{dB}}, \quad (5.49)$$

and $\widetilde{G}_{\text{dB}}(Q_k)$ and $\widetilde{\Sigma}(Q_k)$ denote the mean vector and covariance matrix of the multi-variate Gaussian distribution characterizing the channel powers at the POIs in the

dB domain.

Proof. The proof is similar to the proof of Theorem 5.2.3. The minimum energy occurs when the stability margin is zero. By setting $\Delta_k = 0$ in (5.41), and based on Assumptions 5.2.1, 5.2.2 and 5.2.3, we obtain

$$E_{\min,\text{ave},k} = \mathbb{E}\left\{E_k^*\right\} = \left[\frac{P_{\text{loss},k}}{\left(1 - m_k \frac{\rho}{\alpha_k}\right) v_{\max,k}} + w_k\right] \mathbb{E}\big\{d(\mathcal{H}_k)\big\} \tag{5.50}$$
$$+ t_c P_{\text{TH}} \int_{\mathcal{W}} \cdots \int_{\mathcal{W}} \mathbb{E}\left\{\frac{1}{\max_{i\in\mathcal{V}_k} G(q_i)}\middle| Q_k\right\} \psi(q_1)\cdots\psi(q_{m_k}) dQ_k.$$

Let us define $G_{\max} = \max_{i\in\mathcal{V}_k}\big\{G_{\text{dB}}(q_i)\big\}$. Then, the cumulative density function (cdf) of $G_{\max}$ is given as follows:

$$\mathbb{P}\{G_{\max} \le x\} = \int_{-\infty}^{x}\cdots\int_{-\infty}^{x} \frac{\exp\left(-\frac{1}{2}\big(G_{\text{dB}} - \widetilde{G}_{\text{dB}}(Q_k)\big)^{\text{T}} \widetilde{\Sigma}^{-1}(Q_k)\big(G_{\text{dB}} - \widetilde{G}_{\text{dB}}(Q_k)\big)\right)}{(2\pi)^{\frac{m_k}{2}}\left|\widetilde{\Sigma}(Q_k)\right|^{\frac{1}{2}}} dG_{\text{dB}}$$
$$= \Upsilon(x, Q_k). \tag{5.51}$$

We therefore have

$$\mathbb{E}\left\{\frac{1}{\max_{i\in\mathcal{V}_k} G(q_i)}\middle| Q_k\right\} = \int_{-\infty}^{\infty} 10^{-x/10} \frac{\partial}{\partial x}\Upsilon(x, Q_k) dx. \tag{5.52}$$

Also, using Lemma 5.2.2, $\mathbb{E}\big\{d(\mathcal{H}_k)\big\} = \zeta\sqrt{m_k}$ for large m_k. After substituting $\mathbb{E}\left\{\frac{1}{G(q)}\middle| q\right\}$ and $\mathbb{E}\big\{d(\mathcal{H}_k)\big\}$ into (5.50), (5.48) is obtained. □

Note that the average of the minimum energy per period in the communication-efficient case is more complicated than the one derived in the communication-intensive case.

5.4 Simulation Results

In this section, we present our simulation results for the dynamic coverage of a time-varying environment using the proposed framework. The simulation environment

was implemented in C++ and MATLAB. To solve the MILPs, we used IBM ILOG CPLEX Optimization Studio v12.2.

Fig. 5.5 shows the result of applying the proposed dynamic coverage framework to cover 24 POIs using 3 mobile agents, in a 200 m by 200 m workspace. The wireless channel between the mobile agents and the remote station is generated using our probabilistic channel simulator, which can generate path loss, shadowing and multipath fading with realistic spatial correlations. A detailed description of this channel simulator can be found in [54, 56]. The 3D plot of the channel power over the workspace is shown in Fig. 5.4. In this example, the shadowing component of the channel is log-normally distributed in the linear domain (has a zero-mean Gaussian distribution in the dB domain). The multipath fading component is also Rician-distributed in the linear domain. The remote station is located at position $q_b = (-80, 80, 0.5)$ m. The following channel parameters are also used: $K_{\text{dB}} = -5$ dB, $n_{\text{PL}} = 2$, $\vartheta = 5$ dB, $\beta = 30$ m and $\omega = 2$ dB. See Chapter 2 for the descriptions of the channel parameters and the distributions of the shadowing and multipath components. The rest of the parameters are as follows: $\text{SNR}_{\text{TH}} = 25$ dB, $BN_0 = -90$ dB, $\alpha_{i,k} = 100$, $T_{\max} = 6000$ s, $E_{\max,k} = 40$ J, $v_{\max,k} = 0.1$ m/s, $P_{\text{TX},\max,k} = 800$ mW, $P_{\text{loss},m,k} = 0.1$ mW, $P_{\text{loss},s,k} = 0.2$ mW, $w_k = 0.1$ J/m (corresponding to a small-size light-load robot) and $\Delta_k = 0$, for $i = 1, \cdots, 24$ and $k = 1, 2, 3$. Furthermore, we set $\varpi_k = \frac{1}{3}$, for $k = 1, 2, 3$, and $t_c = 20$ s in both communication-intensive and communication-efficient cases. Note that the value of t_c is small enough such that communication can be done while stopping at the positions of the POIs (or while being very close to them).

Fig. 5.5 (left) and Fig. 5.5 (right) show the optimal trajectories of the mobile agents in the communication-intensive and communication-efficient cases respectively and for the case of known channel. The optimal communication points for each mobile agent in the communication-efficient case is also specified by a circle in Fig. 5.5

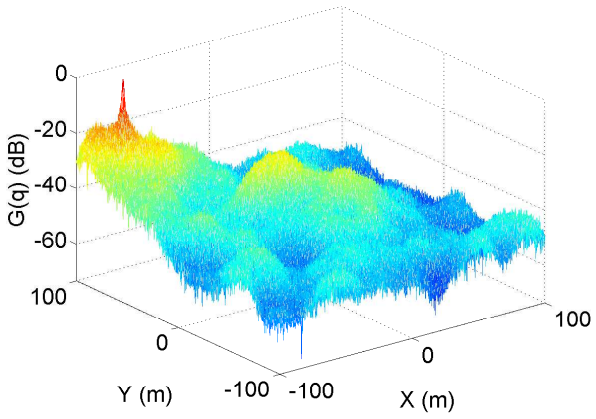

Figure 5.4: The 3D plot of the channel power $G(q)$ over the workspace of Fig. 5.5.

(right). The values of ρ_i and $G(q_i)$ for all the POIs are listed in Table 5.1. The optimal stop times at all the POIs, in both communication-intensive and communication-efficient cases, are listed in Table 5.2. The optimal period, optimal total energy per period, optimal motion energy per period and optimal communication energy per period, in both communication-intensive and communication-efficient cases and for all the mobile agents, are also listed in Table 5.3.

In can be seen that the optimal period and the optimal motion energy per period are larger for longer routes, as expected. The optimal communication energy per period, on the other hand, is a function of channel qualities at the POIs. For instance, in the communication-intensive case, Agent 2 (dashed-blue trajectory) is assigned to 5 POIs only. However, the optimal communication energy per period is the largest for this agent. This is due to the fact that the POIs assigned to this agent experience the lowest channel qualities among the POIs, as can be seen from Table 5.1. On the other hand, Agent 1 (solid-red trajectory) consumes the minimum communication energy in the communication-intensive case as its assigned POIs experience highest channel qualities. The same discussion applies to the optimal motion and communication energies in the communication-efficient case.

POI	ρ_i	$G(q_i)$ (dB)	POI	ρ_i	$G(q_i)$ (dB)	POI	ρ_i	$G(q_i)$ (dB)
1	2.01	-48.3	9	2.89	-42.8	17	2.38	-43.2
2	1.47	-49.3	10	1.92	-62.7	18	1.26	-30.3
3	1.23	-46.3	11	1.78	-51	19	1.74	-40.1
4	2.84	-45.9	12	1.54	-56.4	20	2.78	-43.7
5	2.91	-37.1	13	2.97	-51.4	21	1.34	-35.5
6	2.71	-46.5	14	1.59	-53.8	22	2.85	-54.1
7	1.19	-45.2	15	1.78	-49.4	23	2.42	-42.9
8	1.71	-39.8	16	1.39	-41.7	24	2.07	-34.9

Table 5.1: The value of ρ_i and $G(q_i)$ at the POIs in Fig. 5.5.

From Table 5.3, one can also see that the communication energy per period in the communication-efficient case is much less than the one in the communication-intensive case, as expected. Furthermore, it can be confirmed that the optimal communication point for each mobile agent in the communication-efficient case is the POI that experiences the maximum channel power among all the POIs assigned to that agent. It is worth mentioning that in this example the mobile agents are identical. Therefore, we can alternatively assign any mobile agent to any partition, in both communication-intensive and communication-efficient cases, without changing the optimal solution. Another important note is that for a given $E_{\max,k}$, the communication-efficient case imposes less constraint on the motion, since less communication energy is consumed as compared to the communication-intensive case (same t_c is used for both cases).

Note that the optimal partition found for the communication-efficient case cannot be used for the communication-intensive case as it violates the constraint on the total energy per period.

Fig. 5.28 (left) and Fig. 5.28 (right) show the plots of $\Psi_i(t)$ at the remote station for one sample POI in Fig. 5.5 (POI #4), in communication-intensive and communication-efficient cases respectively. In the communication-efficient case, the

Communication-Intensive Case				Communication-Efficient Case			
POI	$t^*_{i,k}$	POI	$t^*_{i,k}$	POI	$t^*_{i,k}$	POI	$t^*_{i,k}$
1	63.3 s	13	93.5 s	1	107 s	13	158 s
2	46.1 s	14	50 s	2	77.6 s	14	84.2 s
3	54.4 s	15	78.5 s	3	49.9 s	15	72 s
4	50.2 s	16	24.4 s	4	151 s	16	56.1 s
5	91.6 s	17	105 s	5	154 s	17	96.2 s
6	47.8 s	18	55.6 s	6	144 s	18	6.2 s
7	52.6 s	19	76.8 s	7	48.2 s	19	8.56 s
8	75.6 s	20	123 s	8	69.4 s	20	113 s
9	128 s	21	42.1 s	9	117 s	21	70.9 s
10	33.8 s	22	89.7 s	10	101 s	22	151 s
11	56 s	23	76 s	11	94.4 s	23	128 s
12	27.1 s	24	91.6 s	12	81.4 s	24	84 s

Table 5.2: The optimal stop times at all the POIs in Fig. 5.5 in both communication-intensive and communication-efficient cases.

plot of $\Phi_i(t)$ is also shown. Without loss of generality, in both figures we assume that at $t = 0$ the robot starts at POI 4. In the communication-efficient case, we also assume that communication happens at the end of visiting the POI that is selected as the optimal communication point (POI 21 in this case). In can be seen that $\Psi_i(t)$ remains bounded at the remote station in both cases. Similar plots can also be obtained for other POIs in Fig. 5.5.

Note that for a fixed $\mathcal{V}_k$, the maximum value of $\Psi_i(t)$ for any $i \in \mathcal{V}_k$ is larger in the

Communication-Intensive Case					Communication-Efficient Case				
k	T^*_k	E^*_k	$E^*_{m,k}$	$E^*_{c,k}$	k	T^*_k	E^*_k	$E^*_{m,k}$	$E^*_{c,k}$
1	4414 s	37.85 J	36.26 J	1.587 J	1	4050 s	33.94 J	33.92 J	0.01939 J
2	1764 s	31.14 J	16 J	15.14 J	2	5298 s	38.67 J	38.64 J	0.02229 J
3	3144 s	31.66 J	25.74 J	5.924 J	3	492.1 s	4.831 J	4.824 J	0.006781 J

Table 5.3: The optimal period, optimal total energy per period, optimal motion energy per period and optimal communication energy per period in both communication-intensive and communication-efficient cases and for all the mobile agents in Fig. 5.5.

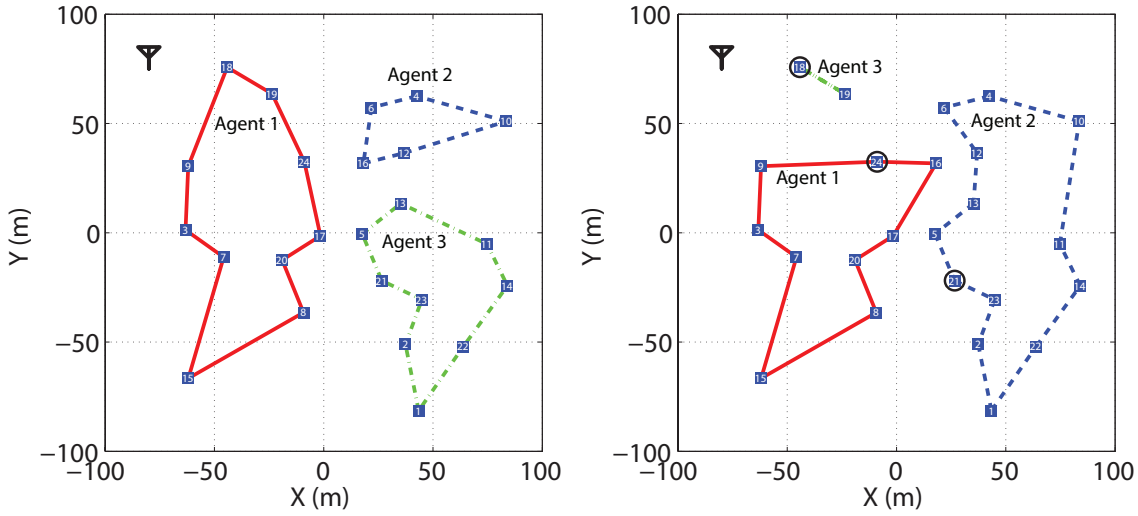

Figure 5.5: The optimal trajectories of the mobile agents in the communication-intensive (left) and communication-efficient (right) cases for the case of known channel. The solid red, dashed blue and dot-dashed green lines correspond to the trajectories of Agent 1, 2 and 3 respectively. The location of the remote station is denoted at the top left corner of the figures. The optimal communication points for each mobile agent in the communication-efficient case is also specified by a circle in the right figure.

communication-efficient case, as compared to the communication-intensive case. This is due to the fact that in the communication-efficient case, there is generally a delay in reporting the observation of each POI, which results in a non-zero minimum for $\Psi_i(t)$. However, the communication-efficient case can stabilize the dynamic coverage task with less constraints on the connectivity.

Next, consider the case where the channel powers at the POIs are not known and are assessed probabilistically. Assume the same workspace and channel of Fig. 5.5. In order to show our results more clearly, assume that only one mobile agent is used to cover the POIs. The system parameters are taken to be the same as the previous case, except we have $\alpha_i = 200$, $T_{\max} = 12000$ s, $E_{\max} = 200$ J, and $\Delta = 2000$ in this case. Note that we dropped the dependency of the system parameters on k, as we have only one mobile agent in this case. In this example, we assume that the channel is assessed using 0.5% of the total channel power samples (804 samples in a 401×401

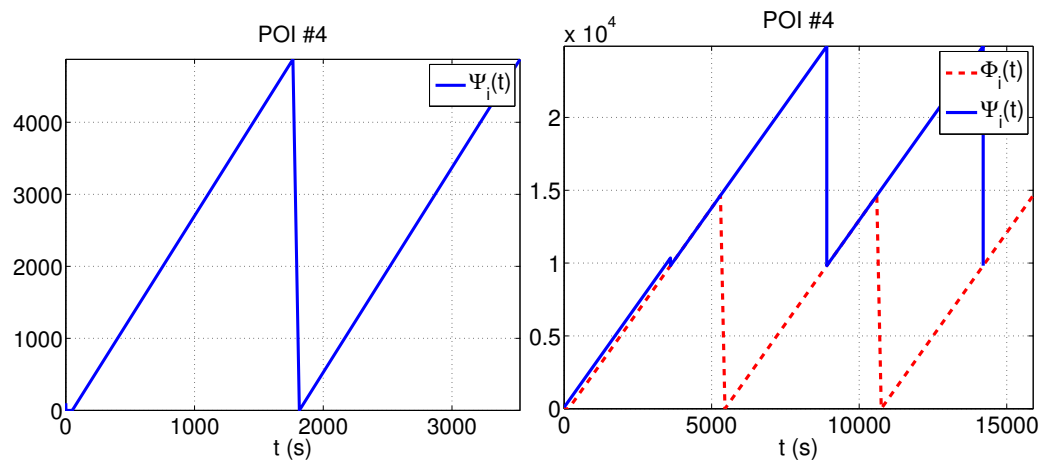

Figure 5.6: The plot of $\Psi_i(t)$ at the remote station for POI #4 in Fig. 5.5 in communication-intensive (left) and communication-efficient (right) cases. In the communication-efficient case, the plot of $\Phi_i(t)$ at the mobile agent is also provided.

grid), which are assumed to be randomly collected during an offline survey of the channel (see Chapter 2 for a detailed discussion on our probabilistic channel assessment framework). Fig. 5.7 (left) compares the estimated and actual channel powers at the positions of the POIs. Fig. 5.7 (right) then shows the optimal trajectory of the mobile agent in both communication-intensive and communication-efficient cases respectively. Note that, as proved by Theorems 5.2.1 and 5.3.1, the optimal trajectory in case of a single mobile agent is the minimum-length Hamiltonian cycle, in both communication-intensive and communication efficient cases. The optimal communication point in the communication efficient case, i.e., the POI with the smallest $\Gamma(q_i, \chi)$ (see Section 5.3.3), is also specified by a circle in Fig. 5.7 (right). Table 5.4 lists the optimal stop times and the value of $\Gamma(q_i, \chi)$ at all the POIs. For the sake of comparison, this table also shows the minimum required transmit power for the case of known channel powers, i.e., $\frac{P_{\text{TH}}}{G(q_i)}$, for all the POIs. The optimal period, optimal total energy per period, optimal motion energy per period and optimal communication energy per period, in both communication-intensive and communication-efficient

cases, are listed in Table 5.5.[11] In this example, we set $\chi = 0.95$. From Table 5.4, one can see that $\Gamma(q_i, \chi)$ is larger than the minimum required transmit power in case of known channel power, i.e., $\frac{P_{\text{TH}}}{G(q_i)}$, at each POI. This is to guarantee that, based on the variance of channel estimation, the probability of connectivity is larger than χ. Note that in Table 5.4, the optimal periods are the same for both communication-intensive and communication-efficient cases, since we only have one mobile agent. Also, as can be seen from Table 5.4, the optimal communication energy per period and, as a direct result, the optimal total energy per period is larger in the communication-intensive case, as expected (t_c is taken to be the same for both cases).

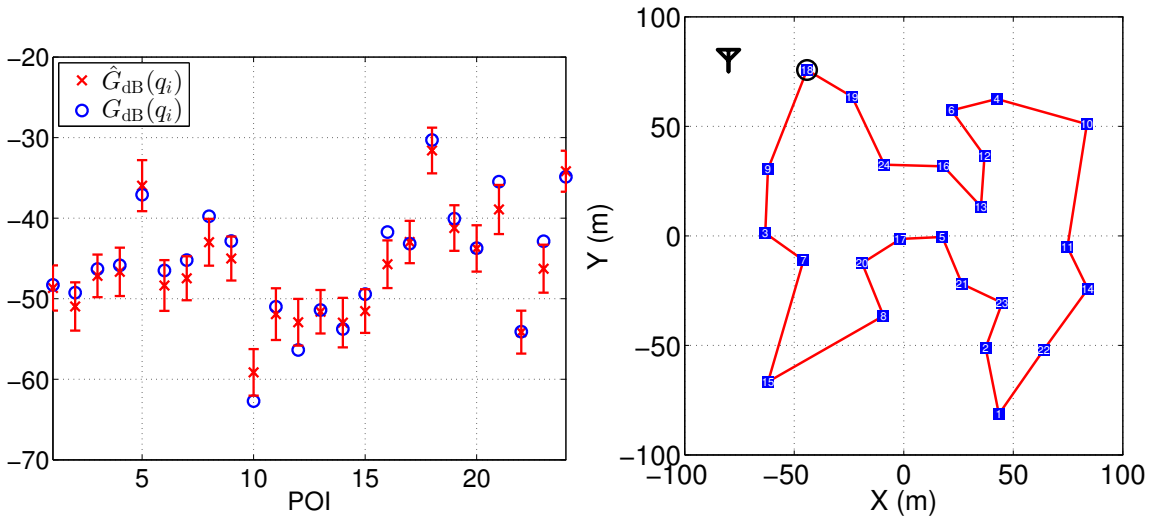

Figure 5.7: The comparison of the estimated and real channel powers at the POIs (left) and the optimal trajectories of one mobile agent in both communication-intensive and communication-efficient cases and for the case of unknown channel powers (right). The location of the remote station is denoted at the top left corner of the right figure. The optimal communication point for the mobile agent in the communication-efficient case is also specified by a circle in the right figure. It can be seen that the optimal trajectory is the Hamiltonian cycle over the set of POIs.

[11] The calculated energy values are based on assuming that the mobile agent will use the *a priori* found optimal channel powers, based on the probabilistic channel assessment at the POIs. Alternatively, the agent can measure the channel at the POIs after deployment and better adapt its transmission powers at the POIs, resulting in less total energy consumption.

POI	t_i^*	$\Gamma(q_i, \chi)$	$\frac{P_{\text{TH}}}{G(q_i)}$	POI	t_i^*	$\Gamma(q_i, \chi)$	$\frac{P_{\text{TH}}}{G(q_i)}$
1	113.13 s	67.259 mW	21.316 mW	13	162.38 s	127.25 mW	43.702 mW
2	85.084 s	122.72 mW	26.615 mW	14	91.422 s	200.61 mW	74.99 mW
3	73.151 s	44.735 mW	13.532 mW	15	101.09 s	125.84 mW	27.739 mW
4	155.76 s	45.637 mW	12.171 mW	16	81.005 s	36.209 mW	4.7053 mW
5	159.26 s	4.1431 mW	1.6186 mW	17	131.75 s	16.905 mW	6.5547 mW
6	148.9 s	71.488 mW	14.09 mW	18	74.563 s	1.338 mW	0.33904 mW
7	71.034 s	49.583 mW	10.496 mW	19	99.129 s	12.229 mW	3.206 mW
8	97.799 s	18.894 mW	2.9919 mW	20	152.51 s	22.329 mW	7.4526 mW
9	158.17 s	28.176 mW	6.0823 mW	21	78.6 s	7.8333 mW	1.1143 mW
10	108.17 s	774.54 mW	589.35 mW	22	156.13 s	224.98 mW	80.994 mW
11	101.33 s	165.64 mW	39.749 mW	23	133.92 s	41.428 mW	6.118 mW
12	88.73 s	185.93 mW	136.71 mW	24	116.3 s	2.1681 mW	0.96975 mW

Table 5.4: The optimal stop times (for both communication-intensive and communication-efficient cases), and the values of $\frac{P_{\text{TH}}}{G(q_i)}$ and $\Gamma(q_i, \chi)$ for all the POIs in Fig. 5.7.

Communication-Intensive Case				Communication-Efficient Case			
T^*	E^*	E_m^*	E_c^*	T^*	E^*	E_m^*	E_c^*
10250 s	124.36 J	76.403 J	47.957 J	10250 s	76.43 J	76.403 J	0.02676 J

Table 5.5: The optimal period, optimal total energy per period, optimal motion energy per period and optimal communication energy per period in both communication-intensive and communication-efficient cases and for all the mobile agents in Fig. 5.7. Note that the dependency on k has been dropped as there is one mobile agent in this case.

Fig. 5.8 (left) and Fig. 5.8 (right) show the plots of $\Psi_i(t)$ at the remote station for two sample POIs in Fig. 5.7 (POI #4 and POI #10). For the sake of comparison, each figure shows the plots of $\Psi_i(t)$ at the remote station for three cases: communication-intensive, communication-efficient and communication-unaware. By communication-unaware we mean the case where the same transmission power is used at all the POIs, without adapting to channel powers. To have a fair comparison, we set this fixed communication energy budget to be the same as the optimal communication energy found in the communication-intensive case (47.9573 J). The transmission power at every POI is then fixed to $\frac{1}{m}\sum_{i\in\mathcal{V}}\Gamma(q_i, \chi) = 99.91$ mW in this case. It can be seen

that in communication-intensive and communication-efficient cases, both of the POIs could be stably covered. The communication-unaware case, however, could stabilize the sensing of only one POI (POI #4). This is due to the fact that the robot is not connected to the remote station at the position of POI #10 in the communication-unaware case. This has been explained visually in Fig. 5.9. This figure shows the positions of the POIs superimposed on the connectivity map to the remote station for the communication-unaware case, assuming that the fixed transmission power of 99.91 mW is used. It can be seen that POI #10 and POI #12 are disconnected, resulting in $\Psi_i(t)$ becoming unstable at these points.

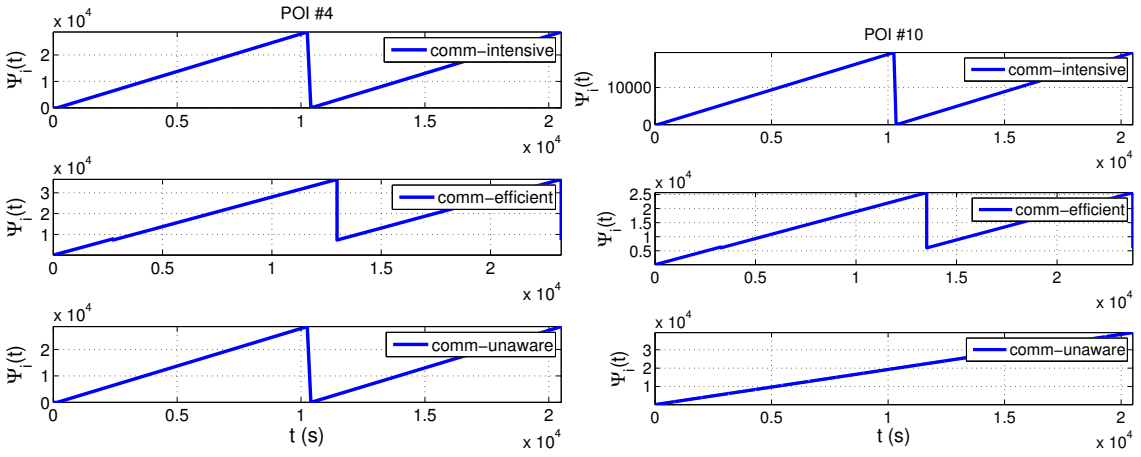

Figure 5.8: The plots of $\Psi_i(t)$ at the remote station for POI #4 (left) and POI #10 (right) in Fig. 5.7. These figures compare the time evolution of $\Psi_i(t)$ in communication-intensive, communication-efficient and communication-unaware cases.

Note that after solving the proposed MILP to find the feasible stabilizing policy in this specific example, all the POIs in the communication-intensive case or the optimal communication point in the communication-efficient case are connected, although the channel is assessed probabilistically. This may or may not be the case in general, depending on the quality of the channel assessment, especially the power of the multipath fading component of the channel. Since multipath fading is not predictable using sparse sampling of the channel, one expects that by increasing the

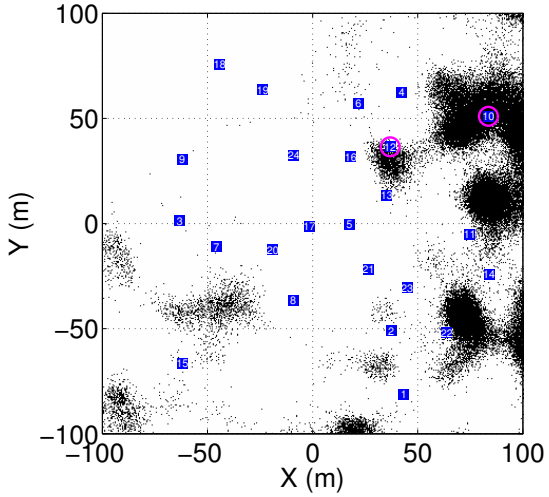

Figure 5.9: Positions of the POIs superimposed on the connectivity map to the remote station, assuming that the fixed transmission power $\frac{1}{m}\sum_{i\in\mathcal{V}}\Gamma(q_i,\chi)$ is used in the communication-unaware case. The disconnected POIs are circled on the figure.

power of multipath fading the number of POIs that can be covered decreases. This is shown in Fig. 5.10. Fig. 5.10 (left) shows the percentage of the connected POIs in Fig. 5.7 that can be covered by the mobile agent in the communication-intensive case, as a function of the power of the multipath fading component. The figure also shows the results for the non-adaptive communication-unaware case. The communication energy per period in the communication-intensive case is calculated to guarantee for $\chi = 0.95$. The same energy budget is then used in the communication-unaware case, where the power is uniformly distributed among all the POIs. The results are averaged for 500 different realizations of the channel. In this example, the path loss and shadowing components are kept fixed and only the multipath fading component is regenerated in each realization. Similar to Fig. 5.7, the channel is assessed using 0.5% of the total channel power samples. Interesting results can be observed. First, it can be seen that the percentage of the POIs that can be covered in the communication-intensive case decreases as the power of multipath fading increases. Second, for a fixed multipath power, the percentage of POIs, covered in the communication-unaware case, is lower than the communication-intensive case,

unless multipath power is very large. Third, for a very large multipath power, the percentage of the POIs covered by the communication-intensive case converges to that of the communication-unaware case. These results can be justified as follows:

As the multipath fading power increases, the quality of channel assessment degrades considerably. Although the optimal energy allocated for communication, i.e., $\sum_{i\in\mathcal{V}}\Gamma(q_i,\chi)$, also increases as the power of multipath fading increases, the overall number of connected POIs decreases in the communication-intensive case. The increase in the optimal energy allocated for communication, however, results in an opposite effect in the communication-unaware case. Since the power is distributed uniformly among all the POIs in this case, the increase in the allocated transmission power, along with more randomness in channel variations, increases the chance of connectivity at the POIs. Finally, for very large multipath fading power, adaptation of the transmission power in the communication-intensive case is not effective anymore due to large channel variations, resulting in almost the same percentage of connected POIs as of the communication-unaware case. Note that we used Rician multipath fading in this example. Therefore, the maximum possible multipath fading power is $\omega = 5.1195$ dB, which corresponds to the case when Rician distribution becomes a Raleigh distribution [54, 59]. To get a better idea about how the channel looks like for very small and very large multipath fading powers, Fig. 5.11 shows two sample channels with $\omega = 0.8730$ dB (left) and $\omega = 5.0941$ dB (right). The Rician K-parameter (the ratio of the power of the non-multipath component to that of the multipath component [59]) is equal to 50 for the left figure and 0.2 for the right one.

The probability of connectivity of the optimal transmission point found in the communication-efficient case also presents a similar behavior. Fig. 5.10 (middle) shows the plot of the probability of connectivity of the optimal transmission point in the communication-efficient case, as a function of the multipath power. The result is averaged over 500 realizations of the channel. Similar to the communication-intensive

case, it can be seen that the probability of connectivity decreases as multipath power increases. Finally, Fig. 5.10 (right) shows the total optimal communication energy as a function of multipath power for both communication-intensive and communication-efficient cases. As expected, the energy increases as the multipath power increases.

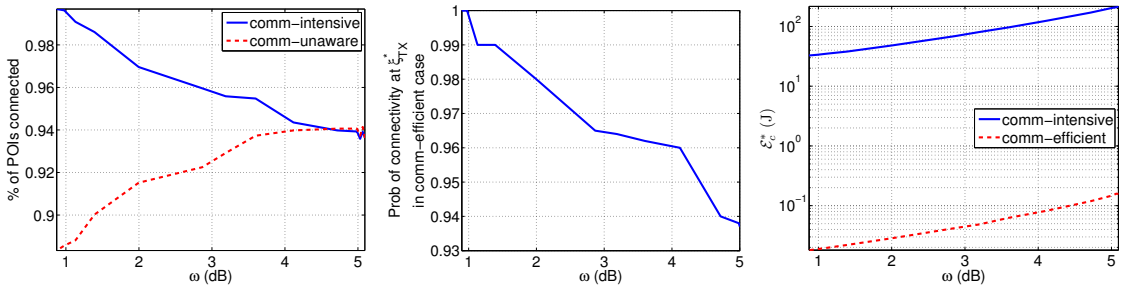

Figure 5.10: The percentage of the POIs that can be covered by the mobile agent of Fig. 5.7 in the communication-intensive case (left), the probability of connectivity of the optimal transmission point in the communication-efficient case (middle), and the total optimal communication energy (right) as a function of multipath power.

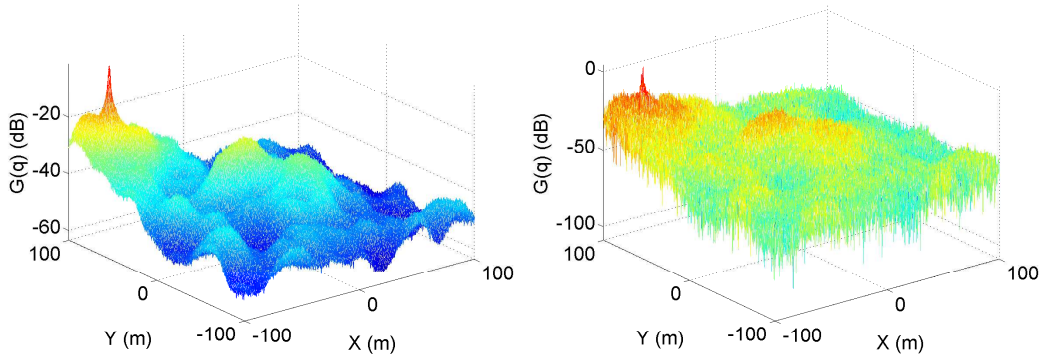

Figure 5.11: Two sample channels with $\omega = 0.8730$ dB (left) and $\omega = 5.0941$ dB (right). The path loss and shadowing components of both channels are the same as in Fig. 5.4

Finally, in order to confirm the probabilistic analysis of Sections 5.2.4 and 5.3.4 for a large number of POIs, Fig. 5.12 compares the actual and theoretical average minimum total energy per period, consumed to cover a set of POIs by one mobile agent, as a function of the number of POIs. Fig. 5.13 (left) and Fig. 5.13 (right) also show the average minimum communication energy per period for communication-intensive and communication-efficient cases respectively. The results for every m are

calculated by averaging over 500 different channels and sets of POIs. The POIs are distributed according to a uniform pdf over the workspace of Fig. 5.7. The channel in the dB domain is generated using a Gaussian distribution, with a mean equal to the path loss component of the channel of Fig. 5.5 and a standard deviation equal to $\vartheta = 5$ dB. Also, in this example we set $P_{\text{loss},m} = P_{\text{loss},s} = P_{\text{loss}} = 0.1$ mW, $\rho = 1$ and $\alpha = 200$ for all the POIs. The rest of the parameters are the same as in Fig. 5.5. Note that we dropped the dependency of the parameters on i and k as there is only one mobile agent and the parameters are the same for all the POIs. Fig. 5.13 shows that the average minimum communication energy per period is an increasing function of the number of POIs in the communication-intensive case, as expected. However, it is a decreasing function of the number of POIs in the communication-efficient case. This is explained by the fact that by increasing the number of POIs in an environment, the chance of finding a higher channel power at one of the POIs increases. Also, it can be seen that overall the theoretical values provide a good approximation to the simulated ones.

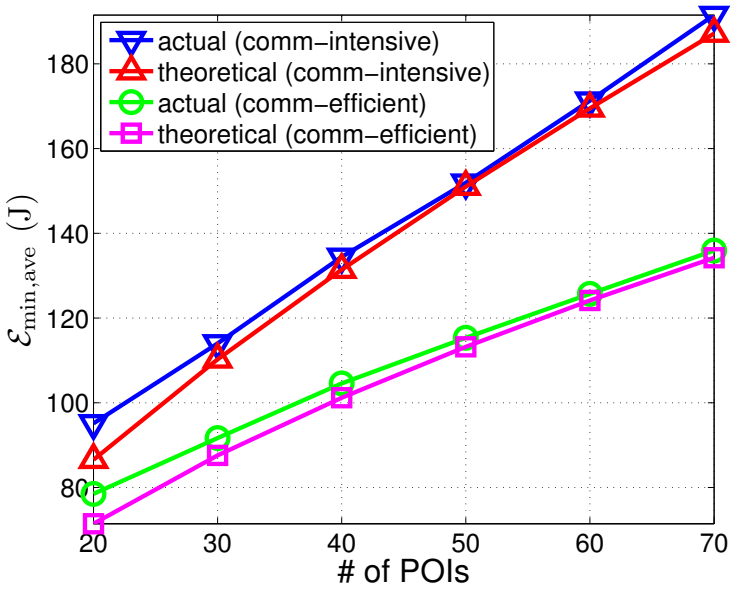

Figure 5.12: The actual and theoretical average minimum total energy consumed in each period to cover a set of POIs, as a function of the number of POIs.

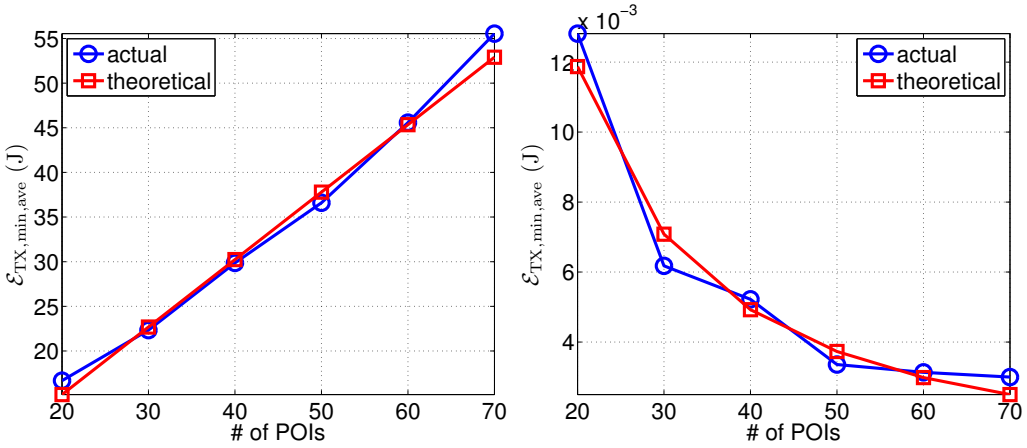

Figure 5.13: The actual and theoretical average minimum communication energy consumed in each period to cover a set of POIs as a function of the number of POIs, in the communication-intensive (left) and communication-efficient (right) cases.

5.5 Further Extension of the Dynamic Coverage Problem

In this section, we extend our dynamic coverage results by considering a non-zero range for the sensing/actuation device of the mobile agents and adapting their velocities and transmission rates (in addition to their transmission powers) along their trajectories. Unlike our previous results, here we take into account the number of information bits that are transmitted to and correctly received by the remote station. We, however, assume only one robot in this section to facilitate mathematical derivations.[12]

We assume an obstacle-free workspace $\mathcal{W} \subset \mathbb{R}^2$, which contains a set of m POIs $\mathcal{Q} = \{q_1, \cdots, q_m\} \subset \mathcal{W}$. Let $\mathcal{V} = \{1, \cdots, m\}$ denotes the indices of the POIs. In this section, we specifically consider a scenario where information bits are generated with certain rates at the POIs (e.g., consider the case where the POIs are data loggers that are distributed over the workspace to log time variations of a physical

[12]Extension to the case of multiple mobile agents in this case is under our consideration.

quantity in an environment). The mobile agent is then tasked with collecting the information bits from the POIs and transmitting them to a remote station. Similar to the previous, the trajectory of the mobile agent is uniquely defined by a Hamiltonian cycle, denoted by $\mathcal{C}$, on the set of POIs in $\mathcal{V}$. The range of the data collection device of the mobile agent is, however, not zero in this case. Let $\mathcal{S}(t) \subset \mathbb{R}^2$ denote the area covered by the mobile agent at time t. Generally, $\mathcal{S}(t)$ is a function of the position and orientation of the mobile agent at time t, i.e., $\mathcal{S}(t) = \mathcal{S}\big(\xi(t), \theta(t)\big)$, where $\xi(t) \in \mathcal{W}$ and $\theta(t) \in (-\pi, \pi]$ are the position and orientation of the mobile agent at time t, respectively. Whenever a POI i falls within $\mathcal{S}(t)$, the information bits at this POI are collected with a distance-dependent rate $\alpha\big(\|\xi(t) - q_i\|\big)$ by the mobile agent. The physical quantity under control at the i^{th} POI, $\Psi_i(t)$, is then the number of information bits to be collected from the i^{th} POI at time t. Similar to dynamic coverage for surveillance, we consider the following linear dynamics for $\Psi_i(t)$:

$$\dot{\Psi}_i(t) = \mathrm{I}\big(\Psi_i(t) \geq 0\big)\Big[\rho_i - \mathrm{I}\big(q_i \in \mathcal{S}(t)\big)\alpha\big(\|\xi(t) - q_i\|\big)\Big], \tag{5.53}$$

where ρ_i is rate at which the information bits are generated/stored at the i^{th} POI and I(.) denotes the indicator function.[13]

5.5.1 Motion Model

The velocity of the mobile agent at time t is shown by $v(t) \in [v_{\min},\ v_{\max}]$. For a periodic trajectory, $v(t)$ is also periodic and given by $v(t) = v\big(\xi(t)\big)$, where $v(q)$ is the velocity of the mobile agent at position q along its trajectory. The mobile agent adapts its velocity along its trajectory based on its data collection rate, in order to

[13]It should be noted that in practice the number of information bits, $\Psi_i(t)$, is an integer value. Here, in order to simplify the problem, we approximate $\Psi_i(t)$ with a real value and consider a continuous-time dynamics for it. The case of integer $\Psi_i(t)$ can be similarly considered by using a discrete linear dynamics and properly choosing ρ_i and $\alpha(.)$.

increase the number of information bits it collects in each period. This is done by slowing down at positions with good data collection rate, i.e., the positions where one or more POIs are within $\mathcal{S}(t)$ and $\alpha\big(\|\xi(t)-q_i\|\big)$ attains a large value. On the other hand, spending time at positions with good data collection rate increases the motion energy consumed by the robot in each period (according to the motion power model that was introduced previously in this chapter), resulting in a trade-off between the motion energy consumed and the number of information bits collected in one period. To see this more clearly, let us calculate the number of information bits collected while the mobile agent from POI i to POI j along the trajectory of the mobile agent: $N_{i,j}=\sum_{\ell=1}^{m} N_{i,j,\ell}$, where

$$N_{i,j,\ell}=\int_{q_i}^{q_j}\frac{1}{v(q)}\mathrm{I}\big(q_\ell\in\mathcal{S}(q,\theta_{i,j})\big)\alpha\big(\|q-q_\ell\|\big)dq, \tag{5.54}$$

and $\theta_{i,j}=\mathrm{atan2}(q_j-q_i)$. Clearly, for a given trajectory, $N_{i,j}$ increases by decreasing $v(q)$ in positions where the data collection rate is larger. On the other hand, by adopting the first-order motion power model used in the previous part, the motion power of the mobile agent at time t is given by $P_m(t)=P_{\text{loss}}+wv(t)$, where P_{loss} denotes the motion power loss and w is a positive constant. By integrating $P_m(t)$ in time we obtain the motion energy consumed in one period as follows:

$$E_m=\int_T P_m(t)dt=P_{\text{loss}}T+w\mathrm{d}(\mathcal{C}), \tag{5.55}$$

where T is the period and $\mathrm{d}(\mathcal{C})$ denotes the Euclidean length of $\mathcal{C}$. From (5.55), for a given trajectory the motion energy E_m is an increasing function of T, which explains why decreasing $v(q)$ is not preferred for energy minimization purposes. The optimal motion policy, without considering communication issues, provides the right balance between the motion energy E_m and the amount of information bits collected in one period. More specifically, such a motion policy determines the trajectory of the mobile agent as well as the its velocity profile $v(q)$ along this trajectory such that E_m is minimized, while guaranteeing that enough information bits are collected from the POIs to make $\Psi_i(t)$ bounded for all i.

5.5.2 Communication Model

The information bits collected from the POIs are transmitted to the remote station along the trajectory of the mobile agent. Unlike our previous dynamic coverage results, in this case it is important to consider how the information bits are transmitted to the remote station. The mobile agent is capable of adapting its transmission power and rate based on the quality of the channel to the remote station. By doing so, it can control the number of information bits sent in each period, its consumed communication energy, and the reception quality of the remote station.

We assume that MQAM modulation with n_r different constellation sizes is used by the onboard digital communication device of the mobile agent. Then, by assuming a transmission bandwidth B, we achieve the spectral efficiency of $R_{\mathrm{TX},\ell}$ bits/symbol (bits/s/Hz) or equivalently the transmission rate of $BR_{\mathrm{TX},\ell}$ bits/s by choosing the constellation size $2^{R_{\mathrm{TX},\ell}}$, for $\ell = 1, \cdots, n_r$ [59]. Let $P_{\mathrm{TX}}(t)$ and $R_{\mathrm{TX}}(t)$ denote the transmission power and the spectral efficiency chosen at time t. Then, the number of information bits transmitted to the remote station in one period is given by

$$N_c = B \int_T R_{\mathrm{TX}}(t) dt. \tag{5.56}$$

The communication energy consumed in one period is also

$$E_c = \int_T P_{\mathrm{TX}}(t) dt. \tag{5.57}$$

Note that for a periodic trajectory, $P_{\mathrm{TX}}(t) = P_{\mathrm{TX}}\big(\xi(t)\big)$ and $R_{\mathrm{TX}}(t) = R_{\mathrm{TX}}\big(\xi(t)\big)$, where $P_{\mathrm{TX}}(q)$ and $R_{\mathrm{TX}}(q) \in \{0, R_{\mathrm{TX},1}, \cdots, R_{\mathrm{TX},n_r}\}$ are the transmission power and the spectral efficiency chosen at position q along the trajectory of the mobile agent. The reception quality at the remote station is measured by the resulting BER. For an MQAM modulation, the BER at time t at the remote station is given by

$$\mathrm{BER}(t) \approx 0.2 \exp\left(-\frac{1.5 P_{\mathrm{TX}}(t) G(t)}{\big(2^{R_{\mathrm{TX}}(t)} - 1\big) B N_0} \right), \tag{5.58}$$

where $G(t) = G\big(\xi(t)\big)$, $G(q)$ is the channel power at position q along the trajectory of the mobile agent and $\frac{N_0}{2}$ is the PSD of the thermal noise at the receiver of the remote station. The optimal communication policy, without considering motion issues, then determines the trajectory of the robot, as well as $P_{\mathrm{TX}}(q)$ and $R_{\mathrm{TX}}(q)$ along this trajectory, such that the communication energy E_c is minimized and all the information bits collected in one period are transmitted to the remote station, in the same period, with a BER lower than a given threshold $\mathrm{BER}_{\mathrm{TH}}$. Note that optimizing the motion and communication cannot be done independently. The trajectory of the robot affects both E_m and E_c. Furthermore, the velocity profile of the robot determines the number of the information bits collected in one period, which affects the transmission power and rate required for the transmission. In the next section, we formulate our proposed combined motion and communication optimization problem. Then, in Section 5.6.2, we show how to solve this problem using an MILP.

Before presenting our MILP, we should note that the channel power $G(q)$ may not be deterministically known everywhere, as we also explained in Section 5.2.3. Furthermore, even if the channel is deterministically known, pre-planning based on the rapidly changing multipath fading component of the channel is not preferred in practical applications. In such case, instead of a deterministic $G(q)$, the pdf of $G(q)$, given by our channel assessment framework of Chapter 2, is used to calculate $\mathbb{P}\big\{\mathrm{BER}(t) \leq \mathrm{BER}_{\mathrm{TH}}\big\}$. Then, $P_{\mathrm{TX}}(q)$ and $R_{\mathrm{TX}}(q)$ are selected to guarantee $\mathbb{P}\big\{\mathrm{BER}(t) \leq \mathrm{BER}_{\mathrm{TH}}\big\} \geq 1 - \epsilon$, for a small ϵ, whenever $P_{\mathrm{TX}}(t) > 0$ and $R_{\mathrm{TX}}(t) > 0$. This is explained in more details in Section 5.6.2.

5.6 Extended Dynamic Coverage of Time-Varying Environments

In this section, we formulate the problem of dynamic coverage for information collection in time-varying environments, which requires adapting the velocity, transmission

power and transmission rate of the mobile agent along its trajectory. We then propose an MILP to find the optimal solution of the problem. We furthermore analyze the solution of the MILP and its special cases mathematically.

5.6.1 Problem Formulation

Based on the discussions of the previous sections, the dynamic coverage policy for information collection in time-varying environments is defined as follows

Definition 5.6.1. *A dynamic coverage policy for information collection in a time-varying environment using a single mobile agent is a tuple* $\mathcal{P} = (\mathcal{C}, P_{\text{TX}}, R_{\text{TX}}, v)$*, where* $\mathcal{C}$ *denote the Hamiltonian cycle defined on the set of POIs and functions* $P_{\text{TX}} : \mathcal{W} \to \mathbb{R}_{\geq 0}$*,* $R_{\text{TX}} : \mathcal{W} \to \{0, R_{\text{TX},1}, \cdots, R_{\text{TX},n_r}\}$ *and* $v : \mathcal{W} \to [v_{\min},\ v_{\max}]$ *determine the transmission power, spectral efficiency and velocity of the mobile agent for any position* $q \in \mathcal{W}$ *along the trajectory defined by* $\mathcal{C}$*, respectively.*

Our goal in this section is then to determine the dynamic coverage policy $\mathcal{P}$ such that the total energy $E = E_m + E_c$ is minimized and the following hold:

1. There exist $\overline{\Psi} \geq 0$ such that $\Psi_i(t) \leq \overline{\Psi}$ for all $t \geq 0$ and $i = 1, \cdots, m$.

2. All the information bits collected in one period are transmitted to the remote station, in the same period, and $\mathbb{P}\{\text{BER}(t) \leq \text{BER}_{\text{TH}}\} \geq 1 - \epsilon$ whenever $P_{\text{TX}}(t) > 0$ and $R_{\text{TX}}(t) > 0$.

3. The total information bits collected in one period is no larger than the maximum memory size of the the mobile agent $L_{\max}$.

The first condition implies that the dynamical system (5.53) is stable for all POIs.

In Section 5.2 we showed that this is equivalent to the following:

$$T\rho_i - \int_T \mathrm{I}\big(q_i \in \mathcal{S}(t)\big)\alpha\big(\|\xi(t) - q_i\|\big)dt \leq 0,\ i = 1, \cdots, m, \tag{5.59}$$

which implies that the total information bits collected from the i^{th} POI is no smaller that the number of bits generated at this POI. Furthermore, if this condition holds, the total information bits collected in one period becomes $T\sum_{i=1}^{m}\rho_i$. Therefore, the first part of the second condition is equivalent to $N_c = B\int_T R_{\text{TX}}(t)dt \geq T\sum_{i=1}^{m}\rho_i$. Finally, the third condition implies that $T\sum_{i=1}^{m}\rho_i \leq L_{\max}$. The optimization problem to solve is then given as follows:

Problem 5.6.1. *The minimum-energy dynamic coverage policy for information collection in a time-varying environment is given as follows:*

$$\begin{aligned}
&\min_{\mathcal{P}} \int_T P_{\text{TX}}(t)dt + P_{\text{loss}}T + w\mathrm{d}(\mathcal{C}),\\
&\text{s.t.}\\
&1)\ T\rho_i - \int_T \mathrm{I}\big(q_i \in \mathcal{S}(t)\big)\alpha\big(\|\xi(t) - q_i\|\big)dt \leq 0,\ \ \forall i = 1, \cdots, m\\
&2)\ B\int_T R_{\text{TX}}(t)dt \geq T\sum_{i=1}^{m}\rho_i,\\
&3)\ \textit{if } P_{\text{TX}}(t) > 0 \textit{ and } R_{\text{TX}}(t) > 0 \textit{ then } \mathbb{P}\big\{\mathrm{BER}(t) \leq \mathrm{BER}_{\text{TH}}\big\} \geq 1 - \epsilon,\ \ \forall t \geq 0,\\
&4)\ T\sum_{i=1}^{m}\rho_i \leq L_{\max},
\end{aligned} \tag{5.60}$$

where T the period of movement, which is a function of the velocity profile of the mobile agent $v(t)$. Furthermore, $v(t) = v\big(\xi(t)\big)$, $P_{\text{TX}}(t) = P_{\text{TX}}\big(\xi(t)\big)$, and $R_{\text{TX}}(t) = R_{\text{TX}}\big(\xi(t)\big)$.

As can be seen, Problem 5.6.1 is generally complicated to solve. Next, we show how to solve this problem by discretizing the trajectory of the mobile agent and by using an MILP.

5.6.2 Optimal Solution of the Dynamic Coverage in Case of Non-zero Ranges and Adaptive Velocities, Transmission Powers and Transmission Rates

Let us discretize each possible trajectory of the mobile agent into a number of small line segments with maximum length $\delta_{\max}$ and minimum length $\delta_{\min}$. $\delta_{\max}$ is selected small enough such that the channel can be considered stationary along each segment.[14] Define binary variables $z_{i,j} \in \{0,1\}$ such that $z_{i,j} = 1$ when $\mathcal{C}$ includes a path from POI i to POI j, and $z_{i,j} = 0$ otherwise. Let $\mathcal{L}_{i,j,k}$ denote the k^{th} line segment along the path from POI i to POI j. Also, let $n_{i,j}$ denote the number of such line segments. Define the continuous variables $\tau_{i,j,k,\ell}$ as the amount of time that mobile agent transmits information bits with the spectral efficiency of $R_{\text{TX},\ell}$, for $\ell = 1, \cdots, n_r$, along $\mathcal{L}_{i,j,k}$. Also, define the continuous variables $\varrho_{i,j,k}$ as the inverse of the constant velocity of the mobile agent along $\mathcal{L}_{i,j,k}$. We set $\varrho_{i,j,k} = 0$ whenever $z_{i,j} = 0$, which can be guaranteed by the linear constraints $z_{i,j} v_{\max}^{-1} \leq \varrho_{i,j,k} \leq z_{i,j} v_{\min}^{-1}$. Based on the definition of these variable we have

$$\int_T \mathrm{I}\big(q_\ell \in \mathcal{S}(t)\big)\alpha\big(\|\xi(t) - q_\ell\|\big)dt = \sum_{i=1}^{m}\sum_{\substack{j=1\\ j\neq i}}^{m} z_{i,j} N_{i,j,\ell}. \tag{5.61}$$

We can then confirm that the first condition in Problem 5.6.1 is equivalent to the following for all $\ell = 1, \cdots, m$:

$$\sum_{i=1}^{m}\sum_{\substack{j=1\\ j\neq i}}^{m}\sum_{k=1}^{n_{i,j}} \nu_{i,j,k,\ell}\, \varrho_{i,j,k} - \rho_\ell \sum_{i=1}^{m}\sum_{\substack{j=1\\ j\neq i}}^{m}\sum_{k=1}^{n_{i,j}} d_{i,j,k}\, \varrho_{i,j,k} \geq 0, \tag{5.62}$$

where the weights $\nu_{i,j,k,\ell}$ are given by

$$\nu_{i,j,k,\ell} = \int_{\mathcal{L}_{i,j,k}} \mathrm{I}\big(q_\ell \in \mathcal{S}(q,\theta_{i,j})\big)\alpha\big(\|q - q_\ell\|\big)dq. \tag{5.63}$$

[14] Note that in practical applications pre-planning based on rapidly-changing multipath fading is not desired.

Here, $d_{i,j,k}$ denotes the length of $\mathcal{L}_{i,j,k}$. Similarly, the second condition in Problem 5.6.1 is equivalent to the following:

$$\sum_{i=1}^{m}\sum_{\substack{j=1\\j\neq i}}^{m}\sum_{k=1}^{n_{i,j}}\sum_{\ell=1}^{n_r} R_{\mathrm{TX},\ell}\,\tau_{i,j,k,\ell} \geq \frac{\sum_{i=1}^{m}\rho_i}{B}\sum_{i=1}^{m}\sum_{\substack{j=1\\j\neq i}}^{m}\sum_{k=1}^{n_{i,j}} d_{i,j,k}\varrho_{i,j,k}. \tag{5.64}$$

Finally, for the third condition in Problem 5.6.1 we have

$$\sum_{i=1}^{m}\sum_{\substack{j=1\\j\neq i}}^{m}\sum_{k=1}^{n_{i,j}} d_{i,j,k}\;\varrho_{i,j,k} \leq \frac{L_{\max}}{\sum_{i=1}^{m}\rho_i}. \tag{5.65}$$

The motion and communication energies can also be found as functions of the newly defined variables. For the motion energy we have

$$E_m = P_{\mathrm{loss}}\sum_{i=1}^{m}\sum_{\substack{j=1\\j\neq i}}^{m}\sum_{k=1}^{n_{i,j}} d_{i,j,k}\;\varrho_{i,j,k} + w\sum_{i=1}^{m}\sum_{\substack{j=1\\j\neq i}}^{m} d_{i,j}\;z_{i,j}, \tag{5.66}$$

where $d_{i,j} = \|q_i - q_j\|$. Given the transmission times $\tau_{i,j,k,\ell}$, the communication energy to be minimized is also the minimum required communication energy to guarantee $\mathbb{P}\big\{\mathrm{BER}(t) \leq \mathrm{BER}_{\mathrm{TH}}\big\} \geq 1-\epsilon$ along each line segment $\mathcal{L}_{i,j,k}$ for which $\sum_{\ell=1}^{n_r}\tau_{i,j,k,\ell} > 0$. We have

$$\mathbb{P}\big\{\mathrm{BER}(t) \leq \mathrm{BER}_{\mathrm{TH}}\big\} = \mathbb{P}\left\{G(t) \geq \kappa\frac{(2^{R_{\mathrm{TX}}(t)}-1)}{P_{\mathrm{TX}}(t)}\right\}, \tag{5.67}$$

where $\kappa \triangleq -\frac{\log(5\mathrm{BER}_{\mathrm{TH}})BN_0}{1.5}$. Assume that the channel is known only at a number of *a priori* channel measurements. According to the channel assessment framework of Chapter 2, the distribution of $G(q)$ in the dB domain, conditioned on the channel measurements, is given by a Gaussian pdf with mean $\hat{G}_{\mathrm{dB}}(q)$ and variance $\sigma^2(q)$. Note that similar to dynamic coverage for for surveillance, we dropped the dependency of the channel assessment to t and k, since there is only one mobile agent and the channel is assessed before the operation starts. Along each line segment the channel is stationary and, therefore, $\hat{G}_{\mathrm{dB}}(q)$ and $\sigma^2(q)$ can be assumed constant. Let us define $\hat{G}(q) \triangleq 10^{\frac{\hat{G}_{\mathrm{dB}}(q)}{10}}$. Also, let $\hat{G}_{i,j,k}$ and $\sigma_{i,j,k}$ denote the constant values of $\hat{G}(q)$ and

$\sigma(q)$ along $\mathcal{L}_{i,j,k}$, respectively. After some straightforward calculations, we can then find the minimum required communication energy, that guarantees $\mathbb{P}\big\{\text{BER}(t) \leq \text{BER}_{\text{TH}}\big\} \geq 1-\epsilon$ along each $\mathcal{L}_{i,j,k}$ for which $\sum_{\ell=1}^{n_r} \tau_{i,j,k,\ell} > 0$, as follows:

$$E_c = \kappa \sum_{i=1}^{m} \sum_{\substack{j=1 \\ j\neq i}}^{m} \sum_{k=1}^{n_{i,j}} \sum_{\ell=1}^{n_r} \tau_{i,j,k,\ell} \frac{(2^{R_{\text{TX},\ell}}-1)}{\overline{G}_{i,j,k}}, \tag{5.68}$$

where $\overline{G}_{i,j,k} \triangleq \hat{G}_{i,j,k} 10^{\frac{Q^{-1}(1-\epsilon)\sigma_{i,j,k}}{10}}$ and $Q^{-1}(.)$ denotes the inverse of the Q-function (the tail probability of the Gaussian distribution).

The total transmission time in each segment, i.e., $\sum_{\ell=1}^{m} \tau_{i,j,k,\ell}$, determines how much time in each segment is dedicated to communication. Generally, two different types of constraints can be considered on $\sum_{\ell=1}^{n_r} \tau_{i,j,k,\ell}$. The first type of constraints guarantee that $\sum_{\ell=1}^{n_r} \tau_{i,j,k,\ell}$ is no larger than a fixed transmission time $t_c \leq \min_{i,j,k} \frac{d_{i,j,k}}{v_{\max}}$:

$$\text{Type I constraints:} \quad \sum_{\ell=1}^{n_r} \tau_{i,j,k,\ell} \leq z_{i,j} t_c, \qquad \forall i,j,k. \tag{5.69}$$

The total transmission time in each segment is not affected by the velocity of the mobile agent in this case. The second type of constraints, on the other hand, guarantee $\sum_{\ell=1}^{n_r} \tau_{i,j,k,\ell}$ is no larger than the time required to move along $\mathcal{L}_{i,j,k}$:

$$\text{Type II constraints:} \quad \sum_{\ell=1}^{n_r} \tau_{i,j,k,\ell} \leq d_{i,j,k}\, \varrho_{i,j,k}, \qquad \forall i,j,k, \tag{5.70}$$

where we set $\varrho_{i,j,k} = 0$ whenever $z_{i,j} = 0$. By adding the second type of constraints, the velocity of the mobile agent along its trajectory affects not only data collection but also data transmission. This is due to the fact that by increasing $\varrho_{i,j,k}$ in some areas (e.g. areas with good channel quality) more information bits can be transmitted to the remote station.

Based on the discretized version of Problem 5.6.1, we then propose the MILP of Program 3 for finding the optimal dynamic coverage policy.

Program 3 MILP for solving Problem 5.6.1

$$\min\ E = E_m + E_c = P_{\text{loss}} \sum_{i=1}^{m} \sum_{\substack{j=1 \\ j\neq i}}^{m} \sum_{k=1}^{n_{i,j}} d_{i,j,k}\, \varrho_{i,j,k} + w \sum_{i=1}^{m} \sum_{\substack{j=1 \\ j\neq i}}^{m} d_{i,j}\, z_{i,j} + \kappa \sum_{i=1}^{m} \sum_{\substack{j=1 \\ j\neq i}}^{m} \sum_{k=1}^{n_{i,j}} \sum_{\ell=1}^{n_r} \tau_{i,j,k,\ell} \frac{(2^{R_{\text{TX},\ell}}-1)}{\overline{G}_{i,j,k}}$$

1) $\sum_{i=1}^{m} \sum_{\substack{j=1 \\ j\neq i}}^{m} \sum_{k=1}^{n_{i,j}} \nu_{i,j,k,\ell}\, \varrho_{i,j,k} - \rho_\ell \sum_{i=1}^{m} \sum_{\substack{j=1 \\ j\neq i}}^{m} \sum_{k=1}^{n_{i,j}} d_{i,j,k}\, \varrho_{i,j,k} \geq 0, \qquad \forall \ell,$

2) $\sum_{i=1}^{m} \sum_{\substack{j=1 \\ j\neq i}}^{m} \sum_{k=1}^{n_{i,j}} \sum_{\ell=1}^{n_r} R_{\text{TX},\ell}\, \tau_{i,j,k,\ell} \geq \frac{\sum_{i=1}^{m} \rho_i}{B} \sum_{i=1}^{m} \sum_{\substack{j=1 \\ j\neq i}}^{m} \sum_{k=1}^{n_{i,j}} d_{i,j,k} \varrho_{i,j,k},$

3) $\sum_{i=1}^{m} \sum_{\substack{j=1 \\ j\neq i}}^{m} \sum_{k=1}^{n_{i,j}} d_{i,j,k}\, \varrho_{i,j,k} \leq \frac{L_{\max}}{\sum_{i=1}^{m} \rho_i},$

4) $\sum_{\ell=1}^{n_r} \tau_{i,j,k,\ell} \leq z_{i,j} t_c$ or $\sum_{\ell=1}^{n_r} \tau_{i,j,k,\ell} \leq d_{i,j,k}\, \varrho_{i,j,k}, \qquad \forall i,j,k,$

5) $z_{i,j} v_{\max}^{-1} \leq \varrho_{i,j,k} \leq z_{i,j} v_{\min}^{-1}, \qquad \forall i,j,k,$

6) $\sum_{\substack{j=1 \\ j\neq i}}^{m} z_{i,j} = 1, \ \sum_{\substack{j=1 \\ j\neq i}}^{m} z_{j,i} = 1, \qquad \forall i,$

7) $u_i - u_j + (m-1) z_{i,j} \leq (m-2),\ \forall i \neq 1, j \neq 1,$

8) $2 \leq u_i \leq m,\ \forall i \neq 1,$

9) $z_{i,j} \in \{0,1\},\ \tau_{i,j,k,\ell} \in \mathbb{R}_{\geq 0},\ \varrho_{i,j,k} \in \mathbb{R}_{\geq 0},\ u_i \in \mathbb{Z}_{\geq 0},$

Here, we have introduced $m-1$ extra integer variables $u_2, \cdots, u_m$. In this MILP, in addition to constraints 1 to 5, which we introduced previously, constraint 6 enforces each POI to have exactly one degree in and one degree out. Constraints 7 and 8 are the Miller-Tucker-Zemlin (MTZ) constraints [106,111], which are added to eliminate the subtours. This MILP can be solved using several efficient solvers, such as IBM ILOG CPLEX [104] and SAS/OR [105].

Note that the optimal transmission times $\tau_{i,j,k,\ell}$, given by the solution of the MILP of Program 3, are sufficient to find the optimal transmission power and transmission rate profiles. More specifically, along any line segment $\mathcal{L}_{i,j,k}$ and for $\ell = 1, \cdots, n_r$, we set the transmission power to $\kappa \frac{2^{R_{\text{TX},\ell}}-1}{\overline{G}_{i,j,k}}$ and transmit the information bits with the spectral efficiency of $R_{\text{TX},\ell}$ for time interval $\tau_{i,j,k,\ell}$, if $\tau_{i,j,k,\ell} > 0$. Therefore, by discretizing Problem 5.6.1, the solution of this MILP uniquely gives the optimal $\mathcal{P}$.

Also, note that the concept of virtual POIs, introduced in Section 5.3, can be also used in this case as well. The virtual POIs are located at regions with good channel qualities which are also close to the actual POIs. By ensuring that the mobile agent passes through these points, we can then decrease the optimal communication energy considerably.

5.6.3 Mathematical Analysis and Special Cases

In this section, we mathematically analyze the solution of the MILP of Program 3 and its special cases. We present our results in the form of the following theorems:

Theorem 5.6.1. *Assume that the trajectory of the mobile agent is given by a Hamiltonian cycle $\mathcal{C}$ beforehand. Also, assume that the constraints in (5.69) are used for the total transmission time in each segment. Then, the following are true:*

1. *The optimal velocity profile along the trajectory is given by the following linear program (LP):*

$$\min \sum_{(i,j)\in\mathcal{C}} \sum_{k=1}^{n_{i,j}} d_{i,j,k}\varrho_{i,j,k} \tag{5.71}$$

s.t.

$$1)\ \sum_{(i,j)\in\mathcal{C}} \sum_{k=1}^{n_{i,j}} \big(\nu_{i,j,k,\ell} - \rho_\ell d_{i,j,k}\big)\varrho_{i,j,k} \geq 0, \quad \forall \ell,$$

$$2)\ \sum_{(i,j)\in\mathcal{C}} \sum_{k=1}^{n_{i,j}} d_{i,j,k}\varrho_{i,j,k} \leq \frac{L_{\max}}{\sum_{i=1}^{m}\rho_i},$$

$$3)\ v_{\max}^{-1} \leq \varrho_{i,j,k} \leq v_{\min}^{-1}, \qquad \forall i,j,k.$$

2. *The optimal transmission time profile along the trajectory is given by the fol-*

lowing LP:

$$\min \sum_{(i,j)\in\mathcal{C}} \sum_{k=1}^{n_{i,j}} \sum_{\ell=1}^{n_r} \tau_{i,j,k,\ell} \frac{(2^{R_{\mathrm{TX},\ell}}-1)}{\overline{G}_{i,j,k}} \tag{5.72}$$

s.t.

$$1)\ \sum_{(i,j)\in\mathcal{C}} \sum_{k=1}^{n_{i,j}} \sum_{\ell=1}^{n_r} R_{\mathrm{TX},\ell}\tau_{i,j,k,\ell} \geq \frac{\sum_{i=1}^{m}\rho_i}{B} T^*,$$

$$2)\ \sum_{\ell=1}^{n_r} \tau_{i,j,k,\ell} \leq t_c, \qquad \forall i,j,k,$$

where $T^* = \sum_{(i,j)\in\mathcal{C}} \sum_{k=1}^{n_{i,j}} d_{i,j,k}\varrho^*_{i,j,k}$ *is the optimal period found using the solution of (5.71).*

3. *In the optimal solution,* $v^*_{i,j,k} = v_{\max}$ *in any segment for which* $\sum_{\ell=1}^{m}\nu_{i,j,k,\ell} = 0$. *In other segments, the optimal velocities are the maximum possible velocities that do not violate the stability constraint (5.62).*

4. *In the optimal solution,* $\sum_{\ell=1}^{n_r}\tau^*_{i,j,k,\ell} > 0$ *only in a number of segments where* $\overline{G}_{i,j,k}$ *is the largest. Also, if for two segments* (i_1,j_1,k_1) *and* (i_2,j_2,k_2) *we have* $\overline{G}_{i_1,j_1,k_1} > \overline{G}_{i_2,j_2,k_2}$*, then, necessarily,*

$$\sum_{\ell=1}^{n_r} \tau^*_{i_1,j_1,k_1,\ell}\big(2^{R_{\mathrm{TX},\ell}}-1\big) \geq \sum_{\ell=1}^{n_r} \tau^*_{i_2,j_2,k_2,\ell}\big(2^{R_{\mathrm{TX},\ell}}-1\big). \tag{5.73}$$

Proof. In case the trajectory of the mobile agent is given and the constraints in (5.69) are used for the total transmission time in each segment, the problem of optimizing the velocity and transmission times becomes decoupled. The velocity of the mobile agent is then found to minimize the motion energy and the total information bits collected in one period, while meeting the constraints on the stability and the total memory size. Note that minimizing the number of collected information bits is in favor of minimizing the communication energy and, as a direct result, the total energy. In case the trajectory is given, the motion energy as well as the number of

information bits collected are minimized when the period is minimized. This results in the LP of (5.71) for finding the optimal velocity profile in the first part of the theorem. The resulting optimal period is then used to find the optimal transmission times such that the total communication energy is minimized, resulting in the LP of (5.72) in the second part of the theorem.

From (5.71), it is clear that whenever $\sum_{\ell=1}^{m} \nu_{i,j,k,\ell} = 0$ in a segment, i.e., whenever none of the POIs are being covered by the onboard data collection device of the mobile agent, the optimal velocity is necessarily $v_{\max}$ such that the period is minimized. Furthermore, in the other segments, where at least one of the POIs is covered, the optimal velocities are the maximum possible velocities that do not violate the stability constraint. This proves third part of the theorem.

The proof of the forth part is by contradiction. Consider two segments (i_1, j_1, k_1) and (i_2, j_2, k_2) for which $\overline{G}_{i_1,j_1,k_1} > \overline{G}_{i_2,j_2,k_2}$. Assume that for these two segments $\sum_{\ell=1}^{n_r} \tau^*_{i_1,j_1,k_1,\ell}\big(2^{R_{\text{TX},\ell}} - 1\big) < \sum_{\ell=1}^{n_r} \tau^*_{i_2,j_2,k_2,\ell}\big(2^{R_{\text{TX},\ell}} - 1\big)$. Then, if the optimal transmission times of segment (i_1, j_1, k_1) are used for segment (i_2, j_2, k_2) instead and vice versa, none of the constraints of (5.72) are violated. However, the total communication energy becomes smaller, since

$$\begin{aligned}
&\sum_{\ell=1}^{n_r} \tau^*_{i_1,j_1,k_1,\ell} \frac{(2^{R_{\text{TX},\ell}} - 1)}{\overline{G}_{i_1,j_1,k_1}} + \sum_{\ell=1}^{n_r} \tau^*_{i_2,j_2,k_2,\ell} \frac{(2^{R_{\text{TX},\ell}} - 1)}{\overline{G}_{i_2,j_2,k_2}} - \sum_{\ell=1}^{n_r} \tau^*_{i_1,j_1,k_1,\ell} \frac{(2^{R_{\text{TX},\ell}} - 1)}{\overline{G}_{i_2,j_2,k_2}} \\
&\qquad - \sum_{\ell=1}^{n_r} \tau^*_{i_2,j_2,k_2,\ell} \frac{(2^{R_{\text{TX},\ell}} - 1)}{\overline{G}_{i_1,j_1,k_1}} \qquad (5.74) \\
&= \left(\frac{1}{\overline{G}_{i_2,j_2,k_2}} - \frac{1}{\overline{G}_{i_1,j_1,k_1}}\right) \left(\sum_{\ell=1}^{n_r} \tau^*_{i_2,j_2,k_2,\ell}\big(2^{R_{\text{TX},\ell}} - 1\big) - \sum_{\ell=1}^{n_r} \tau^*_{i_1,j_1,k_1,\ell}\big(2^{R_{\text{TX},\ell}} - 1\big)\right) > 0.
\end{aligned}$$

This is a contradiction which proves the forth part of the theorem. □

From Theorem 5.6.1, by choosing the constraints in (5.69) and by assuming a given trajectory, the problem of finding the optimal motion and communication

policies becomes decoupled. This is, however, not the case when the constraints in (5.70) are used for the total transmission time in each segment.

Next, we consider the special case of the MILP of Program 3 when the area covered by the onboard data collection device of the mobile agent is very small, i.e., $|\mathcal{S}(t)| = 0$. In this case, the mobile agent can only collect the information bits at the positions of the POIs. The dynamics of $\Psi_i(t)$ is given by the following in this case, which is similar to the one considered in Section 5.1:

$$\dot{\Psi}_i(t) = \mathrm{I}\big(\Psi_i(t) \geq 0\big)\Big[\rho_i - \mathrm{I}\big(\xi(t) = q_i\big)\alpha_0\Big], \tag{5.75}$$

where we have defined $\alpha_0 \triangleq \alpha(0)$. As explained in Section 5.1, in order to guarantee the boundedness of the $\Psi_i(t)$, the mobile agent is then required to stop for some time at each POI. Let t_i denote the stop time at the i^{th} POI. Given the trajectory of the mobile agent, the optimal velocity and stop times at the POIs are then given by the following lemma in this case:

Lemma 5.6.1. *Assume that the trajectory of the mobile agent is given by a Hamiltonian cycle $\mathcal{C}$ and $\sum_{i=1}^{m} \rho_i < \alpha_0$. Then the following hold in the case of $|\mathcal{S}(t)| = 0$:*

1. *If the constraints in (5.69) are used for the total transmission time in each segment, the optimal motion policy, which minimizes the total energy and guarantees the boundedness of $\Psi_i(t)$ for all $i = 1, \cdots, m$, is to choose the fixed maximum velocity $v_{\max}$ for moving along the trajectory and to stop at the i^{th} POI for time $t_i^* = \frac{\rho_i}{\phi\alpha_0}\frac{\mathrm{d}(\mathcal{C})}{v_{\max}}$, where $\phi \triangleq 1 - \frac{1}{\alpha_0}\sum_{i=1}^{m}\rho_i$.*

2. *If the constraints in (5.70) are used for the total transmission time in each segment, the optimal motion is not necessarily to move with the maximum velocity along the trajectory. Also, for a given velocity profile along the trajectory, the optimal stop time at POI i is $t_i^* = \frac{\rho_i}{\phi\alpha_0}\sum_{(i,j)\in\mathcal{C}}\sum_{k=1}^{n_{i,j}} d_{i,j,k}\,\varrho_{i,j,k}$.*

Proof. The proof is similar to the proof of Theorem 5.2.1 and is omitted for brevity. □

Using Lemma 5.6.1, the MILP of Program 3 can be modified to find the optimal motion and communication policies in the case of $|\mathcal{S}(t)| = 0$, as shown by the following two theorems:

Theorem 5.6.2. *Assume that the constraints in (5.69) are used for the total transmission time in each segment. Then, the optimal motion policy is to move with the maximum velocity $v_{\max}$. Also, the optimal trajectory and transmission times in the case of $|\mathcal{S}(t)| = 0$ are given by the following MILP:*

$$\min\ \overline{w}\sum_{i=1}^{m}\sum_{\substack{j=1\\j\neq i}}^{m} z_{i,j}d_{i,j} + \kappa\sum_{i=1}^{m}\sum_{\substack{j=1\\j\neq i}}^{m}\sum_{k=1}^{n_{i,j}}\sum_{\ell=1}^{n_r}\tau_{i,j,k,\ell}\frac{(2^{R_{\mathrm{TX},\ell}}-1)}{\overline{G}_{i,j,k}}$$

s.t.

$$1)\ \sum_{i=1}^{m}\sum_{\substack{j=1\\j\neq i}}^{m}\sum_{k=1}^{n_{i,j}}\sum_{\ell=1}^{n_r} R_{\mathrm{TX},\ell}\tau_{i,j,k,\ell} \geq \frac{1}{B}\frac{\sum_{i=1}^{m}\rho_i}{\phi v_{\max}}\sum_{i=1}^{m}\sum_{\substack{j=1\\j\neq i}}^{m} z_{i,j}d_{i,j},$$

$$2)\ \frac{\sum_{i=1}^{m}\rho_i}{\phi v_{\max}}\sum_{i=1}^{m}\sum_{\substack{j=1\\j\neq i}}^{m} z_{i,j}d_{i,j} \leq L_{\max},$$

$$3)\ \sum_{\ell=1}^{n_r}\tau_{i,j,k,\ell} \leq z_{i,j}t_c, \qquad \forall i,j,k,$$

$$4)\ \textit{Constraints 6, 7, 8 and 9 in MILP of Program 3}, \tag{5.76}$$

where $\overline{w} \triangleq \frac{1}{\phi}\frac{P_{\mathrm{loss}}}{v_{\max}} + w$.

Proof. The proof is based on the fact that in this case the minimum period T required for stability is given by $T = \frac{1}{\phi v_{\max}}\sum_{i=1}^{m}\sum_{\substack{j=1\\j\neq i}}^{m} z_{i,j}d_{i,j}$. This results in the following motion energy in each period: $E_m = \overline{w}\sum_{i=1}^{m}\sum_{\substack{j=1\\j\neq i}}^{m} z_{i,j}d_{i,j}$. By substituting T and E_m in Program 3, the MILP of (5.76) results. □

Note that by setting $T^* = \frac{\mathrm{d}(\mathcal{C})}{\phi v_{\max}}$, the results of parts 2 and 4 of Theorem 5.6.1 hold for the MILP of (5.76) as well.

Theorem 5.6.3. *Assume that the constraints in (5.70) are used for the total transmission time in each segment. Then, the MILP, that gives the optimal motion and communication policies in the case of $|\mathcal{S}(t)| = 0$, is the same MILP of Program 3, without the stability constraints in (5.62) and after replacing $\varrho_{i,j,k}$ with $\frac{1}{\phi}\varrho_{i,j,k}$ in (5.64), (5.65) and (5.66).*

Proof. In case the constraints in (5.70) are used for the total transmission time in each segment, the minimum period T required for stability is given by $T = \frac{1}{\phi}\sum_{i=1}^{m}\sum_{\substack{j=1\\ j\neq i}}^{m}\sum_{k=1}^{n_{i,j}} d_{i,j,k}\varrho_{i,j,k}$. By substituting T in the MILP of Program 3 and removing the constraints on stability (the stability is already guaranteed by choosing proper stop times), it becomes clear that the optimal policies are the solution of the this MILP without the stability constraints and after replacing $\varrho_{i,j,k}$ with $\frac{1}{\phi}\varrho_{i,j,k}$. □

Another special case happens when the mobile agent is forced to transmits its collected information bits at the positions of the POIs only. This may be the case when the actual POIs are located in a region with a poor channel quality and a number of virtual POIs are added to improve the communication. In this case, the mobile agent needs to stop for some time at a number of POIs to transmit its collected information bits. Let $\tau_{i,\ell}$ represent the time spent for transmission with the spectral efficiency of $R_{\mathrm{TX},\ell}$ at the i^{th} POI. The following theorem then gives the optimal motion and communication policies in this case, when we additionally have $|\mathcal{S}(t)| = 0$:

Theorem 5.6.4. *Assume that the mobile agent only transmits at the location of the POIs and $|\mathcal{S}(t)| = 0$. Then, the following hold:*

1. *The optimal trajectory is given by the minimum-length Hamiltonian cycle on*

the POIs, $\mathcal{H}$, which is given by the solution of a Traveling Salesman Problem (TSP). Also, the optimal velocity along the trajectory is $v_{\max}$.

2. *The optimal stop times and transmission times are given by the solution of the following LP:*

$$
\begin{aligned}
&\min\ P_{\text{loss}} \sum_{i=1}^{m} t_i + \kappa \sum_{i=1}^{m} \sum_{\ell=1}^{n_r} \tau_{i,\ell} \frac{(2^{R_{\text{TX},\ell}} - 1)}{\overline{G}_i} \\
&\text{s.t.} \\
&1)\ \alpha_0 t_i - \rho_i \left(\frac{\mathrm{d}(\mathcal{H})}{v_{\max}} + \sum_{i=1}^{m} t_i \right) \geq 0, \qquad \forall i, \\
&2)\ \sum_{i=1}^{m} \sum_{\ell=1}^{n_r} \tau_{i,\ell}\, R_{\text{TX},\ell} \geq \frac{\sum_{i=1}^{m} \rho_i}{B} \left(\frac{\mathrm{d}(\mathcal{H})}{v_{\max}} + \sum_{i=1}^{m} t_i \right), \\
&3)\ \sum_{\ell=1}^{n_r} \tau_{i,\ell} \leq t_i, \qquad \forall i, \\
&4)\ \tau_{i,\ell} \geq 0,\ \ t_i \geq 0, \qquad \forall i, \ell,
\end{aligned}
\tag{5.77}
$$

where $\overline{G}_i \triangleq \hat{G}(q_i) 10^{\frac{Q^{-1}(1-\epsilon)\sigma(q_i)}{10}}$.

Proof. Since, the trajectory of the mobile agent affects neither the data collection nor the data transmission, the optimal trajectory which results in the minimum total energy is simply the one that results in the minimum period. This happens after choosing the minimum-length Hamiltonian cycle, $\mathcal{H}$, and the maximum velocity, $v_{\max}$. The rest of the proof is straightforward and uses the fact that $T = \frac{\mathrm{d}(\mathcal{H})}{v_{\max}} + \sum_{i=1}^{m} t_i$ in this case. □

The more general case where $|\mathcal{S}(t)| > 0$ and the mobile agent transmits at the positions of the POIs only can be considered in a similar fashion. The results are, however, omitted for lack of space.

5.7 Simulation Results for the Extended Dynamic Coverage Problem

In this section, we present the results of applying the proposed MILP approach to a persistent information collection scenario using a mobile agent. The workspace is a 100m by 100m rectangular region that includes 10 POIs. We assume the mobile agent is equipped with an omni-directional data collection device with the following distance-dependant data collection rate: $\alpha(d) = \alpha_0 e^{-d/\iota}$, where α_0 and ι are positive constants. The area covered by the data collection device is also given by $\mathcal{S}(q) = \{q' \in \mathcal{W} \mid \|q' - q\| \leq d_{\max}\}$.

The channel power $G(q)$ is generated using our probabilistic channel simulator. The remote station is located at position $q_b = (0, 0, 1.0)$ m. The following channel parameters are also used: path loss constant $K_{\text{dB}} = -25$ dB, path loss exponent $n_{\text{PL}} = 2$, standard deviation of shadowing component $\vartheta = 5$ dB, decorrelation distance of shadowing component $\beta = 20$ m, and standard deviation of multipath component $\omega = 2$ dB. The 3D plot of the channel power $G(q)$ in dB is shown in Fig. 5.14. The rest of the parameters are selected as follows: $\alpha_0 = 10^6$ bits/s, $\iota = 8$ m, $d_{\max} = 8$ m, $\delta_{\max} = 2$ m, $v_{\max} = 1$ m/s, $v_{\min} = 0.1$ m/s, $w = 0.1$ J/m, $P_{\text{loss}} = 0.2$ W, $\text{BER}_{\text{TH}} = 0.05$, $B = 1$ MHz, $N_0 = 10^{-11}$ W/Hz, $\kappa = 9.24 \times 10^{-6}$, $\rho_i = 6 \times 10^4$ bits/s, for $i = 1, \cdots, 10$, $t_c = 2$ s, and $L_{\max} = 10^{10}$ bits. We also consider $n_r = 3$ different spectral efficiencies of $R_{\text{TX},1} = 2$ bits/symbol, $R_{\text{TX},2} = 4$ bits/symbol and $R_{\text{TX},3} = 6$ bits/symbol (corresponding to 4QAM, 16QAM and 64QAM modulations).

Fig. 5.15 shows the optimal trajectory of the mobile agent in case Type I constraints in (5.69) are used for the total transmission time in each segment. The green parts of the trajectory in the left figure show the segments where the mobile agent slows down, i.e., the segments where the robot does not move with the maximum velocity ($\varrho^*_{i,j,k} > v^{-1}_{\max}$). The green parts in the right figure also show the segments

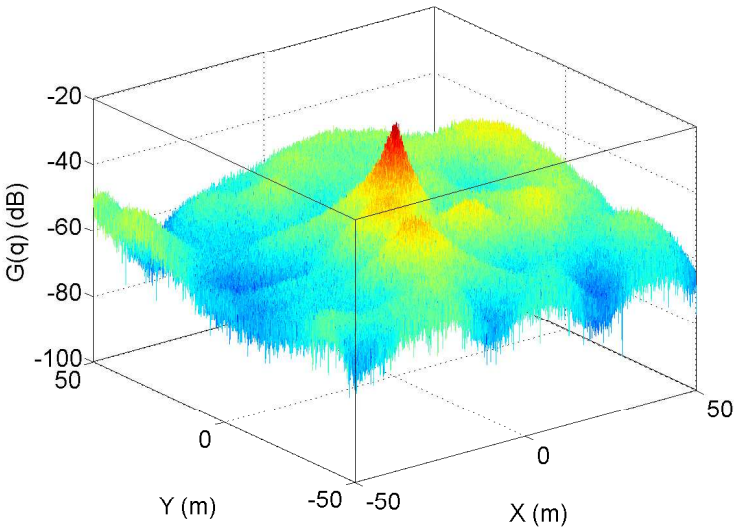

Figure 5.14: The 3D plot of the channel power $G(q)$ over the workspace.

where the information bits are transmitted to the remote station, i.e., the segments where $\sum_{\ell=1}^{n_r} \tau^*_{i,j,k,\ell} > 0$.[15] The velocity profile of the mobile agent long the optimal trajectory is shown in Fig. 5.16 (left). The optimal transmission times along the optimal trajectory, for sending with the three different spectral efficiencies of $R_{\mathrm{TX},1} = 2$ bits/symbol, $R_{\mathrm{TX},2} = 4$ bits/symbol and $R_{\mathrm{TX},3} = 6$ bits/symbol, are also shown in Fig. 5.16 (right). In both figures, we have specified the paths between any two POIs along the trajectory of mobile agent. It can be seen that the mobile agent slows down along the segments close to the POIs to collect the information bits. However, it moves with velocity $v_{\max}$ when there is no information bits to collect. The optimal motion energy, communication energy and period are also shown in Table 5.6. It is worth mentioning that since the communication energy is much larger than the motion energy (due to poor predicted channel quality), the optimal trajectory passes through the regions close to the remote station as much as possible to minimize the communication energy. In other words, the minimum-length Hamiltonian cycle

[15]Note that the planning is based on a probabilistic prediction of the channel quality.

(which provides the minimum motion energy) is not the optimal Hamiltonian cycle in this case.

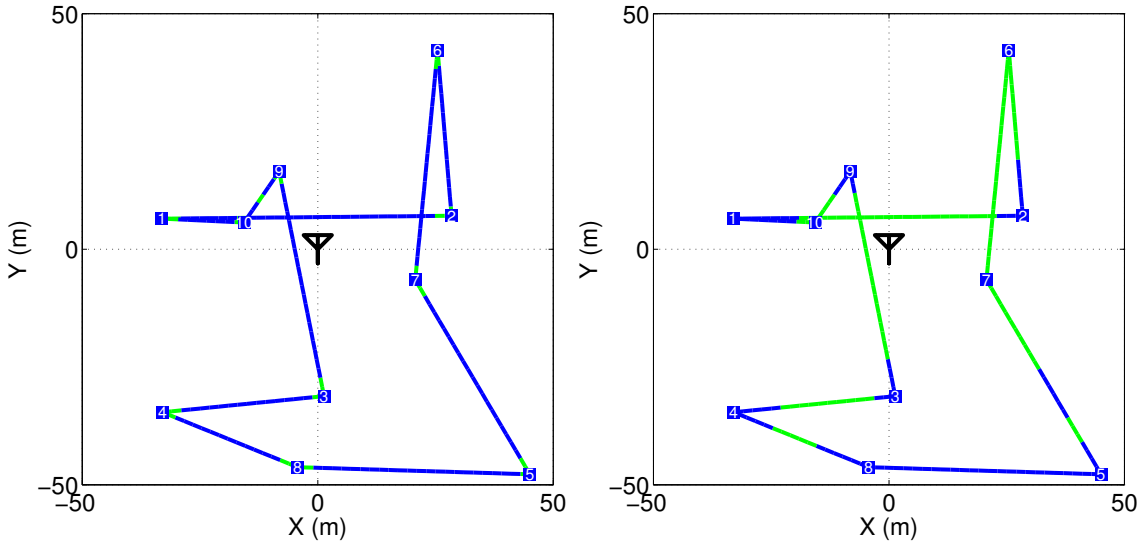

Figure 5.15: The optimal trajectory of the mobile agent in case Type I constraints in (5.69) are used for the total transmission time in each segment. The location of the remote station is denoted at the center of the figures. The green parts of the trajectory in the left figure show the segments where the mobile agent slows down, i.e., the segments where $\varrho^*_{i,j,k} > v_{\max}^{-1}$. The green parts in the right figure also show the segments where the information bits are transmitted to the remote station, i.e., the segments where $\sum_{\ell=1}^{n_r} \tau^*_{i,j,k,\ell} > 0$.

In order to see how information bits are transmitted along the trajectory, Fig. 5.17 shows the plots of $\sum_{\ell=1}^{n_r} \tau^*_{i,j,k,\ell}\big(2^{R_{\mathrm{TX},\ell}} - 1\big)$ and $\overline{G}_{i,j,k}$ (as a measure of the predicted channel quality) along the optimal trajectory of the mobile agent. It can be seen that in this case whenever for any two segments (i_1, j_1, k_1) and (i_2, j_2, k_2) we have $\overline{G}_{i_1,j_1,k_1} > \overline{G}_{i_2,j_2,k_2}$, then, necessarily $\sum_{\ell=1}^{n_r} \tau^*_{i_1,j_1,k_1,\ell}\big(2^{R_{\mathrm{TX},\ell}}-1\big) \geq \sum_{\ell=1}^{n_r} \tau^*_{i_2,j_2,k_2,\ell}\big(2^{R_{\mathrm{TX},\ell}}-1\big)$, as proved by Theorem 5.6.1. In other words, information bits are sent in the regions with good predicted channel quality.

Next consider the case where Type II constraints in (5.70) are used for the total transmission time in each segment. The optimal trajectory of the mobile agent in this case is shown in Fig. 5.18. Note that Type II constraints are more relaxed than

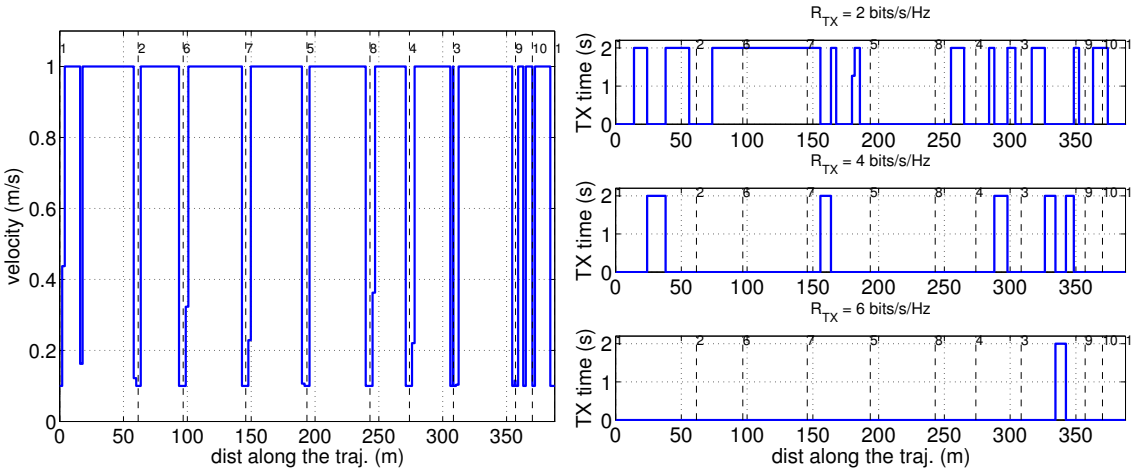

Figure 5.16: The velocity profile (left) and the transmission time profile (right) of the mobile agent along the optimal trajectory of Fig. 5.15. We have specified the paths between any two POIs along the trajectory on both figures.

Type I ones. Therefore, the mobile agent can optimize the transmission times more freely, resulting in less total energy, as shown in Table 5.6. This can be justified by slowing down and spending more time for transmission in regions with good predicted channel qualities (e.g., the regions close to the remote station). The velocity profile and the transmission time profile of the mobile agent long the optimal trajectory of Fig. 5.18 are shown in Fig. 5.19. The plots of $\sum_{\ell=1}^{n_r} \tau^*_{i,j,k,\ell}\big(2^{R_{\mathrm{TX},\ell}}-1\big)$ and $\overline{G}_{i,j,k}$ along the optimal trajectory of the mobile agent are also shown in Fig. 5.20. As can be seen, unlike Fig. 5.17, part 4 of Theorem 5.6.1 does not hold for this case. Also, in this example, the mobile agent slows down in two regions: along the segments close to the POIs to collect more information bits, and along a number of segments with high predicted channel quality to transmit more information bits. Due to the high channel quality along the segments close to the remote station, the mobile agent transmits most of its collected information bits in these region, as can be seen from Fig. 5.20.

In both of the previous examples, the communication energy is much higher than the motion energy due to poor predicted channel quality. In other words,

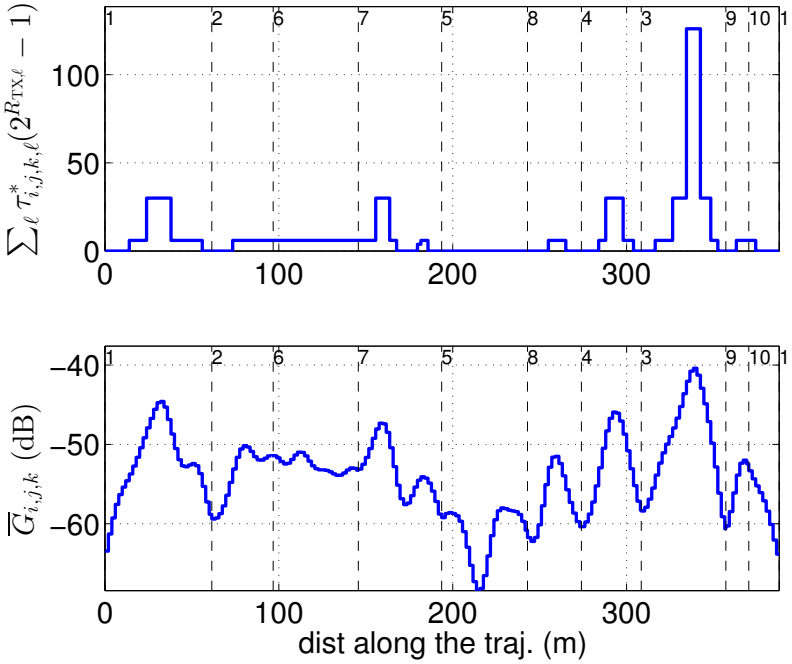

Figure 5.17: The plots of $\sum_{\ell=1}^{n_r} \tau^*_{i,j,k,\ell}\big(2^{R_{\mathrm{TX},\ell}}-1\big)$ (top) and $\overline{G}_{i,j,k}$ (as a measure of the predicted channel quality) (bottom) along the optimal trajectory of Fig. 5.15.

the optimal trajectory is very similar to the Hamiltonian tour that minimizes the communication energy as opposed to the one with minimum length that minimizes the motion energy. On the other hand, when the channel quality is very high, the motion energy becomes the dominant factor, as compared to the communication energy, and the optimal trajectory becomes the minimum-length Hamiltonian tour on the POIs. In order to show this, we find the optimal trajectory for both of the previous examples when the channel power is 20 dB larger (100 times larger in the linear domain) at every point in the workspace. Fig. 5.21 shows the optimal trajectory of the mobile agent in this case when Type I constraints are used for the total transmission time in each segment. It can be seen that the optimal trajectory is the minimum-length Hamiltonian cycle. The velocity profile and the transmission time profile of the mobile agent along the optimal trajectory of Fig. 5.21 are also shown in Fig. 5.22. The plots of $\sum_{\ell=1}^{n_r} \tau^*_{i,j,k,\ell}\big(2^{R_{\mathrm{TX},\ell}}-1\big)$ and $\overline{G}_{i,j,k}$ along the optimal

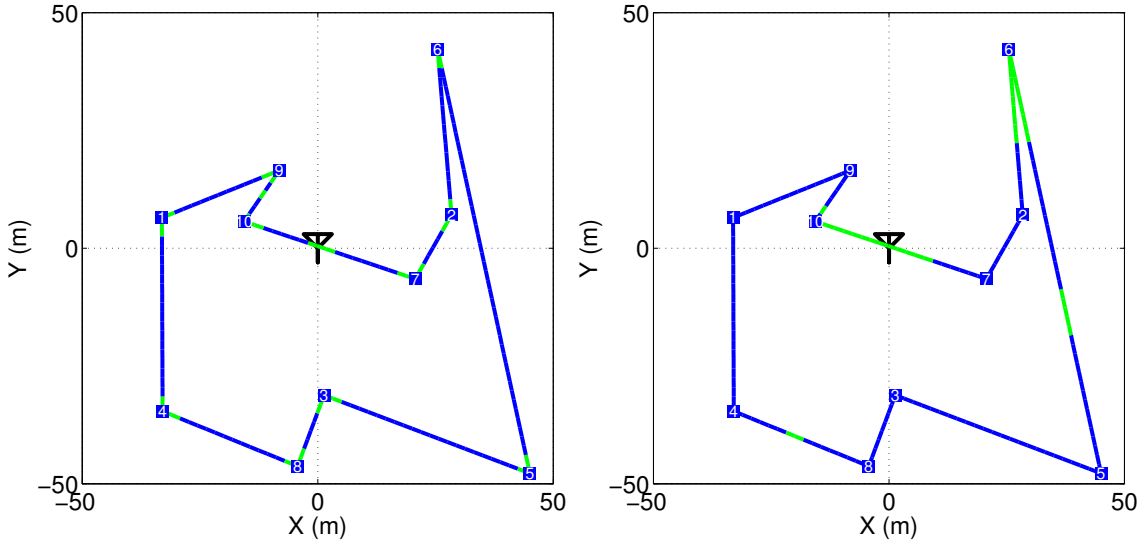

Figure 5.18: The optimal trajectory of the mobile agent in case Type II constraints in (5.70) are used for the total transmission time in each segment. The location of the remote station is denoted at the center of the figures. The green parts of the trajectory in the left figure show the segments where the mobile agent slows down, i.e., the segments where $\varrho^*_{i,j,k} > v_{\max}^{-1}$. The green parts in the right figure also show the segments where the information bits are transmitted to the remote station, i.e., the segments where $\sum_{\ell=1}^{n_r} \tau^*_{i,j,k,\ell} > 0$.

trajectory of the mobile agent are additionally shown in Fig. 5.23. The same behavior as in the first example can be observed. Also, from Table 5.6, it can be seen that both motion and communication energies are smaller than those of the first example, with the motion energy being the dominant factor.

The trajectory of the mobile agent for the case that Type II constraints are used instead for the total transmission time in each segment and the channel power is 20 dB larger at every point is shown in Fig. 5.24. The optimal trajectory is again the minimum-length Hamiltonian cycle. The optimal velocity and transmission time profiles in this case are shown in Fig. 5.25. The plots of $\sum_{\ell=1}^{n_r} \tau^*_{i,j,k,\ell}\big(2^{R_{\mathrm{TX},\ell}} - 1\big)$ and $\overline{G}_{i,j,k}$ along the optimal trajectory of the mobile agent are also shown in Fig. 5.26. The same behavior as in the second example can be observed. From Table 5.6, both motion and communication energies are smaller than their corresponding values in

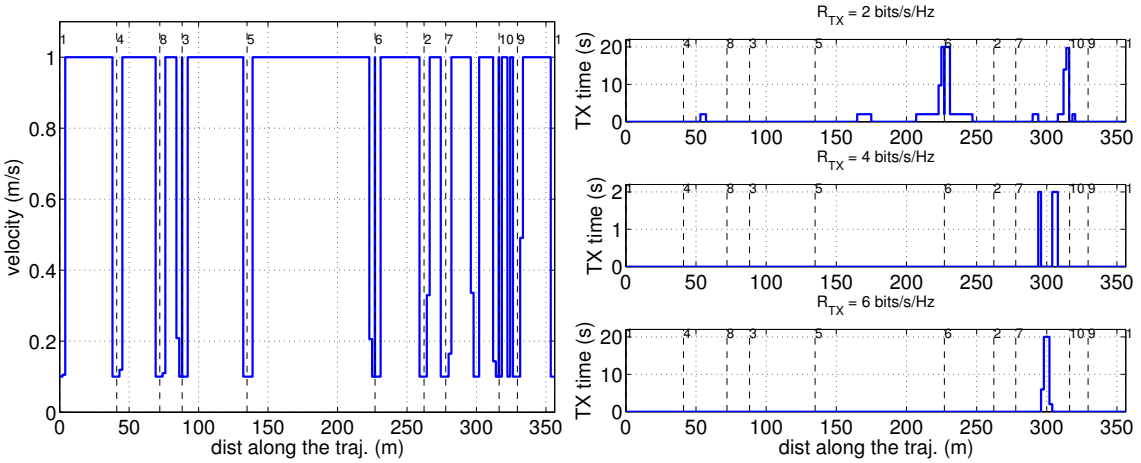

Figure 5.19: The velocity profile (left) and the transmission time profile (right) of the mobile agent along the optimal trajectory of Fig. 5.18. We have specified the paths between any two POIs along the trajectory in both figures.

	Fig. 5.15	Fig. 5.18	Fig. 5.21	Fig. 5.24
E_c^*	1136.6 J	654.1 J	15.00 J	9.24 J
E_m^*	227.6 J	247.18 J	157.14 J	157.14 J
E^*	1364.2 J	901.22 J	172.13 J	166.38 J
T^*	884.2 s	989.15 s	610.36 s	610.36 s

Table 5.6: The optimal communication energy, motion energy, total energy and period in all the examples of Figs. 5.15, 5.18, 5.21 and 5.24.

the second example. Also, since Type II constraints are less restrictive, the total energy in this case is less than that of the third example. In fact, this case results in the least total energy among all the examples. Fig. 5.27 graphically explains how the optimal energy and the length of the optimal Hamiltonian cycle change as a function of the channel quality.

Finally, the time evolution of $\Psi_i(t)$ for POI #4 in all the previous examples is shown in Fig. 5.28. Without loss of generality, we have assumed that at time $t = 0$ the mobile agent starts from POI #4 and $\Psi_i(0) = 0$. It can be seen $\Psi_i(t)$ remains bounded in time. The same behavior can be shown for other POIs.

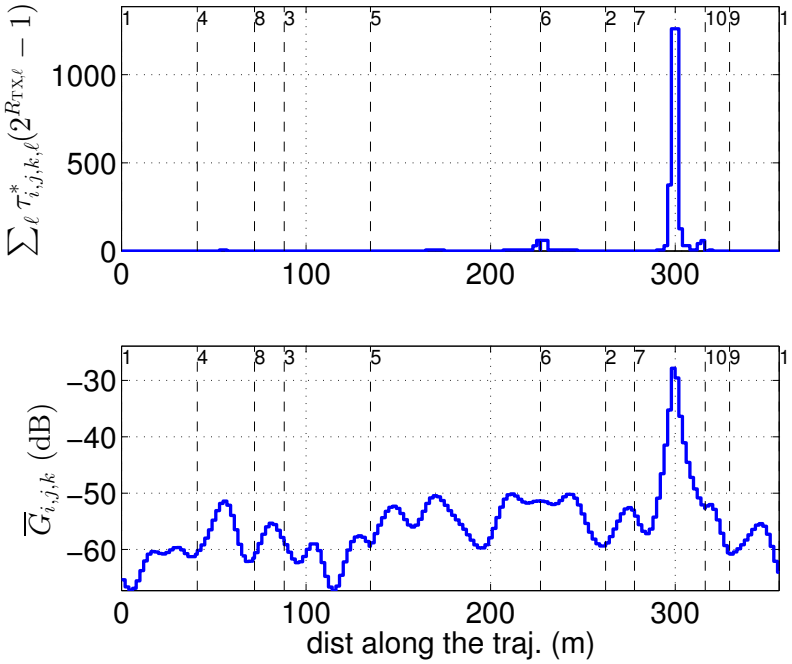

Figure 5.20: The plots of $\sum_{\ell=1}^{n_r} \tau^*_{i,j,k,\ell}\big(2^{R_{\mathrm{TX},\ell}}-1\big)$ (top) and $\overline{G}_{i,j,k}$ (as a measure of the predicted channel quality) (bottom) along the optimal trajectory of Fig. 5.18.

5.8 Summary

In this chapter, we considered the problem of dynamic coverage of a number of POIs using a group of mobile agents in a time-varying environment and in the presence of realistic fading channels. By a time-varying environment, we referred to an environment where a physical quantity is constantly growing at certain rates at the POIs. We considered a linear dynamics for the time-variation of a quantity of interest at the POIs. We then proposed motion and communication policies for the mobile agents to minimize the total energy consumption of the mobile agents in each period, while guaranteeing that the quantity of interest at the POIs remains bounded, and the constraints on the connectivity of the mobile agents, the frequency of covering the POIs, and the total energy budget of the mobile agents are satisfied.

We started with the case where the sensing/actuation range of the mobile agents

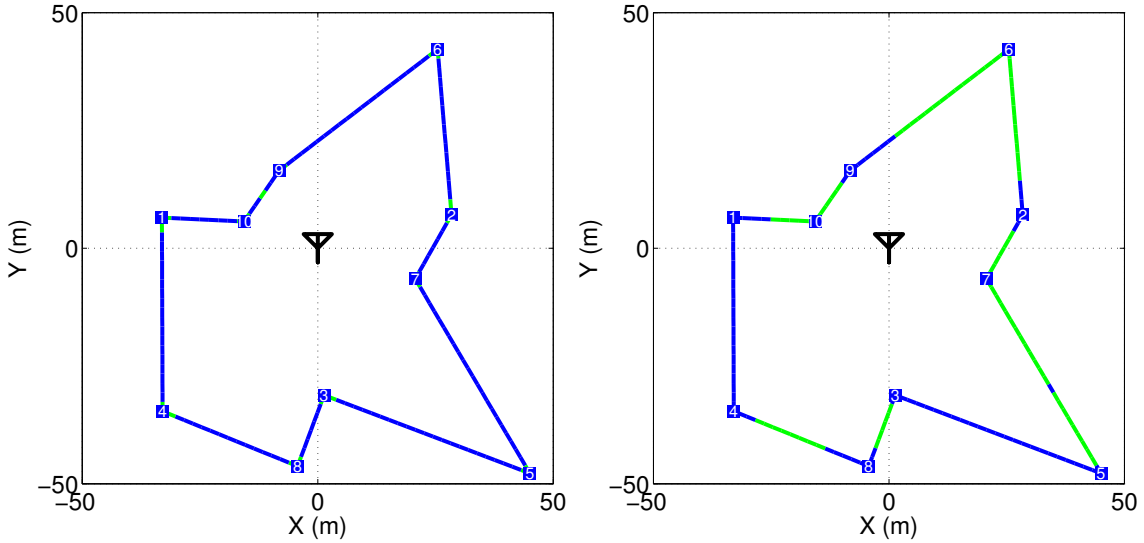

Figure 5.21: The optimal trajectory of the mobile agent in case Type I constraints in (5.69) are used for the total transmission time in each segment and the channel power is 20 dB larger. The location of the remote station is denoted at the center of the figures. The green parts of the trajectory in the left figure show the segments where the mobile agent slows down, i.e., the segments where $\varrho^*_{i,j,k} > v_{\max}^{-1}$. The green parts in the right figure also show the segments where the information bits are transmitted to the remote station, i.e., the segments where $\sum_{\ell=1}^{n_r} \tau^*_{i,j,k,\ell} > 0$.

is small such that each agent is required to move to the position of each POI and stop there for some time to sense/service it. We also assumed a limited total energy budget for the mobile agents. We considered two variants of the problem: *communication-intensive* and *communication-efficient*. Communication-intensive case refers to the case where the mobile agents are required to be connected at all the POIs they visit, in order to send their collected information to the remote station in real-time. Communication-efficient case, on the other hand, refers to the case where the mobile agents are only required to connect to the remote station once along their trajectories, decreasing the communication burden considerably. In both cases, we showed how to optimally find the trajectories of the mobile agents, as well as their stop times and transmission powers at the POIs, using mixed-integer linear programs (MILPs). The properties of the optimal solutions of the MILPs, as well as their asymptotic

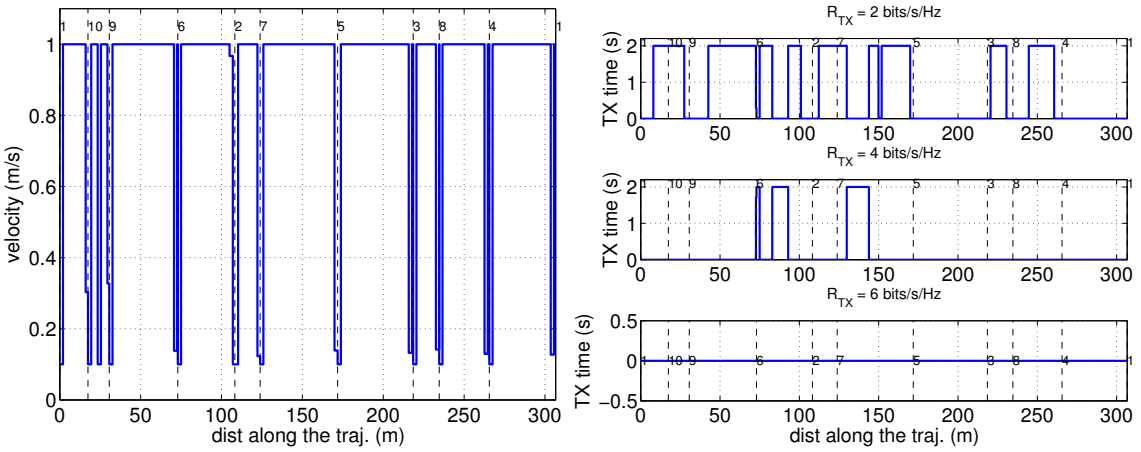

Figure 5.22: The velocity profile (left) and the transmission time profile (right) of the mobile agent along the optimal trajectory of Fig. 5.21. We have specified the paths between any two POIs along the trajectory in both figures.

properties, were also characterized mathematically. At the end of this chapter, we extended our framework by considering a non-zero range for the sensing/actuation device of the mobile agents and adapting their velocities and transmission rates (in addition to their transmission powers) along their trajectories. For the sake of simplicity, however, we considered only one mobile agent. For this case, we similarly proposed an MILP to optimally plan the trajectory of the mobile agent, as well as its transmission power, transmission rate and velocity. The solution of the proposed MILP was also characterized mathematically in this case.

Through theoretical analysis and simulation results, we showed that our proposed dynamic framework enables dynamic coverage of time-varying environments in the presence of realistic fading channels, which is not possible using the previous methods in the literature.

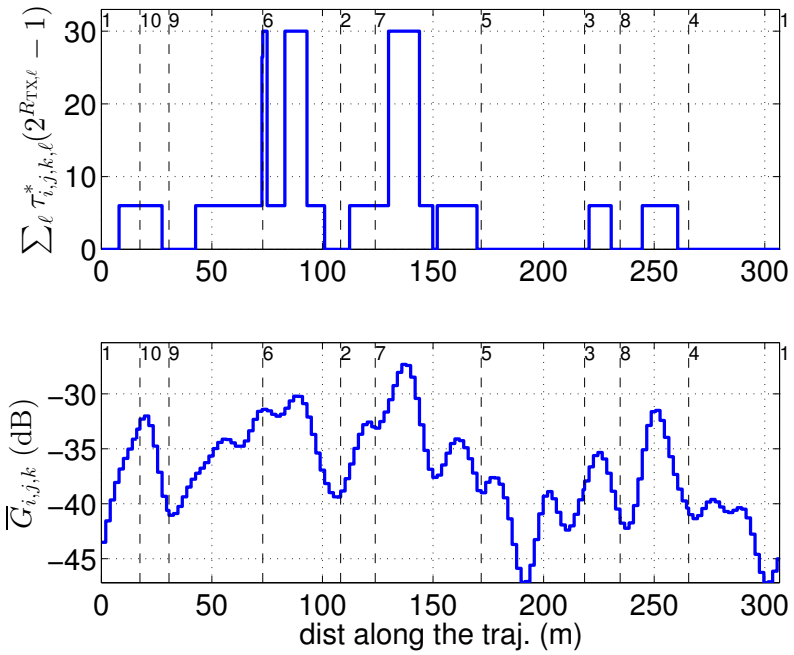

Figure 5.23: The plots of $\sum_{\ell=1}^{n_r} \tau^*_{i,j,k,\ell}\big(2^{R_{\mathrm{TX},\ell}}-1\big)$ (top) and $\overline{G}_{i,j,k}$ (as a measure of the predicted channel quality) (bottom) along the optimal trajectory of Fig. 5.21.

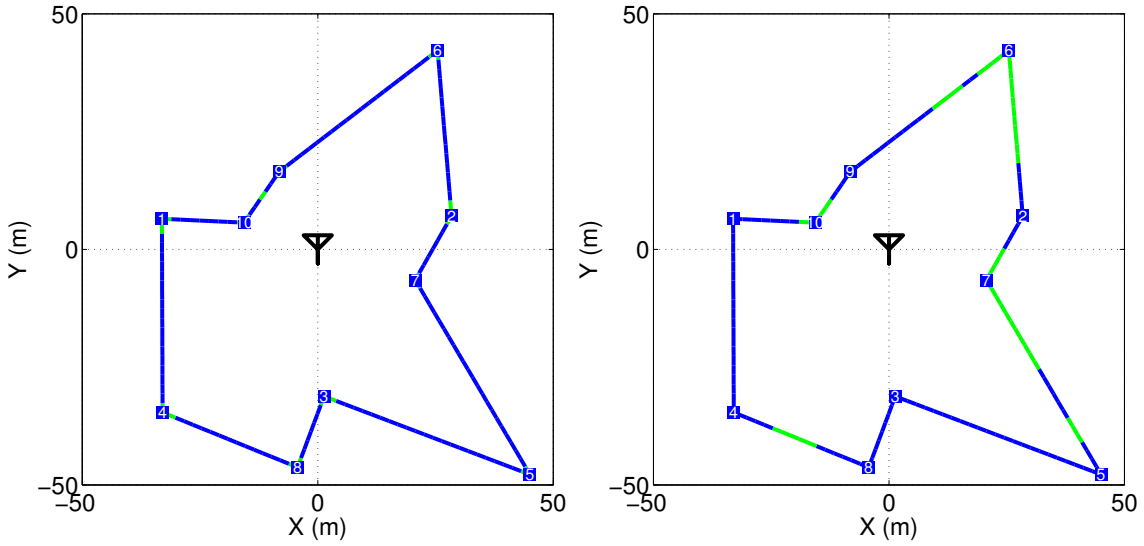

Figure 5.24: The optimal trajectory of the mobile agent in case Type II constraints in (5.70) are used for the total transmission time in each segment and the channel power is 20 dB larger. The location of the remote station is denoted at the center of the figures. The green parts of the trajectory in the left figure show the segments where the mobile agent slows down, i.e., the segments where $\varrho^*_{i,j,k} > v_{\max}^{-1}$. The green parts in the right figure also show the segments where the information bits are transmitted to the remote station, i.e., the segments where $\sum_{\ell=1}^{n_r} \tau^*_{i,j,k,\ell} > 0$.

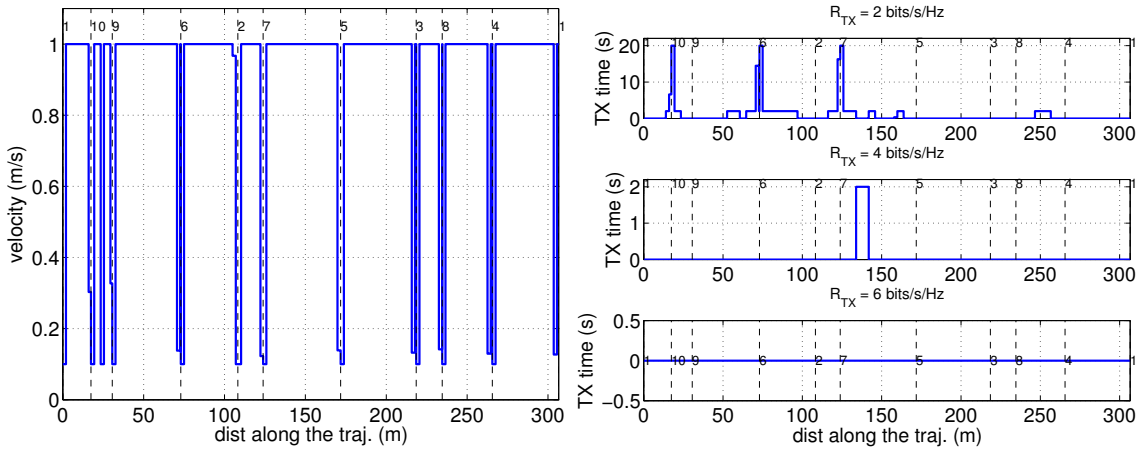

Figure 5.25: The velocity profile (left) and the transmission time profile (right) of the mobile agent along the optimal trajectory of Fig. 5.24. We have specified the paths between any two POIs along the trajectory in both figures.

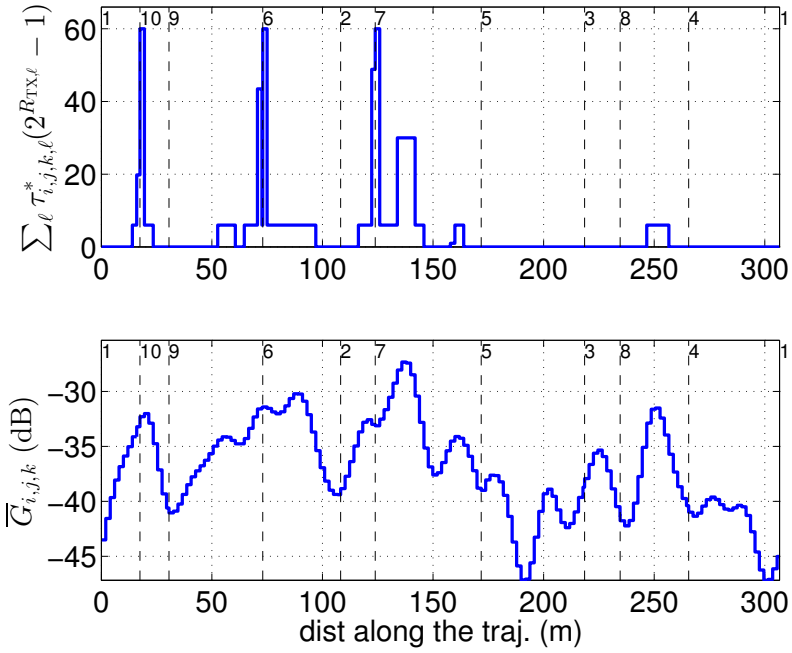

Figure 5.26: The plots of $\sum_{\ell=1}^{n_r} \tau^*_{i,j,k,\ell}\big(2^{R_{\mathrm{TX},\ell}}-1\big)$ (top) and $\overline{G}_{i,j,k}$ (as a measure of the predicted channel quality) (bottom) along the optimal trajectory of Fig. 5.24.

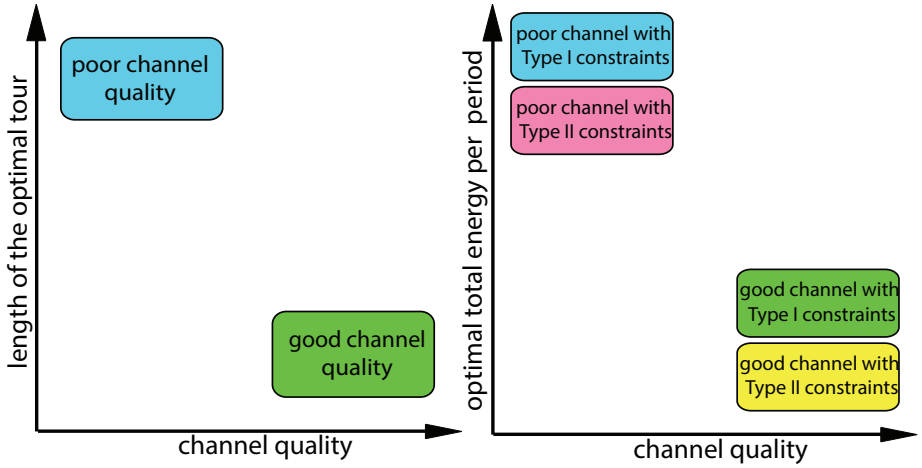

Figure 5.27: The graphical explanation of how optimal energy and the length of the optimal Hamiltonian cycle change as functions of the channel quality.

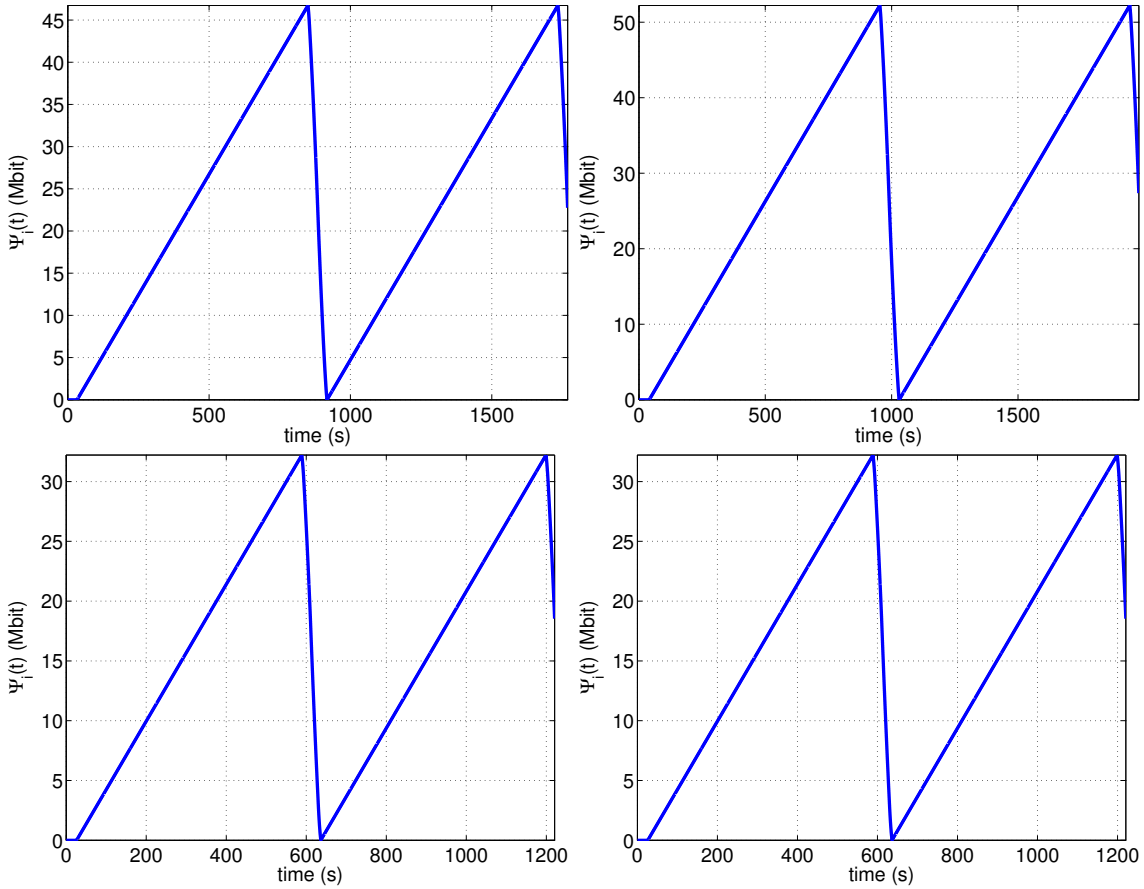

Figure 5.28: The time evolution of $\Psi_i(t)$ in all the previous examples and for POI #4. The top left, top right, bottom left and bottom rights plots correspond to Fig. 5.15, Fig. 5.18, Fig. 5.21, and Fig. 5.24, respectively.

Chapter 6

Conclusions and Further Extensions

In this dissertation, we proposed a new framework for communication-aware motion planning in mobile sensor networks. Our proposed approach enables robust task accomplishment in mobile networks by properly integrating communication, sensing and navigation objectives for motion planning. Through several examples from robotics and mobile sensors literature, we showed that our framework can be used to optimize the trajectories of the mobile sensors (and possibly their transmission powers and rates) to accomplish the sensing task of the network, while satisfying the constraints on the connectivity of the mobile sensors (and their motion and energy consumption).

Next we continue with summarizing the results of each chapter and providing possible directions for further extension of the results of this dissertation.

In Chapter 2, we considered the problem of assessing (predicting) the spatial variations of a wireless channel based on a small number of channel measurements. We used a multi-scale probabilistic model to characterize the channel variations and de-

veloped a channel assessment framework based on that. More specifically, we showed how to plan the motion of the mobile sensors to improve their channel assessment. We first showed how a mobile sensor can plan its trajectory to improve its estimation of the underlying model parameters. This was then followed by planning the motion to decrease the channel assessment error variance. The proposed approaches can be used to provide a good assessment of the wireless channels for the purpose of communication-aware networked task accomplishment.

In Chapter 3, we considered our first communication-aware task accomplishment example. We proposed a communication-aware motion planning framework to remotely track a moving target in realistic fading communication environments. We formulated the Kalman filtering equations for estimating the position of the target over realistic communication links and in the presence of a packet-dropping receiver at the remote station. By using the probabilistic channel assessment framework of Chapter 2, we then designed communication-aware motion planning approaches that properly combine sensing and communication objectives with the goal of maximizing received Fisher information at the remote station.

In Chapter 4, we considered our second example of communication-aware task accomplishment using a mobile network. We assumed the scenario where a team of mobile sensors are deployed by a remote station to explore a given environment, detect an unknown number of static targets and inform the remote station of their findings. We studied the problem of designing the trajectories of the mobile sensors to minimize the probability of target detection error at the remote station, while satisfying the requirements on the connectivity of the mobile sensors to the remote station. First, we considered the case where the mobile sensors need to constantly update the remote station on the locations of the targets. For this case, we proposed our *communication-constrained* motion planning approach which enables the mobile sensors to explore the workspace while maximizing their probability of connectivity

to the remote station during the entire operation. We proved that the overall motion optimization objective function, in this case, is a multiplication of a sensing function that maximizes the Kullback-Leibler (KL) divergence between the maximum uncertainty state and the current one, by a communication function, that maximizes the probability of connectivity to the remote station. Second, we considered the case where the remote station only needs to be informed of the locations of the targets at the end of a given operation time. By building on our communication-constrained results, we proposed our *hybrid* motion planning approach for this case. This approach plans the motion of the mobile sensors such that they explore the workspace with less connectivity constraint on their motion, as compared to the communication-constrained approach, while maximizing their probability of connectivity at the end of the operation. Both of the proposed communication-constrained and hybrid approaches make use of a switching structure. We mathematically characterized the asymptotic behavior of our proposed approaches under certain conditions. We showed that, in terms of the final detection error probability at the remote station, the hybrid approach outperforms the communication-constrained one, while the latter has a higher chance of constant connectivity and, therefore, is more robust to the abrupt termination of the operation. We finally proposed strategies to further increase the robustness of both approaches to multipath fading and under channel assessment errors/uncertainties.

Finally, in Chapter 5, we considered our third communication-aware task accomplishment example. In this chapter, we studied the problem of dynamic coverage of a number of POIs using a group of mobile agents in a time-varying environment and in the presence of realistic fading channels. We considered a linear dynamics for the time-variation of a quantity of interest at the POIs. We then proposed motion and communication policies for the mobile agents to minimize the total energy consumption of the mobile agents in each period, while guaranteeing that the quantity of interest at the POIs remains bounded, and the constraints on the con-

nectivity of the mobile agents, the frequency of covering the POIs, and the total energy budget of the mobile agents are satisfied. We started with the case where the sensing/actuation range of the mobile agents is small such that each agent is required to move to the position of each POI and stop there for some time to sense/service it. We also assumed a limited total energy budget for the mobile agents. We considered two variants of the problem: *communication-intensive* and *communication-efficient*. Communication-intensive case refers to the case where the mobile agents are required to be connected at all the POIs they visit, in order to send their collected information to the remote station in real-time. Communication-efficient case, on the other hand, refers to the case where the mobile agents are only required to connect to the remote station once along their trajectories, decreasing the communication burden considerably. In both cases, we showed how to optimally find the trajectories of the mobile agents, as well as their stop times and transmission powers at the POIs, using mixed-integer linear programs (MILPs). The properties of the optimal solutions of the MILPs, as well as their asymptotic properties, were also characterized mathematically. At the end of this chapter, we extended our framework by considering a non-zero range for the sensing/actuation device of the mobile agents and adapting their velocities and transmission rates (in addition to their transmission powers) along their trajectories. For the sake of simplicity, however, we considered only one mobile agent. For this case, we similarly proposed an MILP to optimally plan the trajectory of the mobile agent, as well as its transmission power, transmission rate and velocity. The solution of the proposed MILP was also characterized mathematically in this case.

There are several possible extensions of the results of this dissertation. A number of possible extensions are as follows:

1. In this dissertation, we considered a wide range of examples when proposing our communication-aware motion planning approaches. The examples considered

in this dissertation demonstrate different aspects of communication-aware task accomplishment in mobile networks. Our ultimate goal is to have a unified framework for communication-aware task accomplishment that can handle any general form of information generation and thus can be applicable to several different applications.

2. In this dissertation, we mainly considered assessing a channel between a mobile sensor and a fixed remote station. The reason for this is as follows. While the distributions of the underlying channel dynamics are readily applicable to the case of two mobile sensors, there are very few work that address the modeling of the channel spatial correlation in this case. We expect a more advanced version of the exponential function to be a good match in this case. However, assessing this hypothesis requires further experimental validations. We expect that our channel prediction framework would then be easily extendable to the case of mobile-to-mobile channels.

3. The proposed motion planning approaches of Chapters 2, 3 and 4 are greedy approaches. As explained previously, the reason for choosing greedy approaches are twofold. First, the form of the objective functions (and constraints) that arise in communication-aware motion planning problems are highly nonlinear. Second, greedy approaches can easily support adaptation to channel assessment, which is a very useful property in case the channel is assessed online by the mobile sensors. There are, however, more optimal solutions based on receding horizon approaches that can be used. Although receding horizon motion planning naturally increases the complexity of the motion planning approaches, studying the improvement achieved by using such approaches is still valuable.

References

[1] I. F. Akyildiz, S. Weilian, Y. Sankarasubramaniam, and E. Cayirci, "A Survey on Sensor Networks," *IEEE Communications Magazine*, vol. 40, no. 8, pp. 102–114, Aug. 2002.

[2] V. Kumar, D. Rus, and S. Singh, "Robot and Sensor Networks for First Responders," *IEEE Pervasive Computing*, vol. 3, no. 4, pp. 24–33, Oct.-Dec. 2004.

[3] W. B. Heinzelman, A. P. Chandrakasan, and H. Balakrishnan, "An Application-Specific Protocol Architecture for Wireless Microsensor Networks," *IEEE Transactions on Wireless Communications*, vol. 1, no. 4, pp. 660–670, Oct. 2002.

[4] I. Nourbakhsh, K. Sycara, M. Koes, M. Yong, M. Lewis, and S. Burion, "Human-robot teaming for search and rescue," *IEEE Pervasive Computing*, vol. 4, no. 1, pp. 72–79, 2005.

[5] J. Casper and R. Murphy, "Human-robot interactions during the robot-assisted urban search and rescue response at the world trade center," *Systems, Man, and Cybernetics, Part B: Cybernetics, IEEE Transactions on*, vol. 33, no. 3, pp. 367–385, June 2003.

[6] A. Ghaffarkhah and Y. Mostofi, "Communication-Aware Motion Planning in Mobile Networks," *IEEE Transactions on Automatic Control*, vol. 56, no. 10, pp. 2478–2485, Oct. 2011.

[7] ——, "Channel Learning and Communication-Aware Motion Planning in Mobile Networks," in *Proceedings of the American Control Conference (ACC)*, Baltimore, MD, June 2010, pp. 5413–5420.

[8] B. S. Y. Rao, H. F. Durrant-Whyte, and J. A. Sheen, "A Fully Decentralized Multi-Sensor System For Tracking and Surveillance,."

[9] S. Martinez and F. Bullo, "Optimal Sensor Placement and Motion Coordination for Target Tracking," vol. 42, no. 4, pp. 661–668, 2006.

[10] B. Grocholsky, "Information-theoretic control of multiple sensor platforms," Ph.D. dissertation, The University of Sydney, 2002.

[11] T. H. Chung, V. Gupta, J. W. Burdick, and R. M. Murray, "On a decentralized active sensing strategy using mobile sensor platforms in a network," in *Proceedings of 43rd IEEE Conference on Decision and Control (CDC)*, 2004, pp. 1914–1919.

[12] E. W. Frew, D. A. Lawrence, and S. Morris, "Coordinated Standoff Tracking of Moving Targets using Lyapunov Guidance Vector Fields," *AIAA Journal of Guidance, Control, and Dynamics*, vol. 31, no. 2, pp. 290–306, Mar. 2008.

[13] A. Ghaffarkhah and Y. Mostofi, "Path Planning for Networked Robotic Surveillance," *IEEE Transactions on Signal Processing*, vol. 60, no. 7, pp. 3560–3575, July 2012.

[14] ——, "Communication-Aware Surveillance in Mobile Sensor Networks," in *Proceedings of the American Control Conference (ACC)*, San Francisco, CA, July 2011, pp. 4032–4038.

[15] B. Grocholsky, J. Keller, V. Kumar, and G. Pappas, "Cooperative Air and Ground Surveillance," *IEEE Robotics and Automation Magazine*, vol. 13, no. 3, pp. 16–25, 2006.

[16] A. Ghaffarkhah and Y. Mostofi, "A communication-aware framework for robotic field estimation," in *Proceedings of 50th IEEE Conference on Decision and Control and European Control Conference (CDC-ECC)*, Dec. 2011, pp. 3553–3558.

[17] Y. Wang and I. Hussein, "Awareness Coverage Control Over Large-Scale Domains With Intermittent Communications," *IEEE Transactions on Automatic Control*, vol. 55, no. 8, pp. 1850–1859, Aug. 2010.

[18] I. I. Hussein and D. M. Stipanovic, "Effective Coverage Control for Mobile Sensor Networks With Guaranteed Collision Avoidance," *IEEE Transactions on Control Systems Technology*, vol. 15, no. 4, pp. 642–657, July 2007.

[19] J. Cortes, "Distributed Kriged Kalman Filter for Spatial Estimation," *IEEE Transactions on Automatic Control*, vol. 54, no. 12, pp. 2816–2827, Dec. 2009.

[20] J. Le Ny and G. Pappas, "On trajectory optimization for active sensing in Gaussian process models," in *Proceedings of the IEEE Conference on Decision and Control and Chinese Control Conference (CDC-CCC)*, Dec. 2009, pp. 6286–6292.

[21] N. E. Leonard, D. A. Paley, F. Lekien, R. Sepulchre, D. M. Fratantoni, and R. E. Davis, "Collective Motion, Sensor Networks, and Ocean Sampling," *Proceedings of the IEEE*, vol. 95, no. 1, pp. 48–74, Jan. 2007.

[22] N. Yilmaz, C. Evangelinos, P. Lermusiaux, and N. Patrikalakis, "Path Planning of Autonomous Underwater Vehicles for Adaptive Sampling Using Mixed Integer Linear Programming," *IEEE Journal of Oceanic Engineering*, vol. 33, no. 4, pp. 522–537, Oct. 2008.

[23] P. E. Rybski, N. P. Papanikolopoulos, S. A. Stoeter, D. G. Krantz, K. B. Yesin, M. Gini, R. Voyles, D. F. Hougen, B. Nelson, and M. D. Erickson, "Enlisting rangers and scouts for reconnaissance and surveillance," *IEEE Robotics Automation Magazine*, vol. 7, no. 4, pp. 14–24, Dec. 2000.

[24] T. Samad, J. Bay, and D. Godbole, "Network-Centric Systems for Military Operations in Urban Terrain: The Role of UAVs," *Proceedings of the IEEE*, vol. 95, no. 1, pp. 92–107, Jan. 2007.

[25] R. Olfati-Saber, J. A. Fax, and R. M. Murray, "Consensus and Cooperation in Networked Multi-Agent Systems," *Proceedings of the IEEE*, vol. 95, no. 1, pp. 215–233, Jan. 2007.

[26] R. Olfati-Saber and R. Murray, "Distributed structural stabilization and tracking for formations of dynamic multi-agents," in *Proceedings of the 41st IEEE Conference on Decision and Control (CDC)*, Las Vegas, Nevada, Dec. 2002.

[27] H. G. Tanner, A. Jadbabaie, and G. J. Pappas, "Stable flocking of mobile agents, part I: Fixed topology," in *Proceedings of IEEE Conference on Decision and Control (CDC)*, Maui, Hawaii, Dec. 2003, pp. 2010–2015.

[28] J. C. Latombe, *Robot Motion Planning*. Springer, 1990.

[29] S. M. LaValle, *Planning Algorithms*. Cambridge University Press, 2006.

[30] J. Desai and V. Kumar, "Motion planning for cooperating mobile manipulators," *Journal of robotic systems*, vol. 16, no. 10, pp. 557–579, 1999.

[31] C. Belta and V. Kumar, "Abstraction and control for groups of robots," *IEEE Transactions on robotics*, vol. 20, no. 5, pp. 865–875, Oct. 2004.

[32] J. S. Bellingham, M. Tillerson, M. Alighanbari, and J. P. How, "Cooperative path planning for multiple UAVs in dynamic and uncertain environments," in *Proceedings of the 41st IEEE Conference on Decision and Control*, Dec. 2002, pp. 2816–2822.

[33] C. Belta and V. Kumar, "Optimal motion generation for groups of robots: a geometric approach," *ASME journal of mechanical design*, vol. 126, pp. 63–70, 2004.

[34] W. Wong and R. Brockett, "Systems with finite communication bandwidth constraints-Part I: State estimation problems," *IEEE Transactions on Automatic Control*, vol. 42, no. 9, pp. 1294–1299, Sept. 1997.

[35] ——, "Systems with finite communication bandwidth constraints-Part II: Stabilization with limited information feedback," *IEEE Transactions on Automatic Control*, vol. 44, no. 5, pp. 1049–1053, May 1999.

[36] S. Tatikonda, "Control under communication constraints," Ph.D. dissertation, MIT, 2000.

[37] A. Ortega, J. Hespanha, and L. Vasudevan, "Towards the control of linear systems with minimum bit-rate," in *Proceedings of Int. Symp. on the Mathematical Theory of Networks and Systems*, Aug. 2002.

[38] F. Fagnani and S. Zampieri, "Stability analysis and synthesis for scalar linear systems with a quantized feedback," *IEEE Transactions on Automatic Control*, vol. 48, no. 9, pp. 1569–1584, Sept. 2003.

[39] N. Elia and S. K. Mitter, "Stabilization of linear systems with limited information," *IEEE Transactions on Automatic Control*, vol. 46, no. 9, pp. 1384–1400, September 2001.

[40] L. Feng-Li, J. Moyne, and D. Tilbury, "Network design consideration for distributed control systems," *IEEE Transactions on Control Systems Technology*, vol. 10, no. 2, pp. 297–307, Mar. 2002.

[41] Y. Mostofi and R. Murray, "To Drop or Not to Drop: Design Principles for Kalman Filtering over Wireless Fading Channels," *IEEE Transactions on Automatic Control*, vol. 54, no. 2, pp. 376–381, Feb. 2009.

[42] ——, "Effect of Time-Varying Fading Channels on the Control Performance of a Mobile Sensor Node," in *Proceedings of IEEE 1st International Conference on Sensor and Ad Hoc Communications and Networks (Secon)*, Santa Clara, CA, Oct. 2004, pp. 317–324.

[43] Q. Qu, L. B. Milstein, and D. R. Vaman, "Cross-Layer Distributed Joint Power Control and Scheduling for Delay-Constrained Applications over CDMA-Based Wireless Ad-Hoc Networks," *IEEE Transactions on Communications*, vol. 58, no. 2, pp. 669–680, Feb. 2010.

[44] W. L. Huang and K. B. Letaief, "Cross-Layer Scheduling and Power Control Combined With Adaptive Modulation for Wireless Ad Hoc Networks," *IEEE Transactions on Communications*, vol. 55, no. 4, pp. 728–739, Apr. 2007.

[45] A. J. Goldsmith and S. B. Wicker, "Design Challenges for Energy-Constrained Ad Hoc Wireless Networks," *IEEE Wireless Communications*, vol. 9, no. 4, pp. 8–27, Aug. 2002.

[46] N. Sarshar, B. A. Rezaei, and V. P. Roychowdhury, "Low Latency Wireless Ad Hoc Networking: Power and Bandwidth Challenges and a Solution," *IEEE/ACM Transactions on Networking*, vol. 16, no. 2, pp. 335–346, Apr. 2008.

[47] R. C. Shah and J. M. Rabaey, "Energy Aware Routing for Low Energy Ad Hoc Sensor Networks," in *Proceedings of IEEE Wireless Communications and Networking Conference (WCNC2002)*, vol. 1, Mar. 2002.

[48] J. Broch, D. A. Maltz, D. B. Johnson, Y. C. Hu, and J. Jetcheva, "A Performance Comparison of Multi-Hop Wireless Ad Hoc Network Routing Protocols," in *Proceedings of the 4th annual ACM/IEEE international conference on Mobile computing and networking*, ser. MobiCom '98. New York, NY, USA: ACM, 1998, pp. 85–97.

[49] D. B. Johnson and D. A. Maltz, *Dynamic Source Routing in Ad Hoc Wireless Networks*. Kluwer Academic Publishers, 1996, vol. 353, ch. 5, pp. 153–181.

[50] J. Laneman, D. Tse, and G. Wornell, "Cooperative Diversity in Wireless Networks: Efficient Protocols and Outage Behavior," *IEEE Transaction on Information Theory*, vol. 50, no. 12, pp. 3062–3080, Dec. 2004.

[51] M. Haenggi, "Analysis and Design of Diversity Schemes for Ad Hoc Wireless Networks," *IEEE Journal on Selected Areas in Communication*, vol. 23, no. 1, pp. 19–27, Jan. 2005.

[52] M. Grossglauser and D. N. C. Tse, "Mobility Increases the Capacity of Adhoc Wireless Networks," *IEEE/ACM Transactions on Networking*, vol. 10, pp. 477–486, Aug. 2002.

[53] C. Comaniciu and H. V. Poor, "On the Capacity of Mobile Ad Hoc Networks with Delay Constraints," *IEEE Transactions on Wireless Communications*, vol. 5, no. 8, pp. 2061–2071, Aug. 2006.

[54] A. Gonzalez-Ruiz, A. Ghaffarkhah, and Y. Mostofi, "A Comprehensive Overview and Characterization of Wireless Channels for Networked Robotic and Control Systems," *Journal of Robotics,*, vol. 2011, 2011.

[55] Y. Mostofi, M. Malmirchegini, and A. Ghaffarkhah, "Estimation of Communication Signal Strength in Robotic Networks," in *Proceedings of IEEE International Conference on Robotics and Automation (ICRA)*, Anchorage, AK, May 2010, pp. 1946–1951.

[56] Y. Mostofi, A. Gonzalez-Ruiz, A. Ghaffarkhah, and D. Li, "Characterization and Modeling of Wireless Channels for Networked Robotic and Control Systems - A Comprehensive Overview," in *Proceedings of 2009 IEEE/RSJ International Conference on Intelligent Robots and Systems (IROS)*, St. Louis, MO, Oct. 2009, pp. 4849–4854.

[57] A. Ghaffarkhah and Y. Mostofi, "Dynamic Coverage of Time-Varying Fading Environments," *submitted, ACM Transactions on Sensor Networks*, 2012.

[58] ——, "Optimal Motion and Communication for Persistent Information Collection using a Mobile Robot," in *submitted, IEEE Globecom International Workshop on Wireless Networking for Unmanned Autonomous Vehicles (Wi-UAV)*, Anaheim, CA, Dec. 2012.

[59] A. Goldsmith, *Wireless Communications*. Cambridge University Press, 2005.

[60] W. C. Jakes, *Microwave Mobile Communications*. New York: Wiley-IEEE Press, 1994.

[61] M. L. Stein, *Interpolation of Spatial Data: Some Theory for Kriging (Springer Series in Statistics)*. New York: Springer, 1999.

[62] A. Krause and C. Guestrin, "Nonmyopic active learning of Gaussian processes: an exploration-exploitation approach," in *Proceedings of the 24th international conference on Machine learning*, ser. ICML '07. New York, NY, USA: ACM, 2007, pp. 449–456. [Online]. Available: http://doi.acm.org/10.1145/1273496.1273553

[63] K. Seung-Jun, E. Dall'Anese, and G. B. Giannakis, "Cooperative Spectrum Sensing for Cognitive Radios Using Kriged Kalman Filtering," *IEEE Journal of Selected Topics in Signal Processing*, vol. 5, no. 1, pp. 24–36, Feb. 2011.

[64] J. Fink and V. Kumar, "Online methods for radio signal mapping with mobile robots," in *IEEE International Conference on Robotics and Automation (ICRA)*, May 2010, pp. 1940–1945.

[65] Y. Yan and Y. Y. Mostofi, "Robotic Router Formation in Realistic Communication Environments," *IEEE Transactions on Robotics*, vol. 28, no. 4, pp. 810–827, Aug. 2012.

[66] M. Malmirchegini, A. Ghaffarkhah, and Y. Mostofi, "Impact of Motion and Channel Parameters on the Estimation of Transmitter Position in Robotic Networks," in *Proceedings of IEEE Globecom International Workshop on Wireless Networking for Unmanned Autonomous Vehicles (Wi-UAV)*, Dec. 2012.

[67] Y. Bar-Shalom, X. R. Li, and T. Kirubarajan, *Estimation with Applications to Tracking and Navigation*. New York: John Wiley, 2001.

[68] B. Sinopoli, L. Schenato, M. Franceschetti, K. Poolla, M. I. Jordan, and S. S. Sastry, "Kalman filtering with intermittent observations," *IEEE Transactions on Automatic Control*, vol. 49, no. 9, pp. 1453 – 1464, Sept. 2004.

[69] L. Schenato, B. Sinopoli, M. Franceschetti, K. Poolla, and S. S. Sastry, "Foundations of Control and Estimation Over Lossy Networks," *Proceedings of the IEEE*, vol. 95, no. 1, pp. 163–187, Jan. 2007.

[70] M. Stachura, A. Carfang, and E. W. Frew, "Cooperative Target Tracking with a Communication Limited Active Sensor Network," in *International Workshop on Robotic Wireless Sensor Networks*, Marina Del Rey, CA, June 2009.

[71] Y. Mostofi, T. Chung, R. Murray, and J. Burdick, "Communication and Sensing Trade Offs in Decentralized Mobile Sensor Networks: A Cross-Layer Design Approach," in *4th International Conference on Information Processing in Sensor Networks (IPSN)*, Los Angeles, California, Apr. 2005, pp. 118–125.

[72] Y. Mostofi, "Decentralized Communication-Aware Motion Planning in Mobile Networks: An Information-Gain Approach," *Journal of Intelligent and Robotic Systems, Special Issue on Unmanned Autonomous Vehicles*, vol. 56, no. 2, pp. 233–256, Sept. 2009.

[73] J. Cortés, S. Martínez, T. Karatas, and F. Bullo, "Coverage control for mobile sensing networks," *IEEE Transactions on Robotics and Automation*, vol. 20, no. 2, pp. 243–255, 2004.

[74] J. Cortés, S. Martínez, and F. Bullo, "Spatially-distributed coverage optimization and control with limited-range interactions," *ESAIM: Control, Optimisation and Calculus of Variations*, vol. 11, pp. 691–719, 2005.

[75] S. L. Smith, M. Schwager, and D. Rus, "Persistent Robotic Tasks: Monitoring and Sweeping in Changing Environments," *IEEE Transactions on Robotics*, vol. 28, no. 2, pp. 410–426, Apr. 2012.

[76] H. Choset, "Coverage for robotics - A survey of recent results," *Annals of Mathematics and Artificial Intelligence*, vol. 31, pp. 113–126, May 2001.

[77] E. U. Acar and H. Choset, "Sensor-based Coverage of Unknown Environments: Incremental Construction of Morse Decompositions," *The International Journal of Robotics Research*, vol. 21, no. 4, pp. 345–366, 2002.

[78] E. U. Acar, H. Choset, and Y. L. Ji, "Sensor-based coverage with extended range detectors," *IEEE Transactions on Robotics*, vol. 22, no. 1, pp. 189–198, Feb. 2006.

[79] M. Li, W. Cheng, K. Liu, Y. He, X. Li, and X. Liao, "Sweep Coverage with Mobile Sensors," *IEEE Transactions on Mobile Computing*, vol. 10, no. 11, pp. 1534–1545, Nov. 2011.

[80] Y. Chevaleyre, "Theoretical analysis of the multi-agent patrolling problem," in *Proceeding of IEEE/WIC/ACM International Conference on Intelligent Agent Technology (IAT)*, Sept. 2004, pp. 302–308.

[81] A. Machado, G. Ramalho, J. D. Zucker, and A. Drogoul, "Multi-agent patrolling: an empirical analysis of alternative architectures," in *Proceedings of the 3rd international conference on Multi-agent-based simulation II*, ser. MABS'02. Berlin, Heidelberg: Springer-Verlag, 2003, pp. 155–170.

[82] N. Agmon, D. Urieli, and P. Stone, "Multiagent Patrol Generalized to Complex Environmental Conditions," in *Proceedings of the Twenty-Fifth Conference on Artificial Intelligence*, Aug. 2011.

[83] Y. Elmaliach, N. Agmon, and G. Kaminka, "Multi-robot area patrol under frequency constraints," *Annals of Mathematics and Artificial Intelligence*, vol. 57, pp. 293–320, 2009.

[84] P. F. Hokayem, D. Stipanovic, and M. W. Spong, "On persistent coverage control," in *Proceedings of 46th IEEE Conference on Decision and Control (CDC)*, Dec. 2007, pp. 6130–6135.

[85] R. N. Smith, M. Schwager, S. L. Smith, B. H. Jones, D. Rus, and G. S. Sukhatme, "Persistent Ocean Monitoring with Underwater Gliders: Adapting Sampling Resolution," *Journal of Field Robotics*, vol. 28, no. 5, pp. 714–741, 2011. [Online]. Available: http://dx.doi.org/10.1002/rob.20405

[86] M. Lindhe and K. Johansson, "Using robot mobility to exploit multipath fading," *IEEE Wireless Communications*, vol. 16, no. 1, pp. 30–37, Feb. 2009.

[87] H. V. Poor, *An Introduction to Signal Detection and Estimation (2nd ed.)*. New York, NY, USA: Springer-Verlag, 1994.

[88] W. M. Smith, "Urban propagation modeling for wireless systems," Ph.D. dissertation, Stanford University, 2004.

[89] M. Malmirchegini and Y. Mostofi, "On the Spatial Predictability of Communication Channels," *IEEE Transactions on Wireless Communications*, vol. 11, no. 3, pp. 964–978, Mar. 2012.

[90] R. A. Horn and C. R. Johnson, *Matrix Analysis*. Cambridge University Press, 1999.

[91] W. Rudin, *Principles of Mathematical Analysis, Third Edition*. McGraw-Hill, 1976.

[92] A. Ghaffarkhah and Y. Mostofi, "Communication-Aware Navigation Functions for Robotic Networks," in *Proceedings of the American Control Conference (ACC)*, St. Louis, MO, June 2009, pp. 1316–1322.

[93] D. Son, B. Krishnamachari, and J. Heidemann, "Experimental Study of Concurrent Transmission in Wireless Sensor Networks," in *Proc. of the 4th Intl. Conf. on Embedded Networked Sensor Systems*, 2006, pp. 237–250.

[94] K. V. Ramachandra, *Kalman Filtering Techniques for Radar Tracking*. Marcel Dekker, 2000.

[95] T. Kailath, A. H. Sayed, and B. Hassibi, *Linear Estimation*. Prentice Hall, 2000.

[96] E. Rimon and D. E. Koditschek, "Exact Robot Navigation using Artificial Potential Functions," *IEEE Transactions on Robotics and Automation*, vol. 8, no. 5, pp. 501–518, Oct. 1992.

[97] D. V. Dimarogonas and K. H. Johansson, "Bounded control of network connectivity in multi-agent systems," *IET Control Theory Applications*, vol. 4, no. 8, pp. 1330–1338, Aug. 2010.

[98] M. Ji and M. Egerstedt, "Distributed Coordination Control of Multiagent Systems While Preserving Connectedness," *IEEE Transactions on Robotics*, vol. 23, no. 4, pp. 693–703, Aug. 2007.

[99] S. A. Mohamed and M. M. Fahmy, "Binary image compression using efficient partitioning into rectangular regions," *IEEE Transactions on Communications*, vol. 43, no. 5, pp. 1888–1893, May 1995.

[100] R. M. Murray, Z. Li, and S. S. Sastry, *A Mathematical Introduction to Robotic Manipulation*. CRC Press, 1994.

[101] T. ElBatt and A. Ephremides, "Joint Scheduling and Power Control for Wireless Ad-hoc Networks," *IEEE Transactions on Wireless Communications*, vol. 3, no. 1, pp. 74–85, Jan. 2004.

[102] Y. Mei, Y. Lu, Y. C. Hu, and C. S. G. Lee, "Deployment of Mobile Robots With Energy and Timing Constraints," *IEEE Transactions on Robotics*, vol. 22, no. 3, pp. 507–522, June 2006.

[103] ——, "A Case Study of Mobile Robots Energy Consumption and Conservation Techniques," in *Proceeding of the 12th International Conference on Advanced Robotics (ICAR)*, July 2005, pp. 492–497.

[104] IBM ILOG CPLEX Optimizer, Available: http://www-01.ibm.com/software/integration/optimization/cplex-optimizer/.

[105] SAS/OR Software Package, http://www.sas.com/technologies/analytics/optimization/or/.

[106] G. Gutin and A. P. Punnen, *The Traveling Salesman Problem and Its Variations (Combinatorial Optimization)*. Kluwer Academic Press, 2004.

[107] B. Na, "Heurisic approaches for no-depot k-traveling salesmen problem with a minmax objective," Master's thesis, Texas A&M University, 2007.

[108] T. Bektas, "The multiple traveling salesman problem: an overview of formulations and solution procedures," *Omega*, vol. 34, no. 3, pp. 209–219, June 2006. [Online]. Available: http://ideas.repec.org/a/eee/jomega/v34y2006i3p209-219.html

[109] A. Shapiro, D. Dentcheva, and A. Ruszczynski, *Lectures on Stochastic Programming: Modeling and Theory*. SIAM, 2009.

[110] R. C. Larson and A. R. Odoni, *Urban Operations Research*. Englewood Cliffs, NJ: Prentice-Hall.

[111] A. Ghaffarkhah, Y. Yan, and Y. Mostofi, "Dynamic Coverage of Time-Varying Environments Using a Mobile Robot - a Communication-Aware Perspective,"

in *Proceedings of IEEE Globecom International Workshop on Wireless Networking for Unmanned Autonomous Vehicles (Wi-UAV)*, Houston, TX, Dec. 2011.